AN ABSTRACT OF THE DISSERTATION OF

Lapyote Prasittisopin for the degree of Doctor of Philosophy in Civil Engineering presented on December 4, 2013

Title: Chemical Transformation of Rice Husk Ash for Sustainable, Constructable, and Durable Binary Cementitious System

Abstract approved:

_____

David Trejo

The production of cement and concrete results in the production of large amounts of CO_2 emissions which can have significant negative environmental impacts. Using supplementary cementing materials (SCMs) as a cement replacement is an effective solution to reduce these negative environmental impacts, as most SCMs are waste by-products from other industries. Rice husk ash (RHA) is one such by-product material. RHA is produced from the burning of rice husks for the production of electricity. This material consists mostly of amorphous silica and has high potential to be used as a SCM. However, the use of RHA is limited. This is due to its cellular, honeycomb-like morphology. This morphology absorbs mix water and reduces the workability of fresh mixtures containing RHA. Reducing RHA particle size can improve the workability of cementitious systems containing RHA. However, reducing RHA particle size with mechanical grinding is time-consuming and costly. This dissertation evaluates the development of a new chemical transformation method to reduce particle size and to eliminate the RHA cellular, honeycomb-like morphology of the RHA. This dissertation focuses on developing a chemical transformation process for RHA, assessing the

performance of systems containing chemically transformed RHA (t-RHA), and evaluating the influence of mixing and transport variables on the characteristics of RHA blended cement systems.

Results indicate that using the chemical transformation process can be an alternative method to reduce RHA particle size and eliminate the cellular, honeycomb-like morphology of the RHA. This results in the improved flowability, higher chemical shrinkage, faster set, reduced porosity, and increased early-age strength of blended cementitious systems when compared to the 100% portland cement (PC) system. When mixing time and mixer revolution counts increase, using t-RHA exhibits lower flow reduction rates and lower chloride diffusivity than the 100% PC system. However, the performance of the t-RHA and the as-receive RHA (AR-RHA) system are similar with increasing mixing time and mixer revolutions count.

CHEMICAL TRANSFORMATION OF RICE HUSK ASH FOR SUSTAINABLE, CONSTRUCTABLE, AND DURABLE BINARY CEMENTITIOUS SYSTEM

by
LAPYOTE PRASITTISOPIN

A DISSERTATION

Submitted to

Oregon State University

in partial fulfillment of
the requirements for the
degree of

Doctor of Philosophy

Presented December 4, 2013
Commencement June 2014

Doctor of Philosophy dissertation of Lapyote Prasittisopin presented on December 4, 2013

APPROVED:

Major Professor, representing Civil Engineering

Head of the School of Civil and Construction Engineering

Dean of the Graduate School

I understand that my dissertation will become part of the permanent collection of Oregon State University libraries. My signature below authorizes release of my dissertation to any reader upon request.

Lapyote Prasittisopin, Author

ACKNOWLEDGEMENTS

I would like to highly express my appreciations to acknowledgement the excellent academic guidance and financial support offered by Dr. David Trejo, my main advisor, during my four-year doctorate study at Oregon State University. His guidance was my memorable experience in my life. I also appreciate the excellent input of the other committee members, Dr. Chris A. Bell, Dr. Burkan O. Isgor, Dr. Lech Muszyński, and Dr. Karl R. Haapala. I am also grateful to Dr. Jonathan D. Istok for his advices on the thermodynamic modeling and ion chromatography testing. I also wish to thank Dr. Jason H. Ideker for his timely guidance and advice on the research, especially on pore solution extraction and on calcium aluminate cement. I wish to thank Dr. Thomas Shellhammer for his time to advise on particle size analysis, Kathryn Motter for her assistance on atomic absorption spectroscopy and ultraviolet-visible spectroscopy, Dr. Wenping Li of Agrilectric Companies for RHA, Manfred Dittrich for his kind and friendly assistance, Dr. Khomson Suttisintong who provided me a assistance on chemical reactions, Dr. Paravee Vas-Umnuay of Chemical Engineering who assisted with Scanning Electron Microscope (SEM), Dr. Lalita Attanatho and Matthew Coblyn of Chemical Engineering who assisted with the preparation of the micrograph specimens, Weekit Sirisaksoontorn of the Department of Chemistry, and Noon Prasertpalichatr of Materials Science program who assisted with X-Ray Diffraction Analysis (XRD).

I appreciate the assistance of my colleague for their helping this dissertation comes to fruition; colleagues include Dr. Ceki Halmen of University of Missouri–Kansas City, Dr. Young Hoon Kim of University of Louisville, Dr. Radhadkrishna Pillai of Indian Institute of Technology, Madras, and Passrin Jongvisuttisun of Georgia Institute of Technology. I appreciate assistance from Yisen Guo, Jiaming Chen, Tim Link, Greg Hendrix, and other student members of my research group. Special thanks also go to Tyler Deboodt, Dr. Tengfei Fu, and Chang Li.

I acknowledge the support provided by the Washington Department of Transportation through as part of Project GCA6766, *Extended Discharge Time and Revolution Count for Cast-In-Place Concrete*."

As always, I sincerely thank my father, mother, and two brothers (Leryote and Dr. Lerdyote) for their endless love and continuously encouragement throughout my doctoral study.

TABLE OF CONTENTS

TABLE OF CONTENTS (Continued)

Page

TABLE OF CONTENTS (Continued)

Page

TABLE OF CONTENTS (Continued)

Page

TABLE OF CONTENTS (Continued)

Page

TABLE OF CONTENTS (Continued)

Page

LIST OF FIGURES

LIST OF FIGURES (Continued)

Figure Page

LIST OF FIGURES (Continued)

Figure Page

LIST OF FIGURES (Continued)

Figure Page

LIST OF FIGURES (Continued)

Figure Page

LIST OF FIGURES (Continued)

Figure Page

LIST OF FIGURES (Continued)

Figure Page

LIST OF TABLES

LIST OF TABLES (Continued)

Table Page

NOTATION

μ	Mean Value
A	Alite
A, B	Debye-Huckel Parameter
AAR	Alkali-Aggregate Reaction
AASHTO	American Association of State Highway and Transportation Officials
ACI	American Concrete Institute
ACS	American Chemical Society
a_i	Activity of *i* Ion
ANOVA	Analysis of Variances
AR-RHA	As-Received Rice Husk Ash
AR-RHA+R	As-received Rice Husk Ash Containing Retarder
ASR	Alkali-Silica Reaction
ASTM	American Society for Testing and Materials
B	Belite
$C_{(x,t)}$	Percent Chloride Ion Concentration
$Ca(OH)_2$	Calcium Hydroxide, Portlandite
$Ca_4Al_2(SO_4)(OH)_{12}\cdot 6H_2O$	Monosulphate.

NOTATION (Continued)

$Ca_4Al_2(SO_4)(OH)_{12}\cdot 6H_2O$	Monosulphate.
$Ca_6Al_2(SO_4)_3(OH)_{12}\cdot 26H_2O$	Ettringite
$CaSO_4\cdot 2H_2O$	Gypsum
C_i	Percent Initial Chloride Ion Concentration of Mortar Before Solution Exposure
$c_{i,t}$	Concentration of ion, *i* and Time *t*
C-RHA	Combination of AR-RHA and t-RHA
C_s	Predicted Percent Chloride Ion Concentration at the Surface of the Exposed Mortar
CS	Chemical Shrinkage
C-S-H	Calcium Silicate Hydrates, Pozzolanic
D_a	Apparent Chloride Diffusion Coefficient
DI	De-Ionized
E	Ettringite
EDX	Energy-Dispersive X-Ray Analysis
erf	Error Function
(F)AAS	(Flame) Atomic Absorption Spectroscopy
FAO	Food and Agriculture Organization
f_c	Compressive Strength

NOTATION (Continued)

G	Gypsum
H_0	Null Hypothesis
H_a	Alternative Hypothesis
HCl	Hydrochloric Acid
HPC	Hydrated Portland Cement
I	Ionic Strength
IAP	Ion Activity Product
IC	Ion Chromatography
ITZ	Interfacial Transition Zone
KOH	Potassium Hydroxide
Ksp	Equilibrium Solubility Product
M	Monosulphate
NaOH	Sodium Hydroxide
P	Portlandite
PC	Portland Cement
PCA	Portland Cement Association
PVA	Poly Vinyl Alcohol
R	Gas Constant

NOTATION (Continued)

R_D	Rate of Dissolution
RHA	Rice Husk Ash
R_P	Rate of Precipitation
SCC	Self-Consolidating Concrete
SCM	Supplementary Cementing Materials
SD	Standard Deviation
SEM	Scanning Electron Microscope
SHA	State Highway Agency
SI	Saturation Index
ST	Setting Time
T	Temperature
t-RHA	Chemically Transformed Rice Husk Ash
UCP	Unhydrated Cement Particle
UPC	Unhydrated Portland Cement
ut-RHA	Untransformed Rice Husk Ash
w/b	Water-to-Binder Ratio
w/c	Water-to-Cement Ratio
w/cm	Water-to-Cementitious Material Ratio

NOTATIONS (Continued)

XRD	X-Ray Diffraction
z	Charge of Ion
ΔH_r	Enthalpy

1 INTRODUCTION

1.1 SUSTAINABILITY TO CEMENTITIOUS SYSTEMS

Sustainability is increasingly becoming an everyday issue in our society. Many government agencies and companies focus on policies and resources to minimize environmental impacts. Sustainability focuses on three interdependent considerations: ecological, social, and economic issues (Hutchins and Sutherland 2008). These three issues should be considered when developing the sustainable materials or systems, including materials and systems in the cement and concrete industries.

Concrete is the most widely used man-made materials in the world (Mehta and Monteiro 2006). Mehta (2004) reported that the concrete construction industry is not sustainable. This is due to the large consumptions of virgin materials, the large CO_2 emissions from cement manufacturing process, and deterioration of concrete structures over time. Sustainability is one of the most important challenges confronting the cement and concrete industries today. The use of supplementary cementing materials (SCMs) is one of the most ubiquitous methods to make concrete more ecological and more economic. This is often done by replacing portland cement (PC) with SCMs, thereby requiring less PC in the concrete. Common SCMs include fly ash, silica fume, and blast-furnace slag. Other SCMs are available and could be used, but research is needed.

1.2 RICE HUSK ASH

Rice husk ash (RHA) is an agricultural waste product from the burning of rice husks for energy production. Rice husks are hard coatings that protect the rice seed during the growth period. The pre-burnt composition of the rice husk consists of approximately 75 to 80 percent by weight of organic components (approximately 50 percent of lignin and 25 to 30 percent of cellulose) and 15 to 20 percent of inorganic components. The burning process efficiently removes these organic components, leaving behind an inorganic ash consisting mostly of silica. The size, morphology, and specific surface area of RHA

particles depend on the burning conditions. Proper burning conditions can lead to RHA with higher amorphous silica contents. As a result of the high amorphous silica contents, RHA becomes a highly reactive pozzalanic materials (similar to silica fume (Mehta 1983)). After burning, RHA maintains its original morphology, that is, it maintains its cellular, honeycomb morphology. Figure 1-1 shows a scanning electron microscope (SEM) image of RHA particles.

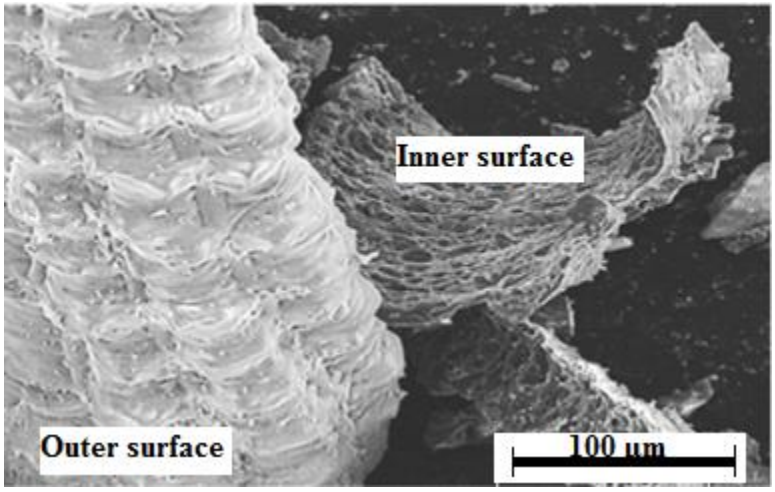

Figure 1-1. SEM image of RHA.

The Food and Agriculture Organization (FAO) of the United Nations (2009) reported that 20 percent of the volume of rice is rice husk and that approximately 690 million tons of rice is generated worldwide each year. Even though a large quantity of RHA is generated, there are few commercial applications for this product – RHA is considered a waste product. This leads to challenges with disposal and storage at power plants (Naiya et al. 2009). Current disposal methods include dumping into landfills. This can create long-term environmental problems. Broadening the application of RHA, as a sustainable resource, can increase economic value and reduce environmental impacts.

RHA has a high potential to be used as a SCM. The use of RHA in cementitious systems could lead to increased sustainability and may offer ecological, economic, energy, and durability benefits. Although potentially beneficial when used in the

cementitious systems, consumers often favor using SCMs that are readily available and do not negatively impact *workability*. The workability is defined in ASTM C125, *Standard Terminology Relating to Concrete and Concrete Aggregates*, as "the property determining the effort required to manipulate freshly mixed quantity of concrete without minimum loss of homogeneity." This workability issue with systems containing RHA is due to the cellular, honeycomb-like morphology of the RHA. This cellular, honeycomb-like morphology is shown in Figure 1-2.

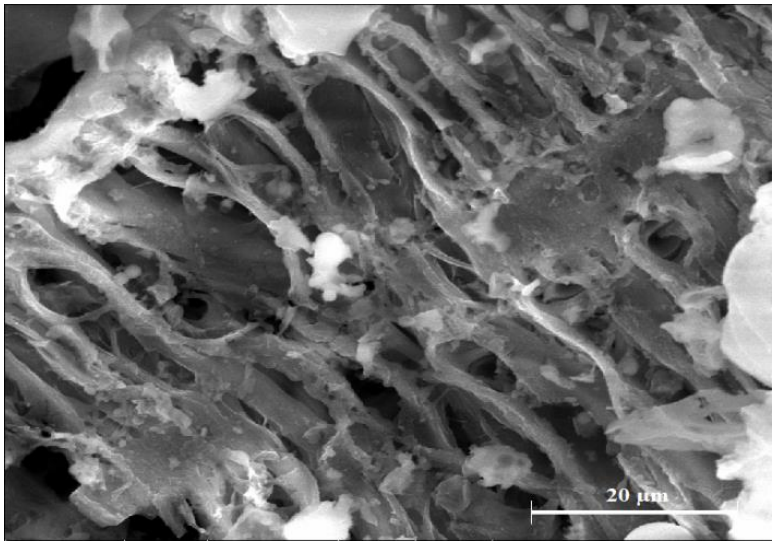

Figure 1-2. Cellular, honeycomb-like morphology of RHA.

The workability issue can be mitigated by reducing RHA particle size. This can be accomplished by mechanical pulverization. Previous studies (Stroeven et al. 1999; Bui et al. 2005) investigated the effects of RHA particle size on concrete performance and reported that smaller RHA particle sizes result in an increased cement hydration reaction rates, reduced $Ca(OH)_2$ content in the hydrated paste, improved flow, earlier strength gain, and improved durability. These improvements are believed to be a result of the breakdown of the cellular, honeycomb-like morphology. Van Tuan (2011) suggested that the appropriate mean particle size of RHA to make a concrete ranges from 5.6 to 9.0 µm. The most common procedure in reducing RHA particle size into these sizes is with ball-

and vibratory milling. However, this process is reported to consume significant time and energy (Chandrasekhar et al. 2002; Datta and Rajamani 2002).

Due to the inefficiencies in mechanical pulverization, this work presents the development of an alternative method to reduce RHA particle size and eliminate the cellular, honeycomb-like morphology, that is, a chemical transformation process.

1.3 OBJECTIVE AND SCOPES

The main objective of this dissertation is to develop a new chemical transformation process to reduce RHA particle size to the target size of 5.6 to 9.0 μm and also break down RHA cellular, honeycomb-like morphology. Specifically, this dissertation assesses the feasibility of using chemically transformed RHA (t-RHA) on the fresh and hardened characteristics of cementitious systems and assesses effects of mixing on systems containing t-RHA.

1.4 ORGANIZATION OF DISSERTATION

The dissertation is organized using a manuscript document format. There are eight chapters in this dissertation. The first chapter is this introduction. Chapters 2 through 7 include six manuscripts. Chapter 8 includes a summary and discusses needed future research. Each manuscript is a stand-alone document and addresses a specific issue related to the chemical transformation process and its influence on cementitious system performance. Following is a brief explanation of the chapters in the dissertation.

- Chapter 2 (manuscript 1) presents the development of the chemical transformation process of RHA morphology. The particle size analysis, observation of the morphology, and silicate ion concentration in solution of the t-RHA slurry are assessed. This manuscript follows a format of the American Concrete Institute (ACI) Materials Journal.

- Chapter 3 (manuscript 2) reports on the hydration and phase formation of blended cementitious systems incorporating t-RHA. The ion concentrations as a function of time, degree of saturation solubility, and solid phase composition of RHA blended cementitious systems are assessed. This manuscript follows a format of Cement and Concrete Composites Journal.
- Chapter 4 (manuscript 3) presents the performance characteristics of blended cementitious paste and mortar systems incorporating t-RHA. The characteristics of the t-RHA cementitious systems reported include the early-age and hardened characteristics of blended systems. This manuscript follows a format of the Cement and Concrete Composites Journal.
- Most standard specifications include limits on mixing of PC concrete systems. To better understand the influence of mixing variables on the characteristics of RHA systems, research was needed to assess the influence of mixing variables on PC systems. Chapters 5 and 6 (manuscripts 4 and 5) present results on the laboratory evaluation of the effects of mixing time and mixer revolution counts on the early-age and hardened characteristics of portland cement paste and mortar systems. Both manuscripts follow a format of ACI Materials Journal.
- Chapter 7 (manuscript 6) presents results of the laboratory evaluation of the effects of mixing time and mixer revolution counts on the fresh and hardened characteristics of RHA blended cementitious systems. The different RHA systems evaluated include AR-RHA, t-RHA, and AR-RHA+retarder (AR-RHA+R). This manuscript follows a format of the ACI Materials Journal.
- Chapter 8 presents a summary and recommendations for future research.

1.5 REFERENCE

Bui, D. D., J. Hu, and P. Stroeven (2005). "Particle size effect on the strength of rice husk ash blended gap-graded portland cement concrete." *Cem. & Con. Comp.* **27**(3): 357-366.

Chandrasekhar, S., P. N. Pramada, P. Raghavan, K. G. Satyanarayana, and T. N. Gupta (2002). "Microsilica from rice husk as a possible substitute for condensed silica fume for high performance concrete." *J. Mater. Sci. Letters* **21**(16): 1245-1247.

Datta, A., and R. K. Rajamani (2002). "A direct approach of modeling batch grinding in ball mills using population balance principles and impact energy distribution." *Inter. J. Mineral Processing* **64**(4): 181-200.

Food and Agriculture Organization of the United Nations (2009). FAO statistical databases.

Hutchins, M. J., and J. W. Sutherland (2008). "An exploration of measures of social sustainability and their application to supply chain decisions." *Journal of Cleaner Production* **16**(15): 1688-1698.

Mehta, P. K. (1983). "Pozzolanic and cementitious by-products as mineral admixtures for concrete - a critical review." *ACI SP*. **79**: 1-46.

Mehta, P. K. (2004). *High-performance, high-volume fly ash concrete for sustainable development*. Intern. Workshop Sustain. Develop. Concr. Tech., Beijing, China, Iowa State University.

Mehta, P. K., and P. J. M. Monteiro (2006). *Concrete: Structure, properties, and materials*. New York, McGraw-Hill.

Naiya, T. K., A. K. Bhattacharya, and S. K. Das (2009). "Adsorptive removal of Cd(II) ions from aqueous solutions by rice husk ash." *Env. Prog. Sustain. Energy* **28**(4): 535-546.

Stroeven, P., D. D. Bui, and E. Sabuni (1999). "Ash of vegetable waste used for economic production of low to high strength hydraulic binders." *Fuel* **78**(2): 153-159.

van Tuan, N., G. Ye, K. van Breugel, and O. Copuroglu (2011). "Hydration and microstructure of ultra high performance concrete incorporating rice husk ash." *Cem. Con. Res.* **41**(11): 1104-1111.

2 CHEMICAL TRANSFORMATION OF RICE HUSK ASH MORPHOLOGY

ABSTRACT

Rice husk ash (RHA) has significant potential to be used as a supplementary cementing material (SCM). However, RHA contains a cellular, honeycomb-like morphology of amorphous silica and this morphology results in high water absorption. Due to this morphology, the use of RHA in concrete results in reduced workability and higher water demands. Reduced workability and higher water demands can be mitigated by using smaller RHA particles. These smaller particles can be obtained by mechanical grinding. However, this grinding requires significant energy. This paper presents a novel method to transform the RHA morphology using a chemical transformation process; specifically, an alkali transformation method. Results indicate that the process can effectively reduce RHA particle size, and eliminate the cellular and honeycomb-like morphology.

Keywords: Rice Husk Ash, Chemical Transformation, Solution, Alkali, Particle Size, Silicate ions

Submitted to
ACI Material Journal

2.1 INTRODUCTION

2.1.1 *Rice Husk Ash*

Supplementary cementing materials (SCMs) are commonly used in the cement and concrete industries, added either separately in the concrete mixer or in blended cements. The use of SCMs can be a viable solution to improve the sustainability of systems made with portland cement (PC), adding ecological, economical, and environmental benefits. The use of SCMs in concrete systems is ubiquitous and includes fly ash, blast-furnace slag, and silica fume.

Rice husk ash (RHA) is an agricultural residue obtained from the combustion process of rice husks for energy production. Prior to burning, rice husks consist of approximately 20% to 23% by weight of the overall rice plant (including rice grain and husks) (Della *et al.* 2002, Rodrigues 2003). The pre-burnt composition of the rice husks consists of approximately 75% to 80% of organic substance and 15% to 20% of inorganic substance. The burning is an efficient way to remove the organic substance while generating energy, leaving behind an inorganic ash consisting of mostly silica. Mehta (1994) reported that after burning no other agricultural residue generates a higher quantity of ash than RHA. Nair *et al.* (2008) reported that a proper burning process of rice husks generates ash with high amorphous silica contents. The resultant ash size, morphology, and specific surface are dependent on the burning conditions. Nair *et al.* (2008) also reported the optimal content of amorphous silica in RHA occurs when burnt at approximately 932 to 1292˚F [500 to 700˚C]. Burning of rice husk in this range typically yields a porous, cellular ash, containing amorphous silica up to approximately 90% (Yu *et al.* 1999). Burnt rice husk, i.e. RHA, maintains its original cellular morphology.

The Food and Agriculture Organization (FAO) of the United Nations (2009) reported that approximately 77 million tons (70 million tonnes) of the RHA is produced worldwide each year. Even though a large amount of RHA is produced, the commercial applications to utilize this material have been reported to be limited (Da Costa *et al.*

2000, Meyer 2009). This can lead to serious challenges with disposal (He *et al.* 2013). Da Costa *et al.* (2000) and Rodriguez de Sensale (2010) reported that the most common method of disposing RHA is dumping in landfills or into rivers. These disposal methods can create environmental problems and are not sustainable over the long term. In addition, after the burning of rice husks, the smaller RHA particles can be suspended in the air, creating air pollution. Because of these environmental challenges, broadening the utilization of RHA would be beneficial.

Fly ash is one of the most widely used SCMs. However, the availability of fly ash from coal power plants is decreasing due to lower natural gas prices and stricter air-emission regulations. Pratson *et al.* (2013) estimated that lower natural gas prices will result in a 9% reduction in coal burning for energy and stricter air-emission regulations will result in another 56% reduction in the coal burning. This reduction will result in a significant reduction in fly ash availability. Hence, finding an alternative resource of SCM that is as "user-friendly" and provides similar long-term durability benefits as fly ash is needed.

RHA has the potential to be used as a SCM and may be used to replace fly ash. It is reported that the pozzolanic activity in RHA systems depends on three parameters: 1) the amorphous silica content, 2) the specific surface area, and 3) the particle size distribution (Hanafi *et al.* 1980, Payá *et al.* 2001, Wang *et al.* 2001, Della *et al.* 2002, Bui *et al.* 2005). RHA systems having higher amorphous silica contents, larger surface areas, and particle size distributions with smaller particles result in higher pozzolanic activity. Taylor (1997) reported that RHA blended systems can result in similar characteristics as silica fume blended systems. The author also reported that the RHA system can exhibit higher pozzolanic activity than the silica fume system. Higher pozzolanic activity of cementitious systems containing RHA can lead to enhanced hydration reactions, increased later-age strength, reduced porosity (especially at the interfacial transition zone (ITZ)), and improved durability (Giaccio *et al.* 2007, Rodríguez de Sensale 2010, van Tuan *et al.* 2011, Sata *et al.* 2012). Although RHA seems to have a high potential for use

in cement and concrete systems, there are existing challenges when using RHA that must be overcome before this material will be widely accepted as a SCM.

The use of RHA in cement and concrete is not widespread because RHA typically has very high specific surface areas ranging from 97,640 to 244,100 ft^2/lb [20 to 50 m^2/g] [compared to Type I portland cement which is less than 4880 ft^2/lb (1 m^2/g)]. As discussed, RHA also contains a cellular, honeycomb-like morphology (Zhang *et al.* 1996, Bapat 2012). This high surface area and cellular, honeycomb-like morphology leads to high water-absorption characteristics. Although the high water-absorption of RHA can be useful for some applications such as making silica gel (Kalapathy *et al.* 2000), metal absorbents (Tiwari *et al.* 1995, Elouear *et al.* 2008), and CO_2 capturing (Bhagiyalakshmi *et al.* 2010), RHA having these characteristics when used in fresh concrete mixtures results in decreased workability and increased water demands. These make the fresh concrete mixtures more difficult to place and consolidate. Although the negative impacts can be easily mitigated by increasing the water content in the mixture proportions, the strength and durability of hardened concrete having higher water contents is consequently reduced. As a result, contractors are reluctant to use RHA because of reduced workability and owners are reluctant to use RHA because of potentially lower strengths and reduced durability. This is especially the case when alternative SCMs are locally available.

In addition to the high water-absorption of RHA, it is known that the use of SCMs can result in delayed compressive strength gain due to the slower pozzalanic reactions (Zhang and Malhotra 1996, Thomas *et al.* 1999, Mehta and Monteiro 2006). Delayed compressive strength reduces the likelihood that contractors will use RHA, as they will have to keep forms on for longer periods before stripping, thereby increasing construction cost. Reinschmidt and Trejo (2006) reported that contractors can realize significant benefits by decreasing construction duration. The use of cementitious systems that can provide higher early strengths is therefore more valuable to the contractors than systems that provide lower early strengths. Because RHA has been reported to result in lower early strengths, the likelihood of the contractors accepting RHA as a commonly used SCM is again limited.

Many researchers have investigated the effect of RHA particle size on the concrete performance and reported that using smaller particles can result in the elimination of the cellular, honeycomb-like morphology (Sugita *et al.* 1992, Bui 2001, Bui *et al.* 2005, Cordeiro *et al.* 2009, Cordeiro *et al.* 2011). Eliminating the cellular, honeycomb-like morphology can lead to reduced water absorption characteristics. As a result, fresh concrete mixtures having smaller RHA particles will exhibit better workability and lower water demands than mixtures having larger RHA particles. To obtain smaller RHA particles, RHA has been mechanically ground (e.g., using a ball-mill) (Bui *et al.* 2005). Hence, using mechanical grinding to reduce RHA particle size could make RHA a more widely used SCM.

Although the challenges of the RHA cellular and honeycomb-like morphology seem to be mitigated by using mechanical grinding, this process is reported to be inefficient because significant grinding energy is required to achieve smaller RHA particles. van Tuan *et al.* (2011) reported that reducing the RHA particle size can be done by extending grinding periods, but this leads to higher energy use and reduced production output. Habeeb and Mahmud (2010) investigated the effect of mechanically grinding period on the average RHA particle size and reported that reducing the average RHA particle sizes from 0.00242 to 0.00123 in [63.4 to 31.3 μm] can be achieved after grinding RHA for 90 minutes [2.25% per minute]. However, to grind these average RHA particle sizes from 0.00123 to 0.00045 in [31.3 to 11.5 μm], the grinding required longer time up to 180 minutes [1.51% per minute]. Reducing RHA particles to moderate sizes has been reported to be relatively economical; however, reducing RHA particle sizes to sizes that can be used in cementitious systems requires significantly more energy and has been reported to be uneconomical (van Tuan 2011). In addition to the significant grinding energy, maintenance from wear of the mills and grinding components is reported to be cost-prohibitive (Halim 2008). van Tuan *et al.* (2011) reported that although extending grinding periods leads to higher energy use and reduced production output, this can be overcome by using higher capacity grinders. However, this leads to increased capital and maintenance costs in the manufacturing process (Mehta 1994).

2.1.2 *Chemical Transformation Method*

Further investigations are needed to identify more economical and more efficient alternatives to mechanical grinding of RHA such that this material can become a more widely used SCM. Earlier studies (Kamath and Proctor 1998, Kalapathy *et al.* 2000, Kalapathy *et al.* 2002) on the chemical treatment of RHA indicate that the amorphous silica in the RHA can be transformed into soluble silicate ions using an alkali extraction process. The objective of these studies was to produce pure silica gel from RHA. The alkali extraction process was prepared by mixing RHA that consists of 61% silica and 36% carbon with 1M NaOH solution for 1 hour. The temperature of the solution was controlled at 212˚F (100˚C). The RHA to water ratio was at 1:6 by weight. After mixing, the solution was filtered using a filter paper. Test results indicated that using this process could produce $Na_2O \bullet xSiO_2$ (sodium silicate) solution from RHA.

The alkali extraction method presented by Kamath and Proctor (1998) and Kalapathy *et al.* (2000, 2002) could be useful for reducing RHA particle size and eliminating the cellular, honeycomb-like morphology. However, more research is needed to investigate the extraction method for transforming RHA to use in cementitious systems. This paper investigates the chemical transformation processes, specifically, the alkali transformation process. The chemically transformed RHA product reported in this paper will be referred to as t-RHA. The chemical process to transform the RHA morphology evaluated herein used sodium hydroxide (NaOH) and potassium hydroxide (KOH). The chemical transformation reactions are assumed as:

$$xSiO_2 + zNaOH \rightarrow (Si_xO_y)^{4x-2y} + zNa^+ + z/2\,H_2O \qquad \text{Eq. (2-1)}$$

$$xSiO_2 + zKOH \rightarrow (Si_xO_y)^{4x-2y} + zK^+ + z/2\,H_2O \qquad \text{Eq. (2-2)}$$

where *x*, *y*, and *z* is a number in moles.

Kamath and Proctor (1998) and Kalapathy *et al.* (2000, 2002) reported that the chemical extraction in their studies resulted in sodium silicate solution. However, it can

be assumed that the amorphous silica in the RHA reacts with NaOH or KOH solution and generates ionic species – i.e., $Si_xO_y^{4x-2y}$ (silicate) anions and Na^+ (sodium) or K^+ (potassium) cations in solution. These chemical reactions in **Eqs. 2-1** and **2-2** are believed to be one factor that results in a reduction of t-RHA particle size and the elimination of the cellular, honeycomb-like morphology.

The objective of this paper was to assess the efficiency of the chemical transformation. As discussed, if the RHA particles become smaller, reduced workability and higher water demands will be mitigated. Hence, the efficiency here is assessed by a reduction of the average RHA particle size. Smaller t-RHA particles are contributed to the more efficient process. It should be noted that the studies of the hydration process and performance characteristics of the t-RHA blended cementitious systems are presented in the other publications (Prasittisopin and Trejo 2014; Trejo and Prasittisopin 2014).

2.2 RESEARCH SIGNIFICANCE

Although RHA has the potential to be used as a SCM, it is not widely used because RHA contains a cellular, honeycomb-like morphology. The use of RHA in concrete results in increased water demands and reduced workability of concrete mixtures. Increased water demands and reduced workability limit the use of RHA in concrete, especially when alternative SCMs are locally available. Previous studies reported that using a mechanical grinding of RHA results in reduced particle size and elimination of the cellular, honeycomb-like morphology. This leads to reduced water demands of fresh mixtures. However, this grinding process is not efficient. This work assesses a chemical method that transforms the RHA morphology. The average RHA particle size, RHA morphology, and silicate ion concentration in solutions were evaluated to assess the feasibility of the chemically transforming RHA to make it a more “user-friendly” SCM.

2.3 MATERIALS AND METHODS

2.3.1 *Materials*

As-received RHA (AR-RHA) was procured from a power plant in Lake Charles, LA. Its chemical composition is shown in **Table 2-1**. The average particle size of the AR-RHA is 0.0076 in (192 μm) with a standard deviation (SD) of 0.00012 in (3.15 μm). **Fig. 2-1** shows the X-Ray Diffraction (XRD) patterns of AR-RHA. The broad peak indicates that the AR-RHA mainly consists of amorphous silica. ASTM Type II de-ionized (DI) water [0.4 MΩ·in (1.0 MΩ·cm) at 77°F (25°C)] was used for all mixtures and experiments. Pellet NaOH and KOH were American Chemical Society (ACS) grade. Polyvinyl alcohol (PVA) powder with molecular weight of 1750 ± 50 atomic mass units was procured and used as dispersing agent.

Table 2-1. Chemical composition of AR-RHA

Composition	(wt %)*
SiO_2	89.65 - 96.90
C	2.09 - 7.59
Al_2O_3	0.006 - 0.039
Fe_2O_3	0.006 - 0.052
CaO	0.48 - 0.81
MgO	0.13 - 0.53
SO_3	0.018 - 0.24
Na_2O	0.018 - 0.18
K_2O	1.74 - 2.69
Ti_2O_3	0.003 - 0.020
P_2O_5	0.74 -1.23
Mn_3O_4	0.00 - 0.20

*Provided by manufacturer

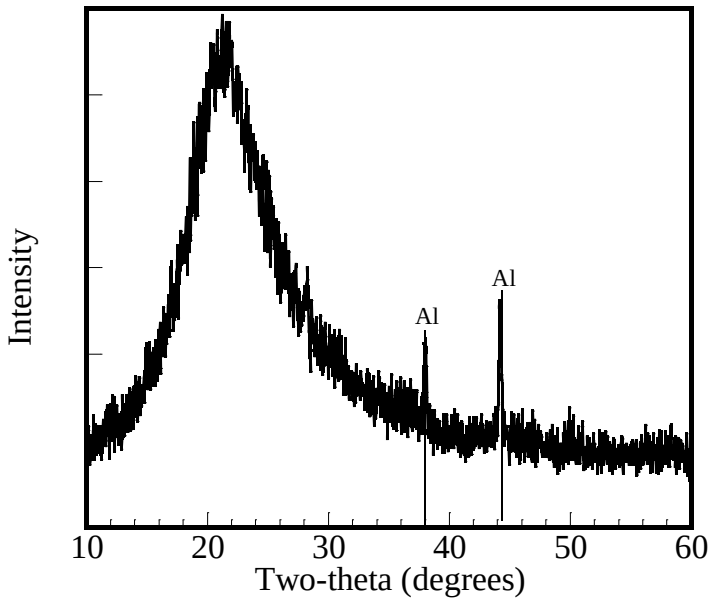

Fig. 2-1–XRD patterns of AR-RHA.

2.3.2 *Preparation of Chemical Morphological Transformation Method*

Chemical transformation processes assessed in this study included NaOH and KOH solutions to produce silicate anions. The t-RHA slurry was prepared by mixing AR-RHA with different concentrations of NaOH and KOH solutions and for different mixing times using a laboratory magnetic stirrer at a mixing speed of 400 rpm. The weight ratio of AR-RHA to NaOH solution was 1:4. Although the studies by Kalapathy *et al.* (2000, 2002) used heat to increase the efficiency of the alkali extraction process, no additional heat was used in this work due to the concerns regarding energy-efficiency of the transformation process. Mixing in this study was performed at 73˚F (23˚C).

2.3.3 *Characterization Methods*

2.3.3.1 Particle Size Analysis

The average particle size of t-RHA was evaluated using a particle size analyzer. RHA mixed with NaOH and KOH solutions at different concentrations and mixing times.

Concentrations included 0, 1, 2, and 4M and mixing times included 0, 0.5, 1, 2, 3, and 8 hours were assessed for the average particle size. The temperature was controlled at 73˚F (23˚C) throughout the experiment. Test results are based on triplicate tests.

It will be discussed later that the most efficient process or smallest resultant RHA particle size is mixing RHA with 2M NaOH solution. This study evaluates the effect of the PVA at 1%, 2%, and 3% by weight of 2M NaOH solution on the resultant average particle size. The addition of PVA was considered due to the concerns of agglomeration of the smaller t-RHA particles.

2.3.3.2 RHA Morphology Assessment

To investigate the effect of the chemical transformation process of RHA, the morphology of the RHA was observed using the Scanning Electron Microscope (SEM). After mixing the RHA with the chemical solution, the t-RHA slurry was filtered from the solution using a No. 40 filter paper and a vacuum pump. The filtrated t-RHA was then soaked with ethyl alcohol and oven-dried at 230˚F (110˚C) for approximately 4 hours to remove water, prior to the SEM analysis.

2.3.3.3 Silicate Ion Concentration

It will be noted later that using NaOH to transform RHA is more efficient than using KOH. This study assesses the silicate ion concentrations to determine the efficiency of alkali transformation process using NaOH solution. The silicate ion concentration in solution was assessed by preparing t-RHA slurry at different concentrations of NaOH solution (1, 2, and 4M) and different mixing times (0, 0.5, 1, 2, 3, and 8 hours). The t-RHA slurry was decanted from the mixing beaker and filtered using a vacuum pump and No. 40 filter paper. 0.034 fl oz (1 ml) of filtered solution was diluted with DI water into 0.34-fl oz (10-ml) solution. The diluted solution used for analyzing silicate ion concentration. The silicate ion concentration was evaluated following the dissolved silica by photometric method section in ASTM C289, *Standard Test Method for Potential*

Alkali-Silica Reactivity of Aggregates (Chemical Method). The DI water was used as a background correction.

2.3.3.4 Statistical Analysis

Two-sample t-test and analysis of variances (ANOVA) analyses were performed to evaluate the means of samples with two groups and more than two groups, respectively. The Shapiro-Wilk test was used to determine if data were normally distributed and the Levene's test was used to determine if the data sets had equal variance prior to the analyses. The statistical hypotheses for the analyses are defined as:

$$\text{Null hypothesis } (H_0): \mu_1 = \mu_2 = \ldots = \mu_a \qquad \text{Eq. (2-3)}$$

$$\text{Alternative hypothesis } (H_a): \mu_i \neq \mu_j \text{ for some } i \neq j \qquad \text{Eq. (2-4)}$$

The 95% confidence interval was used in these analyses. If the H_0 is rejected (p-value ≤ 0.05), it is concluded that there is a statistically significant effect at the 5% level between the means of the different group populations. Alternatively, if the H_0 is not rejected (p-value > 0.05), it is concluded that there is no statistically significant effect at the 5% level between the means of the different group populations.

2.4 RESULTS AND DISCUSSION

2.4.1 *Particle Size Analysis*

This particle size analysis section consists of two parts: 1) effect of alkali and 2) effect of PVA addition.

2.4.1.1 Effect of Alkali

Figs. 2-2a and **2-2b** show the effect of mixing time (0.5, 1, 2, 3, and 8 hours) on the average particle size of t-RHA particles mixed with different concentrations (0, 1, 2, and 4M) of NaOH and KOH solution, respectively. Results indicate that the average

particle size of the AR-RHA system mixed with NaOH solution (**Fig. 2-2a**) decreases with increasing mixing times of up to 3 hours. The average particle size of the AR-RHA mixed with KOH solution (**Fig. 2-2b**) decreased with increasing mixing times of up to 8 hours. The process that results in the smallest average particle size at shortest time is assumed here to be the most efficient process. Thus, the average particle size of t-RHA is smallest when mixed with 2M NaOH solution for 3 hours. The average particle size can be reduced from approximately 0.0076 to 0.0011 in [192 to 28 μm] or 3.8% reduction per minute. As discussed, using mechanical grinding reported by Habeeb and Mahmud (2010) results in the reduction of the resultant particle size by approximately 1.5% to 2.3% per minute. Thus, the chemical transformation process can be an alternative to reduce RHA particle size.

It should be noted in **Figs. 2-2a** and **2-2b** that the RHA mixed with NaOH or KOH solution at early mixing periods (e.g., 0 to 1 hour) results in a faster reduction of the particle size; however, the RHA mixed at longer mixing periods (e.g., from 2 to 3 hours) results in a slower reduction of the particle sizes. As discussed, reducing RHA particles to moderate sizes requires shorter grinding periods; however, reducing RHA particle sizes to even smaller sizes requires longer grinding periods.

Results also show that the average particle size of the t-RHA increases with increasing mixing times from 3 to 8 hours when mixed with the 1M NaOH, 2M NaOH, and 1M KOH solution. The difference in the average particle size is statistically significant (two sample t-test with p-value = 0.013, 0.049, and 0.01, respectively). It has been reported that the pH level of solution or the NaOH and KOH concentration herein strongly affects the agglomeration (Maskara and Smith 1997). It is also reported that silica surfaces possess negative charges over the typical pH range of solution (Double 1983, Sasaki 1993). When the pH levels are more than 12, the roughness of the silica surfaces is reported to increase and this may consequently influence the agglomeration (Maskara and Smith 1997). Therefore, the increase of the t-RHA particle size is likely due to agglomeration of the smaller particles. However, this agglomeration effect is limited when the concentrations of NaOH and KOH solution are high (i.e., 4M NaOH,

2M KOH, and 4M KOH). Minimizing the agglomeration of the RHA particles could make the chemical transformation process more efficient.

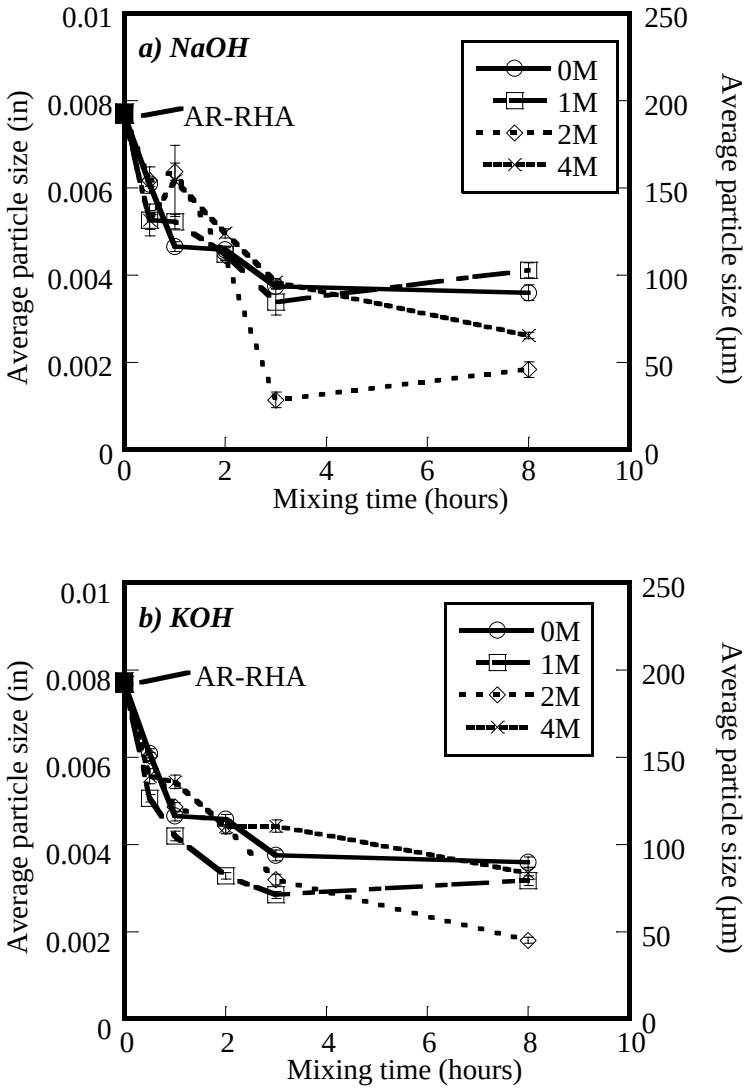

Fig. 2-2–Plots of average particle size of RHA versus mixing time at the different contents of *a)* NaOH and *b)* KOH.

2.4.1.2 Effect of PVA Addition

The chemical transformation process indicates that mixing time greater than 3 hours can lead to increased agglomeration. To minimize this agglomeration, the t-RHA systems

containing a dispersing agent, PVA, were also assessed. PVA has been reported to be both a dispersant (Ahmed *et al.* 2009) and a cross-linking agent (Nakane *et al.* 1999). Adding small amounts of PVA should result in the PVA dispersing the t-RHA particles. Higher PVA amounts can lead to polymer entanglement, and consequently increasing the agglomeration (this is typical behavior for polymeric materials). Because the optimal addition amounts are not known here, the researchers evaluated the effects of PVA addition (1%, 2%, and 4% by weight of NaOH) on the average particle size of the t-RHA systems. As discussed, the process using 2M NaOH solution is the most efficient process; therefore, this test evaluated only the process using 2M NaOH solution.

The effect of mixing time on average particle size of t-RHA for different PVA contents is shown in **Fig. 2-3**.

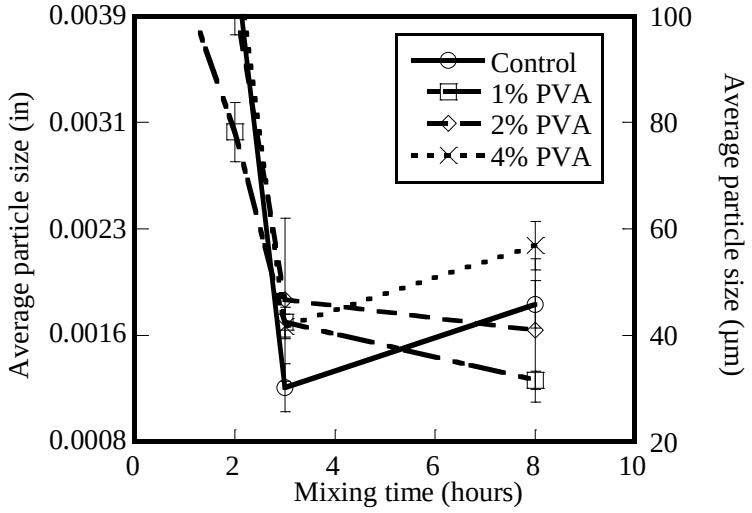

Fig. 2-3–Plot of average particle size of RHA mixed with 2M NaOH solution versus mixing time with different PVA contents.

The control system here is defined as the t-RHA mixed with 2M NaOH solution (no PVA). Results indicate that the average particle size of the t-RHA system mixed with 2M NaOH+1% PVA solution for 8 hours is approximately 26% smaller than the system mixed for 3 hours (reduced from 0.0017 to 0.0012 in [42.45 to 31.57 μm]) (two sample t-

test with p-value = 0.005). These results indicate that adding 1% PVA to the 2M NaOH solution can result in better dispersion of the t-RHA particles. Results from the t-RHA system mixed with 2M NaOH+2% PVA solution indicate no significant difference between the system mixed for 3 hours and 8 hours (two sample t-test with p-value = 0.653). The similar average particle size for the t-RHA system mixed with 2M NaOH+2% PVA solution is likely attributed to the fact that smaller t-RHA particles remain dispersed and some of the PVA is entangled. However, increased mixing time of the t-RHA systems having 2M NaOH+4% PVA results in increased average particle size by 11% [from 0.0016 to 0.0018 in (41.67 to 46.39 μm)] (two sample t-test with p-value = 0.007). It is believed that the further increase of the average t-RHA particle size occurs due to further PVA entanglement. Based on test results, mixing the t-RHA with 2M NaOH+1% PVA solution at 3 hours results in the smallest average particle size and this process is used in this study.

Figs. 2-4a and **2-4b** show micrographs of the t-RHA mixed with 2M NaOH solution (without PVA) for 3 hours and the t-RHA mixed with 2M NaOH+1% PVA solution for 3 hours, respectively. Micrographs were observed using a light-emitting diode (LED) microscope. The micrograph in **Fig. 2-4a** shows that the smaller t-RHA particles are suspended in the NaOH solution but the particles are not randomly distributed – that is, the particles are agglomerating in the lower right corner of the micrograph to form larger particles. This is likely due to the attractive forces between the smaller particles. As expected, the average particle size would become larger due to this agglomeration. In **Fig. 2-4b**, the image shows that when PVA is present in the system, the t-RHA particles remain dispersed and form cross-linking bridges between t-RHA and PVA particles. Although the average particle size of the t-RHA+PVA system [0.0017 in (42.5 μm) in **Fig. 2-3**] is larger than the t-RHA system without PVA [0.0011 in (28.43 μm) in **Fig. 2-3**], the t-RHA+PVA system is preferred because the PVA can reduce the agglomeration effect.

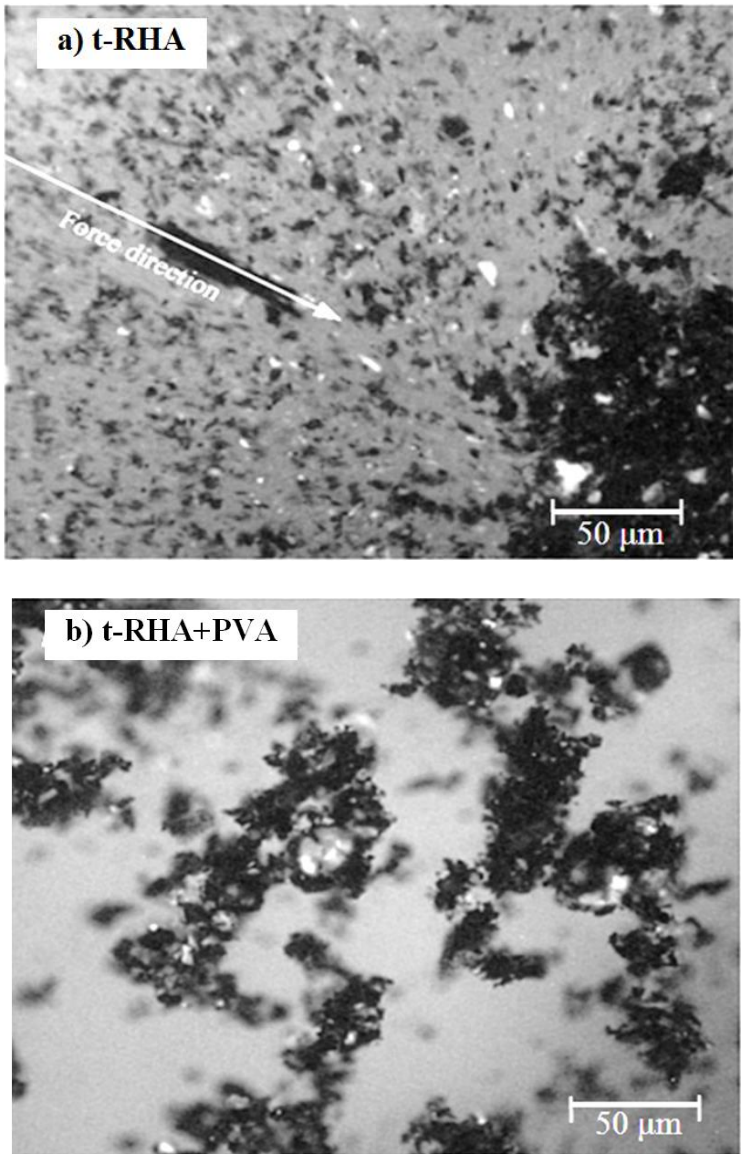

Fig. 2-4–Micrographs of t-RHA mixed with *a)* 2M NaOH solution and *b)* 2M NaOH+1% PVA solution for 3 hours.

2.4.2 *RHA Morphology*

Figs. 2-5a and **2-5b** show SEM images of the AR-RHA particles at different magnifications. The image of the AR-RHA particles exhibits high surface area and contains the cellular, honeycomb-like morphology. As discussed, this leads to high water

absorption characteristics. Water is believed to be absorbed on the surface and in the cellular morphology of AR-RHA due to surface tension and capillary forces. The SEM images of the t-RHA morphology for different magnifications are shown in **Figs. 2-5c** and **2-5d**. The cellular, honeycomb-like morphology is significantly reduced or eliminated for the t-RHA. Using the chemical transformation method not only reduces the average particle size for the t-RHA, but also eliminates much of the cellular, honeycomb-like morphology, associated with reduced workability and higher water demands.

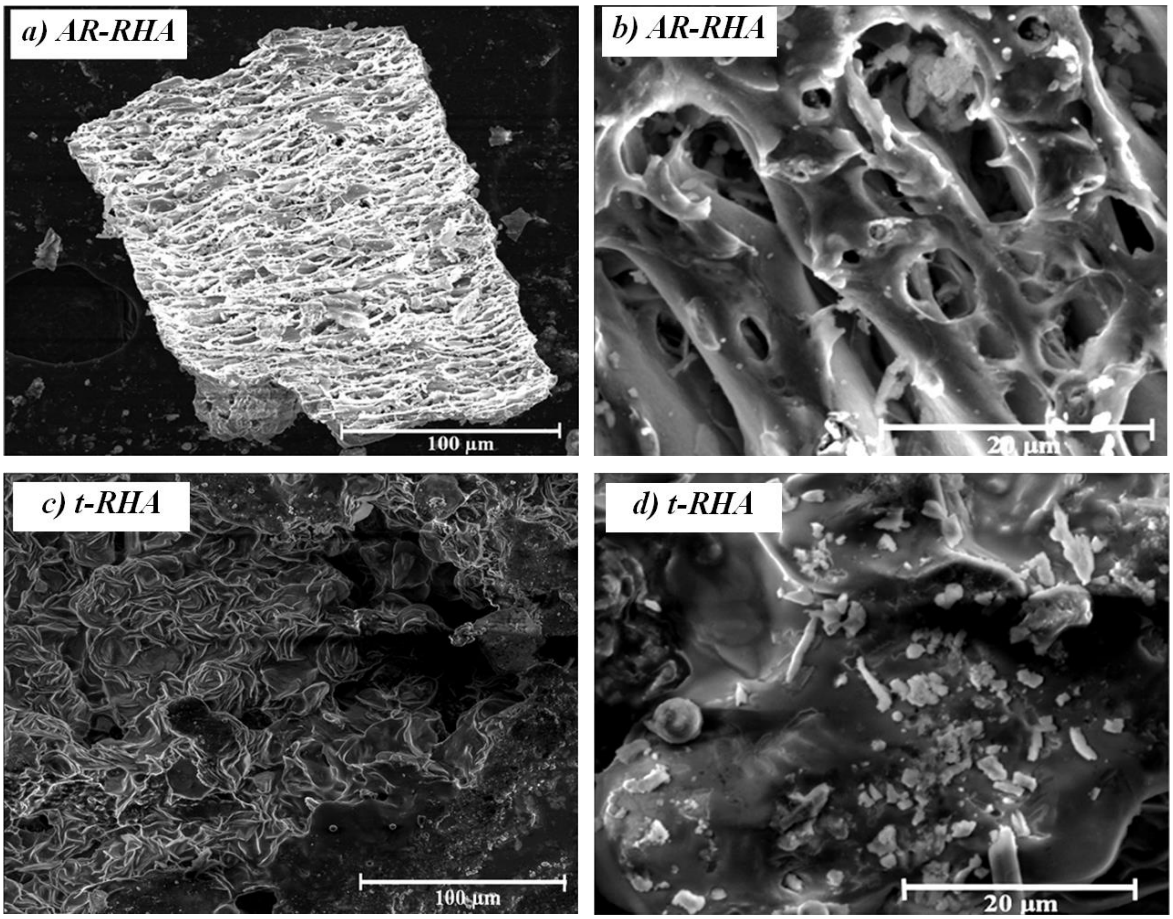

Fig. 2-5–SEM images of *a)* and *b)* AR-RHA; and *c)* and *d)* t-RHA.

2.4.3 *Silicate Ion Concentration*

Fig. 2-6 shows the silicate ion concentration in the t-RHA solution as a function of mixing time (0, 0.5, 1, 2, 3, and 8 hours) mixed with different NaOH concentrations (1, 2, and 4M). Higher concentrations of silicate ions in solution indicate that the silicate ion in the AR-RHA is being reacted at faster rates. Results indicate that the t-RHA system mixed with 2M NaOH solution has higher silicate ion concentration than the systems mixed with 1M and 4M NaOH solution. The silicate ion concentration of the t-RHA mixed with 2M NaOH solution is approximately 11.3 mmol/ft^3 (0.4 mmol/liter) when the mixing time increases from 0 to 3 hours. Results also indicate that the silicate ion concentration of the t-RHA mixed with 2M NaOH solution is significantly reduced when the mixing time increases from 3 to 8 hours. As discussed and shown in **Fig. 2-2a**, this is believed to be a result of the t-RHA particles agglomerating. As the t-RHA particles agglomerate, these larger particles can no longer pass the No. 40 filter paper [pore size of 0.0003 in (8 μm)]. Because the highest concentration of silicate ions was observed when the RHA is mixed with 2M NaOH solution for 3 hours, this process is considered to be the optimal process for the chemical transformation of RHA in this study.

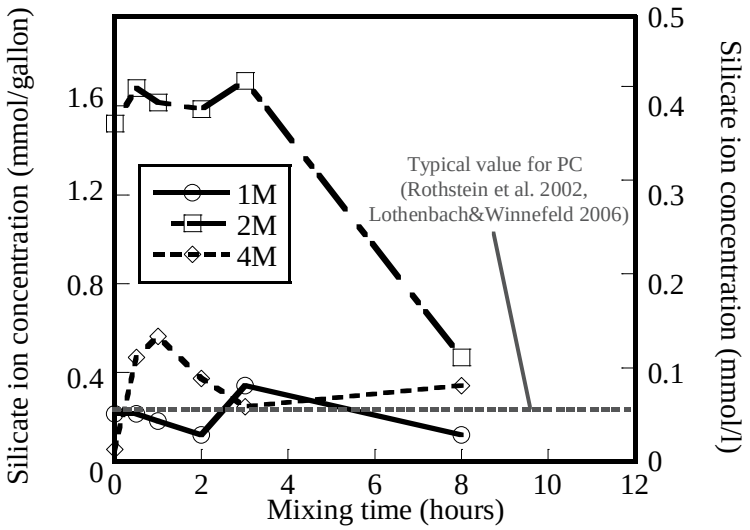

Fig. 2-6–Concentration of silicate ion versus mixing time for different NaOH concentrations and typical concentration of silicate ion of PC (Rothstein et al. 2002, Lothenbach and Winnefeld 2006).

Fig. 2-6 also shows that the typical silicate ion concentration of a PC system at early ages is approximately 0.23 to 0.26 mmol/gallon [0.06 to 0.07 mmol/liter] (Rothstein *et al.* 2002, Lothenbach and Winnefeld 2006). The silicate ion concentration of the t-RHA system mixed with 2M NaOH solution for 3 hours is approximately 5 to 6 times higher than the typical values reported by Rothstein *et al.* (2002) and Lothenbach and Winnefeld (2006). The higher silicate ion concentration in the t-RHA solution could influence cement hydration of blended cementitious systems. This will be presented in the future on-going research (Prasittisopin and Trejo 2014, Trejo and Prasittisopin 2014).

2.5 CONCLUSIONS

A novel method to reduce RHA particle size and eliminate the cellular, honeycomb-like morphology using a chemical transformation process was assessed in this research. The results indicate that:

- The amorphous silica in AR-RHA reacts in alkali solutions.
- A transformation process consisting of 2M NaOH solution mixed with AR-RHA for 3 hours was the most efficient process assessed.
- The average particle size of the RHA transformed with the NaOH solution was approximately 0.0011 in (28 μm) [from 0.0076 in (192 μm)] after 3 hours of mixing.
- PVA when used at 1% acts as a dispersing agent.
- The cellular, honeycomb-like morphology of the AR-RHA particles was eliminated using the chemical transformation process.

Results indicated that the challenges associated with the cellular, honeycomb-like morphology of RHA can be overcome by chemically transforming the RHA. Although further studies are needed to assess the effects of this transformation process on the hydration and performance characteristics of t-RHA blended cementitious system, the process shows promise in making AR-RHA more “user-friendly.” If this chemical

transformation process is feasible, AR-RHA may be more readily accepted as a viable SCM.

2.6 ACKNOWLEDGEMENTS

The authors express gratitude to Dr. Wenping Li, Agrilectric Companies, for providing the rice husk ash, Dr. Thomas Shellhammer, Department of Food Science and Technology, Oregon State University, for advising on the use of particle size analyzer, Kathy Motter of Institute for Water and Watersheds Collaboratory, Oregon State University, and Chang Li for assisting with the assessment of silicate ion concentration in solution.

2.7 REFERENCE

Ahmed, A., Clowes, R., Willneff, E., Ritchie, H., Myers, P., and Zhang, H. (2009), "Synthesis of Uniform Porous Silica Microspheres with Hydrophilic Polymer as Stabilizing Agent," *Indust. & Eng. Chem. Res.*, V. 49, No. 2, pp. 602-608.

Bapat, J. D., *Rice Husk Ash*, in *Mineral Admixtures in Cement and Concrete*, 2012, CRC Press: Boca Raton, FL, pp. 75-96.

Bhagiyalakshmi, M., Yun, L. J., Anuradha, R., and Jang, H. T. (2010), "Utilization of Rice Husk Ash as Silica Source for the Synthesis of Mesoporous Silicas and Their Application to CO_2 Adsorption through TREN/TEPA Grafting," *J. Hazard. Mater.*, V. 175, No. 1-3, pp. 928-938.

Bui, D. D., Rice Husk Ash as a Mineral Admixture for High Performance Concrete, 2001, Delft University of Technology, 122 pp.

Bui, D. D., Hu, J., and Stroeven, P. (2005), "Particle Size Effect on the Strength of Rice Husk Ash Blended Gap-Graded Portland Cement Concrete," *Cem. & Con. Comp.*, V. 27, No. 3, pp. 357-366.

Cordeiro, G., Toledo Filho, R., and Moraes Rego Fairbairn, E. (2009), "Use of Ultrafine Rice Husk Ash with High-Carbon Content as Pozzolan in High Performance Concrete," *Mater. Struct.*, V. 42, No. 7, pp. 983-992.

Cordeiro, G. C., Toledo Filho, R. D., Tavares, L. M., Fairbairn, E. d. M. R., and Hempel, S. (2011), "Influence of Particle Size and Specific Surface Area on the Pozzolanic Activity of Residual Rice Husk Ash," *Cem. Con. Comp.*, V. 33, No. 5, pp. 529-534.

Da Costa, H. M., Visconte, L. L. Y., Nunes, R. C. R., and Furtado, C. R. G. (2000), "The Effect of Coupling Agent and Chemical Treatment on Rice Husk Ash-Filled Natural Rubber Composites," *J. Appl. Polymer Sci.*, V. 76, No. 7, pp. 1019-1027.

Della, V. P., Kuhn, I., and Hotza, D. (2002), "Rice Husk Ash as an Alternate Source for Active Silica Production," *Mater. Letter*, V. 57, No. 4, pp. 818-821.

Double, D. D. (1983), "New Developments in Understanding the Chemistry of Cement Hydration," *Phil. Trans. R. Soc. Lond.*, V. A 310, No., pp. 53-66.

Food and Agriculture Organization of the United Nations, *FAO Statistical Databases*, 2009.

Giaccio, G., de Sensale, G. R., and Zerbino, R. (2007), "Failure Mechanism of Normal and High-Strength Concrete with Rice-Husk Ash," *Cem. Con. Comp.*, V. 29, No. 7, pp. 566-574.

Habeeb, G. A. and Mahmud, H. B. (2010), "Study on Properties of Rice Husk Ash and Its Use as Cement Replacement Material," *Mater Res*, V. 13, No. 2, pp. 185-190.

Halim, S. C., Application of Reactive and Partly Soluble Nanomaterials, in Department of Chemistry and Applied Biosciences, 2008, ETH Zurich.

Hanafi, S., Abo-El-Enein, S. A., Ibrahim, D. M., and El-Hemaly, S. A. (1980), "Surface Properties of Silicas Produced by Thermal Treatment of Rice-Husk Ash," *Thermochemical Acta*, V. 37, No. 2, pp. 137-143.

He, J., Jie, Y., Zhang, J., Yu, Y., and Zhang, G. (2013), "Synthesis and Characterization of Red Mud and Rice Husk Ash-Based Geopolymer Composites," *Cem. Con. Comp.*, V. 37, No., pp. 108-118.

Kalapathy, U., Proctor, A., and Shultz, J. (2000), "Silica Xerogels from Rice Hull Ash: Structure, Density and Mechanical Strength as Affected by Gelation pH and Silica Concentration," *J. Chem. Tech. & Biotech.*, V. 75, No. 6, pp. 464-468.

Kalapathy, U., Proctor, A., and Shultz, J. (2000), "A Simple Method for Production of Pure Silica from Rice Hull Ash," *Bioresor. Tech.*, V. 73, No. 3, pp. 257-262.

Kalapathy, U., Proctor, A., and Shultz, J. (2002), "An Improved Method for Production of Silica from Rice Hull Ash," *Bioresor. Tech.*, V. 85, No. 3, pp. 285-289.

Kamath, S. R. and Proctor, A. (1998), "Silica Gel from Rice Hull Ash: Preparation and Characterization," *Cereal Chem.*, V. 75, No. 4, pp. 484-487.

Lothenbach, B. and Winnefeld, F. (2006), "Thermodynamic Modelling of the Hydration of Portland Cement," *Cem. Con. Res.*, V. 36, No. 2, pp. 209-226.

Maskara, A. and Smith, D. M. (1997), "Agglomeration During the Drying of Fine Silica Powders, Part II: The Role of Particle Solubility," *J. Am. Ceram. Soc.*, V. 80, No. 7, pp. 1715-1722.

Mehta, P. K. (1994), "Rice Husk Ash - a Unique Supplementary Cementing Material," in *Proc. Intern. Advances in Concrete Tech.*, CANMET.

Mehta, P. K. and Monteiro, P. J. M. (2006), *Concrete: Structure, Properties, and Materials*, 3rd ed., New York, McGraw-Hill.

Meyer, C. (2009), "The Greening of the Concrete Industry," *Cem. Con. Comp.*, V. 31, No. 8, pp. 601-605.

Nair, D. G., Fraaij, A., Klaassen, A. A. K., and Kentgens, A. P. M. (2008), "A Structural Investigation Relating to the Pozzolanic Activity of Rice Husk Ashes," *Cem. Con. Res.*, V. 38, No. 6, pp. 861-869.

Nakane, K., Yamashita, T., Iwakura, K., and Suzuki, F. (1999), "Properties and Structure of Poly(Vinyl Alcohol)/Silica Composites," *J. Appl. Polymer*, V. 74, No. 1, pp. 133-138.

Payá, J., Monzó, J., Borrachero, M. V., Mellado, A., and Ordoñez, L. M. (2001), "Determination of Amorphous Silica in Rice Husk Ash by a Rapid Analytical Method," *Cem. Con. Res.*, V. 31, No. 2, pp. 227-231.

Prasittisopin, L. and Trejo, D., "Hydration and Phase Formation of Blended Cementitious Systems Incorporating Chemically Transformed Rice Husk Ash," 2014 (Under review)

Pratson, L. F., Haerer, D., and Patiño-Echeverri, D. (2013), "Fuel Prices, Emission Standards, and Generation Costs for Coal vs Natural Gas Power Plants," *Environ. Sci. Technol.*, V. 47, No. 9, pp. 4926-4933.

Reinschmidt, K. and Trejo, D. (2006), "Economic Value of Building Faster," *J. Construc. Eng. Management*, V. 132, No. 7, pp. 759-766.

Rodrigues, F. A. (2003), "Low-Temperature Synthesis of Cements from Rice Hull Ash," *Cem. Con. Res.*, V. 33, No. 10, pp. 1525-1529.

Rodríguez de Sensale, G. (2010), "Effect of Rice-Husk Ash on Durability of Cementitious Materials," *Cem. Con. Comp.*, V. 32, No. 9, pp. 718-725.

Rothstein, D., Thomas, J. J., Christensen, B. J., and Jennings, H. M. (2002), "Solubility Behavior of Ca-, S-, Al-, and Si-Bearing Solid Phases in Portland Cement

Pore Solutions as a Function of Hydration Time," *Cem. Con. Res.*, V. 32, No. 10, pp. 1663-1671.

Sasaki, S., Method for Preventing Agglomeration of Colloidal Silica and Silicon Wafter olishing Composition Using the Same, in U.S. Patent, Yokkaichi, Editor, 1993, Monsanto Japan, Ltd., 5 pp.

Sata, V., Tangpagasit, J., Jaturapitakkul, C., and Chindaprasirt, P. (2012), "Effect of W/B Ratios on Pozzolanic Reaction of Biomass Ashes in Portland Cement Matrix," *Cem. Con. Comp.*, V. 34, No. 1, pp. 94-100.

Sugita, S., Shoya, M., and Tokuda, H. (1992), "Evaluation of Pozzolanic Activity of Rice Husk Ash," *ACI SP*, V. 132, No., pp. 495-512.

Taylor, H. F. W. (1997), *Cement Chemistry*, 2nd ed., Thomas Telford Publishing.

Thomas, J. J., Jennings, H. M., and Allen, A. J. (1999), "The Surface Area of Hardened Cement Paste as Measured by Various Techniques," *Concr. Sci. Eng.*, V. 1, No. 1, pp. 45-64.

Trejo, D. and Prasittisopin, L., "Performance Characteristics of Blended Cementitious Systems Incorporating Chemically Transformed Rice Husk Ash," 2014 (Under review)

van Tuan, N., *Rice Husk Ash as a Mineral Admixture for Ultra High Performance Concrete*, 2011, Delft University of Technology, Delft, Netherlands, 183 pp.

van Tuan, N., Ye, G., van Breugel, K., and Copuroglu, O. (2011), "Hydration and Microstructure of Ultra High Performance Concrete Incorporating Rice Husk Ash," *Cem. Con. Res.*, V. 41, No. 11, pp. 1104-1111.

Wang, L., Seals, R. K., and Roy, A. (2001), "Investigation of Utilization of Amorphous Silica Residues as Supplementary Cementing Materials," *Adv. Cem. Res.*, V. 13, No. 2, pp. 85-89.

Yu, Q., Sawayama, K., Sugita, S., Shoya, M., and Isojima, Y. (1999), "The Reaction between Rice Husk Ash and $Ca(OH)_2$ Solution and the Nature of Its Product," *Cem. Con. Res.*, V. 29, No. 1, pp. 37-43.

Zhang, M. H., Lastra, R., and Malhotra, V. M. (1996), "Rice-Husk Ash Paste and Concrete: Some Aspects of Hydration and the Microstructure of the Interfacial Zone between the Aggregate and Paste," *Cem. Con. Res.*, V. 26, No. 6, pp. 963-977.

Zhang, M. H. and Malhotra, V. M. (1996), "High-Performance Concrete Incorporating Rice Husk Ash as a Supplementary Cementing Material," *ACI Mater. J.*, V. 93, No. 6, pp. 629-636.

3 HYDRATION AND PHASE FORMATION OF BLENDED CEMENTITIOUS SYSTEMS INCORPORATING CHEMICALLY TRANSFORMED RICE HUSK ASH

ABSTRACT

Rice husk ash (RHA) can be used as a supplementary cementing material (SCM). However, because RHA contains a cellular, honeycomb-like morphology, the use of RHA in concrete results in reduced workability and increased water requirements. Reduced workability and increased water requirements can be mitigated by reducing the RHA particles. The smaller RHA particles are commonly obtained by mechanical grinding. However, mechanical grinding is inefficient because significant energy is required. A recent study assessed a chemical transformation process and reported that using this process results in reduced RHA particle size and an altered cellular morphology. This paper reports results on the early-age hydration and phase formation of the cementitious systems containing chemically transformed RHA (t-RHA). Results indicate that the hydration and phase formation of the t-RHA system is different from the as-received RHA (AR-RHA).

Keywords: Rice Husk Ash; Chemical Transformation; Hydration; Pore Solution; Solubility; X-Ray Diffraction; Thermodynamic Calculations

Summited to
Journal of Cement and Concrete Composites

3.1 INTRODUCTION

Rice husk ash (RHA) is an agricultural waste product and is produced from incineration of rice husks for energy. This incineration is an efficient process to remove organic substances of rice husks, leaving behind inorganic substances – silica ash. Mehta [1] reported that after incineration, approximately 20 percent by mass of rice husk remains as RHA. The Food and Agriculture Organization (FAO) of the United Nations [2] reported that approximately 70 million metric tons of the RHA are produced worldwide each year. Although millions of tons of RHA are produced worldwide each year, the commercial applications to utilize this material have been reported to be limited [3, 4]. This leads to serious challenges with disposal [5]. Da Costa et al. [4] and Rodriguez de Sensale [6] reported that the most common method of disposing RHA is dumping in landfills or into rivers. This disposal method can create environmental challenges and is not sustainable over the long term. Broadening the utilization of RHA is needed to mitigate these challenges.

RHA has a potential to be used as a supplementary cementing material (SCM). Replacing cement with RHA results in an increase in sustainability by reducing the cement content of concrete mixtures. The Portland Cement Association (PCA) [7] reported that cement production accounts for approximately 5 percent of the global carbon dioxide (CO_2) emissions. Reducing cement content by substitution of the RHA can lead to the reduction of CO_2 emissions from cement production.

When burnt under controlled incineration conditions, RHA is composed of mostly amorphous silica. The amorphous silica can be up to 90% by mass of the RHA. This RHA can be used to provide additional C-S-H (pozzolanic) products in cementitious systems [8, 9]. Taylor [10] reported that systems containing RHA not only perform similar to systems containing silica fume, but the RHA systems also exhibit higher pozzolanic activity. This higher pozzolanic activity leads to improved performance characteristics of the systems. Thus, the RHA blended cementitious systems can exhibit good early- and later-age characteristics. Replacement of cement with RHA is reported to

lead to improved mechanical properties of concrete [11-14], good resistance to chloride penetration and sulphate attack [15, 16], good freeze-thaw performance [17-19], good resistance to alkali-silica reaction (ASR) expansion [20], and improved resistance to dicing salt scaling [21].

The use of RHA in cementitious systems not only provides economic and environmental benefits but also can improve mixture performance. However, owners and contractors are not accepting RHA as a viable SCM product. This is especially the case when other SCMs are locally available. This is because RHA has high water absorption characteristics. These high water absorption characteristics occur because RHA contains a cellular, honeycomb-like morphology and has high surface area. RHA having these characteristics when used in concrete results in a reduction of flow [6]. Reduced flow can be mitigated by increasing the amount of water. However, increasing the amount of water in the mixtures results in a reduction of strength and durability. Thus, in addition to reduced flowability, the reduction of strength and durability also limits the use of RHA in cement and concrete systems.

Many studies [22-24] have investigated mechanical grinding methods (e.g., dry vibratory- and ball-milling) to reduce RHA particle size and eliminate the cellular, honeycomb-like morphology. The reduction of RHA particle size and elimination of its honeycomb morphology results in an increase of flowability and reduction of water demand [22-24]. Reducing RHA particle size and elimination of the honeycomb morphology can make RHA a more widely accepted SCM. To do this, alternatives to mechanical grinding processes should be identified [1, 25]. Additional research is required to identify more economical and more efficient alternatives to mechanical grinding of RHA such that this material can be a more widely accepted SCM.

A RHA chemical transformation process has been reported to reduce the honeycomb morphology and reduce RHA particle size [26]. The chemically transformed RHA here is defined as “t-RHA.” The process also resulted in larger amounts of silicate ions dissolved in the t-RHA slurry [26]. The larger amounts of silicate ions and the

smaller RHA particles could affect the early-age hydration rates and setting behavior of the RHA blended cement products.

The use of the t-RHA in blended cementitious systems may influence the hydration. This work evaluates the time-variant concentrations of ions in t-RHA blended cementitious solutions. The control system [100% portland cement (PC)] and the systems containing as-received RHA (AR-RHA) were also assessed for comparison. After collecting ion concentration data from the RHA blended cementitious solutions, saturation levels of portlandite, $CaSO_4 \cdot 2H_2O$ (gypsum), $Ca_6Al_2(SO_4)_3(OH)_{12} \cdot 26H_2O$ (ettringite), and $Ca_4Al_2(SO_4)(OH)_{12} \cdot 6H_2O$ (monosulphate) were assessed by calculating the Ion Activity Product (IAP) and dividing by the equilibrium solubility products. Results from X-Ray Diffraction (XRD) analysis were assessed with results from the solubility calculation for comparison.

3.2 MATERIAL AND METHODS

3.2.1 *Material*

Type I/II PC was used for all systems. The chemical composition and Bogue calculations for the cement are shown in Table 3-1. The PC met ASTM C150, Standard Specification for Portland Cement requirements. AR-RHA was procured from a power plant in Lake Charles, LA and the chemical composition is shown in Table 3-2. The average particle size of the AR-RHA is 192 μm with a standard deviation (SD) in average particle size of 3.15 μm (triplicate tests). ASTM Type II de-ionized (DI) water (1 MΩ•cm at 25˚C) was used for all mixtures and experiments. Pellet sodium hydroxide (NaOH) was American Chemical Society (ACS) grade.

Table 3-1. Chemical composition and Bogue calculation of PC

	(mass %)
Element	
SiO_2	20.30
Al_2O_3	4.80
Fe_2O_3	3.50
MgO	0.70
SO_3	2.80
CaO	63.9
Loss on Ignition	2.60
Insoluble Residue	0.11
Limestone	3.20
$CaCO_3$ in Limestone	97.80
Na_{eq}	0.54
Bogue calculations	
Ca_3SiO_5 (Alite)	60.6
Ca_2SiO_4 (Belite)	12.5
$Ca_3Al_2O_6$ (Calcium aluminate)	6.8
$Ca_4Al_2Fe_2O_{10}$ (Calcium aluminate ferrite)	11.9

Table 3-2. Chemical composition of AR-RHA

Composition	(mass %)*
SiO_2	89.65 - 96.90
C	2.09 - 7.59
Al_2O_3	0.006 - 0.039
Fe_2O_3	0.006 - 0.052
CaO	0.48 - 0.81
MgO	0.13 - 0.53
SO_3	0.018 - 0.24
Na_2O	0.018 - 0.18
K_2O	1.74 - 2.69
Ti_2O_3	0.003 - 0.020
P_2O_5	0.74 -1.23
Mn_3O_4	0.00 - 0.20

* Provided by manufacturer; ranges represent variation over 1 year

3.2.2 *Preparation of Chemical Transformation Process*

The chemical transformation process was performed using NaOH. The t-RHA slurry was prepared by mixing AR-RHA with 2M NaOH solution for 3 hours. Mixing was carried

out at 23˚C. Details on the chemical transformation process are provided in Trejo and Prasittisopin [26].

3.2.3 *Preparation of RHA Blended Cementitious Systems*

After obtaining t-RHA slurry, the t-RHA was mixed with PC at 10% and 15% replacement levels. The water-binder ratio (w/b) was 4.0. Mixing of the systems was performed using a magnetic stirrer (at 400 rpm) and continued throughout the test (up to 420 minutes). The temperature during mixing was 23 ± 1˚C. The control system and the systems containing AR-RHA at 10% and 15% replacement levels were also assessed for comparison.

3.2.4 *Characterization Methods*

3.2.4.1 Ion Concentration

The time elapsed after introducing the cementing materials to the solution will be referred to here as the "hydration time." Ion concentrations were analyzed at hydration times of 5, 10, 15, 30, 45, 60, 90, 120, 150, 180, 210, 240, 300, 360, and 420 minutes. Hydroxyl ion concentrations were evaluated using a pH electrode. Aluminate and calcium ion concentrations were determined using flame atomic absorption spectroscopy (FAAS). Sulphate ion concentrations were determined using ion chromatography (IC).

At each hydration time, test solution (30 ml) was decanted from the mixing beaker and filtered using a vacuum pump and No. 40 filter paper. Ten ml of filtered solution was used for analyzing aluminate ion concentration and 1 ml of filtered solution was used for analyzing calcium and sulphate ion concentrations. Because high concentrations of calcium and sulphate ions occur at early ages, filtered solutions for analyzing calcium and sulphate ion concentrations were diluted prior to the ion analyses. Filtered solutions for determining calcium and sulphate ion concentrations were diluted with 9 ml of DI water to obtain the solution within the detection range of the FAAS and IC. After decanting and diluting, 1 ml of lanthanum acid solution [50 g/l lanthanum oxide

(La_2O_3) in 3M hydrochloric acid (HCl)] was added to the solutions for the FAAS analysis. Concentrations of aluminate ions were determined using the FAAS with nitrous oxide-acetylene gas at a wavelength of 309.3 nm ignited at the temperature of 2600 to 2800 ˚C. The calcium concentrations were determined using air-acetylene gas at a wavelength of 422.7 nm ignited at the temperature of 2100 to 2400 ˚C. A blank sample (only DI water) was also analyzed and used as a background correction. Silicate ion concentrations were not determined in this study due to limitations in equipment viability.

3.2.4.2 Phase Composition

Crystalline compositions of three systems were analyzed using XRD. After mixing t-RHA with PC and water for 420 minutes, solutions were decanted from the mixing and filtrated to remove the liquid phase. The filtrated specimens were soaked with ethanol and then oven-dried at 110 ˚C for 4 hours to remove remaining water. The dried specimens were then ground using a ceramic mortar and pestle to particle sizes of less than 450 μm. XRD patterns of the hydrated products in the range of 8–45 ˚2θ were obtained with Cu Kα radiation and a graphite monochromator. The XRD instrument was operated at the voltage of 40 kV, 40 mA, scan rate of 5˚ per minute, and chopper increment of 0.2˚. The unhydrated PC (UPC) was also assessed for comparison.

3.2.5 *Saturation Calculation*

After obtaining the actual ion concentrations in solution, the activity (a_i) of each ion is calculated as follows:

$$a_i = \gamma_i c_{i,t} \tag{3-1}$$

where γ_i is the activity coefficient and $c_{i,t}$ is concentration of ion, i and time, t.

Rothstein *et al.* [27] reported that the PC system has high ionic strength (I) and equals 0.4. For the solution with ionic strength ranges from 0.1 to 0.5, the γ_i value can be calculated using the WATEQ extended Debye-Huckel equation. Samson *et al.* [28] also

reported using the modified Davies equation of an ionic species in concrete pore solution. The extended WATEQ Debye-Huckel equation was used to determine γ_i. The modified Davies equation can be used when the Debye-Huckel parameters are not known. The extended WATEQ Debye-Huckel equation and the modified Davies equations are shown in Equations. 3-2 and 3-3, respectively.

$$\log\gamma_i = \left(\frac{-Az_i^2\sqrt{I}}{1+Ba_i\sqrt{I}} + b_i I \right) \tag{3-2}$$

$$\ln\gamma_i = -\left(\frac{Az_i^2\sqrt{I}}{1+a_iB\sqrt{I}} \right) + \frac{(0.2-4.17\times10^{-5}I)Az_i^2I}{\sqrt{1000}} \tag{3-3}$$

where A and B are parameters that are temperature dependent, a_i is the parameter obtained from Kielland [29] and Samson *et al.* [28], z is the charge of the ion, and I is ionic strength, of i element. The Debye-Huckel parameters used here were reported by Ball and Nordstrom [30] and are shown in Table 3-3. The I can be calculated as follows:

$$I = \frac{1}{2}\sum_i z_i^2 c_{i,t} \tag{3-4}$$

where c_i is concentration of i element.

Table 3-3. Thermodynamic data for activity coefficient calculations

Species	a_i	b_i
Ca^{2+}	5	0.165
H^+	9	0
SO_4^{2-}	5	-0.04
$Al(OH)_4^-$	Modified Davies Equation	

Table 3-4 shows the IAP equations and the K_{sp} of portlandite, gypsum, ettringite, and monosulphate. These IAP equations were used to assess the solid phases at 25˚C. However, the experiment in this study was carried out at 23˚C. Therefore, the standard K_{sp} was modified using the van Hoff equation as follows:

$$\ln(K_{sp}) = \ln(K_{sp@25C}) + \frac{\Delta H_r}{R}\left(\frac{1}{298} - \frac{1}{T}\right) \quad (3\text{-}5)$$

where $K_{sp@25C}$ is the equilibrium solubility product at 25˚C, ΔH_r is the enthalpy of the reaction, R is the gas constant (0.00831 KJ/mol•K), and T is temperature in Kelvin.

Table 3-4. Thermodynamic data for solubility calculation at 25˚C

Phase	IAP	$\log(K_{sp})$ at 25˚C	ΔH_r (kJ/mol)	Reference
Portlandite	$[Ca^{+2}][OH^-]^2$	-5.18	-17.88	[39]
Gypsum	$[Ca^{+2}][SO_4^{-2}][H_2O]^2$	-4.58	-0.46	[39]
Ettringite	$[Ca^{+2}]^6[Al(OH)_4^-]^2[SO_4^{-2}]^3[OH^-]^4[H_2O]^{26}$	-44.90	204.60	[40]
Monosulphate	$[Ca^{+2}]^4[Al(OH)_4^-]^2[SO_4^{-2}][OH^-]^4[H_2O]^6$	-29.43	45.57	[41]

After calculating the IAP value for each phase, the Saturation Index (SI) for the product was calculated as follows:

$$\mathrm{SI} = \log\left(\frac{\mathrm{IAP}}{K_{sp}}\right) \quad (3\text{-}6)$$

- A SI value of approximately zero (IAP = K_{sp}) indicates that the phase is at saturation, i.e., the product should neither dissolve nor propitiate;
- A SI value greater than zero (IAP > K_{sp}) indicates that the phase is supersaturated, i.e., the solution should precipitate some of the dissolved ions; and
- A SI value less than zero (IAP< K_{sp}) indicates that the product is at an undersaturated stage, i.e., some more of the UPC can be dissolved.

However, note that the actual dissolution rate of the UPC in an undersaturated solution or precipitation rate from a supersaturated solution will depend on kinetics factors [31].

3.3 RESULTS AND DISCUSSION

3.3.1 *Ion Concentration of RHA Blended Cementitious System*

The hydroxyl ion concentrations as a function of hydration time for the control system and the systems containing AR-RHA and t-RHA are shown in Figures 3-1a and 3- 1b, respectively. Results in Figure 3-1a indicate that the hydroxyl ion concentration increases with increasing hydration time up to approximately 240 minutes. The hydroxyl ion concentration then decreases. This is followed by later increases for the 0 and 10% AR-RHA systems. The hydroxyl ion concentration of the control system is higher than the both 10 and 15% AR-RHA systems. This is likely because the control system has higher cement content than the AR-RHA systems. Increased AR-RHA replacement levels result in a reduction of hydroxyl ion concentration. Results in Figure 3-1b for the t-RHA systems indicate that the hydroxyl ion concentration is significantly higher than the AR-RHA systems (note change in scale). The hydroxyl ion concentration of the control system is lower than the hydroxyl ion concentrations of the 10 and 15% t-RHA systems. This is likely due to NaOH solution added to the RHA during the chemical transformation process. Higher hydroxyl ion concentration would be expected to result in a change in phase formation.

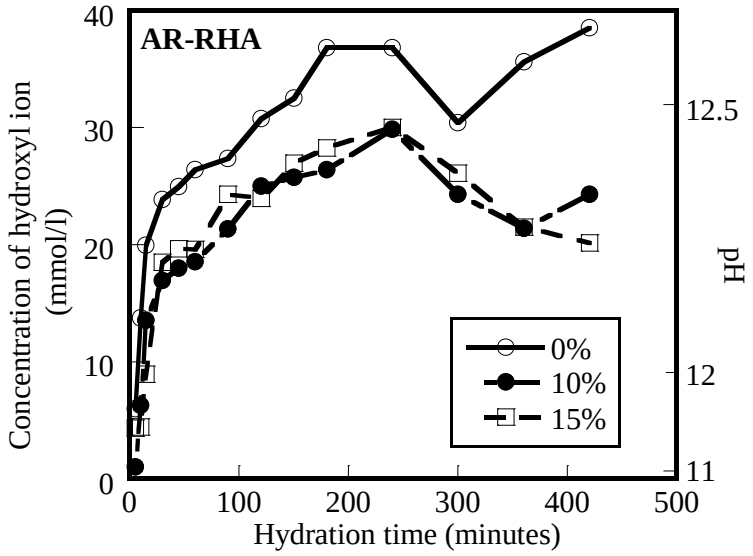

a)

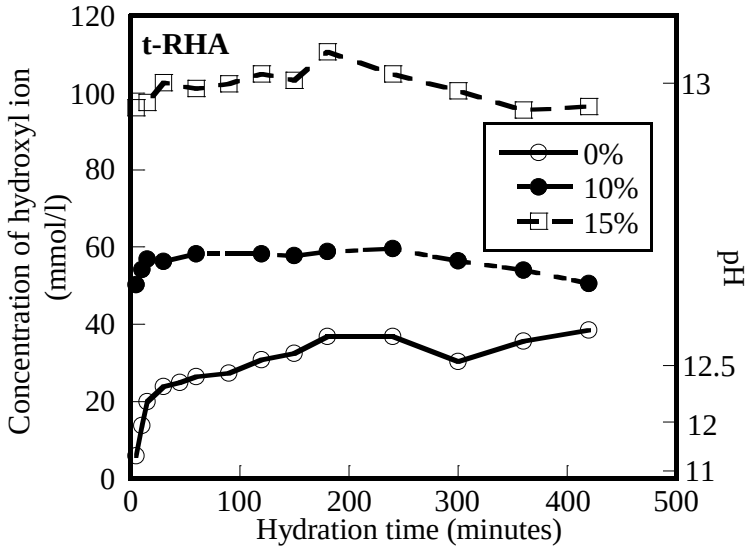

b)

Figure 3-1. Concentration of hydroxyl ion in a) AR-RHA and b) t-RHA blended cementitious systems versus hydration time.

Figures 3-2a and 3-2b show the aluminate ion concentration as a function of hydration time for the AR-RHA and t-RHA systems, respectively. Results indicate that

increased replacement levels of both AR-RHA and t-RHA systems result in increased aluminate ion concentrations. In addition, the aluminate ion concentrations for both systems (AR-RHA and t-RHA) are similar. Tishmack *et al.* [32] investigated the ion concentration in pore solution of cement paste containing SCMs and reported that these systems have higher aluminate ion concentration when compared with the control system.

Figures 3-3a and 3-3b show calcium ion concentration as a function of hydration time for the AR-RHA and t-RHA systems, respectively. The calcium ion concentrations for all systems range from 12 to 32 mmol/l. Results indicate that the control system has higher calcium ion concentrations than the 10 and 15% RHA systems (both AR-RHA and t-RHA). Results also indicate that the calcium ion concentration of the t-RHA systems is lower than the AR-RHA systems at similar replacement levels. This is likely a result of the t-RHA systems having higher silicate ion concentrations than the AR-RHA systems. Trejo and Prasittisopin [26] reported that the silicate ions in the t-RHA systems are approximately 5 to 6 times higher than the typical values for PC systems [26]. Higher silicate ion concentrations should result in larger consumption of portlandite to form pozzolanic products. The t-RHA systems evaluated have lower concentrations of calcium ions than the AR-RHA systems, indicating that this is the case.

The presence of RHA has been reported in the literature to result in the reduction of calcium ion concentration at early ages due to increased silicate ion concentration in solution [33, 34]. Lagier and Kurtis [35] reported that blending PC with SCMs results in larger consumption of portlandite to form pozzolanic products at early ages, when compared with the 100% PC system. Once portlandite is consumed, calcium ion concentrations are reduced. Therefore, increased RHA replacement levels should result in reduced calcium ion concentration.

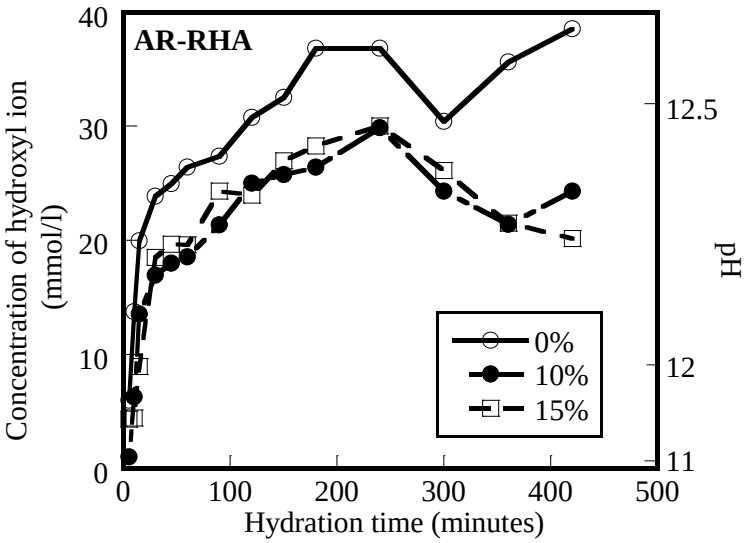

a)

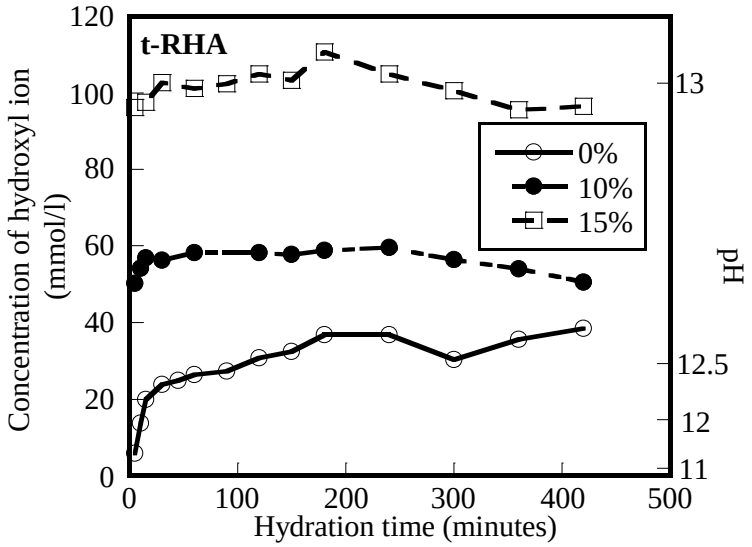

b)

Figure 3-2. Concentration of aluminate ion in a) AR-RHA and b) t-RHA blended cementitious systems versus hydration time.

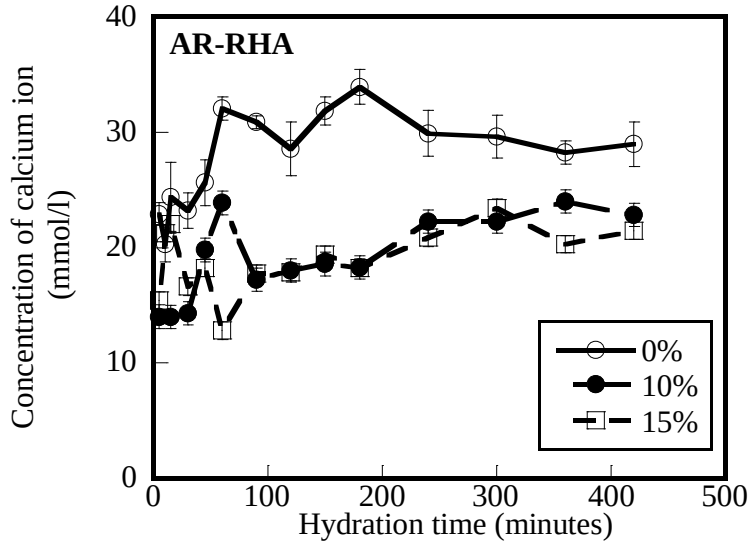

a)

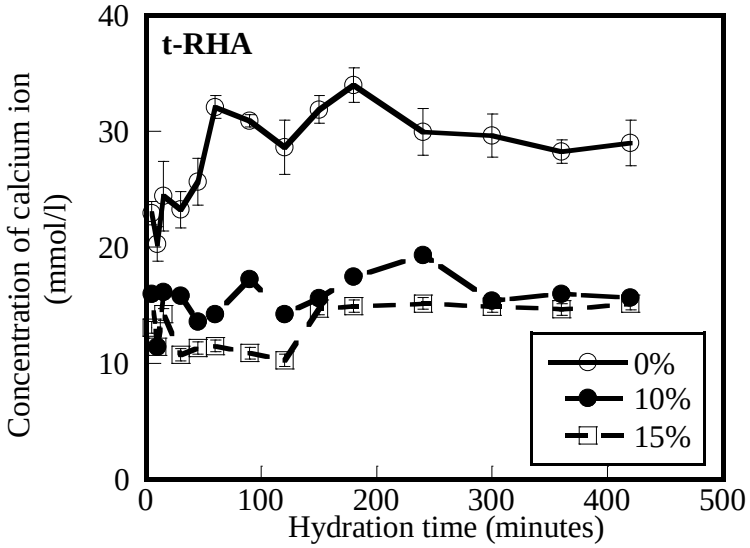

b)

Figure 3-3. Concentration of calcium ion in a) AR-RHA and b) t-RHA blended cementitious systems versus hydration time.

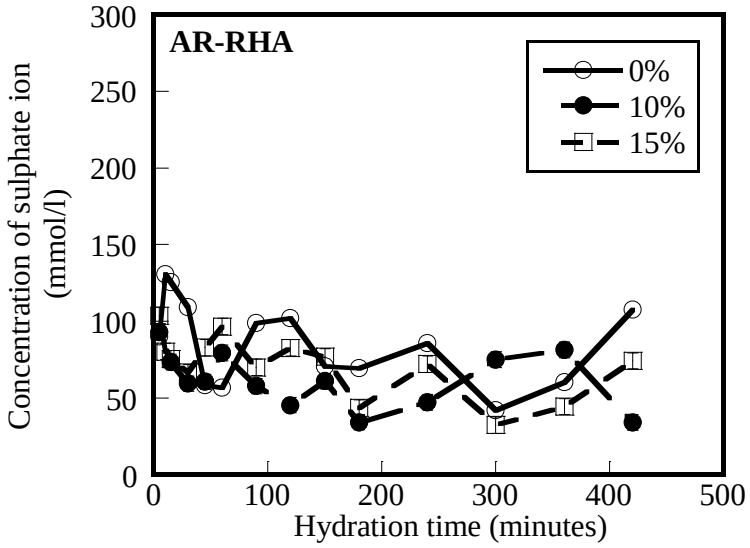

a)

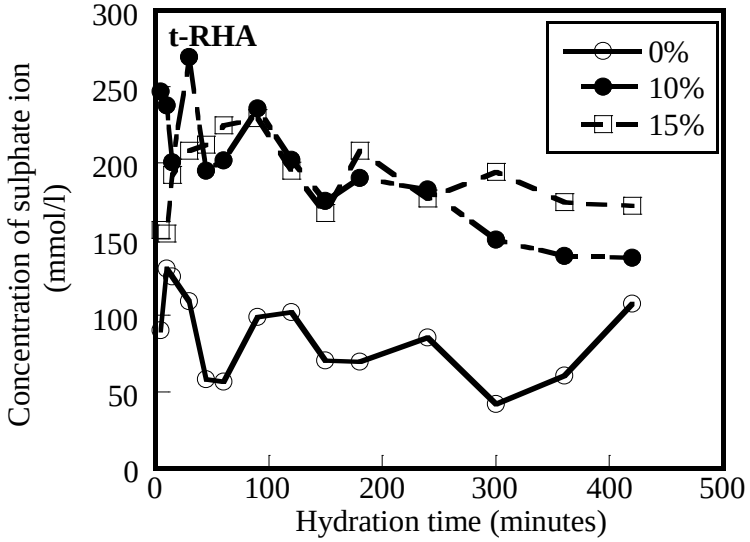

b)

Figure 3-4. Concentration of sulphate ion in a) AR-RHA and b) t-RHA blended cementitious systems versus hydration time.

Figure 3-4a shows the sulphate ion concentration in solution for the AR-RHA systems as a function of hydration time. Results indicate that increased AR-RHA

replacement levels do not significantly influence the sulphate ion concentration in solution. However, there are variations in the concentrations and the concentrations cycle over time. This is likely a result of sulphate levels becoming supersaturated, and precipitating out of solution, then new sulphates dissolving and super-saturating the solution again. Figure 3-4b shows sulphate ion concentration of the t-RHA systems as a function of hydration time. Results indicate that the sulphate ion concentration significantly increases with increasing t-RHA replacement levels. Diamond and Ong [36] reported that the alkali hydroxides react with gypsum and convert the alkali hydroxides and gypsum into alkali sulphate ions. This occurs immediately after the cement is introduced to the NaOH solution. As a result, the additional NaOH solution in the t-RHA system results in increased concentrations of sulphate ions.

3.3.2 *Saturation Calculation*

After obtaining the concentrations of each element from the experimental studies, IAP values can be determined. The SI values of portlandite, gypsum, ettringite, and monosulphate were determined using these IAP values obtained from Equations 3-1 to 3-6. The SI values for portalndite in the AR-RHA and t-RHA systems as a function of hydration time are shown in Figures 3-5a and 3-5b, respectively.

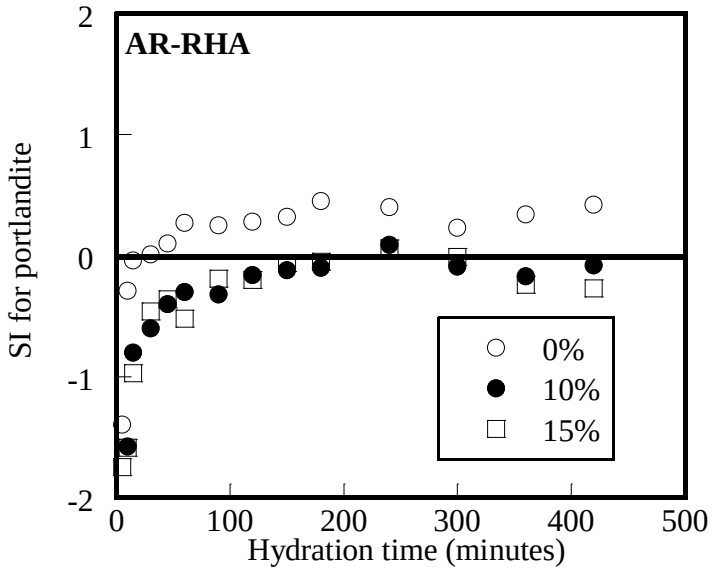

a)

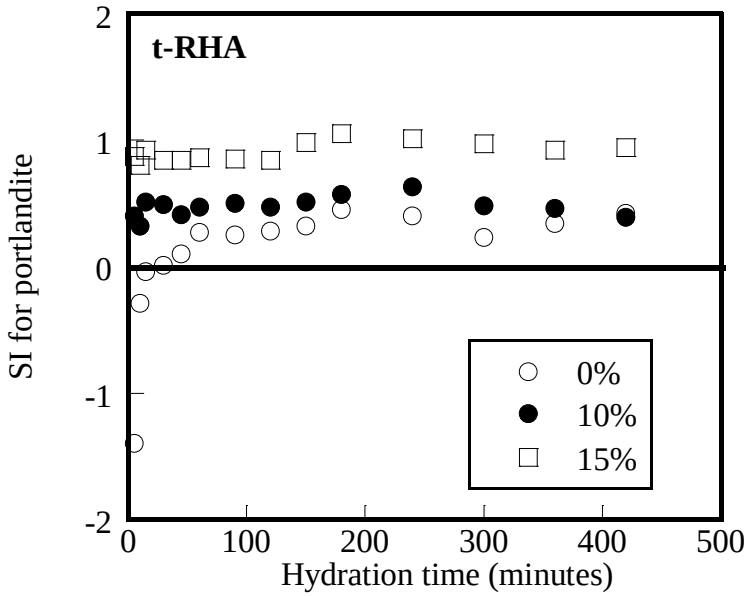

b)

Figure 3-5. SI value for Portlandite in a) AR-RHA and b) t-RHA blended cementitious systems versus hydration time.

Results in Figure 3-5a show that the SI values for portlandite in the control system increases at early times and then reaches a steady state – the SI value stays above zero up to 420 minutes. The SI values for portlandite in the 10 and 15% AR-RHA systems also increase and cycle between supersaturation and undersaturation, indicating that the calcium and hydroxyl ions are dissolving into and precipitating from solution. Results also indicate that as the AR-RHA replacement levels increase, the SI values for portlandite decrease. This indicates that less portlandite product will precipitate from solutions when higher quantities of AR-RHA are used. Figure 3-5b shows results from the t-RHA system. The figure shows that all systems are in the supersaturated range (i.e., SI values > 0). Increased t-RHA replacement levels result in increased SI values for the portlandite, indicating that larger amounts of portlandite product precipitate from solution when higher t-RHA is present. This is likely a result of the NaOH used to transform the RHA.

The SI values for gypsum as a function of time in the AR-RHA systems are shown in Figure 3-6a. Results indicate that the gypsum in the AR-RHA systems cycles between supersaturation and undersaturation. The gypsum in the control system can stay in the supersaturation range. Rothstein *et al.* [27] reported that the gypsum of PC mixtures stays in the supersaturation range for up to 7 hours. Increasing AR-RHA replacement levels result in the reduction of the SI value for gypsum. As a result, less calcium and sulphate ions are consumed in the AR-RHA systems. Because gypsum is added to cement to delay the set, it would be expected that the set of the AR-RHA systems would be delayed. Prasittisopin and Trejo [37] reported that the set for the AR-RHA systems was delayed. Figure 3-6b shows the SI values for gypsum as a function of hydration time for the t-RHA systems. Results indicate that the gypsum in all systems is in the supersaturation range. Although increased t-RHA replacement levels exhibit higher SI values, all values are in the supersaturation range.

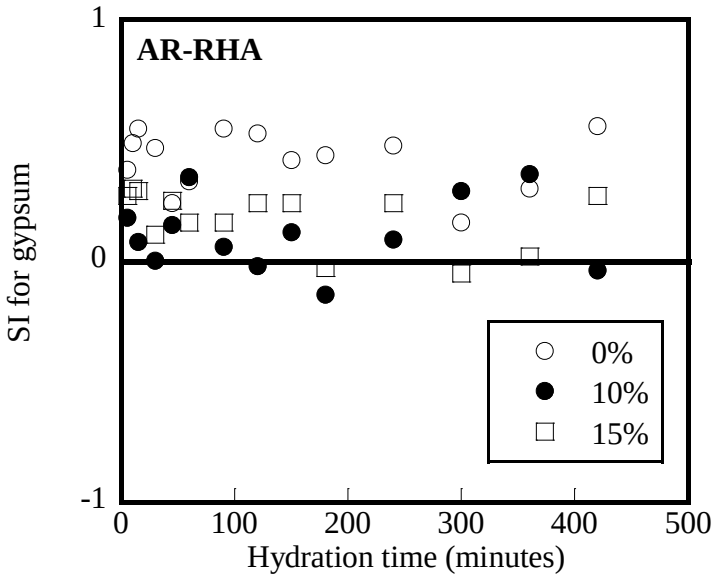

a)

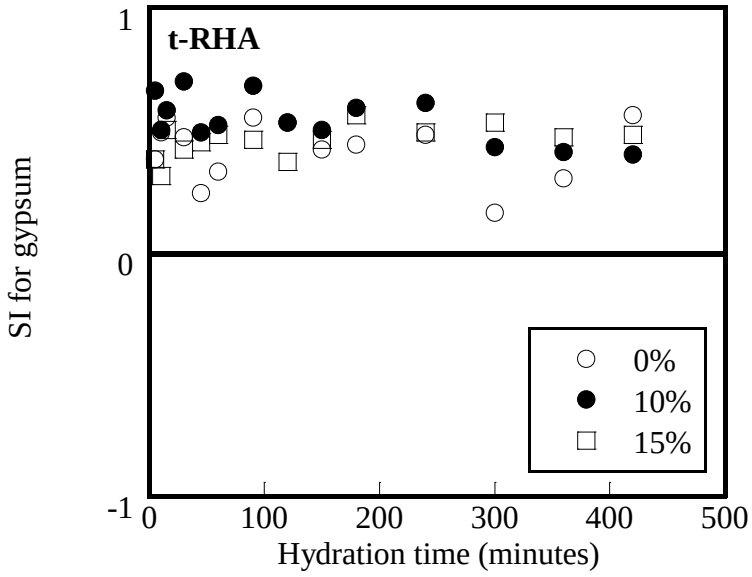

b)

Figure 3-6. SI value for gypsum in a) AR-RHA and b) t-RHA blended cementitious systems versus hydration time.

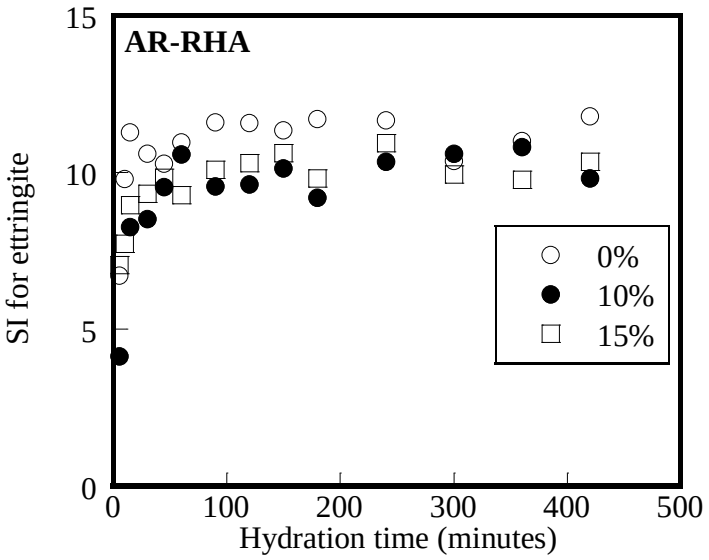

a)

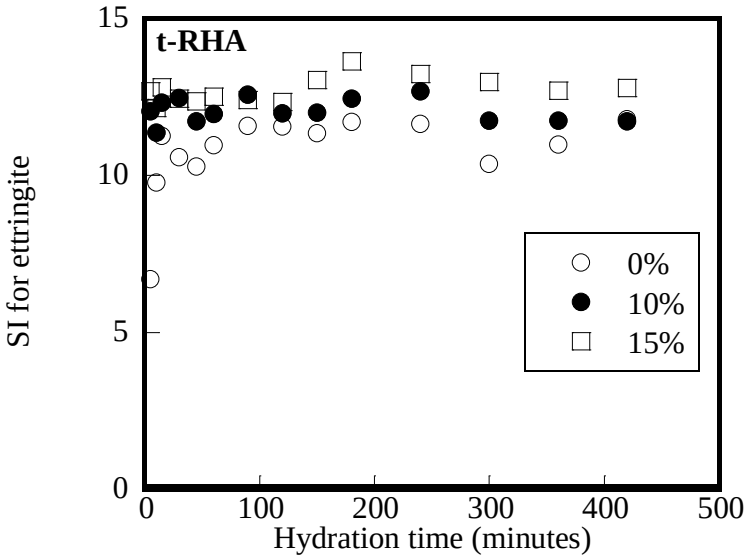

b)

Figure 3-7. SI value for ettringite in a) AR-RHA and b) t-RHA blended cementitious systems versus hydration time.

Figures 3-7a and 3-7b show the SI values for ettringite in the AR-RHA and t-RHA systems as a function of hydration time, respectively.

Results indicate that the solutions are in the supersaturated range for all systems (control, AR-RHA, and t-RHA) Note the scale change on the ordinate between Figures 3-6 and 3-7. This indicates that ettringite is being precipitated for all systems. Results also indicate that the presence of AR-RHA results in a reduction of the SI values for ettringite. This is likely a result of the lower cement content (RHA is a replacement). Figure 3-7b shows that the presence of t-RHA results in an increase in the SI value for ettringite. In addition, there is a small increase with increasing t-RHA replacement level. Note that the SI values for ettringite (shown in Figures 3-7a and 3-7b) are significantly high (from 4 to 13) compared to other products. This is due to the large stoichiometric coefficients of ettringite in the IAP equation (see Table 3-4).

The SI values for monosulphate as a function of hydration time for the AR-RHA and t-RHA systems are shown in Figures 3-8a and 3-8b, respectively. Similar to the SI results for ettringite (shown in Figures 3-7a and 3-7b), all systems (control, AR-RHA, and t-RHA) are in the supersaturated range. Increased AR-RHA replacement levels result in a reduction in the SI values for monosulphate. However, increased t-RHA replacement levels result in an increase in the SI values for monosulphate. Results also indicate that the SI values of monosulphate (in Figures 3-8a and 3-8b) are lower than the SI values of ettringite (in Figures 3-7a and 3-7b) at all hydration times.

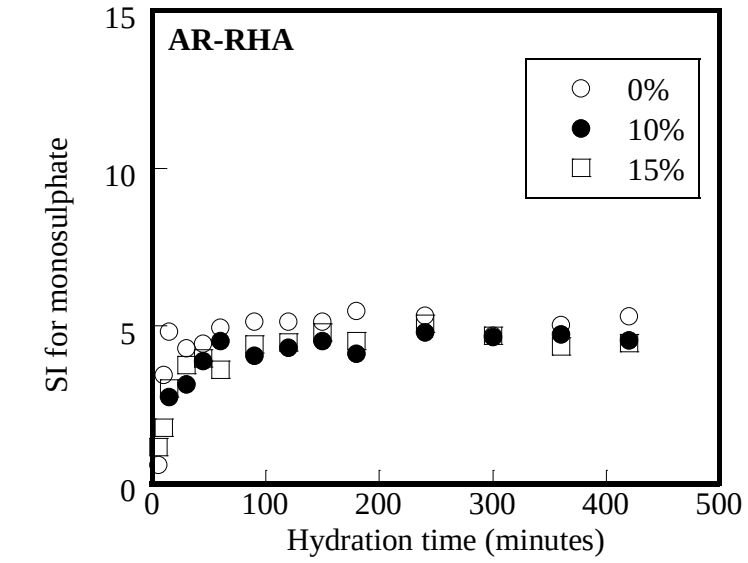

a)

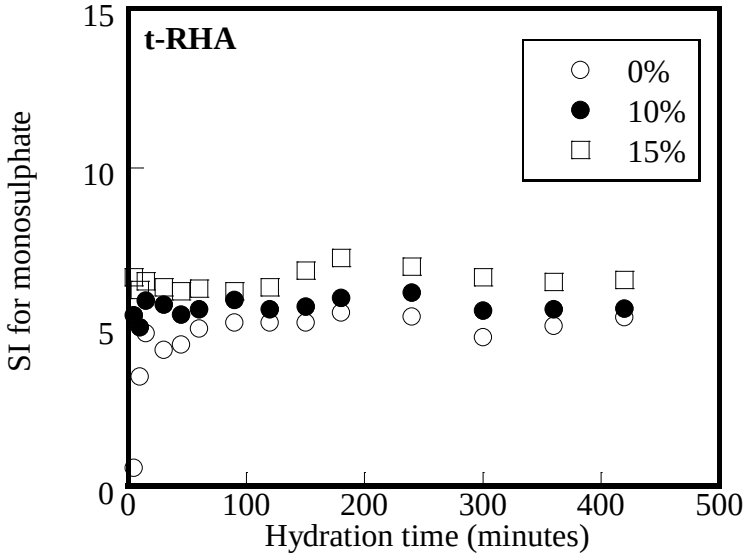

b)

Figure 3-8. SI value for monosulphate in a) AR-RHA and b) t-RHA blended cementitious systems versus hydration time.

A summary of the influence of AR-RHA and t-RHA replacement levels on SI value for the different phases is shown in Table 3-5. The presence of AR-RHA results in similar or lower SI values when compared to the control system. This indicates that less product precipitates from solution and indicates that lower amounts of hydrated products are forming at early ages. Increased t-RHA replacement levels result in similar or higher SI values. The higher SI values indicates that more product is precipitated and formed at early ages. This is likely because the AR-RHA lowers the sulphate ion concentration (as shown in Figure 4a and reported by Diamond and Ong [36]) and results in the reduction of the SI value for gypsum (as shown in Figure 3-6a). Once larger quantities of gypsum are present in the AR-RHA systems, the hydration is retarded. However, t-RHA replacements allow for higher sulphate ions to dissolve in solution (as shown in Figure 3-4b) and this results in an increase in the SI value for gypsum (as shown in Figure 3-6b). Increased SI value for gypsum indicates that more gypsum precipitates and forms sulphate products (e.g., ettringite and monosulphate). Therefore, less gypsum is present in the system and this consequently results in faster hydration.

Table 3-5. SI values of the solid phase with presence of RHA type

RHA type	SI value of hydrated product			
	Portlandite	Gypsum	Ettringite	Monosulphate
AR-RHA	↓	↓	↓	↓
t-RHA	↑	↑	↑	↑

3.3.3 *Phase Composition*

Solubility calculations provide theoretical information on the hydrated products for RHA blended systems. To complement these theoretical analyses, an XRD analysis was performed. This analysis provides information on the solid phases present in the systems after 420 minutes of hydration time.

The XRD patterns for the UPC and HPC mixed for 420 minutes are shown in Figure 3-9.

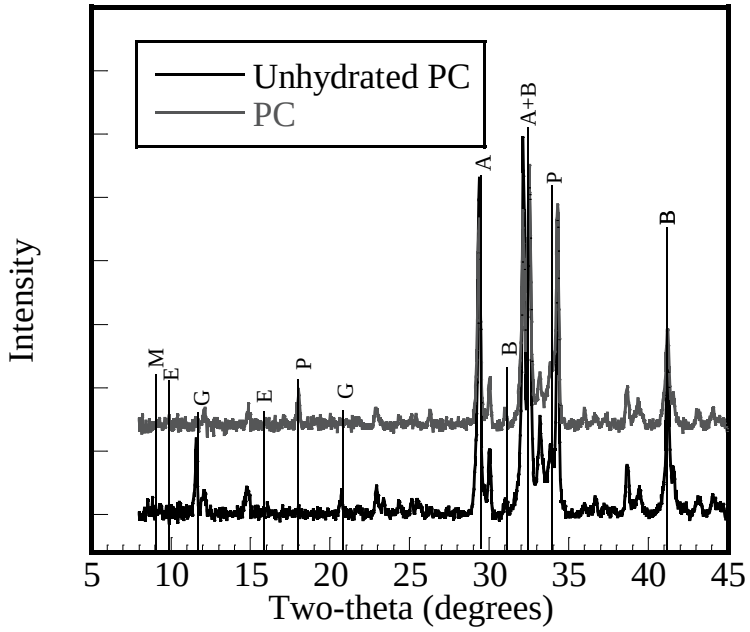

Figure 3-9. XRD pattern of the unhydrated PC and PC system mixed for 420 minutes (A is alite; B is belite; P is portlandite; G is gypsum; E is ettringite; and M is monosulphate).

Results indicate that the alite and belite phases (˚2θ peaks at 29.4, 31.0, 32.5, and 41.2) for the HPC are significantly lower than these phase in the UPC. This would be expected as the unhydrated phases of alite and belite are hydrating and forming new products. In addition, the peaks for gypsum (˚2θ at11.6 and 20.9) for the HPC is also significantly lower than the UPC, indicating that gypsum is consumed. The portlandite peaks (˚2θ at 18.0 and 34.1) for the UPC is lower than the peaks for HPC, indicating the early formation of portlandite. The figure also indicates that trace amounts of ettringite (˚2θ at 9.6 and 15.9) are present. The monosulphate phase (˚2θ at 9.0) was not detected. The XRD patterns indicate that alite, belite, and gypsum are consumed and portlandite and trace amounts of ettringite are formed within 420 minutes.

Figure 3-10 shows XRD patterns of the HPC system and systems containing 10 and 15% AR-RHA. Results for all systems indicate that unhydrated products are the major phases (alite and belite). The HPC system contains portlandite, while the 10% AR-RHA system exhibited lower peaks at the ˚2θ for portlandite. The 15% AR-RHA system

exhibited no portlandite. The amount of portlandite is decreasing with increasing AR-RHA replacement levels. The gypsum peaks for the AR-RHA systems are significantly higher than the control HPC system. Trace amounts of ettringite and monosulphate were observed in the AR-RHA systems. A summary of the phase composition of HPC and systems containing AR-RHA and t-RHA at 10% and 15% replacement levels is shown in Table 3-6.

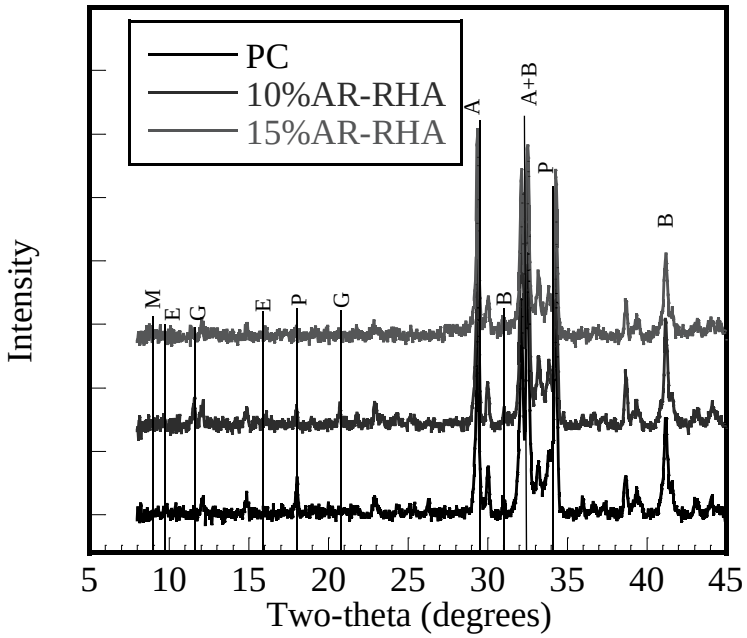

Figure 3-10. XRD pattern of the PC, 10% AR-RHA, and 15% AR-RHA system mixed for 420 minutes (A is alite; B is belite; P is portlandite; G is gypsum; E is ettringite; and M is monosulphate).

Table 3-6. Phase composition of PC system, and systems containing AR-RHA and t-RHA at 10% and 15% replacement levels and mixed at 420 minutes

System	XRD phase composition					
	Portlandite	Gypsum	Ettringite	Monosulphate	Alite	Belite
PC	**	*	*	*	***	***
AR-RHA	*	**	*	-	***	***
t-RHA	*	*	*	*	***	***

*** major phase; ** minor phase; * trace phase; and - undetected phase

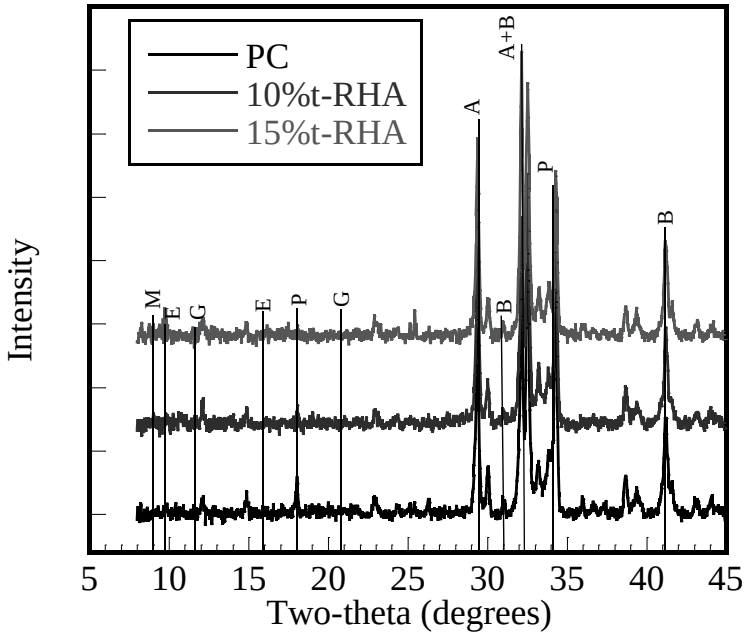

Figure 3-11. XRD pattern of the PC, 10% t-RHA, and 15% t-RHA system mixed for 420 minutes (A is alite; B is belite; P is portlandite; G is gypsum; E is ettringite; and M is monosulphate).

XRD patterns for the t-RHA systems are shown in Figure 3-11. Results of all systems indicate that alite and belite are the major phases. Lower amounts of portlandite were detected in the t-RHA systems when compared with the HPC system. These results contradict the solubility calculations shown in Figure 3-5b. However, Trejo and Prasittisopin [26] reported that during the transformation process the amorphous silica in the t-RHA reacts with NaOH solution and results in higher silicate ion concentrations in solution. Because of this, the silicate ions are readily available to react with portlandite to form pozzolanic products. Therefore, even though results in Figure 3-5b indicate that larger amounts of portlandite may precipitate, it is possible that less portlandite was detected due to early pozzolanic reactions. Results indicate that trace amounts of gypsum, ettringite, and monosulphate were detected for all systems.

3.3.4 *Effects of Chemistry on Early-age Characteristics*

Using the chemical transformation process for RHA can alter the phase formation of cementitious systems at early ages. Quennoz and Scriverner [38] reported that the presence of sulphate ions can control the dissolution rates of alite. In the t-RHA systems, when sulphate ions from the gypsum dissolve into solution (shown in Figure 3-4b), less aluminate and calcium ions are observed (shown in Figures 3-2b and 3-3b). This higher sulphate ion concentration results in increased SI values, indicating that more gypsum is consumed. Quennoz and Scriverner [38] also reported that immediately after all gypsum is reacted, accelerated hydration reactions could occur. Prasittisopin and Trejo [37] reported that the blended cement system containing t-RHA had shorter setting time, increased early strength development, and higher chemical shrinkage at early ages when compared with the control and AR-RHA systems. Hence, using the chemical transformation process will result in accelerated early-age characteristics. Shorter setting times and increased early strength development can result in a shorter construction periods and this may be beneficial to construction purpose. Issues with increased chemical shrinkage will have to be further assessed

3.4 **CONCLUSIONS**

A study assessing the hydration process and phase formation for a chemically transformed RHA (t-RHA) was performed. Results indicate that:

- The t-RHA systems have higher concentrations of hydroxyl and sulphate ions than the AR-RHA systems, but had lower concentrations of aluminate and calcium ions than the AR-RHA systems.
- The SI values for portlandite, gypsum, ettringite, and monosulphate of the t-RHA systems are higher than the AR-RHA systems.

- Results indicate that gypsum in the t-RHA systems quickly dissolves in solution and precipitates into sulphate-containing products. This likely will result in accelerated hydration.
- The gypsum in the AR-RHA systems also dissolves quickly, but the SI values for gypsum indicate cycling between supersaturated and undersaturated ranges. Because the sulphates are not continuously in the supersaturated range, reactions with sulphates are depressed, keeping sulphates in solution for longer periods. This likely will lead to retarded hydration.

Earlier studies reported that the chemical transformation process of the RHA morphology could be a promising alternative to mechanical grinding. This study indicates that the early-age phase formation of the t-RHA systems is altered and may lead to accelerated hydration. Although promising, the economics to determine the feasibility of the chemical transformation process is needed to be assessed.

3.5 ACKNOWLEDGEMENTS

The authors express gratitude to Dr. Wenping Li, Agrilectric Companies, for providing the rice husk ash and Dr. Jack Istok for advising the IC testing.

3.6 REFERENCES

[1] Mehta PK. Rice husk ash - a unique supplementary cementing material. In: Malhotra VM, editor. Proc Intern Advances in Concrete Tech. 2nd ed: CANMET; 1994. p. 419-43.

[2] Food and Agriculture Organization of the United Nations. FAO statistical databases. 2009.

[3] Meyer C. The greening of the concrete industry. Cem Con Comp. 2009;31(8):601-5.

[4] Da Costa HM, Visconte LLY, Nunes RCR, Furtado CRG. The effect of coupling agent and chemical treatment on rice husk ash-filled natural rubber composites. J Appl Polymer Sci. 2000;76(7):1019-27.

[5] He J, Jie Y, Zhang J, Yu Y, Zhang G. Synthesis and characterization of red mud and rice husk ash-based geopolymer composites. Cem Con Comp. 2013;37:108-18.

[6] Rodríguez de Sensale G. Effect of rice-husk ash on durability of cementitious materials. Cem Con Comp. 2010;32(9):718-25.

[7] PCA. Green in practice 102 - concrete, cement, and CO_2. Portland Cement Association; 2010.

[8] Yu Q, Sawayama K, Sugita S, Shoya M, Isojima Y. The reaction between rice husk ash and $Ca(OH)_2$ solution and the nature of its product. Cem Con Res. 1999;29(1):37-43.

[9] Salas A, Delvasto S, de Gutierrez RM, Lange D. Comparison of two processes for treating rice husk ash for use in high performance concrete. Cem Con Res. 2009;39(9):773-8.

[10] Taylor HFW. Cement chemistry. 2nd ed: Thomas Telford Publishing; 1997.

[11] Muthadhi A, Kothandaraman S. Experimental investigations of performance characteristics of rice husk ash–blended concrete. J Mater Civil Eng. 2013;25(8):1115-8.

[12] Zhang MH, Malhotra VM. High-performance concrete incorporating rice husk ash as a supplementary cementing material. ACI Mater J. 1996;93(6):629-36.

[13] Vayghan A, Khaloo A, Nasiri S, Rajabipour F. Studies on the effect of retention time of rice husk combustion on the ash's chemo-physical properties and performance in cement mixtures. J Mater Civil Eng. 2011;24(6):691-7.

[14] Sujivorakul C, Jaturapitakkul C, Taotip A. Utilization of fly ash, rice husk ash, and palm oil fuel ash in glass fiber–reinforced concrete. J Mater Civil Eng. 2011;23(9):1281-8.

[15] Venkatanarayanan H, Rangaraju P. Evaluation of sulfate resistance of portland cement mortars containing low-carbon rice husk ash. J Mater Civil Eng. 2013.

[16] Sakr K. Effects of silica fume and rice husk ash on the properties of heavy weight concrete. J Mater Civil Eng. 2006;18(3):367-76.

[17] Azevedo AA, Martins MLC, Molin DCD. A study of the penetration of chloride ions in rice-husk ash concrete. In: Malhotra VM, editor. Third CANMET/ACI Intern Symp on Sustainable Development of Cement and Concrete. San Francisco, CA: ACI; 2001. p. 379-96.

[18] Nehdi M, Duqette J, El Damatty A. Performance of rice husk ash produced using a new technology as a mineral admixture in concrete. Cem Con Res. 2003;33(8):1203-10.

[19] Gastaldini ALG, Isaia GC, Gomes NS, Sperb JEK. Chloride penetration and carbonation in concrete with rice husk ash and chemical activators. Cem Con Comp. 2007;29:176-80.

[20] Shuichi S, Shoya M, Tokuda H. Evaluation of pozzolanic activity of rice husk ash. ACI SP. 1992;132:495-512.

[21] Mehta PK, Folliard KJ. Rice husk ash--a unique supplementary cementing material: Durability aspects. ACI SP. 1995;154:531-42.

[22] Cordeiro GC, Toledo Filho RD, Tavares LM, Fairbairn EdMR, Hempel S. Influence of particle size and specific surface area on the pozzolanic activity of residual rice husk ash. Cem Con Comp. 2011;33(5):529-34.

[23] Bui DD, Hu J, Stroeven P. Particle size effect on the strength of rice husk ash blended gap-graded portland cement concrete. Cem & Con Comp. 2005;27(3):357-66.

[24] Gholizadeh Vayghan A, Khaloo AR, Rajabipour F. The effects of a hydrochloric acid pre-treatment on the physicochemical properties and pozzolanic performance of rice husk ash. Cem Con Comp. 2013;39(0):131-40.

[25] Bui DD. Rice husk ash as a mineral admixture for high performance concrete. Delft, Delft University of Technology; 2001.

[26] Trejo D., Prasittisopin L., Chemical transformation of rice husk ash morphology. 2014. (Under review)

[27] Rothstein D, Thomas JJ, Christensen BJ, Jennings HM. Solubility behavior of Ca-, S-, Al-, and Si-bearing solid phases in portland cement pore solutions as a function of hydration time. Cem Con Res. 2002;32(10):1663-71.

[28] Samson E, Lemaire G, Marchand J, Beaudoin JJ. Modeling chemical activity effects in strong ionic solutions. Comp Mater Sci. 1999;15:285-94.

[29] Kielland J. Individual activity coefficients of ions in aqueous solutions. J ACS. 1937;59(9):1675-8.

[30] Ball JW, Nordstrom DK. User's manual for WATEQ4F with revised thermodynamic data base and test cases for calculating speciation of major, trace, and redox elements in natural waters. In: Interior USDot, editor. Menlo Park, CA: U.S. Geological Survey; 1991. p. 55.

[31] Misra KC. Introduction to geochemistry: Principles and appliations. Hoboken, NJ: John Wiley & Sons; 2012.

[32] Tishmack JK, Olek J, Diamond S, Sahu S. Characterization of pore solutions expressed from high-calcium fly-ash–water pastes. Fuel. 2001;80(6):815-9.

[33] Begarin F, Garrault S, Nonat A, Nicoleau L. Hydration of alite containing aluminum. Adv Applied Ceram. 2011;110(3):127-30.

[34] Lothenbach B, Scrivener K, Hooton RD. Supplementary cementitious materials. Cem Con Res. 2011;41(3):217-29.

[35] Lagier F, Kurtis KE. Influence of portland cement composition on early age reactions with metakaolin. Cem Con Res. 2007;37(10):1411-7.

[36] Diamond S, Ong S. Effects of added alkali hydroxides in mix water on long-term SO_4^{2-} concentrations in pore solution. Cem Con Comp. 1994;16(3):219-26.

[37] Prasittisopin L, Trejo D. Performance characteristics of blended cementitious systems incorporating chemically transformed rice husk ash. 2014 (Under review).

[38] Quennoz A, Scrivener KL. Hydration of C_3A–gypsum systems. Cem Con Res. 2012;42(7):1032-41.

[39] Parkhurst DL, Appelo CAJ. User's guide to PHREEQC (version 2)— a computer program for speciation, batch-reaction, one-dimensional transport, and inverse geochemical calculations. In: Interior USDot, editor. Denver, CO 1999.

[40] Perkins RB, Palmer CD. Solubility of ettringite ($Ca_6[Al(OH)_6]_2(SO_4)_3 \cdot 26H_2O$) at 5–75°C. Geochimica et Cosmochimica Acta. 1999;63(13–14):1969-80.

[41] Damidot D, Glasser FP. Thermodynamic investigation of the CaO-Al_2O_3-$CaSO_4$-H_2O system at 25°C and the influence of Na_2O. Cem Con Res. 1993;23(1):221-38.

4 PERFORMANCE CHARACTERISTICS OF BLENDED CEMENTITIOUS SYSTEMS INCORPORATING CHEMICALLY TRANSFORMED RICE HUSK ASH

ABSTRACT

Rice husk ash (RHA) is an abundantly available by-product from the burning of rice husks for energy production – this ash can be used as a supplementary cementing material (SCM). However, RHA contains a cellular, honeycomb-like morphology of amorphous silica and this morphology results in high water absorption. The use of RHA in concrete has been reported to result in reduced workability, reducing the likelihood that RHA will be accepted in the industry. Research has shown that reduced particle size results in improved workability and lower water demands. Mechanical grinding can be used to reduce the cellular morphology and size but results indicate this process requires significant energy and costs. This paper reports on the performance characteristics of cementitious systems containing chemically transformed RHA. Results indicate that this chemical transformation method is promising and can make RHA a more user-friendly SCM, enhancing its likelihood of being utilized.

Keywords: Rice Husk Ash; Morphology; Chemical Transformation; Alkalis; Blended Cement

Submitted to
Journal of Cement and Concrete Composites

4.1 INTRODUCTION

RHA is produced from the de-husking and burning of rice husks for energy production. Rice husks are hard covers that protect a rice grain during the growth period. Prior to burning, rice husks consist of approximately 20% to 23% by mass of the rice plant [1]. The pre-burnt composition of the rice husk consists of approximately 75% to 80% of organic substances (e.g., cellulose and lignin) and 15% to 20% of inorganic substances. The burning process is an efficient way to remove organic substances, leaving behind an inorganic ash composed mostly of silica. Because size, morphology, and specific surface of RHA particles are dependent on burning conditions, a proper burning process can lead to RHA with high amorphous silica contents [2]. The proper burning process of rice husk typically yields a porous, cellular ash, reported to contain amorphous silica up to approximately 90% [3]. After burning, RHA maintains its original cellular morphology.

A large quantity of RHA is generated from power plants and this product is considered to be a waste material, as there are few commercial applications for this material. This leads to challenges with disposal and storage at power plants [4-6]. Current disposal methods include dumping into landfills. Although currently economical, this is not sustainable as RHA can create long-term environmental challenges. In addition, because natural gas is becoming more economical, the availability of fly ash from the burning of coal is decreasing. Broadening the application and use of RHA can increase economic value, reduce environmental impact, and provide an alternative product for fly ash.

RHA blended cementitious systems have been reported to exhibit good early- and later-age characteristics. Chandrasekhar *et al.* [7] reported that a concrete containing RHA exhibited improved mechanical properties. The authors also reported that RHA can be used as a replacement for silica fume. RHA-containing concrete has also been reported to exhibit good resistance to chloride penetration [8], good freeze-thaw performance [9, 10], good resistance to alkali-aggregate reaction (AAR) expansion [11], and improved resistance to dicing salt scaling [12].

RHA blended cementitious systems have the potential to improve sustainability and offer ecological, economic, energy, and durability benefits for the cement and concrete industries. However, existing RHA blended cementitious systems have practical limitations and challenges. These limitations and challenges reduce its acceptance and use in the cement and concrete industries. Limitations and challenges include:

- Increased water requirements, largely due to the cellular, honeycomb-like morphology. The internal surface area of a typical RHA ranges from 20 to 50 m^2/g (compared to Type I portland cement (PC) which is less than 1 m^2/g). This cellular, honeycomb-like morphology and high surface area leads to high absorption characteristics of RHA [9];
- Retarded early-age strength development as a result of the later pozzalanic reactions [7, 13-15]. The amorphous silica in the RHA particles reacts with portlandite [$Ca(OH)_2$] to form calcium-silicate-hydrate (C-S-H) gel. Yu *et al.* [3] reported that C-S-H gel forms from RHA and $Ca(OH)_2$ to produce floccules (groups of particles with relatively low densities and large pore spaces between these particles); and
- Reduced flow and workability characteristics of fresh concrete mixtures containing RHA [13, 16-18].

The challenge of reduced workability of RHA blended cementitious systems can be mitigated by adding more water. However, increasing the water content results in increased water-to-cementitious materials ratios (w/cm), resulting in reduced strength and durability. Because most specifications have strength requirements and earlier strengths are more economical to contractors than later-age strengths [19], the acceptance of RHA in the industry has not been widespread.

Researchers [20-22] have investigated the effect of RHA particle size on concrete performance and reported that smaller RHA particle sizes result in increased cement hydration reaction rates, reduced $Ca(OH)_2$ content, improved flow, earlier strength gain,

and improved durability. Researchers also reported that when smaller RHA particles were used in concrete, less water was required to achieve adequate flow characteristics [20]. The improved flow is reportedly due to improved particle size distribution, decreased cellular, honeycomb-like morphology, and enhanced particle packing [12, 23]. In most studies, researchers used mechanical grinding (e.g., ball-milling) to reduce the particle size of RHA and this process was reported to consume significant effort and energy [18, 24-27]. It has been reported that the energy requirement for grinding RHA particles to smaller sizes significantly increases as the required size decreases. In addition to the significant energy requirements, wear of mill and grinding components is costly. Although successive reductions in particle size can result in improved performance characteristics, obtaining these smaller particles can be cost prohibitive when mechanical grinding is required.

Further research is needed to identify more economical and more efficient alternatives to mechanical grinding of RHA such that this material can become a more widely used supplementary cementing material (SCM). Thus, recent research [28, 29] presented the development of a chemical transformation process; specifically, an alkali transformation process and the hydrated products formation of blended cementitious systems. This process has been reported to reduce the cellular, honeycomb-like morphology and particle size of RHA. The chemically transformed product, referred to as t-RHA, will be assessed herein for its influence on the characteristics of blended cement pastes and mortars. These characteristics include assessing the setting time, the chemical shrinkage (CS), flowability, compressive strength, hardened porosity, apparent chloride diffusivity coefficient (D_a), and morphology analysis of as-received RHA (AR-RHA) and t-RHA paste and mortar systems.

4.2 MATERIAL AND METHODS

4.2.1 *Material*

Type I/II PC with chemical composition as shown in Table 4-1 was used for all specimens. The cement met ASTM C150, *Standard Specification for Portland Cement* requirements. The AR-RHA was procured from a power plant in Lake Charles, LA. Its chemical composition is shown in Table 4-2. The carbon content of RHA (corresponding with the loss in ignition (LOI) of cement) is relatively high (2.09% to 7.59%) compared to PC (maximum limit of 3%). The high carbon content is reported to reduce the workability in fresh mixtures [30]. The average particle size of the AR-RHA is 192 μm with a standard deviation (σ) of 3.15 μm. Fine aggregate, used for the compressive strength specimens, was procured from a local source in Corvallis, OR and met ASTM requirements C33, *Standard Specification for Concrete Aggregates*. The fineness modulus of the fine aggregate is 2.5, determined following ASTM C136, *Standard Test Method for Sieve Analysis of Fine and Coarse Aggregates procedures.* The specific gravity (s.g.) of the fine aggregate is 2.47 and the absorption is 3.08%. The s.g. and absorption were determined following ASTM C128, *Standard Test Method for Density, Relative Density (Specific Gravity), and Absorption of Fine Aggregate*. Ottawa graded sand meeting ASTM C778, *Standard Specification for Standard Sand*, was used for the flowability, D_a, porosity, and morphology specimens. Type II de-ionized (DI) water (1 MΩ·cm at 25˚C) was used for all mixtures and experiments. Pellet sodium hydroxide (NaOH) was American Chemical Society (ACS) grade and was used for the alkali solution. Polyvinyl alcohol (PVA) powder with molecular weight of 1750 ± 50 atomic mass units was used as a dispersing agent for some mixtures.

Table 4-1. Chemical composition and specification requirements meeting ASTM C150 of PC

Composition	Spec. requirement (%)	(%)
SiO_2	-	20.30
Al_2O_3	6.0 max	4.80
Fe_2O_3	6.0 max	3.50
MgO	6.0 max	0.70
SO_3	3.0 max	2.80
CaO	-	63.9
Loss on Ignition	3.0 max	2.60
Insoluble Residue	0.75 max	0.11
Limestone	5.0 max	3.20
$CaCO_3$ in Limestone	70 min	97.80
Na_{eq}	0.6 max	0.54

Table 4-2. Chemical composition of AR-RHA

Composition	(%)*
SiO_2	89.65 - 96.90
C	2.09 - 7.59
Al_2O_3	0.006 - 0.039
Fe_2O_3	0.006 - 0.052
CaO	0.48 - 0.81
MgO	0.13 - 0.53
SO_3	0.018 - 0.24
Na_2O	0.018 - 0.18
K_2O	1.74 - 2.69
Ti_2O_3	0.003 - 0.020
P_2O_5	0.74 -1.23
Mn_3O_4	0.00 - 0.20

*Provided by manufacturer

4.2.2 *Chemical Morphological Transformation Method*

Recent studies [31-33] on the chemical treatment of RHA indicate that the amorphous silica in the RHA can be transformed into soluble silicate ions using an alkali extraction method. Prasittisopin and Trejo [28] provided a comprehensive description of a chemical transformation method based on the extraction method using NaOH. The AR-RHA was mixed with a 2M NaOH solution for 3 hours and resulted in an average particle size of 28 μm (from 192 μm). The RHA chemical transformation method is reported to increase the silicate ion concentration in solution, reduce the particle size, and eliminate the cellular,

honeycomb-like morphology [28]. Reducing particle size and reducing the degree of cellular morphology should make RHA more user-friendly. However, Prasittisopin and Trejo [28] also reported that not only the silicate ions dissolve into solution, but the sodium content is high and could affect other characteristics.

Although the chemical transformation of the RHA can provide benefits, it should be noted that the increase of silicate and sodium ion concentrations can influence the cement hydration and setting behavior of cementitious systems [29]. Schutz [34] reported that silicate ions in solution can affect set behavior. Increasing silicate ions in solution can result in decreased setting time. Juenger and Jennings [35] investigated the effects of sodium ions in solution on cement pastes. The authors reported that cement pastes having 1M NaOH solution exhibits faster hydration reactions and increased early-age strength when compared with cement pastes without NaOH solution. As a result, faster setting time and faster hydration reactions of the t-RHA blended cementitious systems would be expected, although studies are needed.

4.2.3 *Preparation of t-RHA*

The t-RHA slurry was prepared by mixing AR-RHA with 2M NaOH solution using a laboratory magnetic stirrer at a mixing rate of 400 rpm. Mixing was performed at 23˚C ± 2˚C. Although earlier studies by Kalapathy *et al.* [31] and Kamath and Proctor [36] evaluated the alkali extraction method using heat to improve the alkali extraction process, no heat was used to transform the RHA due to concerns regarding energy-consumption and sustainability. Details on the transformation process can be found on Trejo and Prasittisopin [28].

4.2.4 *Experimental Procedures*

4.2.4.1 RHA Blended Cementitious Systems

Six mixtures were assessed in this study: control, AR-RHA, t-RHA, t-RHA+PVA, a combination of 50% AR-RHA and 50% t-RHA (C-RHA), and an untransformed RHA

(ut-RHA). The control system is 100% PC mixture. The AR-RHA system contained the as-received RHA. The t-RHA system contained t-RHA as the SCM. Because of initial concerns with dispersion of the RHA particles, one mixture included PVA as a dispersant. The C-RHA system contained 50% AR-RHA and 50% t-RHA. To compare the influence of the NaOH solution in the t-RHA, the system containing NaOH solution with AR-RHA was also evaluated. Note that the AR-RHA was not processed and transformed. All test results were based on triplicate tests.

Mixing of the cement pastes and mortars followed ASTM C305, *Standard Practice for Mechanical Mixing of Hydraulic Cement Pastes and Mortars of Plastic Consistency*. The w/cm value was 0.4 for all paste specimens (for setting time and CS). The w/cm value of all mortar specimens was 0.485 and the cementitious material-fine aggregate ratio was 1:2.75 (for flowability, compressive strength, porosity, D_a, and morphology). The mixtures were prepared with 10% and 15% (by mass) RHA replacement levels. Table 4-3 shows the experimental program.

Table 4-3. Experimental program and characterization methods

Systems	Characterization methods						
	Flow	Setting time	CS	Compressive strength	Porosity	D_a	SEM-EDX
Control	✓	✓	✓	✓	✓	✓	✓
AR-RHA	✓	✓	✓	✓	✓	✓	✓
t-RHA	✓	✓	✓	✓	✓	✓	✓
t-RHA+PVA	✓	✓	✓	✓	✓	✓	x
C-RHA	✓	✓	✓	x	x	x	x
ut-RHA	x	x	x	✓	x	x	x

✓ – tested x – not tested

The alkali content of the systems containing t-RHA at 10% and 15% replacement levels was 2.96% and 4.18%, respectively. Note that the alkali contents of the systems are high and could result in long-term performance challenges. Because of this, a filtration process to separate the sodium and hydroxyl ions in solution from the t-RHA solids was evaluated to determine if the process can be used to reduce the alkali content. A simple study determined that approximately 70% by weight of the sodium ions in solution can be

removed in as little as 3 minutes. However, all tests in this research assessed the t-RHA solution with high alkali conditions (2.96% and 4.18%). Further research will be performed to assess and characterize the performance of the RHA blended cementitious systems with lower alkali content (i.e., filtered t-RHA).

4.2.4.2 Characterization Methods

The different RHA systems were characterized for flowability, setting time, CS, compressive strength, porosity, D_a, and morphology analysis. The flowability was determined following ASTM C1437, *Standard Test Method for Flow of Hydraulic Cement Mortar*. The setting time was determined following ASTM C191, *Standard Test Methods for Time of Setting of Hydraulic Cement by Vicat Needle.* The CS was assessed following ASTM C1608 (procedure A), *Standard Test Method for Chemical Shrinkage of Hydraulic Cement Paste*. The 1-, 7-, and 28-day compressive strengths were determined following ASTM C109/C109M, *Standard Test Method for Compressive Strength of Hydraulic Cement Mortars (Using 2-in. or [50-mm] Cube Specimens)*. The 28-day porosity of the hardened mortars was determined following a modified procedure of ASTM C642, *Standard Test Method for Density, Absorption, and Voids in Hardened Concrete*. The D_a was evaluated following ASTM C1556, *Apparent Chloride Diffusion Coefficient of Cementitious Mixtures by Bulk Diffusion* and ASTM C1152, *Standard Test Method for Acid-Soluble Chloride in Mortar and Concrete*.

Results of the flowability (discussed later) indicated that increased RHA replacement levels resulted in reduced flow. Reduced flows of the fresh mixtures can lead to additional energy inputs for consolidation. To control the consolidation energy input for each porosity specimen, the consolidation process was standardized in this study. A schematic diagram of the consolidation process for testing the porosity of hardened mortars is shown in Figure 4-1. A hopper placed above the top of a casting mold was used to ensure that each mixture had similar consolidation energy during fabrication. About half of the first layer of mortar was placed in the hopper. After placing the hopper, the bottom trap door was opened, allowing the mortar to free fall into the mold.

Immediately after free-falling, a vibrating table was activated for 5 seconds. After the vibrating table was turned off, the same process was repeated to fill the second layer. After placing and vibrating the fresh mortars, the top surface of the specimens was struck-off and smoothed using a trowel. This process is believed to provide the same consolidation energy input for each specimen, thereby allowing for standardized consolidation process to be used to assess the influence of RHA content on the porosity.

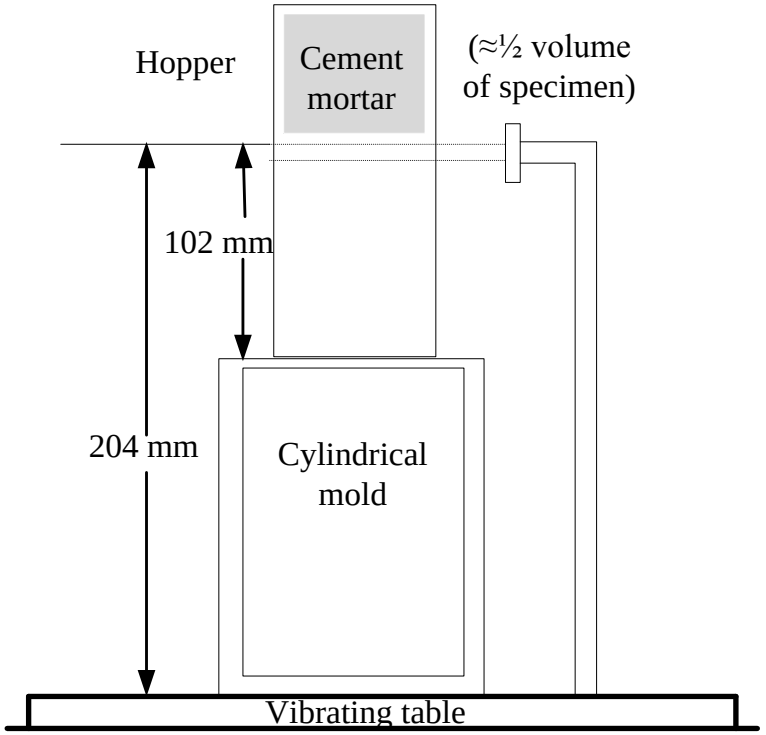

Figure 4-1. Diagram of consolidating equipment for porosity testing.

Specimens for assessing the morphology of the control mortars and the mortars containing AR-RHA and t-RHA were cured for 28 days and then examined using the Scanning Electron Microscope (SEM) and Energy Dispersive X-Ray Analysis (EDX). The SEM and EDX analyses only evaluated specimens containing 10% replacement levels.

4.2.4.3 Statistical Analysis

Two-sample t-test and analysis of variances (ANOVA) analyses were performed to compare the sample means of two groups and more than two groups, respectively. The Shapiro-Wilk test was used to determine if data were normally distributed and the Levene's test was used to determine if the data sets had equal variance prior to the analyses. The statistical hypotheses for the analyses are defined as:

$$\text{Null hypothesis } (H_0): \mu_1 = \mu_2 = \ldots = \mu_a \quad (4\text{-}1)$$

$$\text{Alternative hypothesis } (H_a): \mu_i \neq \mu_j \text{ for some } i \neq j \quad (4\text{-}2)$$

The 95% confidence interval was used in these analyses. If the H_0 is rejected (p-value $\leq$ 0.05), it is concluded that there is a statistically significant effect at the 5% level between the means of the different group populations. Alternatively, if the H_0 is not rejected (p-value > 0.05), it can be concluded that there is no statistically significant effect at the 5% level between the means of the different group populations.

4.3 RESULTS AND DISCUSSION

4.3.1 *Flowability*

The flow of the different RHA blended cementitious systems as a function of RHA content is shown in Figure 4-2. Results for the control mixtures are also shown in this figure. Results indicate there is a significant reduction in flow of fresh mortars when replacing cement with AR-RHA. Replacing the cement with 10% AR-RHA results in a 15% reduction in flow (182 mm to 154 mm) and replacing the cement with 15% AR-RHA results in a 25% reduction in flow (182 mm to 137 mm). As discussed, the reduction of flow of the AR-RHA is caused by the cellular, honeycomb-like morphology of AR-RHA that absorbs water. Therefore, less water is available for flow.

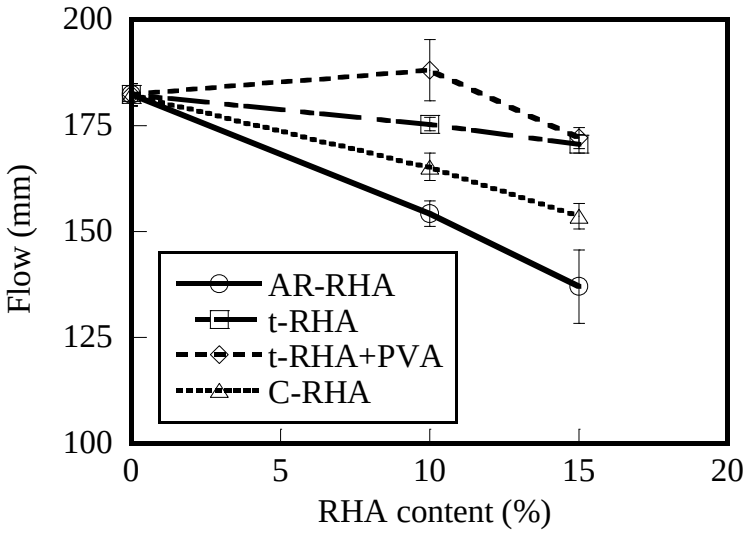

Figure 4-2. Effect of RHA type and content on flow.

Results also indicate that replacing the cement with t-RHA, and C-RHA exhibits reduced flow when compared with the control mixtures. However, the t-RHA and C-RHA systems exhibit higher flow values than the AR-RHA system. Replacing the cement with 10% and 15% t-RHA results in a 4% (182 mm to 175 mm) and 6% (182 mm to 171 mm) reduction in flow when compared with the control system, respectively. There is no significant difference in flow between the control and the 10% t-RHA+PVA system (two-sample t-test with p-value = 0.187). However, the flow of the 15% t-RHA+PVA system is 6% less than the flow of the control system (182 mm to 172 mm). Replacing the cement with 10% and 15% C-RHA results in a 9% (182 mm to 165 mm) and 15% (182 mm to 154 mm) reduction in flow, respectively. Trejo and Prasittisopin [28] reported that the chemical transformation of the RHA eliminates of the cellular, honeycomb-like morphology and should lead to reduced RHA absorption, and improved flow of the mixtures.

4.3.2 *Setting Time*

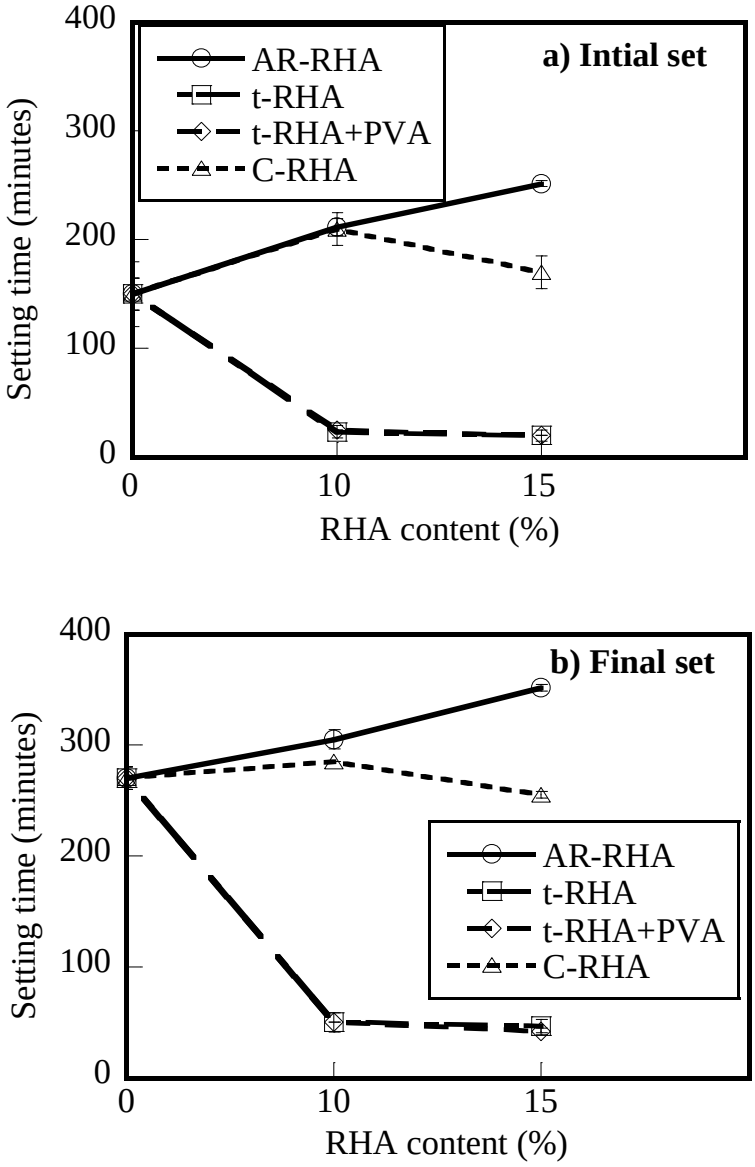

Figure 4-3. Effect of RHA type and content on a) initial setting time and b) final setting time.

The effects of the different RHA systems (AR-RHA, t-RHA, t-RHA+PVA, and C-RHA) and RHA contents (0%, 10%, and 15%) on the initial and final setting times are shown in

Figures 4-3a and 4-3b, respectively. Results indicate that both initial and final setting times of the AR-RHA systems increase with increasing AR-RHA content. Increased setting times tend to correspond with delayed hydration, which is likely a result of the lower cement contents and the slower pozzalanic reactions. Delayed hydration occurs due to more gypsum is present in the AR-RHA systems [29].

the t-RHA and t-RHA+PVA systems exhibit different setting characteristics than the AR-RHA system. The t-RHA and t-RHA+PVA systems exhibit a reduction in setting time. It is believed that the reduction in setting time corresponds with the effect of 1) smaller t-RHA particles, 2) the NaOH addition (for transformation), and 3) increased silicate ion concentration in solution (from transformation). The 1% addition of PVA to the RHA systems shows no significant effect on the setting times.

The 10% and 15% t-RHA systems exhibited initial setting times of approximately 40 and 45 minutes, respectively, which may be too fast for practical applications. The 10% and 15% AR-RHA systems exhibited initial setting times of 205 and 250 minutes, respectively, which could be too long for practical applications. If the setting time is too fast or too slow, construction challenges or higher costs could be encountered. Therefore, the researchers propose to manipulate the setting times of the t-RHA system by proportioning the AR-RHA and t-RHA (i.e., C-RHA as shown in Table 4-3). The 10% and 15% C-RHA systems resulted in the initial setting time of approximately 205 and 165 minutes. The final setting time of the 10% and 15% C-RHA systems were approximately 285 and 255 minutes, respectively. The initial and final setting times of the C-RHA systems are similar to the control system, making them appropriate for most concrete placements. The setting times of the RHA systems can be manipulated by replacing cement with different proportions of AR-RHA and t-RHA.

4.3.3 *Chemical Shrinkage*

The influence of the control system and systems containing AR-RHA, t-RHA, and C-RHA at 10% and 15% replacement levels on the CS at early ages is shown in Figures 4-4a, 4-4b, and 4-4c, respectively.

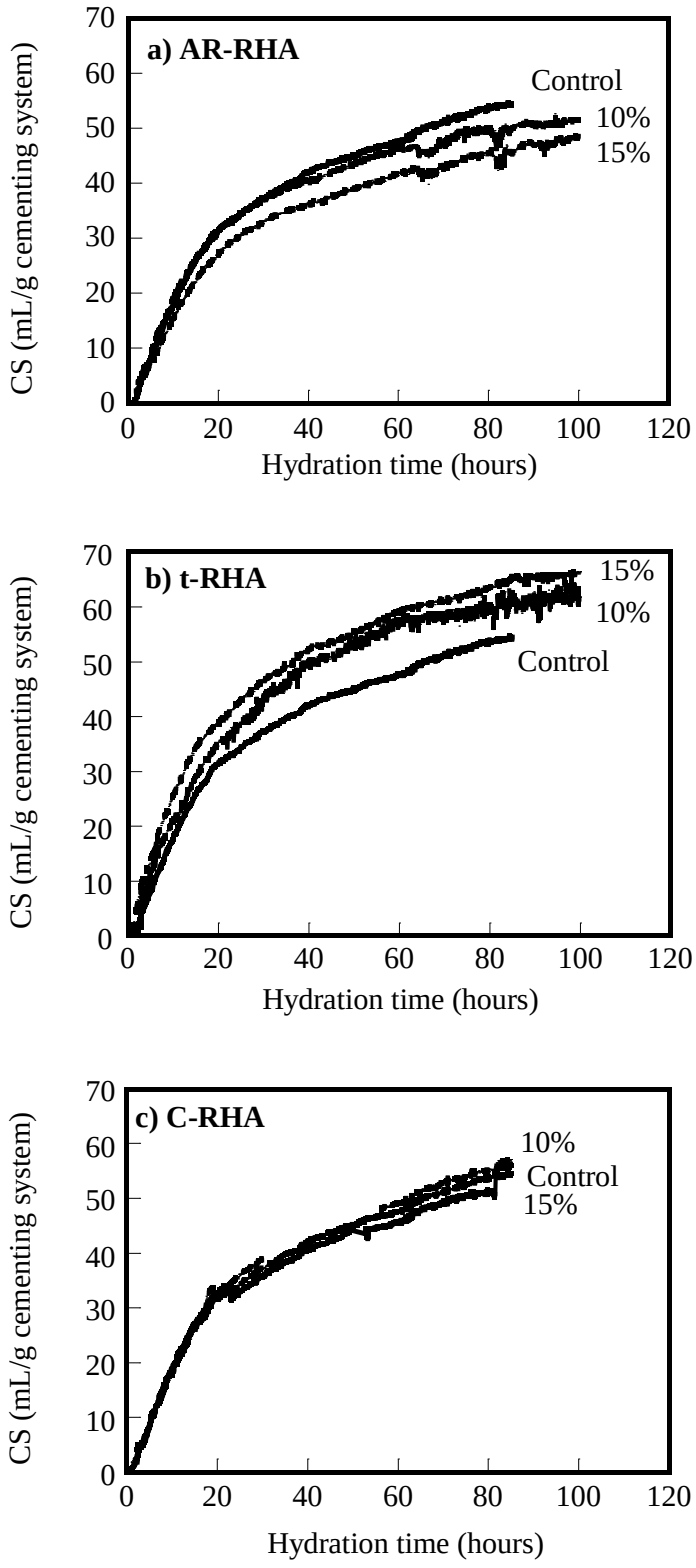

Figure 4-4. Effect of a) AR-RHA, b) t-RHA, and c) C-RHA content on CS.

Results in Figure 4-4a indicate that the CS values of the AR-RHA system are lower than the control system and increasing the replacement level of AR-RHA results in further reduction in CS values. It is believed that the AR-RHA initially acts as an inert filler. In addition, because the overall system contains lower amounts of cement, it would be expected that systems containing these "inert" fillers would exhibit lower CS values. Figure 4-4b shows the CS of the t-RHA systems. Results indicate that the CS values of the t-RHA systems are higher than the control system. Unlike the results of the AR-RHA systems, the t-RHA systems showed increased CS values with increasing t-RHA replacement level. Lura et al. [37] reported that the higher CS is a result of the increased hydration reaction rates. Although these systems contain lower cement contents, the smaller t-RHA particles, the addition of NaOH, and the increase in silicate ion concentration affect the rates of hydration, consequently resulting in faster hydration reactions and increased CS. Increased CS may lead to higher risks of cracking at early ages. Thus, the CS of the C-RHA system was assessed and results are shown in Figure 4-4c. Results for the C-RHA systems indicate that the CS values of the C-RHA seem not to be significantly different from the control. As with the setting time, CS can be manipulated by proportioning the percentage of AR-RHA and t-RHA.

4.3.4 *Compressive Strength*

It has been reported that the early-age compressive strength of RHA blended cementitious systems is lower than systems without RHA [7, 13, 14, 38]. Compressive strength ratios for the different RHA systems and control system are shown in Figures 4-5a, 4-5b, 4-5c, and 4-5d. Note that this ratio is compared for each test time – that is, the compressive strength of the RHA system at day 1 (or day *t*), is divided by the compressive strength of the control at day 1 (or day *t*). The average compressive strength of the control system (PC only) for 1, 7, and 28 days is 15, 25, and 56 MPa, respectively.

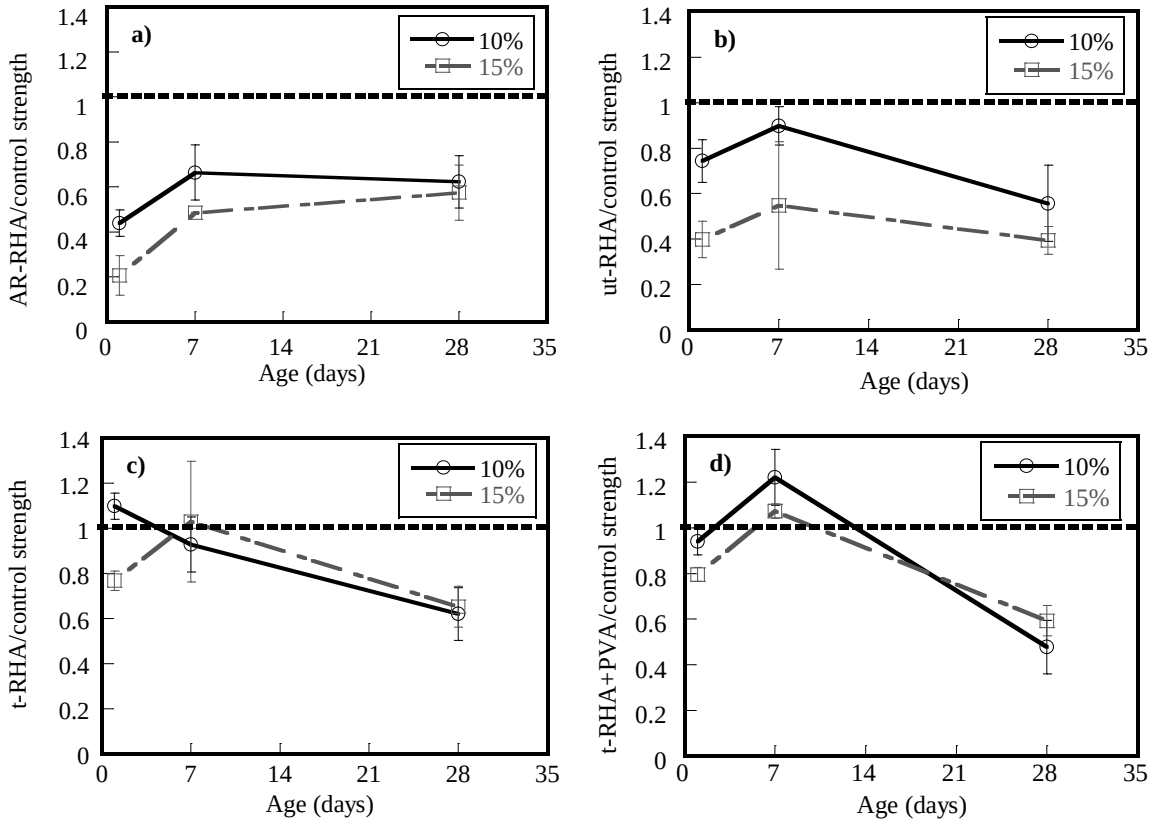

Figure 4-5. Effect of curing age on compressive strength of a) AR-RHA, b) ut-RHA, c) t-RHA, and d) t-RHA+PVA; blended cementitious systems with 10% and 15% replacement levels.

Figure 4-5a shows the compressive strength ratio of AR-RHA/control as a function of age. Results indicate that the ratio of the 10% and 15% AR-RHA systems are significantly lower than the control system at all ages. This lower compressive strength is believed to be a result of the delayed pozzalanic reactions between the PC and AR-RHA. It has been reported that the lower compressive strength of the AR-RHA system could be caused by higher porosity of the AR-RHA system due to less efficient packing of coarse RHA particles [18, 39]. Comparison of means indicates that there is a significant difference between the compressive strength of the AR-RHA and the control system at all ages. In addition, the 1- and 7-day compressive strengths of the 10% AR-RHA system are significantly different from the 15% AR-RHA system (two-sample t-test with p-value =

0.019 and 0.00, respectively). The 28-day compressive strength between the 10% and 15% AR-RHA systems is not significantly different (two-sample t-test with p-value = 0.648). The results here indicate that replacing PC with AR-RHA affects the compressive strength. Replacement levels influence the early-age compressive strengths (i.e., 1- and 7-day), but not the 28-day compressive strength.

The compressive strength ratio of the ut-RHA/control as a function of age is shown in Figure 4-5b. Comparison of means indicates that there is a significant difference of the compressive strengths between the ut-RHA and the control system at all ages. The 1-day compressive strengths of the 10% ut-RHA system is significantly different from the 15% ut-RHA system (two-sample t-test with p-value = 0.009), but the 7- and 28-day compressive strengths of the 10% ut-RHA system are not significantly different from the 15% ut-RHA system (two-sample t-test with p-value = 0.108 and 0.199, respectively). Results also indicate that the 1- and 7-day compressive strengths of the ut-RHA systems are higher than the AR-RHA systems for both replacement levels. The 28-day compressive strength of the 10% ut-RHA system is not significantly different than the 10% AR-RHA system (two-sample t-test with p-value = 0.610). However, the 28-day compressive strength of the 15% ut-RHA system is 31% lower than the 15% AR-RHA system (two-sample t-test with p-value = 0.027). Many researchers [40-42] have reported that the NaOH addition results in higher early-age strengths, but lower ultimate strengths after 28 days.

The plot of compressive strength ratio of t-RHA/control versus age is shown in Figure 4-5c. Results indicate that the 1- and 7-day compressive strengths of the t-RHA systems are similar to the control system. The 28-day compressive strength of the 10% and 15% t-RHA systems is 38% and 35% lower than the control system (two-sample t-test with p-value = 0.011 and 0.009), respectively. There is a significant difference in means for the 1-day compressive strength between the 10% and the 15% t-RHA systems (two-sample t-test with p-value = 0.00), but there is no significant difference for 7- and 28-day compressive strengths (two-sample t-test with p-value = 0.011 and 0.009, respectively). In addition, comparing the compressive strength of the t-RHA systems

(shown in Figure 4-5c) with the AR-RHA systems (shown in Figure 4-5a) indicates that the 1- and 7-day strengths of the t-RHA systems are higher than the AR-RHA systems, but the 28-day strength of the t-RHA systems is not significantly different than the AR-RHA systems (two-sample t-test with p-value = 0.98 for the 10% RHA system and 0.175 for the 15% RHA system). As a result, the addition of NaOH of the t-RHA leads to higher 1- and 7-day compressive strengths than the AR-RHA, but has no effect on 28-day compressive strength. Comparing the compressive strength of the t-RHA systems (shown in Figure 4-5c) with the ut-RHA systems (shown in Figure 4-5b) indicates that the 1- and 7-day strengths of the ut-RHA systems are lower than the t-RHA systems. This difference is a result of the chemical transformation of RHA. The 28-day strength of the 10% ut-RHA system is not significantly different than the 10% t-RHA system (two-sample t-test with p-value = 0.593). However, the 28-day strength of the 15% ut-RHA system is 40% lower than the 15% t-RHA system (two-sample t-test with p-value 0.004). The higher 1- and 7-day compressive strengths of the t-RHA systems is a result of the combination of 1) smaller t-RHA particles and 2) the additional NaOH solution. The smaller t-RHA particles result in faster hydration and denser constituent particle packing (discussed later), and this consequently results in higher strength.

The compressive strength ratio of t-RHA+PVA/control as a function of age is shown in Figure 4-5d. Like the results of the t-RHA systems shown in Figure 4-5c, the 1- and 7-day compressive strengths of the t-RHA+PVA systems are similar to the control system. The 28-day compressive strength is also lower than the control system. In fact, the 1-, 7-, and 28-day strengths of the t-RHA+PVA systems are not significantly different from the t-RHA systems (two-sample t-test with p-value = 0.125, 0.424, and 0.559, respectively), indicating that the PVA addition as a dispersant tends not to influence the strength development of the t-RHA.

Results from this research indicate that the 1- and 7-day compressive strengths of the t-RHA systems are similar to the control system. The compressive strengths of the systems containing t-RHA are also higher than the systems containing AR-RHA. The 28-

day compressive strength of all RHA-containing systems (all types) is significantly lower than the control system (ranges from 40% to 63%).

4.3.5 *Porosity*

Porosity of hardened cementitious systems corresponds to their constituent particle packing and presence of voids. Efficient particle packing is believed to allow the hardened mixture to have fewer inter-particle spaces, lower entrapped air content, higher bulk density, and lower permeability and diffusivity, leading to improved performance characteristics. As discussed, lower compressive strength of the AR-RHA systems may be caused by higher porosity of the system.

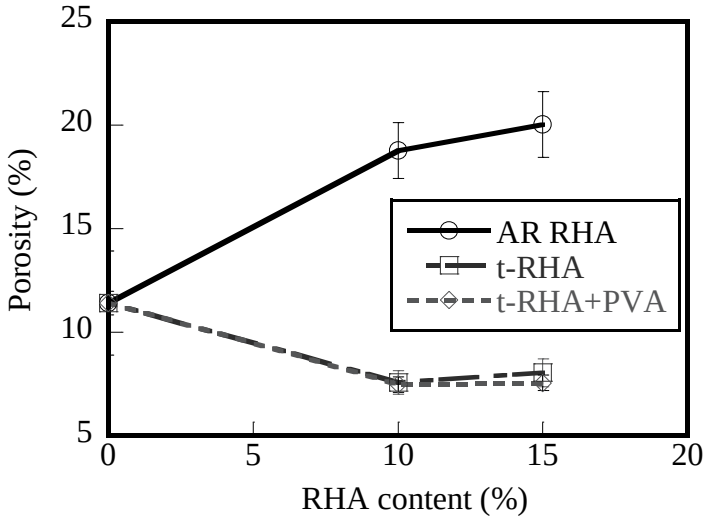

Figure 4-6. Effect of replacement level of AR-RHA, t-RHA, and t-RHA+PVA blended cementitious systems on 28-day porosity.

Figure 4-6 shows the influence of RHA replacement level and RHA type on the 28-day porosity (recall that all systems were cast using the same consolidation energy input). Results indicate that increasing the AR-RHA replacement levels result in increased 28-day porosity. The 28-day porosity of the 10% and 15% AR-RHA systems is

approximately 64% and 75% higher than the control system, respectively. The porosity of the t-RHA system decreases with increasing replacement levels. The porosity of the 10% and 15% t-RHA systems is 34% and 30% lower than the control system, respectively. No significant difference in means was observed for the different replacement levels for the AR-RHA (two-sample t-test with p-value = 0.353) and t-RHA systems (two-sample t-test with p-value = 0.407). Figure 4-6 also shows the porosity of the t-RHA+PVA systems. The addition of PVA seems to have limited effects on the porosity of t-RHA mortars. Replacing cement with t-RHA results in reduced 28-day porosity when compared with the control system, indicating that mixtures containing t-RHA would likely be easier to place when compared with mixtures containing AR-RHA.

4.3.6 *Apparent Chloride Diffusivity*

Figure 4-7 shows the influence of the replacement level of AR-RHA, t-RHA, and t-RHA+PVA systems on the D_a. Results indicate that replacing cement with AR-RHA results in reduced D_a values. The D_a of the 10% and 15% AR-RHA systems are both approximately 60% lower than the control system (two-sample t-test with p-value = 0.007 and 0.009), respectively. Maeda *et al.* [43] reported that the D_a values of concretes containing RHA for different w/cm values was approximately 25% to 57% lower than the 100% PC concretes. Although the hardened porosity of the AR-RHA system is higher than the control system, the D_a of the AR-RHA system is significantly lower than the control system. Rodrigues *et al.* [44] reported that the replacement of cement with RHA resulted in a modified pore structure of the hydrated cement paste. This modified pore structure reduces the interconnection of the pore networks and leads to lower transport rates. The AR-RHA particles, which have high absorption characteristics, may also capture chloride ions in the cellular morphology, thereby "binding" the chloride ions and reducing the transport into the AR-RHA systems.

Results indicate that replacing cement with the t-RHA also results in reduced D_a. The D_a values of the 10% and 15% t-RHA systems are 58% and 62% lower than the control system (two-sample t-test with p-value = 0.026 and 0.009), respectively. Because

the cellular, honeycomb-like morphology of the AR-RHA is no longer present in the t-RHA, the absorption of chloride ions is likely not the reason for the reduced diffusivity. However, it is thought that as the particles of t-RHA become smaller, the system containing the t-RHA exhibits faster hydration, densifying the mixture (more than the control), thus reducing the D_a values. The results indicate that the 10% and 15% AR-RHA systems exhibits little difference in the D_a between the 10% and 15% t-RHA system (two-sample t-test with p-value = 0.687 and 0.814, respectively). Although the RHA transformation process does not seem to significantly reduce the D_a when compared with AR-RHA, different mechanisms of these two systems seem to be present (absorption versus blocking). The study of D_a of the t-RHA+PVA system was also investigated. Results indicate that the D_a of the t-RHA systems is not influenced by the addition of PVA.

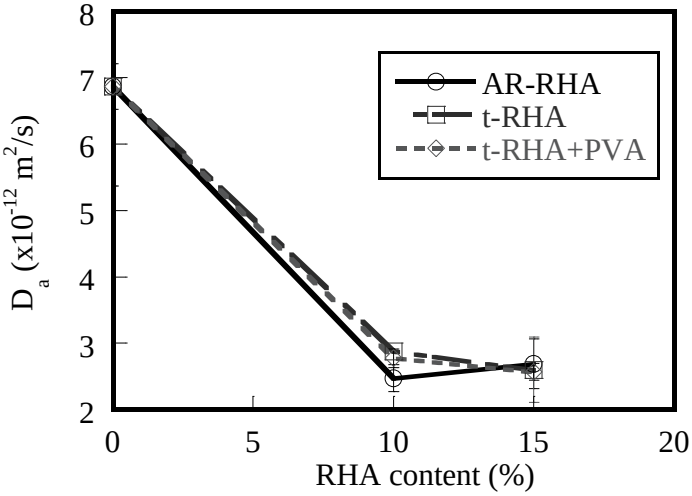

Figure 4-7. Effect of replacement level of AR-RHA, t-RHA, and t-RHA+PVA blended cementitious systems on D_a exposed for 35 days.

4.3.7 *Morphology*

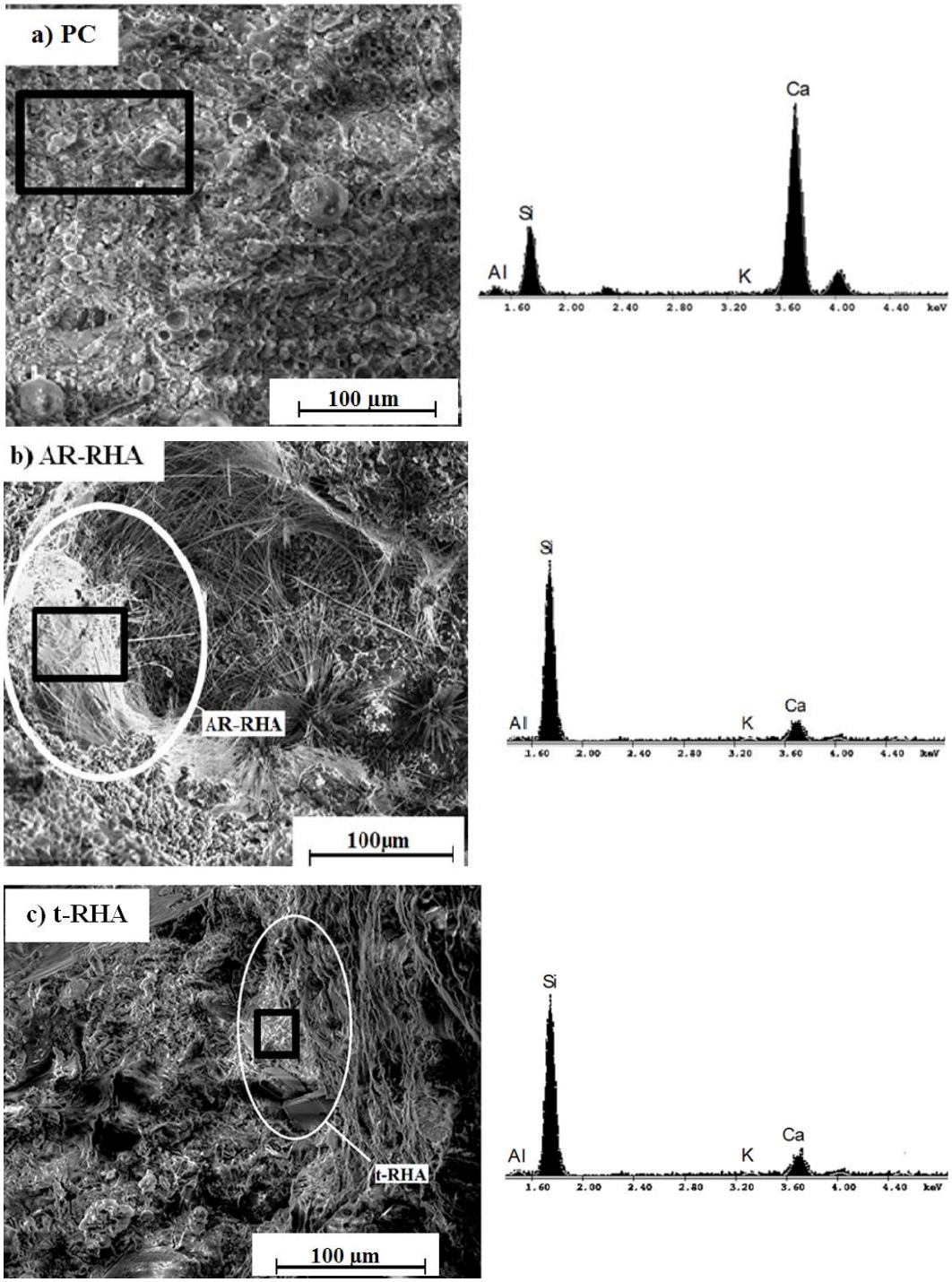

Figure 4-8. SEM images of a) control, b) 10% AR-RHA, and c) 10% t-RHA blended cementitious systems cured for 28 days and EDX spectrums of the areas marked by the black-squares.

The SEM images with the EDX spectra of the hydrated mortars for the control, 10% AR-RHA, and 10% t-RHA systems are shown in Figures 4-8a, 4-8b, and 4-8c, respectively. The morphology of the control system (shown in Figure 4-8a) exhibited relatively smooth surfaces throughout the inspected surfaces and EDX indicates the chemical composition to be mainly calcium and silica. The morphology and EDX spectra of the AR-RHA system (shown in Figure 4-8b) exhibited rougher surfaces and as expected, unhydrated AR-RHA particles are present throughout the matrix (in circle). In addition, fibrous-like particles from the original AR-RHA, which contain mainly silica, are present in the morphology of the system. A SEM image and EDX spectra of the t-RHA system is shown in Figure 4-8c. This figure shows shorter fibrous-like silica particles and particles with the cellular, honeycomb-like morphology were no identified. This was the case for most surfaces observed.

4.3.8 *Correlation of Flowability and Porosity versus RHA Particle Size*

The correlation of flowability and average particle size of RHA of the blended cementitious systems is shown in Figure 4-9a. Results indicate that the flowability of the fresh mortars is lower for systems containing larger RHA particles. Results indicate that an 87% reduction in the RHA particle size results in 12% and 20% increase in flowability of the 10% and 15% RHA systems, respectively. As a result, the chemical transformation process developed to reduce particle size of RHA seems to be a promising method to mitigate the workability challenges of using RHA as an SCM for concrete construction.

Figure 4-9b shows a plot of the 28-day porosity versus the average RHA particle size of the RHA blended systems. Results indicate the 28-day porosity of the mortars is lower for systems containing smaller RHA particles. This indicates that for the same energy input, smaller RHA particles will result in high-degrees of consolidation and/or particle packing.

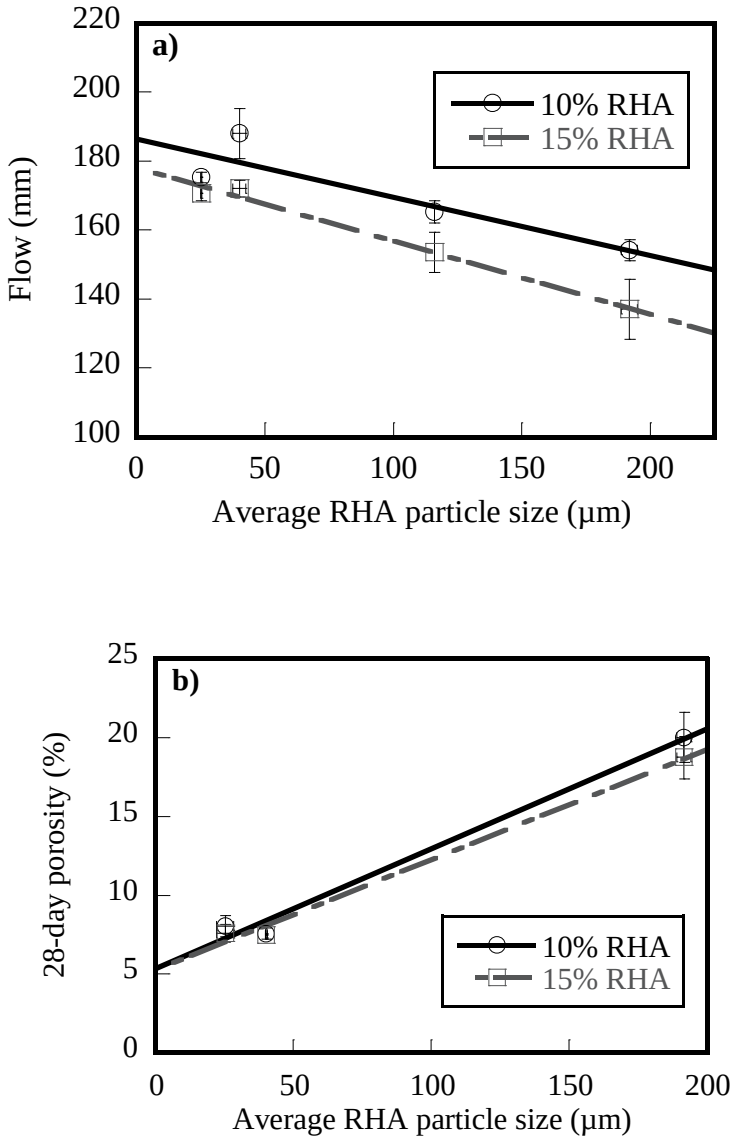

Figure 4-9. Effect of average RHA particle size on a) flow and b) 28-day porosity of RHA blended cementitious systems at 10% and 15% replacement levels.

4.4 CONCLUSIONS

An investigation assessing the influence of chemically transforming the morphology of RHA (t-RHA) and using this product as an SCM was performed. Results indicate that:

- The t-RHA systems exhibited better flow characteristics than the AR-RHA systems and exhibited slightly lower flow values than the control system.
- The t-RHA systems exhibited shorter setting times than the control system; the AR-RHA systems exhibited longer setting times than the control system; and a systems containing combination of these RHAs, C-RHA, exhibited similar setting times as the control system.
- The CS values of the t-RHA systems were higher than the control system, but the CS values of the AR-RHA systems were lower than the control system. The C-RHA systems exhibited similar CS to the control system.
- Compressive strengths of the t-RHA systems at 1 and 7 days were similar to the control PC system and higher than the AR-RHA systems; compressive strength of both AR-RHA and t-RHA systems at 28 days was lower than the control system.
- Porosity of the t-RHA systems was lower than the control and AR-RHA systems. Porosity of the AR-RHA systems was higher than the control system.
- The D_a of the t-RHA systems was lower than the control system but similar to the AR-RHA systems.

Results indicate that the alkali transformation process of the RHA morphology could be a promising alternative to mechanical grinding. This process can transform RHA, a waste product not commonly used in cementitious systems, into a more user friendly SCM. Although the feasibility of using t-RHA in blended cementitious systems is promising, further studies to develop an efficient filtration process to reduce alkali content are needed. In addition, the economy of chemically transforming the RHA needs to be assessed.

4.5 ACKNOWLEDGEMENTS

The authors express gratitude to Dr. W. Li, Agrilectric Companies, for providing the rice husk ash.

4.6 REFERENCES

[1] Della VP, Kuhn I, Hotza D. Rice husk ash as an alternate source for active silica production. Mater Letter. 2002;57(4):818-21.

[2] Nair DG, Fraaij A, Klaassen AAK, Kentgens APM. A structural investigation relating to the pozzolanic activity of rice husk ashes. Cem Con Res. 2008;38(6):861-9.

[3] Yu Q, Sawayama K, Sugita S, Shoya M, Isojima Y. The reaction between rice husk ash and $Ca(OH)_2$ solution and the nature of its product. Cem Con Res. 1999;29(1):37-43.

[4] Naiya TK, Bhattacharya AK, Mandal S, Das SK. The sorption of lead (II) ions on rice husk ash. J Hazard Mater. 2009;163(2-3):1254-64.

[5] Liou TH, Chang FW, Lo JJ. Pyrolysis kinetics of acid-leached rice husk. Indust & Eng Chem Res. 1997;36(3):568-73.

[6] Kibriya T. Performance of blended cement in high strength self compacting concrete. In: Cross B, editor. 17th Analys and Comput Specialty Conf at Structures. St. Louis, MI: 2006.

[7] Zhang MH, Malhotra VM. High-performance concrete incorporating rice husk ash as a supplementary cementing material. ACI Mater J. 1996;93(6):629-36.

[8] Chandrasekhar S, Satyanarayana KG, Pramada N, Raghavan P. Review processing, properties and applications of reactive silica from rice husk—an overview. J Mater Sci. 2003;38(15):3159-68.

[9] Nehdi M, Duqette J, El Damatty A. Performance of rice husk ash produced using a new technology as a mineral admixture in concrete. Cem Con Res. 2003;33(8):1203-10.

[10] Gastaldini ALG, Isaia GC, Gomes NS, Sperb JEK. Chloride penetration and carbonation in concrete with rice husk ash and chemical activators. Cem Con Comp. 2007;29:176-80.

[11] Shuichi S, Shoya M, Tokuda H. Evaluation of pozzolanic activity of rice husk ash. ACI SP. 1992;132:495-512.

[12] Mehta PK, Folliard KJ. Rice husk ash--a unique supplementary cementing material: Durability aspects. ACI SP. 1995;154:531-42.

[13] Mehta PK, Monteiro PJM. Concrete: Structure, properties, and materials. 3rd ed. New York: McGraw-Hill; 2006.

[14] Thomas JJ, Jennings HM, Allen AJ. The surface area of hardened cement paste as measured by various techniques. Concr Sci Eng. 1999;1(1):45-64.

[15] Rukzon S, Chindaprasirt P, Mahachai R. Effect of grinding on chemical and physical properties of rice husk ash. Inter J Minerals, Metall and Mater. 2009;16(2):242-7.

[16] Lothenbach B, Scrivener K, Hooton RD. Supplementary cementitious materials. Cem Con Res. 2011;41(3):217-29.

[17] Massazza F. Pozzolana and pozzolanic cements. In: Hewlett PC, editor. Lea's chemistry of cement and concrete. 4th ed. Oxford, UK: Butterworth-Heinemann;2008. p. 471-635.

[18] Bui DD, Hu J, Stroeven P. Particle size effect on the strength of rice husk ash blended gap-graded portland cement concrete. Cem & Con Comp. 2005;27(3):357-66.

[19] Reinschmidt K, Trejo D. Economic value of building faster. J Construc Eng Management. 2006;132(7):759-66.

[20] Stroeven P, Bui DD, Sabuni E. Ash of vegetable waste used for economic production of low to high strength hydraulic binders. Fuel. 1999;78(2):153-9.

[21] van Tuan N, Ye G, van Breugel K, Copuroglu O. Hydration and microstructure of ultra high performance concrete incorporating rice husk ash. Cem Con Res. 2011;41(11):1104-11.

[22] Feng Q, Yamamichi H, Shoya M, Sugita S. Study on the pozzolanic properties of rice husk ash by hydrochloric acid pretreatment. Cem Con Res. 2004;34(3):521-6.

[23] Rangaraju P, Harish KC. Optimization of use of rice husk ash for use as SCM in cementitious mortars. Conc Sustain Conf. Tempe, AZ: NRMCA; 2010.

[24] Chandrasekhar S, Pramada PN, Raghavan P, Satyanarayana KG, Gupta TN. Microsilica from rice husk as a possible substitute for condensed silica fume for high performance concrete. J Mater Sci Letters. 2002;21(16):1245-7.

[25] Datta A, Rajamani RK. A direct approach of modeling batch grinding in ball mills using population balance principles and impact energy distribution. Inter J Mineral Processing. 2002;64(4):181-200.

[26] Snow RH, Allen E, Ennis BJ, Litster JD. Size reduction and size enlargement. In: Perry RH, Green DW, editors. Perry's chemical engineers' handbook. New York: McGraw-Hill;2008.

[27] Lu D, Wei S. Effect of grinding aids on producing ultrafine particles. Adv Powder Tech. 1992;3(1):47-53.

[28] Trejo D., Prasittisopin L. Chemical transformation of rice husk ash morphology. 2014. (Under review)

[29] Prasittisopin L, Trejo D. Hydration and phase formation of blended cementitious systems incorporating chemically transformed rice husk ash. 2014. (Under review)

[30] Shearer CR, Yeboah N, Kurtis KE, Burns SE. The early-age behavior of biomass fired and co-fired fly ash in concrete. WOCA conf. Denver, CO2011.

[31] Kalapathy U, Proctor A, Shultz J. An improved method for production of silica from rice hull ash. Bioresor Tech. 2002;85(3):285-9.

[32] Kalapathy U, Proctor A, Shultz J. Silica xerogels from rice hull ash: Structure, density and mechanical strength as affected by gelation pH and silica concentration. J Chem Tech & Biotech. 2000;75(6):464-8.

[33] Kalapathy U, Proctor A, Shultz J. A simple method for production of pure silica from rice hull ash. Bioresor Tech. 2000;73(3):257-62.

[34] Schutz RJ. Admixtures and method for accelerating the setting of portland cement compositions. 1981.

[35] Juenger MCG, Jennings HM. Effects of high alkalinity on cement pastes. ACI Mat J. 2001;98(3):251-5.

[36] Kamath SR, Proctor A. Silica gel from rice hull ash: Preparation and characterization. Cereal Chem. 1998;75(4):484-7.

[37] Lura P, Couch J, Jensen OM, Weiss J. Early-age acoustic emission measurements in hydrating cement paste: Evidence for cavitation during solidification due to self-desiccation. Cem Con Res. 2009;39(10):861-7.

[38] Cizer Ö, Van Balen K, Elsen J, Van Gemert D. Carbonation and hydration of calcium hydroxide and calcium silicate binders with rice husk ash. 2nd Intern RILEM Symp "Advances in Concrete Through Science and Engineering". Quebec 2006. p. 13.

[39] Isaia GC, Gastaldini ALG, Moraes R. Physical and pozzolanic action of mineral additions on the mechanical strength of high-performance concrete. Cem Con Comp. 2003;25(1):69-76.

[40] Jawed I, Skalny J. Alkalies in cement: A review: II. Effects of alkalies on hydration and performance of portland cement. Cem Con Res. 1978;8(1):37-51.

[41] Osbaeck B. On the influence of alkalis on strength development of blended cements. British Ceramic Proc 1984. p. 375-83.

[42] Gouda GR. Microstructure and properties of high-alkali clinker. 8th Intern Congress on the Chemistry of Cement. Rio de Janeiro, Brazil: Alba Grafica e Editora Ltda; 1986. p. 234-9.

[43] Maeda N, Wada I, Kawakami M, Ueda T, Pushpalal GKD. Chloride diffusivity of concrete incorporating rice husk ash. ACI SP. 2001;200:291-308.

[44] Souza Rodrigues C, Ghavami K, Stroeven P. Rice husk ash as a supplementary raw material for the production of cellulose–cement composites with improved performance. Waste Biomass Valor. 2010;1(2):241-9.

5 EFFECTS OF MIXING VARIABLES ON EARLY-AGE CHARACTERISTICS OF PORTLAND CEMENT SYSTEMS

ABSTRACT

The performance and economy of infrastructure system is dependent on the specifications used to construct it. Good specifications contain requirements that correlate with improved performance and/or economy. There are several standards and specifications for mixing field concrete (AASHTO M157, ACI 304R, and ASTM C94). These documents provide requirements for the mixing process and limit placement time and the maximum number of truck drum revolutions. Forty-eight state highway agencies (SHAs) limit placement time and thirty SHAs limit number of drum revolutions. However, limited research has been performed on how mixing time and number of drum revolutions affect concrete characteristics. With advanced chemicals and technologies that can delay the set and extend the workability, the current recommendations and limits may not be applicable.

This work presents a laboratory assessment of pastes and mortars mixed for different times and varying number of mixer revolutions. It is anticipated that these results will be correlated with field study results at a later date. Early-age characteristics evaluated include the assessment of time-variant ion concentration in solution, flowability, setting time, and chemical shrinkage. Results indicate that these early-age characteristics of pastes and mortars mixed in the laboratory are influenced by the mixing time and number of mixer revolutions

Keywords: Mixing Time, Number of Mixer Revolutions, Early-age Characteristics, Ion Concentration, Flowability, Setting Time, Chemical Shrinkage.

Submitted to
American Concrete Institute Materials Journal

5.1 INTRODUCTION

The performance and economy of our infrastructure system are highly dependent on the standard specifications used to construct it. It is estimated that there are more than 2000 specifications for concrete in the US (Roumain 2004). Specifications that place limits on materials, suppliers, and/or contractors may result in increased construction and life cycle costs, especially if these specifications do not result in improved economy, constructability, or concrete performance. Hooton (2008) reported that historically prescriptive specifications should be switched to performance-based specifications so as not to limit the development of alternative materials and construction practices. These specifications include the standard specifications and guidelines for ready-mixed concrete.

Standard specifications and guidelines for ready-mixed concrete, including the American Concrete Institute (ACI) 304R, *Guide for Measuring, Mixing, Transporting, and Placing Concrete*, the American Society for Testing and Materials (ASTM) C94/C94M, *Specification for Ready-mixed Concrete*, and the American Association of State Highway and Transportation Officials (AASHTO) M157, *Standard Specification for Ready-Mixed Concrete*, place limits on the mixing time, concrete temperature, and total number of truck drum revolutions. Furthermore, forty-eight state highway agencies (SHAs) limit the mixing time; forty-five SHAs limit the concrete placement temperature; and thirty SHAs limit the total number of drum revolutions. These limits are in place because it is believed that mixing variables can influence the early- and later-age performance characteristics of concrete products. However, limited research has been performed to assess the influence of mixing time and number of drum revolutions on concrete performance. To better correlate specification values with the concrete performance, the influence of mixing variables on the performance of cementitious systems should be performed to better understand if value is being added. This research presents results from an initial research program to evaluate the effects of the laboratory mixing processes on the early-age characteristics of portland cement paste and mortar

system (not concrete). Research is also being performed on the hardened characteristics of pastes and mortars and on concrete systems. Results on the hardened characteristics and on the concrete systems for different mixing conditions will be presented in future publications.

5.2 BACKGROUND OF LABORATORY MIXING PROCESS

The concrete mixing process has been defined as the production method required for the complete blending to produce a homogeneous concrete (Mindess *et al.* 2002). The mixing process has been reported to influence the homogeneity and uniformity of concrete (Roy and Idorn 1993, Ferraris 2001, Rupnow *et al.* 2007). In fact, Rupnow *et al.* (2007) reported that the mixing process might influence the cement hydration and the interfacial transition zone (ITZ) between aggregates and cement paste. Roy and Idorn (1993) also reported that although the dispersion mechanism (mixing) of constituent particles in concrete was related to cement hydration, the quantification between mixing and hydration is needed. Ferraris (2001) reported that the relationship between the mixing process and macroscopic properties has not been clarified. The vagueness in how the mixing limits affect homogeneity and performance requires further investigations.

In addition, Charonnat and Beitzel (1997) studied the mixing of concrete and reported that (1) filling time, (2) mixing time, and (3) discharge time can all influence homogeneity and uniformity of concrete mixtures. The authors also reported that fresh concrete mixtures that were discharged too fast resulted in segregation due to excess mass flow energy. In addition, the degree of homogeneity and uniformity of concrete mixtures is reported to be dependent on mixture proportions, constituent material type and characteristics, velocity of the mixing tool, geometry of the mixer, and material and environmental conditions during mixing (Ferraris 2001). The following sections provide background on the mechanisms of mixing and how these mechanisms affect homogeneity and possibly early- and later-age characteristics of mixtures.

5.2.1 *Deformation Mechanisms of Mixing Process*

When water is first introduced to unhydrated cement particles (UCP) and the mixing process begins, two types of deformations occur between the water and the UCP. Fluid deformation from the constituent materials, referred to as a dispersive transport, occurs first and continues throughout the mixing process. This is typically associated with Brownian motion and no energy inputs. When mixing begins, mechanical deformation occurs, which is also referred to as a convective transport. Both transport types have been reported to influence the homogeneity of the mixtures (Lowke and Schiessl 2007).

The dispersive transport is a deformation process where individual particles (or smaller groups of particles) randomly collide. It is believed that these collisions only occur over relatively short distances, as no external forces are typically involved. Therefore, the dispersive transport results in some dispersion of the cement particles over shorter distance, but does not uniformly distribute these particles over larger volumes. However, this dispersive transport is believed to have a significant effect on the homogeneity of mixtures because it results in a significant increase of contact areas between the cement particles and the water molecules. This promotes localized homogeneous deformation, facilitates faster nucleation process, and improves a void coalescence (Lowke and Schiessl 2007). After water is introduced to the UCP, capillary forces between water molecules and the surfaces and micropores of constituent particles are created. These capillary forces result in surface tension within the water, and consequently make parts of water unable to disperse uniformly.

The convective transport is a forced, directed deformation. This deformation typically occurs over a larger distance because external energy is often being applied. The external energy from the mixing apparatus disperses constituent particles within the mixer. Lowke and Schiessl (2007) reported that the convective transport has less influence on the dispersion of the UCP than the dispersive transport. This is because during the dispersive transport, individual UCPs can disperse, leading to higher contact areas between the UCP and the water, but during the convective transport, the larger

groups of the UCP only move resulting in fewer contact areas. The convective transport can be divided into three distinct periods (adapted from Lowke and Schiessl 2007):

(1) The loading period (defined as the period when the mixing begins);

(2) The mixing period (defined as the period after mixing initiates up to some optimum mixing time); and

(3) The extended-mixing period (defined as the time after the optimum mixing time).

The loading period is the period when the constituent particles (the UCP and water) are introduced using external energy from a mixing apparatus. This typically occurs at lower shear rates. As the external energy is applied to the mixture, particles become more distributed. After the loading period is finished, the process moves into the mixing period. In this period, the degree of dispersion increases while the mixture is mixed at higher energies and higher shear rates. The degree of dispersion gradually increases to some maximum level within some reasonable time. Once (and if) the maximum level is achieved, the ultimate homogeneity of the fresh mixture is achieved, resulting in maximum flowability and/or workability. Mixing is likely to not improve the flowability after maximum dispersion is achieved. This is because the particles are uniformly dispersed and capillary forces between water molecules and the surfaces and micropores are reduced to some minimum value. However, if maximum dispersion is not achieved within the initial mixing period, an extended mixing period can be beneficial. The summary of the relationship between dispersion and deformation mechanisms of the mixing process is shown in **Fig. 5-1**.

The extended-mixing period can result in decreased dispersion and flowability (as shown in **Fig. 5-1**). It is believed that, as the convective deformation progresses, the cement particles become smaller and debris particles are generated due to impact and abrasion forces between the mixing apparatus and the constituent particles. This has been reported to result in a change of concrete microstructures and performance characteristics for self-consolidating concrete (SCC) (Takada 2004). Diamond (2005) reported that a

change of concrete microstructure was observed when concrete mixtures were mixed for longer periods (e.g., mixed for 90 minutes).

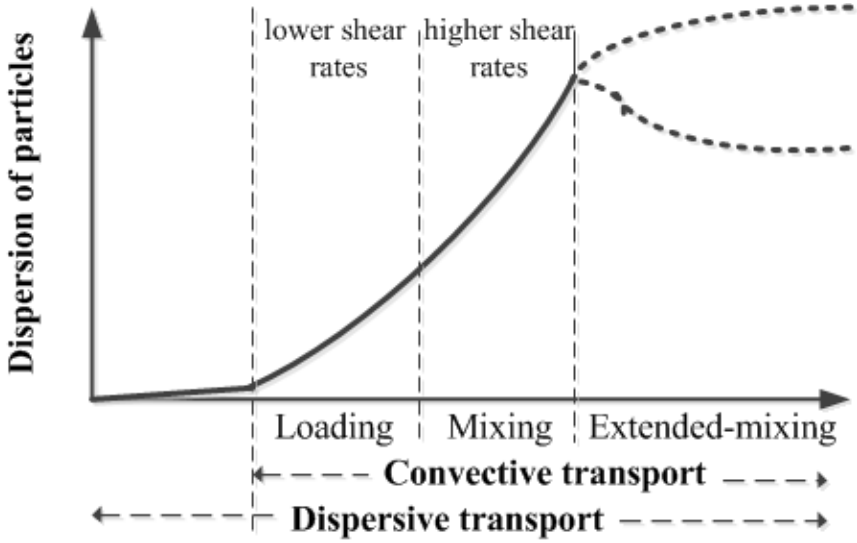

Fig. 5-1–Relationship between dispersion of particles and mixing mechanisms.

Several research programs have reported that mixing influences the homogeneity of the mixture. However, how this homogeneity influences mixture properties and characteristics has not been well documented. More research is needed to better understand a potential impact of mixing time and number of mixer revolutions on the performance of cementitious systems.

5.2.2 *Standard Laboratory Mixing Process*

ASTM C192, *Standard Practice for Making and Curing Concrete Test Specimens in the Laboratory*, is a common method for mixing concrete in the laboratory. The general procedure for mixing is shown in **Fig. 5-2** and includes the following periods:

- The loading period includes initial- and full-load mixing. Initial-load mixing includes adding the coarse aggregates, some of the batched water and liquid admixtures (dry admixtures are added to the cement prior to mixing). The full-

load mixing consists of adding the fine aggregates, the cement, and the remaining water;

- The mixing period includes mixing for 3 minutes, followed by a rest period for 3 minutes, and then mixing again for an additional 2 minutes. Additional mixing is allowed, if necessary; and
- The discharge period includes discharging the mixtures from the mixer.

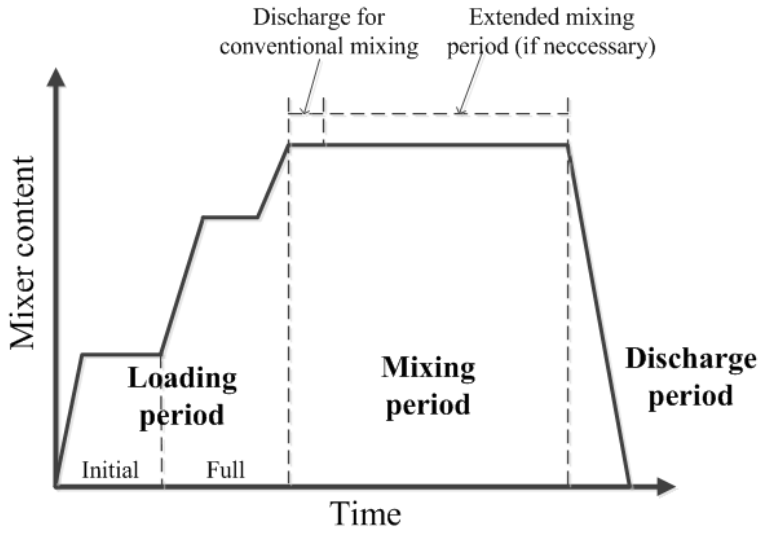

Fig. 5-2–Standard procedures for laboratory mixing and mixing with extended mixing period.

ASTM C192 is the standard procedure for laboratory mixing of concrete; ASTM C305, *Standard Practice for Mechanical Mixing of Hydraulic Cement Pastes and Mortars of Plastic Consistency*, is a standard for mixing cement pastes and mortars. This standard covers a two-stage mixing process: slow-speed mixing in the first stage followed by intermediate-speed mixing. Rejeb (1996) reported that the two-stage mixing process results in increased degree of homogeneity and uniformity of the mixtures because this process increases the available surface area between the hydrating cement particles and water. Although the laboratory mixing procedures are well-documented, the performance

of the final hydrated products between laboratory mixed materials and field mixed materials has not been well-correlated.

5.2.3 *Correlation of the Laboratory and the Field Study*

Correlation between many characteristics of paste, mortar, and concrete mixed in the laboratory and in the field is lacking. Rupnow *et al*. (2007) studied the two-step mixing process for cement paste, laboratory concrete, and field concrete mixing and reported that there was good correlation for concrete strength, slump, and air content between the laboratory and field mixed concretes. Saucier *et al.* (1990) investigated the air-void stability of lab mixed and ready-mixed concrete with superplasticizer admixtures. The results also showed a good correlation of the air-void distribution between these two systems. However, no correlation was reported on other early- and later-age (mechanical and durability) characteristics.

Because the correlation between lab and field mixed concrete is lacking, this paper presents the first work to better define the relationship between laboratory and field mixed concrete. Specifically, this paper will provide a laboratory assessment of portland cement pastes and mortars subjected to different mixing regimes (time and mixer revolutions). It is anticipated that this research will provide basic knowledge on the influence of mixing variables and that the information can then be used to better estimate the influence of mixing variables on concrete mixed in the field. Hardened characteristics mortar and for concrete will be reported in future publications.

5.3 **RESEARCH SIGNIFICANCE**

Specifications and guidelines that limit mixing time and number of drum revolutions are in place. The influence of mixing time and drum revolutions on system characteristics has not been thoroughly studied and research is needed. Better understanding of how mixing variables influence mixture performance is needed to ensure existing specifications do actually add value. This study presents results from a laboratory evaluation of the early-

age characteristics of portland cement paste and mortar systems subjected to different mixing times and different numbers of mixer revolutions. The early-age characteristics assessed include the time-variant concentration of ions in solution, flowability, setting time, and chemical shrinkage.

5.4 EXPERIMENTAL INVESTIGATION

5.4.1 *Materials*

Type I/II portland cement meeting requirements of ASTM C150 was used for all mixtures in this study. The chemical composition and ASTM requirements for the cement are shown in **Table 5-1**. Graded sand meeting ASTM C778, *Standard Specification for Standard Sand*, was used for testing the flowability. ASTM Type II de-ionized (DI) water (0.4 MΩ·in [1 MΩ·cm] at 77˚F [25˚C]) was used for all mixtures and experiments.

Table 5-1–Chemical composition and requirements meeting ASTM C150 of portland cement

Composition	Spec. limit	(%)
SiO_2	-	20.30
Al_2O_3	6.0 max	4.80
Fe_2O_3	6.0 max	3.50
MgO	6.0 max	0.70
SO_3	3.0 max	2.80
CaO	-	63.9
Loss on Ignition	3.0 max	2.60
Insoluble Residue	0.75 max	0.11
CO_2	-	1.80
Limestone	5.0 max	3.20
$CaCO_3$ in Limestone	70 min	97.80
Na_{eq}	0.6 max	0.54

5.4.2 *Methods*

The mixing procedures for the cement pastes and mortars followed ASTM C305. This standard provides guidelines for mixing cement pastes and mortars and includes two

consecutive mixing stages: a low speed mixing (140 rpm) in the first stage followed by an intermediate speed mixing (285 rpm) in the second stage. This evaluation included adjusting the mixing time and mixing speed of the second stage only. **Table 5-2** shows the mixing conditions for the cement pastes and mortars evaluated in this study. Three mixing times (2, 15, and 60 minutes) and two mixing speeds (140 and 285 rpm) were evaluated. This resulted in 210, 355, 2030, 4060, 8330, and 25,435 mixer revolutions for paste mixing and 280, 568, 2170, 4273, 8470, and 17,098 mixer revolutions for mortar mixing. Note that the control mixtures are identified as Mixture No. P2 and M2 (mixing at 140 rpm for a short period) followed by mixing at 285 rpm for another short period. Triplicate specimens were assessed for all tests in this study.

Table 5-2–Mixing conditions for cement pastes and mortars

Mix. No.	Paste				Mix. No.	Mortar			
	First stage		Second stage			First stage		Second stage	
	Time (minutes)	Speed (rpm)	Time (minutes)	Speed (rpm)		Time (minutes)	Speed (rpm)	Time (minutes)	Speed (rpm)
P1	0.5	140	1	140	M1	1	140	1.5	140
P2	0.5	140	1	285	M2	1	140	1.5	285
P3	0.5	140	14	140	M3	1	140	14.5	140
P4	0.5	140	14	285	M4	1	140	14.5	285
P5	0.5	140	59	140	M5	1	140	59.5	140
P6	0.5	140	59	285	M6	1	140	59.5	285

During hydration, the concentrations of ions in solution continuously change. The hydroxyl ion concentration and related solution pH are important parameters that can influence the early-age characteristics and long-term performance of hydrated products. As a result, this study assesses the concentration of hydroxyl ions in solution at early ages. The hydroxyl ion concentration was evaluated using a pH electrode. The water-cement ratio (w/c) of the cement solutions for the hydroxyl ion concentration study was 4.0. Mixing for all systems was performed using a magnetic stirrer rotating at 0, 400, and 800 rpm throughout the test. Note that for the mixtures mixed at 0 rpm, the solutions were first mixed at 400 rpm for 3 minutes and then mixing was stopped. The mixing of the first step allows the UCP to be mixed with water before assessing the influence of the mixing process. The time elapsed after introducing the UCP to the solution is referred to

here as the “hydration time.” Solutions used for evaluating hydroxyl ions were analyzed at 5, 10, 15, 30, 45, 60, 90, 120, 150, 180, 210, and 240 minutes (and mixed at 0, 400, and 800 rpm).

The rates at which calcium, aluminate, and silicate ions dissolve and precipitate from the portland cement are also believed to influence the early-age characteristics. Therefore, to better understand the early-age characteristics of portland cement systems, concentrations of aluminate and calcium ions in portland cement solutions were determined in this study. Silicate concentrations were not assessed due to equipment limitations.

The concentrations of aluminate and calcium ions were determined using flame atomic absorption spectroscopy (FAAS). The mixing process for the aluminate and calcium ion concentration studies was similar to the mixing process for hydroxyl ion concentration study. Ion concentrations were determined at the same hydration times as the hydroxyl ion concentration tests, with additional tests performed at 300, 360, and 420 minutes.

At each hydration time, cement solution was decanted from the mixing container and then filtered using a vacuum pump and No. 40 filter paper. Filtered solution was used for analyzing aluminate (0.338 fl oz [10 ml]) and calcium (0.033 fl oz [1 ml]) ion concentrations, respectively. Because high concentration of calcium ions in solution occurs at early ages, filtered solutions for analyzing calcium ion concentration was diluted prior to the FAAS analyses. Extracted and filtered solution for analyzing calcium ion concentration was diluted with 0.297 fl oz (9 ml) of DI water to obtain the solution within the detection range of the FAAS. After filtering and/or diluting, 0.033 fl oz (1 ml) of lanthanum acid solution (0.42 lb/gal (50 g/l) lanthanum oxide (La_2O_3) in 3M hydrochloric acid (HCl)) was added to the solution. Concentration of aluminate ions was determined using the FAAS with nitrous oxide-acetylene gas at a wavelength of 1.22 x 10^{-5} in (309.3 nm) ignited at a temperature of 4712 to 5072˚F [2600 to 2800˚C]. The calcium concentration was determined using FAAS with air-acetylene gas at a

wavelength of 1.66 x 10^{-5} in (422.7 nm) ignited at the temperature of 3812 to 4352˚F [2100 to 2400˚C]. A blank sample (DI water) was also analyzed and used as a background correction.

Once water contacts the UCP, the hydration reactions begin. Stages of the hydration process, shown in **Fig. 5-3**, occur in four distinct stages: (I) the dissolution stage, (II) the nucleation stage, (III) the precipitation stage, and (IV) the continuing precipitation/dissolution stage (Odler 2008). The dissolution stage (stage I) is referred to as the stage when ions from the UCP dissolve in solution. The ion concentrations significantly increase and reach supersaturated conditions. The nucleation stage (stage II) is an induction stage that allows ions to interact with each other before forming a new hydrated product. In this stage, the ion concentrations remain at the maximum levels. Immediately after hydrated products begin to form, the system moves into the precipitation stage (stage III). In this stage, the ion concentration decreases due to the consumption of ions forming new hydrated products. The concentrations of ions then stabilize and this stage is referred to as the continuous dissolution/precipitation stage (stage IV). Eventually, the rate of dissolution/precipitation of ions is reduced. This is reported to be due to (1) the lack of smaller UCP, (2) the lack of water at the cement grain surface, and (3) the lack of space (Bullard *et al.* 2011). Faster dissolution, nucleation, and/or precipitation tend to result in further reduction in flow, accelerated setting time, and higher chemical shrinkage values.

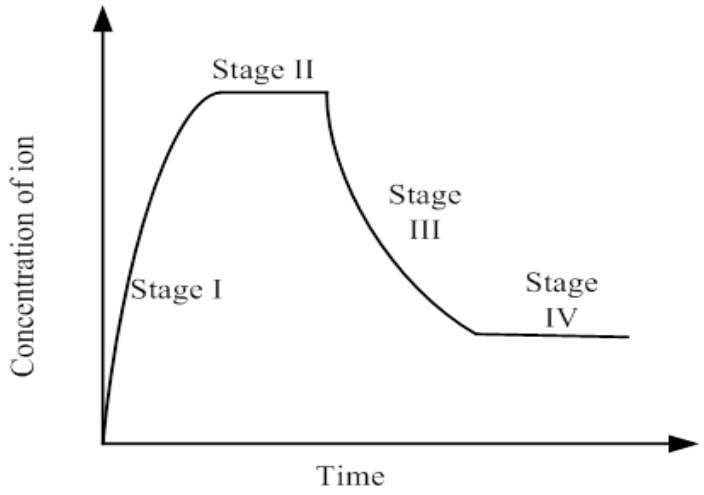

Fig. 5-3–Hydration process of cement systems: dissolution (Stage I), nucleation (Stage II), precipitation (Stage III), and continuous dissolution/precipitation (Stage IV).

The rates of dissolution (R_D) and precipitation (R_P) of ions in this study was determined as follows:

$$R_X \text{ (mmol/l/minute)} = \frac{\text{Average concentation of ions (mmol/l)}}{\text{Hydration time (minute)}} \quad (5\text{-}1)$$

where X is either D for dissolution or P for precipitation.

In addition to the ion concentration studies, the flowability of fresh mortars, setting time, and chemical shrinkage of the pastes were determined.

The flowability was determined following ASTM C1437, *Standard Test Method for Flow of Hydraulic Cement Mortar*. The specimens for the flowability test included mortars with w/c values of 0.4 and 0.485 and the cement-fine aggregate ratio was 1:2.75, as recommended in the standard for mixing mortars. The setting times of all systems were determined following ASTM C191, *Standard Test Methods for Time of Setting of Hydraulic Cement by Vicat Needle.* The w/c values were 0.3 and 0.4. Temperatures of the

pastes were measured immediately after mixing using an infrared thermometer. The chemical shrinkage was assessed following ASTM C1608 (procedure A), *Standard Test Method for Chemical Shrinkage of Hydraulic Cement Paste*. Temperature for shrinkage study was controlled at 73˚F (23˚C) by placing vials containing the materials into a temperature-controlled water bath. The pastes were mixed at the w/c value of 0.4. Data were recorded every 5 minutes using an optical camera and automated data acquisition system.

5.4.3 *Statistical Data Analysis*

Statistical analyses of two sample t-test and analysis of variances (ANOVA) were performed to evaluate the sample means with two groups and more than two groups, respectively. The Shapiro-Wilk test was used to determine if the distribution of data was normal and the Levene's test was used to determine if the data had equal variance before the analyses. The statistical hypotheses are defined as:

$$\text{Null hypothesis } (H_0): \mu_1 = \mu_2 = \ldots = \mu_a \tag{5-2}$$

$$\text{Alternative hypothesis } (H_a): \mu_1 \neq \mu_j \text{ for some } i \neq j \tag{5-3}$$

The 95% confidence interval was used in the analyses herein. If the H_0 is rejected (p-value ≤ 0.05), it can be concluded that there is a statistically significant difference at the 5% level between the means of group population. Alternatively, if the H_0 is not rejected (p-value > 0.05), it can be concluded that there is no statistically significant difference at the 5% level between the means of group population.

5.5 **EXPERIMENTAL RESULTS AND DISCUSSION**

5.5.1 *Ion Concentration*

Unhydrated portland cement consists of large amounts of soluble alkali compounds. Once contacted with water, the pH level of the solution rapidly increases and remains high

(Rothstein *et al.* 2002). This pH affects the solubility of alkali compounds in portland cement systems (Nordstrom and Munoz 2006) and can affect the hydration process. **Figs. 5-4*a*** and **5-4*b*** show the effects of mixing time and number of mixer revolutions on the hydroxyl ion concentration in solution, respectively. Results in **Fig. 5-4*a*** indicate that the hydroxyl ion concentration in solution mixed at 400 rpm increases with increasing mixing time (up to 240 minutes). Results in **Fig. 5-4*b*** also indicate that the hydroxyl ion concentration increases as the number of mixer revolutions increases (up to about 150,000 revolutions). The results indicate that the hydroxyl ion concentration increases rapidly at early ages and lower number of mixer revolutions and then stabilizes (e.g. logarithmic function).

Fig. 5-5 shows the effect of number of mixer revolutions on the R_D of hydroxyl ions in solution. Results indicate that the R_D of hydroxyl ions is influenced by number of mixer revolutions. The R_D for the solution mixed at 0, 96,000, and 192,000 revolutions are 8.4, 16.8, and 16.2 mmol/l/minute, respectively. These results indicate that the R_D in solution mixed at 96,000 revolutions is similar to the R_D in solution mixed at 192,000 revolutions. The R_D of the hydroxyl ions in solution mixed at 96,000 and 192,000 revolutions are 100% and 93% higher than the R_D of hydroxyl ions in solution without mixing (mixed at 0 revolution), respectively. This likely indicates that the number of mixer revolutions does influence the R_D, but the number of mixer revolutions higher than zero does not significantly influence the R_D.

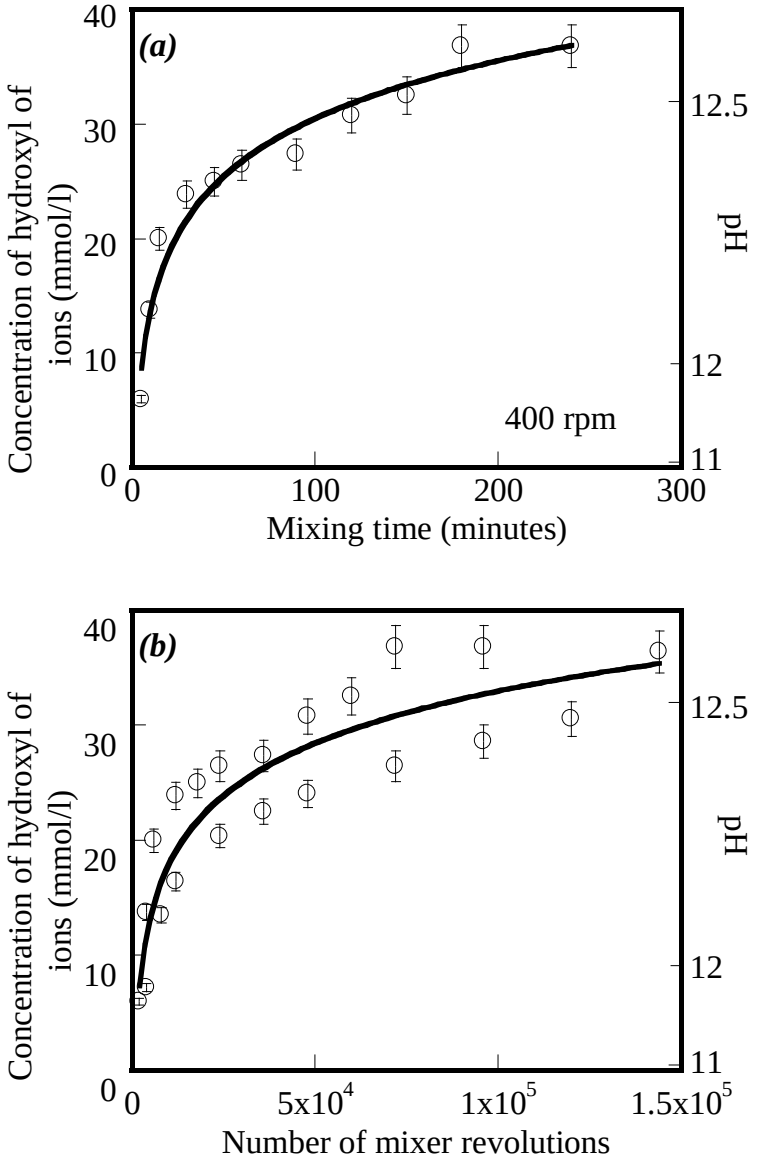

Fig. 5-4–Effect of *a)* mixing time and *b)* number of mixer revolutions on concentration of hydroxyl ions.

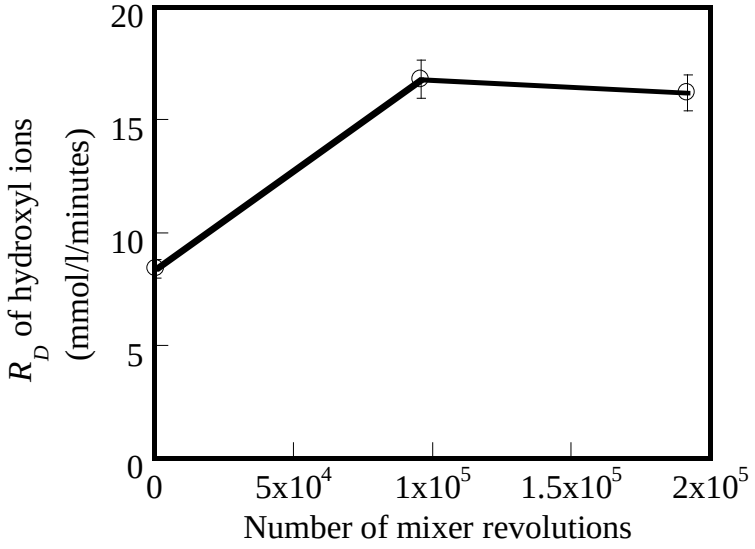

Fig. 5-5–Effect of number of mixer revolutions on R_D of hydroxyl ions.

Figs. 5-6*a* and **5-6*b*** show the plots of mixing time and number of mixer revolutions versus aluminate ion concentration in solution, respectively. Results indicate that the aluminate ion concentration in solution mixed at 400 rpm significantly increases with increasing mixing time from 0 to 15 minutes and then rapidly decreases after mixing for 15 minutes to a stable level. The result of the hydroxyl ion concentration as a function of number of mixer revolutions, as shown in **Fig. 5-6*b***, exhibits a similar trend with the result in **Fig. 5-6*a*.** Aluminate ion concentration increases, decreases, and then stabilizes with increasing number of mixer revolutions.

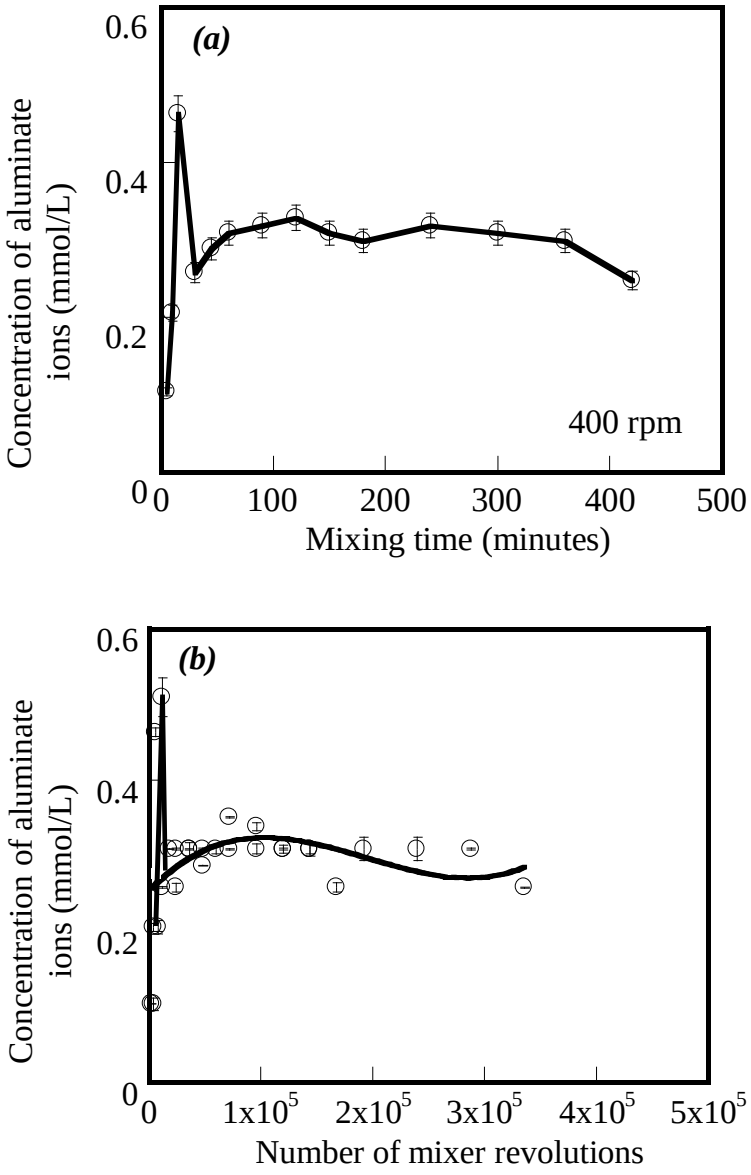

Fig. 5-6–Effect of *a)* mixing time and *b)* number of mixer revolutions on concentration of aluminate ions.

The plot of the R_D and R_P of the aluminate ion concentration in solutions mixed at different numbers of mixer revolutions is shown in **Fig. 5-7**. Results indicate that the R_D of aluminate ions increases with increasing number of mixer revolutions. The R_D of aluminate ions in solutions mixed at 168,000 and 336,000 revolutions are 29% and 37%

higher than the R_D of aluminate ions in solution without mixing (mixed at 0 revolution), respectively This indicates that there is a significant difference in means (ANOVA test with p-value = 0.00). Results also indicate that the R_P of aluminate ions in solution mixed at 168,000 revolutions is not significantly different from the R_P of aluminate ions in solution mixed at 336,000 revolutions (two-sample t-test with p-value = 0.15). These results indicate that R_D is influenced by number of mixer revolutions but R_P is not.

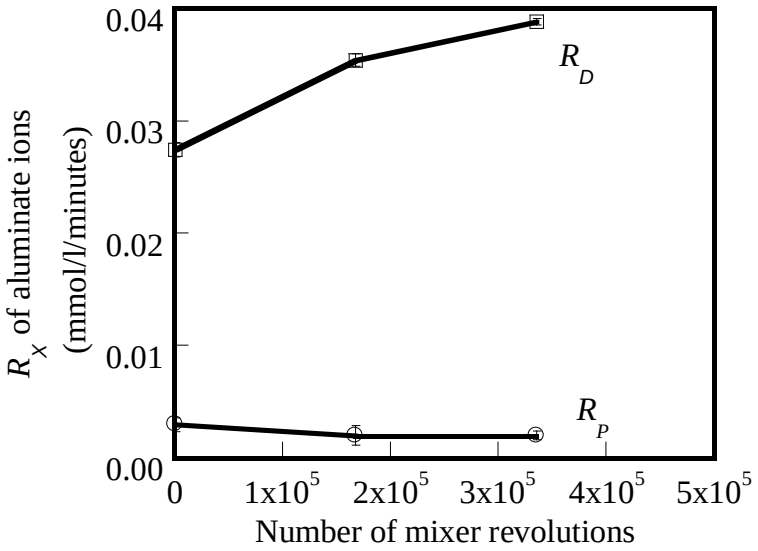

Fig. 5-7–Effect of number of mixer revolutions on R_D and R_P of aluminate ions.

The effects of mixing time and number of mixer revolutions on the R_D and R_P of calcium ion concentration in solutions are shown in **Figs. 5-8*a*** and **5-8*b***, respectively. Results indicate that the calcium ion concentration in solution mixed at 400 rpm tends to increase and achieve maximum concentration of about 34 mmol/L when the solution was mixed for 180 minutes. After achieving the maximum concentration, the calcium ion concentration stabilizes. In **Fig. 5-8*b***, results indicate that the concentration of calcium ions first increases with increasing number of mixer revolutions and then decreases. The concentration then increases again to a maximum level of approximately 36 mmol/L at 120,000 revolutions. After increasing to the maximum concentration, the calcium ion concentration decreases and stabilizes.

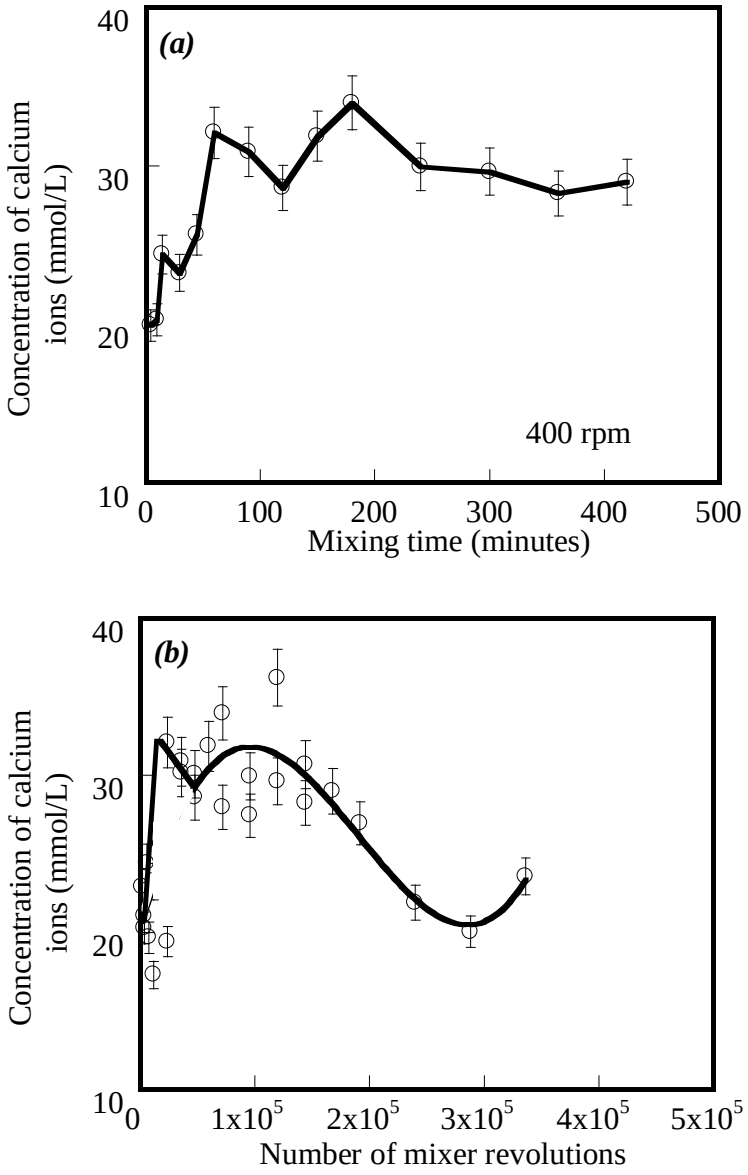

Fig. 5-8–Effect of *a)* mixing time and *b)* number of mixer revolutions on concentration of calcium ions.

The influence of number of mixer revolutions on the R_D and R_P of calcium ion concentration in solutions is shown in **Fig. 5-9**. Results show similar trends to the results of the R_D and R_P of aluminate ion concentration in **Fig. 5-7**. The R_D of calcium ions increases with increasing number of mixer revolutions. The R_D of calcium ions in solution without mixing are 65% and 66% lower than the R_D of calcium ions in solutions mixed 168,000 and 336,000 revolutions, respectively (ANOVA t-test with p-value =

0.00). The R_P of aluminate ion concentration in solution mixed at 168,000 revolutions shows no significant difference from the R_P of aluminate ion concentration in solution mixed at 336,000 revolutions (two-sample t-test with p-value = 0.35). Frigione and Marra (1976) reported that increasing mixing speed or number of mixer revolutions leads to increased rate of hydration reactions and R_D of calcium ions. In fact, results herein indicate that the R_P of calcium ions is not significantly influenced by increasing number of mixer revolutions, but the R_D is.

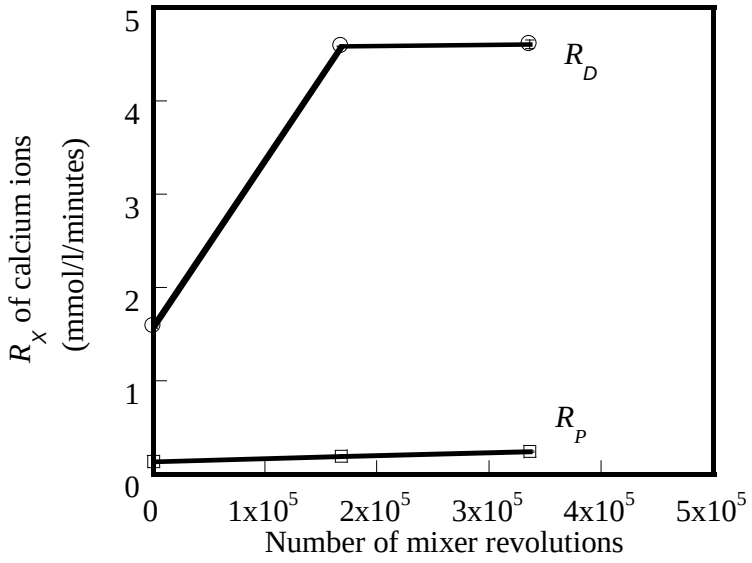

Fig. 5-9–Effect of number of mixer revolutions on R_D and R_P of calcium ions.

As discussed, the hydration reactions are controlled by both the dissolution stage (Stage I in **Fig. 5-3**) and the precipitation stage (Stage III in **Fig. 5-3**). However, the hydration reaction rates can be affected by constituent material variables (e.g, paste temperature and cement particle size). Takada (2004) reported that as cement particles and debris particles become smaller due to abrasion the during mixing process, these particles can influence the hydration reaction rates.

Results herein indicate that the mixing time and number of mixer revolutions do influence the concentrations of both aluminate and calcium ions in solutions. Results also

indicate that the aluminate and calcium ion concentrations begin to increase at the early ages and then decrease and stabilize at later ages. Furthermore, the number of mixer revolutions does influence the R_D of aluminate and calcium ions, but does not influence the R_P.

5.5.2 *Flowability*

The effect of the flowability of fresh cement mortars mixed at 285 rpm and with different w/c values of 0.4 and 0.485 as a function of mixing time is shown in **Fig. 5-10*a***. Results indicate that increased mixing time results in a significant reduction in flow and the mixtures with higher w/c values exhibit higher flow values. Dewar and Anderson (1992) reported that decreased flow likely occurred due to: (1) inadequate water in the mixture proportions, (2) increased water evaporation rates, and/or (3) increased hydration reactions rates. Note that the testing shown in **Fig. 5-10*a*** was discontinued at 60 minutes because the mortars became stiffened and uncastable. Many previous studies on concrete mixed in the field (Baskoca *et al.* 1998, Kirca *et al.* 2002, Nehdi and Al-Martini 2009) have reported that increasing mixing time resulted in reduced workability of fresh concrete mixtures, which is expected.

The relationship between the number of mixer revolutions versus flow of fresh cement mortars with different w/c values of 0.4 and 0.485 is shown in **Fig. 5-10*b***. Results indicate that the flow value of fresh mortars reduces with increasing number of mixer revolutions. Results also indicate that the flow of the fresh mortars with lower w/c values is lower than the mortars with higher w/c values. This is likely due to the fresh mortars with lower w/c values having less available water for flow.

In this work, the decrease in flow is 0.04 in/min [1.1 mm/min] and from 7.3e-5 to 14.1e-5 in/revolution [0.0021 to 0.0036 mm/revolution]. Increasing mixing time resulting in the decrease in flow is not dependent on w/c of the mixtures; whereas, increasing number of mixer revolutions is dependent on w/c of the mixtures It is important to understand the effect of mixing time and number of mixer revolutions on flowability because concrete specifications now put limits on these values.

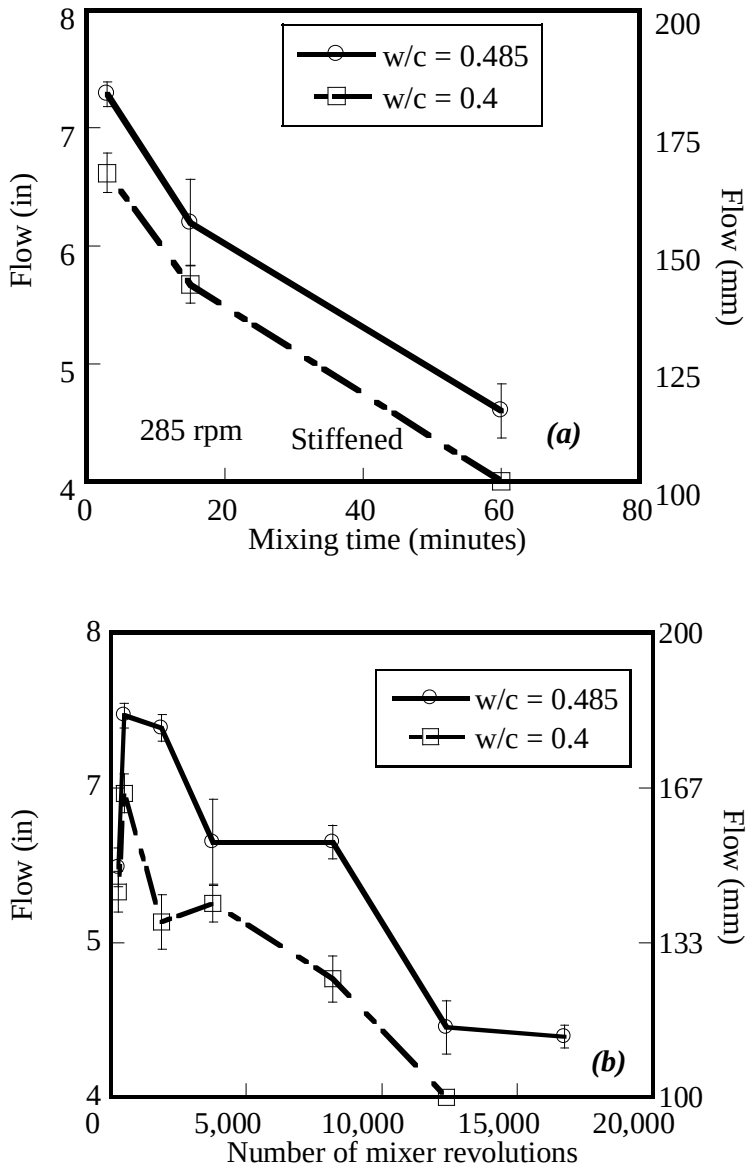

Fig. 5-10–Effect of *a)* mixing time and *b)* number of mixer revolutions on flow of mixtures at different w/c values.

5.5.3 *Setting Time*

Setting time is classified into two times: initial and final setting times. The initial setting time is a time estimate of when the cement paste begins to lose its plasticity and the final setting time is a time estimate of when the cement paste begins to support some

external force without significant deformation (Fajun *et al.* 1985, Fraay 1990). For cementitious systems to be useful to contractors, the setting time must not be too early or too late. Systems that set too early could require removal as there would not be sufficient time to consolidate and finish. Systems that take too long to set are costly as crews have to wait to consolidate and finish the concrete. Suprenant and Malisch (2000) reported that the estimated cost for a finishing crew is approximately $300 to $500 per hour. Therefore, optimal setting time can result in reduced costs.

Figs. 5-11*a* and **5-11*b*** show the plots of the initial setting times for pastes with the w/c values of 0.3 and 0.4 mixed for different mixing times and numbers of mixer revolutions, respectively. Results shown in **Fig. 5-11*a*** indicate that the initial setting time of cement pastes with a w/c value of 0.4 increases with increasing mixing time (ANOVA test with p-value = 0.000). However, the initial setting time of cement pastes with a lower w/c value (0.3) increases with increasing mixing time from 2 to 30 minutes, but then decreases with increasing mixing time from 30 to 60 minutes (ANOVA test with p-value = 0.002). Results in **Fig. 5-11*b*** exhibit similar trends to the results in **Fig. 5-11*a***. Results indicate that the initial setting time of cement pastes with higher w/c values tends to increase as a function of number of mixer revolutions (ANOVA test with p-value = 0.000). Increasing the number of mixer revolutions of the pastes with lower w/c values from 210 to 8330 revolutions results in an increase of the initial setting time (ANOVA test with p-value = 0.0023), but increasing the number of mixer revolutions from 8330 to 25,435 revolutions results in a reduction of the initial setting time (two-sample t-test with p-value = 0.0019).

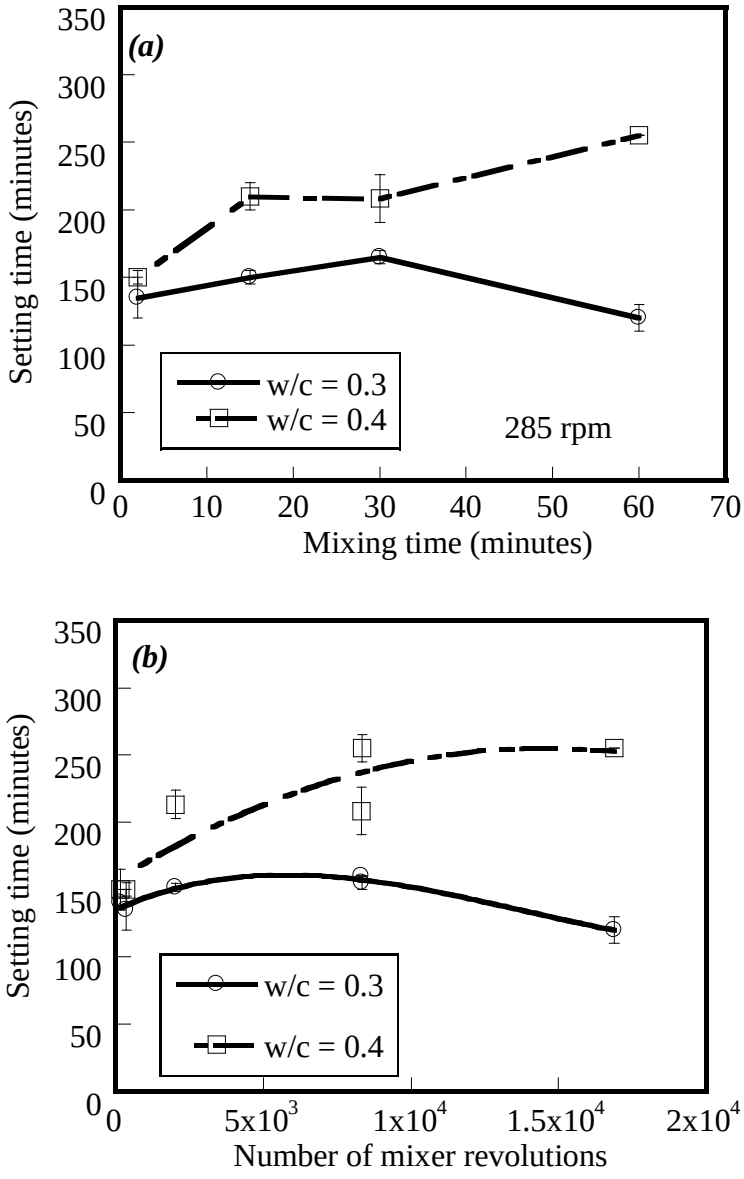

Fig. 5-11–Effect of *a)* mixing time and *b)* number of mixer revolutions on initial setting time of mixtures at different w/c values.

Figs. 5-12*a* and **5-12*b*** show the relationships of the final setting times versus the mixing time and number of mixer revolutions of the pastes with the w/c values of 0.3 and 0.4, respectively. Results indicate that the final setting time exhibits the same trends as the results of the initial setting time, shown in **Figs. 5-11*a*** and **5-11*b***. When mixing time

and number of mixer revolutions increase, the final setting time of the pastes with the w/c value of 0.3 increases slightly and then decreases. However, the final setting time with the pastes with the w/c value of 0.4 increases with increasing mixing time and number of mixer revolutions.

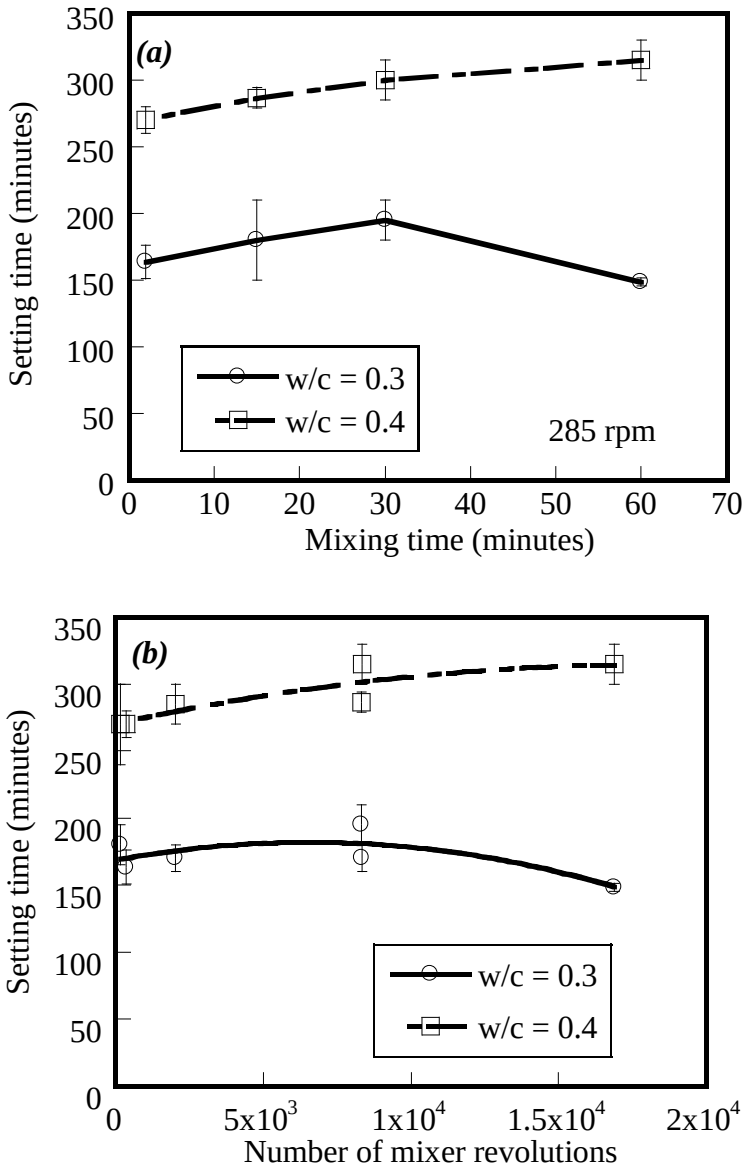

Fig. 5-12–Effect of *a)* mixing time and *b)* number of mixer revolutions on final setting time of mixtures at different w/c values.

The reductions of the initial and final setting times of the pastes with the w/c value of 0.3 mixed at longer mixing times and higher numbers of mixer revolutions, shown in **Figs. 5-11*a***, **5-11*b***, **5-12*a***, and **5-12*b***, correlate with paste temperature [see in **Figs. 5-13*a*** and ***5*-13*b***]. When mixing time and/or number of mixer revolutions increase, the temperature of the pastes with the w/c of 0.3 increases. The average temperature of the pastes with the w/c value of 0.3 mixed for 2 to 60 minutes and from 355 to 25,435 revolutions increased by approximately 0.23˚F/min (0.13˚C/min) and 5.5e-4˚F/rev (3.2e-4˚C/rev), respectively. Kirca *et al.* (2002) investigated the extended mixing of concrete in the field and reported that the increase of concrete temperature from approximately 77 to 82˚F [25 to 28˚C] resulted in a 66% reduction in workability. Baskoca *et al.* (1998) also investigated ready-mixed concrete with admixtures and reported that the concrete temperature increased from approximately 77 to 84 ˚F [25 to 29˚C] mixed for 90 minutes and 135 revolutions. Rupnow *et al.* (2007) reported that increased mixing time results in increased impact and friction, resulting in more heat generated. This leads to increased rates of hydration reactions and shorter setting times. As shown here, increased number of mixer revolutions also increased heat.

As shown in **Figs. 5-11*a***, **5-11*b***, **5-12*a***, and **5-12*b***, the initial and final setting times of cement pastes with higher w/c values (e.g., w/c value of 0.4) significantly increase with increasing mixing time and/or number of mixer revolutions. This is likely because the temperature of pastes with the w/c value of 0.4 does not significantly increase with increasing mixing time and/or number of mixer revolutions [see **Figs. 5-13*a*** and **5-13*b***]. The average temperature of cement pastes with the w/c value of 0.4 increases by 0.033˚F/min (0.016˚C/min) or 7.9e-5˚F/rev (3.9˚C/rev). Results indicate that more water likely leads to lower friction and impact, reduced heat, and extended setting time.

Based on test results, it can be concluded that the mixing variables do affect the setting time. This is likely due to the heat generation from impact and friction. The early-age and hardened characteristics can change due to the increase of mixture temperature.

However, more work is needed to assess the validity of the 300-drum revolution and 90-minute limits.

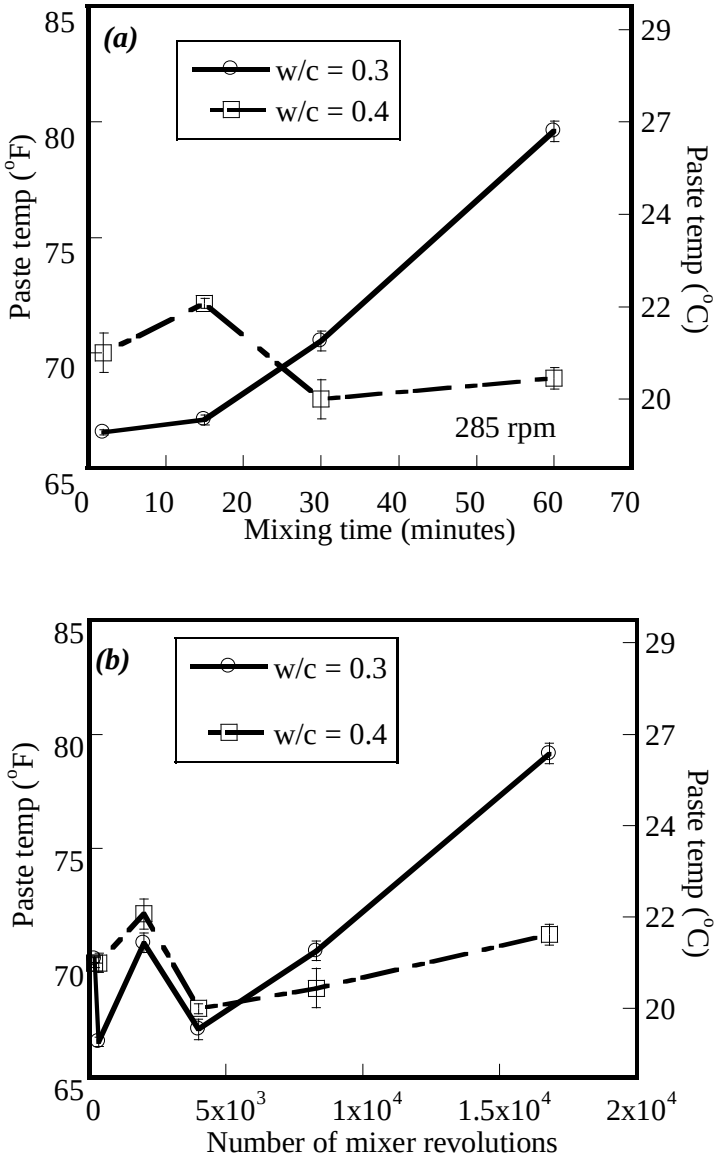

Fig. 5-13–Effect of *a)* mixing time and *b)* number of mixer revolutions on temperature of mixtures at different w/c values.

5.5.4 *Chemical Shrinkage*

Chemical shrinkage is a change in volume of solid and liquid components in the cementitious systems, caused by hydration reactions at early ages. As hydration reactions progress, the hydrated products occupy less volume than the initial unreacted constituents. Prior to setting, this volume change results in a bulk contraction of the entire cement paste which results in micro-voids (Qing *et al.* 2007, Givi *et al.* 2010). Faster hydration reactions can result in increased chemical shrinkage at early ages (Jensen and Hansen 2001, Bentz and Jensen 2004, Lura *et al.* 2009).

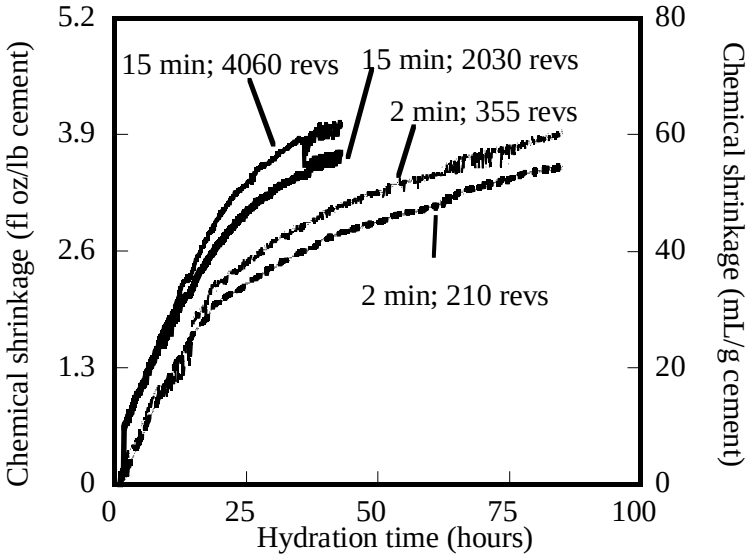

Fig. 5-14–Effect of mixing time and number of revolutions on chemical shrinkage (w/c = 0.4).

The relationship of mixing variables on chemical shrinkage at early ages is shown in **Fig. 5-14.** The chemical shrinkage of specimens with a w/c value of 0.4 and mixed for different mixing times (2 and 15 minutes) and numbers of mixer revolutions (210, 355, 2030, and 4060 revolutions) is shown in the figure. Results indicate that chemical shrinkage value increases with increasing mixing time and/or number of mixer revolutions. The increase of chemical shrinkage value is likely caused by increased

hydration reaction rates. The hydration reaction rates increase due to an increase of paste temperature.

Fig. 5-15 shows the effect of number of mixer revolutions on chemical shrinkage at 45 hours.

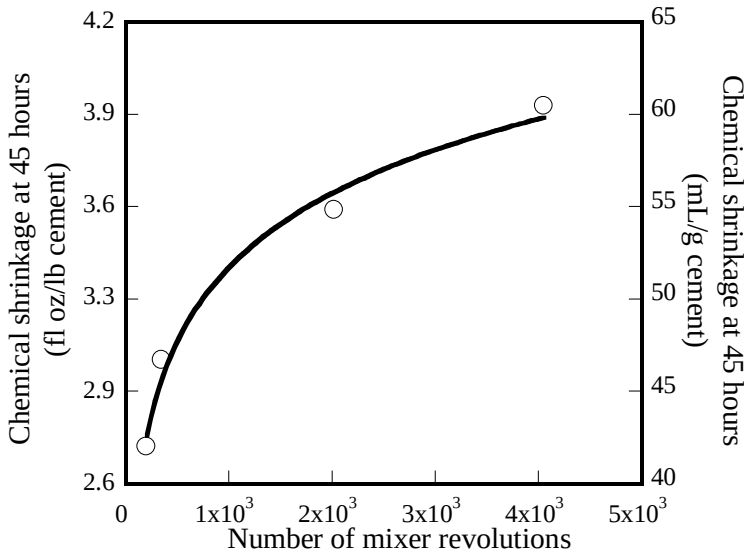

Fig. 5-15–Effect and number of revolutions on chemical shrinkage at 25 hours (w/c = 0.4).

Results indicate that increased number of mixer revolutions results in increased chemical shrinkage value at 45 hours. The chemical shrinkage increases rapidly at lower revolutions and then increases slowly at higher revolutions (e.g., logarithmic function). Note that the chemical shrinkage of the pastes mixed between the number of mixer revolutions lower than 300 and higher than 300 is not significantly distinguished. The number of truck-drum revolutions of 300 limited by SHAs and specifications is not related to significant change in chemical shrinkage.

5.5.5 *Correlation of R_D and R_P of Ions with Early-age Characteristics of Mixtures*

This section provides correlations of the R_D and R_P of ions with the early-age characteristics of the mixtures as increasing number of mixer revolutions, and also discusses possible causes relating to these correlations. The R_D of hydroxyl, aluminate, and calcium ions has a positive correlation on the flowability loss and chemical shrinkage. However, there is no correlation between R_D of these ions on the setting time. The R_P of the ions does not correlate with the early-age characteristics (i.e. flow, setting time, and chemical shrinkage). Increased R_D of ions allows the UCP to dissolve into solution faster which can increase the hydration reaction rates, consequently resulting in accelerated flowability reduction and chemical shrinkage. However, The R_P of aluminate and calcium ions does not influence the flow, setting time, and chemical shrinkage of the mixtures. It is believed that the material variables such as temperature seem to have higher influence on the early-age characteristics.

5.6 **CONCLUSIONS**

Many SHAs and specifications limit the discharge time and truck drum revolutions for ready-mixed concrete. Limited research has been done to deliver whether these limits (i.e. 90-minute discharge time and 300 truck drum revolutions) are applicable. This paper presents laboratory results on the early-age characteristics of portland cement pastes and mortars mixed for different mixing times and number of mixer revolutions. This information will serve as the basis for further studies. The results from this research indicate that:

- The R_D of hydroxyl, aluminate, and calcium ions increased with increasing number of mixer revolutions; increasing number of mixer revolutions had no influence on the R_P the aluminate and calcium ions;
- R_D of ions had a positive correlation with the hydration reaction rates and consequently resulted in the reduction in flow and chemical shrinkage, but not setting time;

- There was no correlation of R_P with the early-age characteristics; the material variables is believed to have greater impact on the early-age characteristics;
- The rate of flow reduction as a function of mixing time was not dependent on w/c of mixtures, but number of mixer revolutions was; Higher w/c resulted in lower rate of flow reduction when number of mixer revolutions increases;
- Increased mixing time and number of mixer revolutions resulted in increased paste temperature of the systems, likely leading to increased hydration reaction rates and shorter setting times; and
- Portland cement pastes that were mixed longer and higher number of mixer revolutions exhibited higher chemical shrinkage value at early ages.

The results provide for better understanding of the relationships of the mixing time and number of mixer revolutions on the early-age characteristics of portland cement systems. The R_D of ions and materials temperature are directly influenced by the mixing process and consequently results in a change in mixture performance, including the flowability, setting time, and chemical shrinkage. Further studies including effects of mixing variables on hardened characteristics and on concrete performance will be presented in future publications.

5.7 ACKNOWLEDGEMENTS

This study was supported by the Washington Department of Transportation (WSDOT) as part of the project, Extended Discharge Time and Revolution Count for Cast-In-Place Concrete.

5.8 REFERENCES

Baskoca, A., Ozkul, M. H., and Artirma, S. (1998), "Effect of Chemical Admixtures on Workability and Strength Properties of Prolonged Agitated Concrete," *Cem. Con. Res.*, V. 28, No. 5, pp. 737-747.

Bentz, D. P. and Jensen, O. M. (2004), "Mitigation Strategies for Autogenous Shrinkage Cracking," *Cem. Con. Res.*, V. 26, No. 6, pp. 677-685.

Bullard, J. W., Jennings, H. M., Livingston, R. A., Nonat, A., Scherer, G. W., Scrivener, K. L., and Thomas, J. J. (2011), "Mechanisms of Cement Hydration," *Cem. Con. Res.*, V. 41, No. 12, pp. 1208-1223.

Charonnat, Y. and Beitzel, H. (1997), "Report: Efficiency of Concrete Mixers Towards Qualification of Mixers," *Mater. Struct.*, V. 30, No. 1, pp. 28-32.

Dewar, J. D. and Anderson, R. (1992), *Manual of Ready Mixed Concrete*, 2nd ed., Glasgow, UK, Blackie Academic and Professional, 72 pp.

Diamond, S. (2005), "The Patch Microstructure in Concrete: Effect of Mixing Time," *Cem. Con. Res.*, V. 35, No. 5, pp. 1014-1016.

Fajun, W., Grutzeck, M. W., and Roy, D. M. (1985), "The Retarding Effects of Fly Ash Upon the Hydration of Cement Pastes: The First 24 Hours," *Cem. Con. Res.*, V. 15, No. 1, pp. 174-184.

Ferraris, C. F. (2001), "Concrete Mixing Methods and Concrete Mixers: State of the Art," *J. Res. Nat. Stand. Technol.*, V. 106, No. 2, pp. 391-399.

Fraay, A. L. A., *Fly Ash a Pozzolan in Concrete*, in *Civil Engineering and Geosciences*, 1990, Delft University of Technology, Delft, Netherlands, 165 pp.

Frigione, G. and Marra, S. (1976), "Relationship between Particle Size Distribution and Compressive Strength in Portland Cement," *Cem. Con. Res.*, V. 6, No. 1, pp. 113-128.

Givi, N. A., Rashid, S. A., Aziz, F. N. A., and Salleh, M. A. M. (2010), "Experimental Investigation of the Size Effects of SO_2 Nano-Particles on the Mechanical Properties of Binary Blended Concrete," *Comp. Part B: Eng.*, V. 41, No. 8, pp. 673–677.

Hooton, R. D. (2008), "Bridging the Gap between Research and Standards," *Cem. Con. Res.*, V. 38, No. 2, pp. 247-258.

Jensen, O. M. and Hansen, P. F. (2001), "Autogenous Deformation and RH-Change in Perspective," *Cem. Con. Res.*, V. 31, No. 12, pp. 1859-1865.

Kirca, O., Turanli, L., and Erdogan, T. Y. (2002), "Effect of Retempering on Consistency and Compressive Strength of Concrete Subjected to Prolonged Mixing," *Cem. Con. Res.*, V. 32, No. 3, pp. 441-445.

Lowke, D. and Schiessl, P., *Effect of Mixing Energy on Fresh Properties of SCC,* 2007, Technical University of Munich, Centre of Building Materials, 6 pp.

Lura, P., Couch, J., Jensen, O. M., and Weiss, J. (2009), "Early-Age Acoustic Emission Measurements in Hydrating Cement Paste: Evidence for Cavitation During Solidification Due to Self-Desiccation," *Cem. Con. Res.*, V. 39, No. 10, pp. 861-867.

Mindess, S., Young, J. F., and Darwin, D. (2002), *Concrete*, 2nd ed., NJ, Prentice Hall.

Nehdi, M. and Al-Martini, S. (2009), "Coupled Effects of High Temperature, Prolonged Mixing Time, and Chemical Admixtures on Rheology of Fresh Concrete," *ACI Mat. J.*, V. 106, No. 3, pp. 231-240.

Nordstrom, D. K. and Munoz, J. L. (2006), *Geochemical Thermodynamics*, 2nd ed., Palo Alto, CA, The Blackburn Press, 504 pp.

Odler, I., *Hydration, Setting and Hardening of Portland Cement*, in *Lea's Chemistry of Cement and Concrete*, P.C. Hewlett, Editor, 2008, Butterworth-Heinemann: Burlinton, MA, pp. 241-297.

Qing, Y., Zenan, Z., Deyu, K., and Rongshen, C. (2007), "Influence of Nano-SiO_2 Addition on Properties of Hardened Cement Paste as Compared with Silica Fume," *Constr. Build. Mater.*, V. 21, No. 3, pp. 539-545.

Rejeb, S. K. (1996), "Improving Compressive Strength of Concrete by a Two-Step Mixing Method," *Cem. Con. Res.*, V. 26, No. 4, pp. 585-592.

Rothstein, D., Thomas, J. J., Christensen, B. J., and Jennings, H. M. (2002), "Solubility Behavior of Ca-, S-, Al-, and Si-Bearing Solid Phases in Portland Cement Pore Solutions as a Function of Hydration Time," *Cem. Con. Res.*, V. 32, No. 10, pp. 1663-1671.

Roumain, J. C., Holcim , 2004. [Personal communication cited by Hooton (2008)]

Roy, D. M. and Idorn, G. M., *Concrete Microstructure*, 1993, Strategic Highway Research Program, Washington DC.

Rupnow, T. D., Schaefer, V. R., Wang, K., and Hermanson, B. L., *Improving Portland Cement Concrete Mix Consistency and Production Rate through Two-Stage Mixing*, 2007, Iowa State University, Ames, IA, 96 pp.

Saucier, F., Pigeon, M., and Plante, P. (1990), "Air-Void Stability, Part III: Field Tests of Superplasticized Concretes," *ACI Mat. J.*, V. 87, No. 1, pp. 3-11.

Suprenant, B. A. and Malisch, W. R., *The Cost of Waiting*, in *Concrete Construction*, 2000, Hanley Wood, Washington DC.

Takada, K., Influence of Admixtures and Mixing Efficiency on the Properties of Self Compacting Concrete: The Birth of Self Compacting Concrete in the Netherlands, in Civil Engineering and Geosciences, 2004, Delft University of Technology, Delfts, Netherlands, 256 pp.

6 EFFECTS OF MIXING VARIABLES ON HARDENED CHARACTERISTICS OF PORTLAND CEMENT SYSTEMS

ABSTRACT

Specifications and guidelines for ready-mixed concrete (AASHTO M157, ACI 304R, and ASTM C94) place limits on placement time, concrete temperature, and/or number of truck drum revolutions. The limits in AASHTO, ACI, and ASTM should correlate with concrete performance; that is, if the limits are exceeded it would be expected that an inferior product would be produced. An earlier paper investigating the effects of mixing time and number of mixer revolutions on cement pastes and mortars concluded that increased mixing time and mixer revolutions resulted in decreased flows, altered setting times, and increased shrinkage. This paper assesses the influence of mixing time and number of mixer revolutions on the hardened characteristics of lab-made mortars. Results indicate that increasing mixing time leads to higher 1-day compressive strengths but lower 28-day strengths. Results also indicate that increased number of mixer revolutions can result in increased porosity, leading to decreased strength.

Keywords: Mixing Time, Number of Mixer Revolutions, Hardened Characteristics, Porosity, Compressive Strength, Microstructure, Chloride Diffusivity.

To be submitted to
American Concrete Institute Materials Journal

6.1 INTRODUCTION

The American Society for Testing and Materials (ASTM) defines ready-mixed concrete as a concrete manufactured and delivered to a purchaser in a fresh state. During the delivery process, fresh concrete can be subjected to a wide range of conditions. Concrete can be agitated or mixed for different time periods and different numbers of drum revolutions (or counts). Longer delivery times and higher drum revolution counts are reported to result in increased mixture temperature, decreased workability, and increased slump loss of fresh concrete mixtures (Cook 1943, Bloem and Gaynor 1971, Ravina 1975, Dewar and Anderson 1992, Ravina 1996, Ozkul *et al.* 1997, Baskoca *et al.* 1998, Mahboub and Cutshaw 2001, Kirca *et al.* 2002, Erdogdu 2005, Al-Negheimish and Alhozaimy 2008, Chen and Struble 2009, Nehdi and Al-Martini 2009, Erdogdu *et al.* 2011). Dewar and Anderson (1992) reported that decreased workability and increased slump loss occurs due to inadequate water in the mixture, increased rate of water evaporation, and increased rates of hydration reactions. Decreased workability of the fresh concrete makes concrete more difficult to properly place and consolidate. This can lead to increased porosity, increased void sizes, and honeycombing of the hardened concrete. An increase in porosity and void size can also lead to reductions in hardened properties and durability (Al-Gahtani *et al.* 1998). Honeycombing can lead to rejection of the concrete element or structure. In addition to producing interior product, Andersen and Hodson (2009) reported that the cost of finishing concrete is approximately two to five times higher than the cost of materials to make concrete. Maintaining adequate workability of fresh concrete should lead to a reduction in construction costs and a better final product. Limited research has been reported on what limits during transport (i.e., time and drum revolutions) correlate with decreased workability and changes in hardened concrete characteristics.

Existing specifications and guidelines for ready-mixed concrete, including the American Concrete Institute (ACI) 304R, *Guide for Measuring, Mixing, Transporting, and Placing Concrete*, the American Association of State Highway and Transportation

Officials (AASHTO) M157, *Standard Specification for Ready-Mixed Concrete*, the ASTM C94/C94M, *Specification for Ready-mixed Concrete*, and many specifications for State Highway Agencies (SHAs) are in place to help "ensure" the delivery of good quality concrete mixtures. In fact, forty-eight SHAs place limits on mixing time, forty-five SHAs place limits on concrete placement temperature, and thirty SHAs place limits on the number of truck drum revolutions. A review of SHAs limits for transporting concrete indicates that:

- The most common limit on allowable mixing time is 90 minutes (42 SHAs). However, maximum allowable mixing times range from 30 to 120 minutes and can be dependent on temperature;
- The most common limit on maximum allowable number of truck drum revolution is 300 revolutions (26 SHAs). However, maximum allowable numbers of truck drum revolutions range from 150 to 320 drum revolutions (when specified), and;
- The most common limit on allowable concrete temperature is 90˚F (32˚C) (31 SHAs). However, maximum allowable temperatures range from 75 to 100˚F [24 to 38˚C], respectively.

The mixing time and number of drum revolutions can influence the workability of fresh concrete mixtures. This was recognized almost 80 years ago when ASTM published the first C94 specification in 1935 that limited placement time. The specification required that ready-mixed concrete must be discharged within 90 minutes after mixing. Although the specifications and guidelines for ready-mixed concrete have been established for some time, limited studies have been performed to assess the effects of the mixing variables on the early-age and hardened characteristics of concrete mixtures. With modern concrete (e.g., concrete containing supplementary cementing materials (SCMs)

and concrete incorporating chemical admixtures), it would be beneficial to determine whether existing specifications and guideline limits are still appropriate and add value. To better correlate specification limits with concrete performance, an investigation evaluating the fresh and hardened characteristics of cementitious systems mixed for different times and drum revolution counts should be performed. This paper presents results from a laboratory study on mortars. A research program is investigating the influence of mixing time and drum revolution counts on concrete performance and this will be published at a later time.

A recent laboratory study investigated the effects of mixing time and number of mixer revolutions on the early-age characteristics of portland cement (PC) paste and mortar systems (Trejo and Prasittisopin 2014). Test results indicated that the paste temperature increased as a function of mixing time and number of mixer revolutions. The authors reported that during mixing, an increased number of mixer revolutions resulted in an increase in friction and impact between constituent particles and the mixer tools. Increased friction and impact leads to more heat generation, potentially resulting in faster hydration. Faster hydration can influence the early-age characteristics of mixtures. Early-age characteristics that can influence constructability and quality of the final product include workability, setting time, and early-age shrinkage. A better understanding of how changes in the early-age characteristics affect the hardened characteristics of cementitious systems is needed.

This paper reports on results from a laboratory research program that assessed the influence of mixing time and number of mixer revolutions on the hardened characteristics of PC mortars. The hardened characteristics investigated include compressive strength, porosity, apparent chloride diffusion coefficient (D_a), and microstructure observation. It is anticipated that this research will provide basic knowledge on the effects of mixing time and number of mixer revolutions on hardened cementitious systems. It is anticipated that test results herein will be correlated with test results obtained from concrete mixed in the field so that the influence of mixing variables on performance can be better understood.

6.2 RESEARCH SIGNIFICANCE

Mixing time and number of truck drum revolutions are mixing variables limited in ready-mixed concrete specifications and guidelines. These specification and guidelines should be responsive to current developments in concrete materials and technology to ensure that value is continually added. To ensure that existing guidelines and specifications add value, a better understanding of how these mixing variables influence concrete performance is needed. More importantly, an assessment of the validity of these limits is needed. Although mixing limits for ready-mixed concrete are well-documented and ubiquitous, understanding of the influence of mixing variables and developing reasonable limits is needed. This study presents results from a laboratory research program evaluating the effects of mixing time and number of mixer revolutions on the hardened characteristics of PC mortars. This information will assist scientists and engineers in maintaining value-adding specifications and guidelines. Future publications will focus on lab and field mixing of concrete.

6.3 EXPERIMENTAL INVESTIGATION

6.3.1 *Materials Used in the Study*

Type I/II PC meeting requirements of ASTM C150 was used for all mixtures in this study. The chemical composition and requirements of PC are shown in **Table 6-1**. ASTM Type II de-ionized (DI) water (0.4 MΩ·in [1 MΩ·cm] at 77˚F [25˚C]) was used for all mixtures and experiments. Fine aggregates, used for the compressive strength study, were procured from a local source in Corvallis, OR and met ASTM requirements C33, *Standard Specification for Concrete Aggregates*. The sieve analysis of the fine aggregates and ASTM C33 limits are shown in **Fig. 6-1**. The fineness modulus of the fine aggregates is 3.1, determined following ASTM C136, *Standard Test Method for Sieve Analysis of Fine and Coarse Aggregates.* The specific gravity of the fine aggregates is 2.47 and the absorption is 3.08%. The specific gravity and absorption were determined following ASTM C128, *Standard Test Method for Density, Relative Density (Specific Gravity), and*

Absorption of Fine Aggregate. Ottawa graded sand meeting ASTM C778, *Standard Specification for Standard Sand*, was used for the analysis of hardened porosity, D_a, and scanning electron microscope (SEM) assessment. The specific gravity and absorption of the Ottawa graded sand is 2.65 and 2.02%, respectively.

Table 6-1. ASTM C150 requirements and actual composition of PC

Composition	Spec limit	% *
SiO_2	-	20.30
Al_2O_3	6.0 max	4.80
Fe_2O_3	6.0 max	3.50
MgO	6.0 max	0.70
SO_3	3.0 max	2.80
CaO	-	63.9
Loss on ignition	3.0 max	2.60
Insoluble residue	0.75 max	0.11
CO_2	-	1.80
Limestone	5.0 max	3.20
$CaCO_3$ in limestone	70 min	97.80
Na_{eq}	0.6 max	0.54

* reported by manufacturer

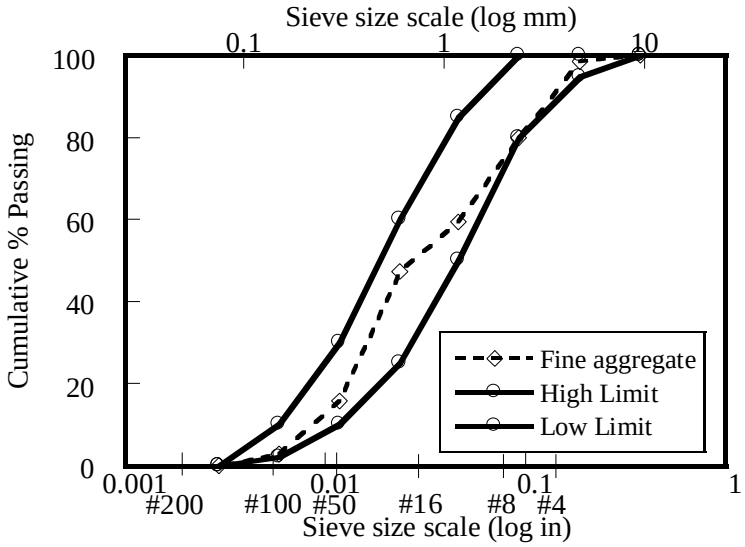

Fig. 6-1–Sieve size analysis and limits of fine aggregate used for compressive strength testing.

6.3.2 *Methods*

6.3.2.1 Preparation Method

The mixing procedure for the PC mortars followed ASTM C305, *Standard Practice for Mechanical Mixing of Hydraulic Cement Pastes and Mortars of Plastic Consistency*. The water to cement ratios (w/c) of the mortars were 0.4 and 0.485 and the cement-fine aggregate ratio was 1:2.75, as recommended in the standard. ASTM C305 provides a guideline for mixing mortars and includes two consecutive mixing stages: a low speed mixing (140 rpm) stage followed by mixing at an intermediate speed (285 rpm). This evaluation included adjusting the mixing time and speed of the second stage only. **Table 6-2** shows the mixing conditions for the PC mortars evaluated in this study. Note that the control mixture is Mixture No. 2 – this is the standard condition reported by ASTM C305. Test results are based on triplicate specimens. Note that the porosity test was also performed for mixtures with a w/c value of 0.485 mixed for 90 minutes and at two different mixing speeds (140 and 285 rpm). These additional mixing conditions resulted in 12,600 and 25,578 revolutions.

Table. 6-2 Mixing conditions for PC mortar

Mix. No.	First stage		Second stage		Number of mixer revolutions
	Time (minutes)	Speed (rpm)	Time[1] (minutes)	Speed (rpm)	
1	1	140	3	140	280
2				285	568
3			15	140	2170
4				285	4273
5			60	140	8470
6				285	17,098
7[2]			90	140	12,670
8[2]				285	25,648

[1] – include 1.5-minute rest period [2] – for porosity testing

6.3.2.2 Characterization Method

Table 6-3 shows the characteristics and mixtures assessed in this research. The 28-day porosity of the hardened mortars was modified following ASTM C642, *Standard Test Method for Density, Absorption, and Voids in Hardened Concrete*. The flow of the fresh mortars was reported to reduce with increased mixing time (Trejo and Prasittisopin 2014). Reduced flows of the fresh mixtures can lead to the need for additional energy inputs for consolidation.

Table. 6-3 Experimental program and characterization methods

w/c	Methods			
	Porosity	Compressive strength	D_a	Microstructure
0.4	✓	✓	✓	✓
0.485	✓	✓	✓	✓

To standardize the consolidation energy input for porosity specimens, a standard consolidation process was used in this study. A schematic diagram of the consolidation equipment used for fabricating the hardened porosity specimens is shown in **Fig. 6-2**. A hopper placed at a constant distance above the top of a casting mold was used to ensure that each mixture had similar consolidation energy during fabrication. About half of the first layer of mortar was placed in the hopper. After placing the mortars in the hopper, the bottom trap door was opened, allowing the mortar to free fall over the constant distance into the mold. Immediately after free-falling, a vibrating table was activated for 5 seconds. After the vibrating table was turned off, the same process was used to fill the second layer. After placing and vibrating the fresh mortars, the top surface of the specimens was struck-off and smoothed using a trowel. This process is believed to provide the same placement and consolidation energy input for each specimen, thereby allowing for the assessment of mixing time and mixer revolution counts on porosity. After fabricating porosity specimens, these specimens were kept in plastic molds for 24

hours and then demolded. Test specimens were then cured in saturated-lime solution until testing the 28-day porosity.

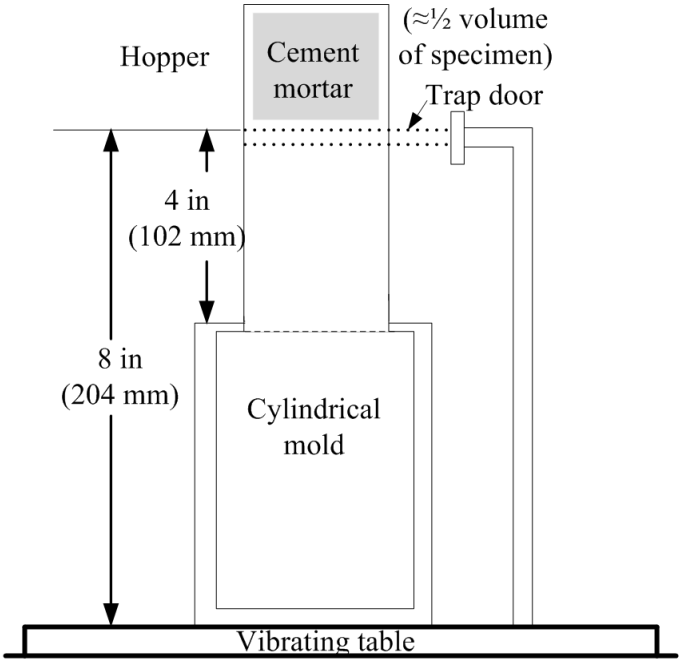

Fig. 6-2–Diagram of standardized consolidation equipment for porosity testing.

The compressive strength of the PC mortars was determined following ASTM C109/C109M, *Standard Test Method for Compressive Strength of Hydraulic Cement Mortars (Using 2-in. or [50-mm] Cube Specimens).* After casting, test specimens were kept in plastic molds for 24 hours and then demolded. Demolded specimens were then cured in saturated-lime solution until testing.

The D_a was determined following ASTM C1556, *Apparent Chloride Diffusion Coefficient of Cementitious Mixtures by Bulk Diffusion*. After casting 3-in by 6-in (75-mm by 150-mm) cylindrical mortar specimens, the specimens were kept in plastic molds for 24 hours and then demolded. Test specimens were then cured in saturated-lime solution for 28 days and then exposed to chloride solution for 35 days. Powder specimens were tested for chloride ion content following ASTM C1152, *Standard Test Method for*

Acid-Soluble Chloride in Mortar and Concrete. A computer controlled potentiometric auto-titrator with a sample changer was used to test chloride ion content. After determining chloride ion content at different depths from the top surface, Fick's second law, as shown in Eq. 6-1, was used to determine the D_a.

$$C(x,t) = C_s - [(C_s - C_i) \times erf\ (\frac{x}{\sqrt{4D_a t}})] \quad \text{Eq. (6-1)}$$

where $C(x,t)$ is percent chloride ion concentration at depth x and time t; C_s is predicted percent chloride ion concentration at the surface of the exposed mortar; C_i is percent initial chloride ion concentration of PC mortars before solution exposure; and *erf* is the error function.

Specimens used to observe representative microstructures of the mortars had a w/c value of 0.485 and cured for 28 days. Specimens were mixed for different periods (3, 60, and 90 minutes). After 28 days of curing, the specimens were crushed and soaked with ethanol. The ethanol-soaked specimens were dried and examined using SEM.

6.3.2.3 Statistical Data Analysis

Two-sample t-test and analysis of variances (ANOVA) analyses were performed to compare the means between two groups and more than two groups, respectively. Prior to the analyses, the Shapiro-Wilk test was used to determine if data were normally distributed and the Levene's test was used to determine if the data had equal variance. The statistical hypotheses for the analyses are defined as:

Null hypothesis (H_0): $\mu_1 = \mu_2 = \ldots - \mu_a$ Eq. (6-2)

Alternative hypothesis (H_a): $\mu_i \neq \mu_j$ for some $i \neq j$ Eq. (6-3)

A 95% confidence interval was used in these analyses. If the H_0 is rejected (p-value ≤ 0.05), it can be concluded that there is a statistically significant effect at the 5% level between the means of the different group populations. Alternatively, if the H_0 is not

rejected (p-value > 0.05), it can be concluded that there is no statistically significant effect at the 5% level between the means of the different group populations.

6.4 RESULTS AND DISCUSSION

6.4.1 *Porosity*

The effect of mixing time (from 3 to 90 minutes) on the 28-day porosity of mixtures mixed at 140 and 285 rpm is shown in **Fig. 6-3a**. Results indicate that the porosity of mixtures rapidly increases as a function of mixing time from 3 to 15 minutes, but increases at significantly lower values thereafter. Note that increasing mixing time longer than 90 minutes made the mortars difficult to cast and this resulted in honeycombing in the hardened mortars. The data from these specimens are not included in **Figs. 6-3**. For mixtures with w/c values of 0.4, increases in mixing time from 3 to 15 minutes result in a significant increase in porosity (two-sample t-test with p-value = 0.004 for 140 rpm and 0.013 for 285 rpm). For the mixtures with w/c values of 0.485, there is no significant difference in means (two-sample t-test with p-value = 0.149 for 140 rpm and 0.418 for 285 rpm). Increased mixing time (from 15 and 90 minutes) does not significantly affect the porosity for all systems (ANOVA test with p-values > 0.05).

Takahashi *et al.* (2011) assessed the effect of mixing time on the microstructure of cementitious materials and reported that the mixtures that were mixed longer have altered microstructure of hydrated products. Diamond (2005) reported that concrete mixed for longer mixing times can generate smaller fragments from aggregates and smaller cement particles due to impact and friction between the mixer tools and the constituent particles. Diamond (2005) also reported denser transition zones from increased mixing times but did not report on the overall porosity of the bulk materials. The literatures indicate that longer mixing times can alter the microstructure, which could result in the change in porosity.

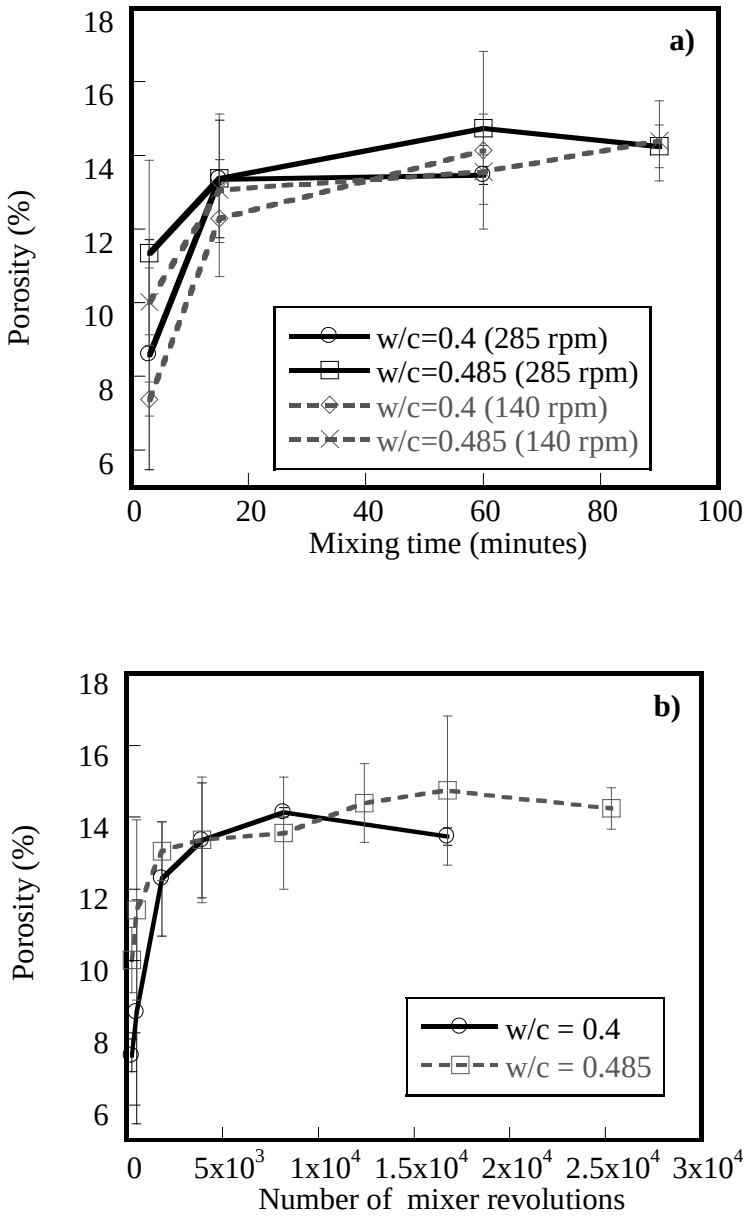

Fig. 6-3–Effect of a) mixing time and b) number of mixer revolutions on 28-day porosity of PC mortars mixed at 140 and 285 rpm for different w/c values.

The influence of mixer revolution counts (from 280 to 25,578 revolutions) on the porosity of mixtures with w/c values of 0.4 and 0.485 is shown in **Fig. 6-3b**. Similar to the results in **Fig. 6-3a**, increasing the mixer revolution counts at lower revolutions (less

than approximately 3000) results in a significant increase in porosity (ANOVA test for mixtures with w/c of 0.4 and 0.485 exhibit p-values of 0.028 and 0.013, respectively). However, increasing the mixer revolution counts at higher revolution counts (more than approximately 3000) has less influence on the porosity of mixtures (p-value = 0.518 and 0.706 for w/c of 0.4 and 0.485, respectively).

Figs. 6-4a and **6-4b** show the flow of the fresh mixtures as a function of mixing time and mixer revolution counts, respectively (Trejo and Prasittisopin 2014). Results indicate that increased mixing time and revolution counts lead to a reduction of flow values. **Fig. 6-5** shows the relationship between the normalized flow and the 28-day porosity mixed for different mixer counts. The flow values are normalized with the average flow for different numbers of mixer revolutions for all mixtures. The increase of the 28-day porosity for mixtures mixed with increased number of mixer revolutions is likely a result from the reduction in flow.

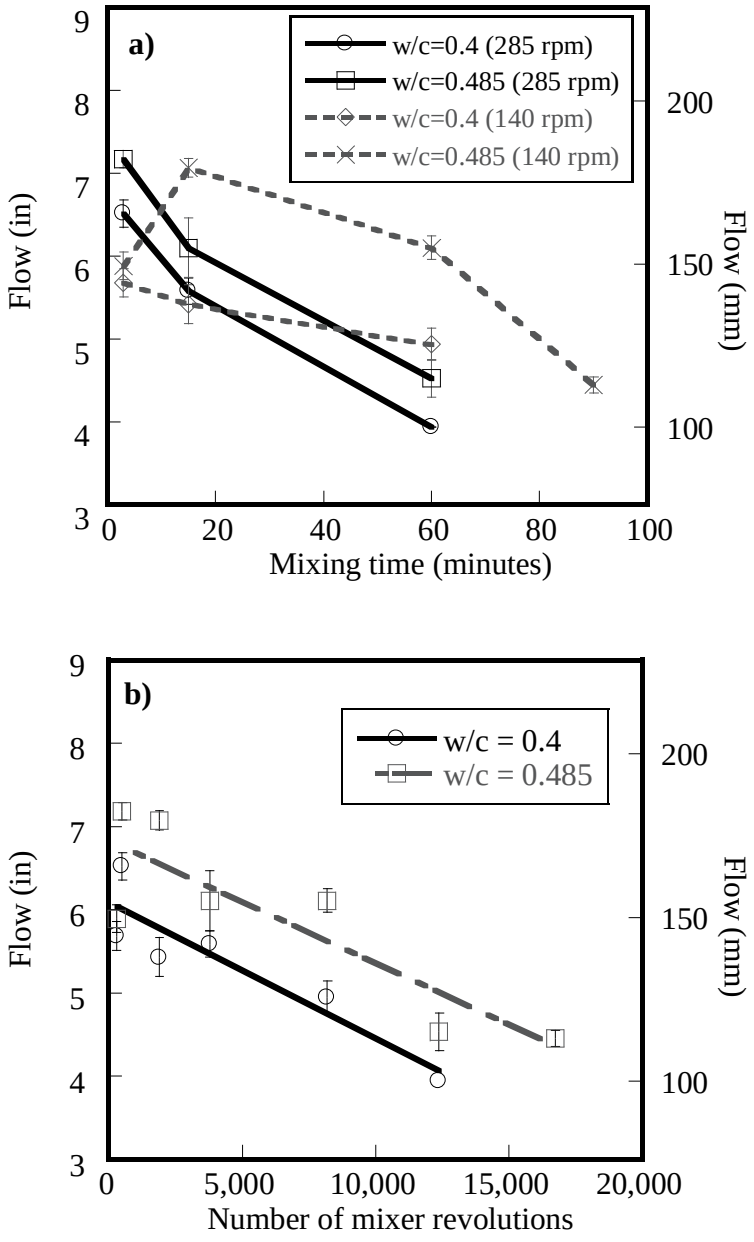

Fig. 6-4–Effect of a) mixing time and b) number of mixer revolutions on flows of PC mortars mixed at 140 and 285 rpm for different w/c values (Trejo and Prasittisopin 2014).

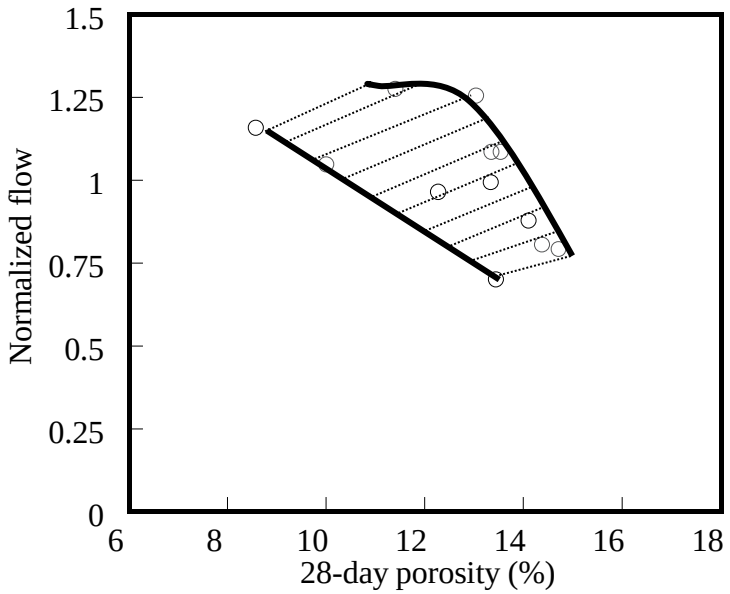

Fig. 6-5–Relationship and area fit between normalized flow and 28-day of mortars with the w/c values of 0.4 and 0.485 and mixed at different number of mixer revolutions.

6.4.2 *Compressive Strength*

Several researchers (Cook 1943, Ravina 1996, Mahboub and Cutshaw 2001, Kirca *et al.* 2002, Erdogdu 2005) investigated the effect of mixing time on the compressive strength of concrete and reported that increased mixing time resulted in increased compressive strength. Kirca *et al.* (2002) reported that increased mixing time led to increased compressive strength and reported that this is due to mixtures (1) having lower w/c values due to the evaporation of water and/or (2) having finer constituent particles generated from the impact and friction between the particles and mixing tools. However, Baskoca (1998) and Han *et al.* (2013) reported that increased mixing time resulted in a reduction in compressive strength of the mixtures. This was reported to be due to the decrease in workability and increase in porosity.

Increases in mixing time and mixer revolution counts could result in altered compressive strengths. Critical to contractors and owners is whether the material meets

the design requirements for compressive strength. To determine whether the compressive strength of mortars mixed for different mixing times and mixer revolution counts can meet compressive strength requirements, the ratio of the actual compressive strength and the specified compressive strength was used. The C150 specification requires 7- and 28-day compressive strength of mortars with w/c values of 0.485 to be 2760 (19.0) and 4060 psi (28.0 MPa), respectively. Because 1-day test was also performed, the 1-day compressive strength of mixtures can be estimated based on an equation reported by Paya *et al.* (1997):

$$\text{compressive strength} = a + b \times \log(\text{age}) \qquad \text{Eq. (6-4)}$$

where a is 935 psi (6.5 MPa) and b is 2160 psi (14.9 MPa).

To determine compressive strength of specimens with w/c of 0.4, a specified compressive strength had to be determined. Lollini *et al.* (2013) reported that the average compressive strength of mortars with w/c = 0.4 is approximately 15% higher than the compressive strength of mixtures with w/c = 0.485. Here, it will be assumed that mortars with w/c = 0.4 have compressive strength values 15% greater than the mortars with w/c = 0.485 and these values will be used for determining the compressive strength ratio. **Table 6-4** shows ASTM C150 required compressive strength values and predicted compressive strength values used to determine the compressive strength ratios for the different mixing conditions. The ratio of actual to specified compressive strength greater than the unity indicates that the compressive strength of the mortars meets the strength requirement and the ratio lower than unity indicates that the compressive strength does not meet the strength requirement.

Table. 6-4 Compressive strength requirements for different ages of PC mortars at w/c values of 0.4 and 0.485

w/c value	C150 compressive strength requirements		
	1-day [psi (MPa)]	7-day [psi (MPa)]	28-day [psi (MPa)]
0.4	1075 (4.7)[1]	3174 (21.9)[1]	4669 (32.2)[1]
0.485	935 (6.5)[1]	2760 (19.0)	4060 (28.0)

[1] estimated data

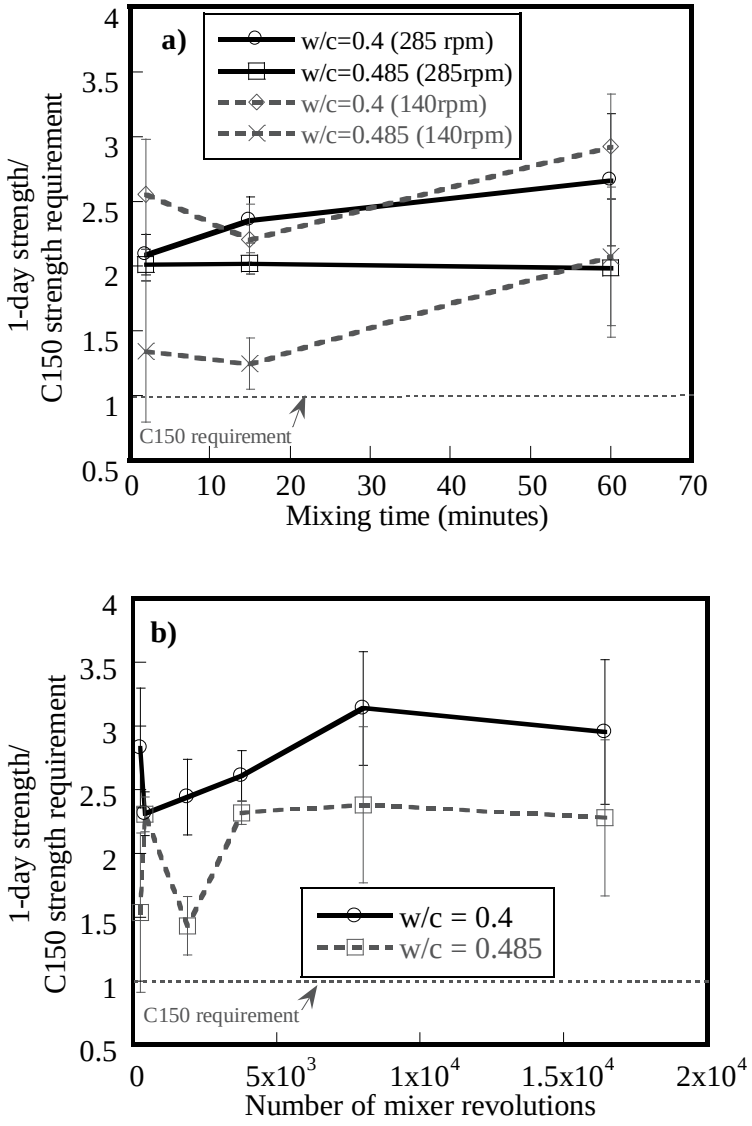

Fig. 6-6–Effect of a) mixing time and b) number of mixer revolutions on 1-day compressive strength/C150 strength requirement of PC mortars.

Fig. 6-6a shows the effect of mixing time on the 1-day compressive strength ratio for mortars mixed with different w/c values and speeds. Results indicate that the 1-day compressive strengths of all mixtures mixed for different times meet the predicted minimum requirements. Increased mixing time results in increased 1-day strength ratios. **Fig. 6-6b** shows the effect of the number of mixer revolutions on the 1-day compressive

strength ratio for mortars mixed with different w/c values. Results indicate that the compressive strengths of all systems meet the "minimum requirements" for the predicted 1-day compressive strength. The ratio values of the mixtures with w/c value of 0.4 are higher than the ratio values of mixtures with w/c value of 0.485.

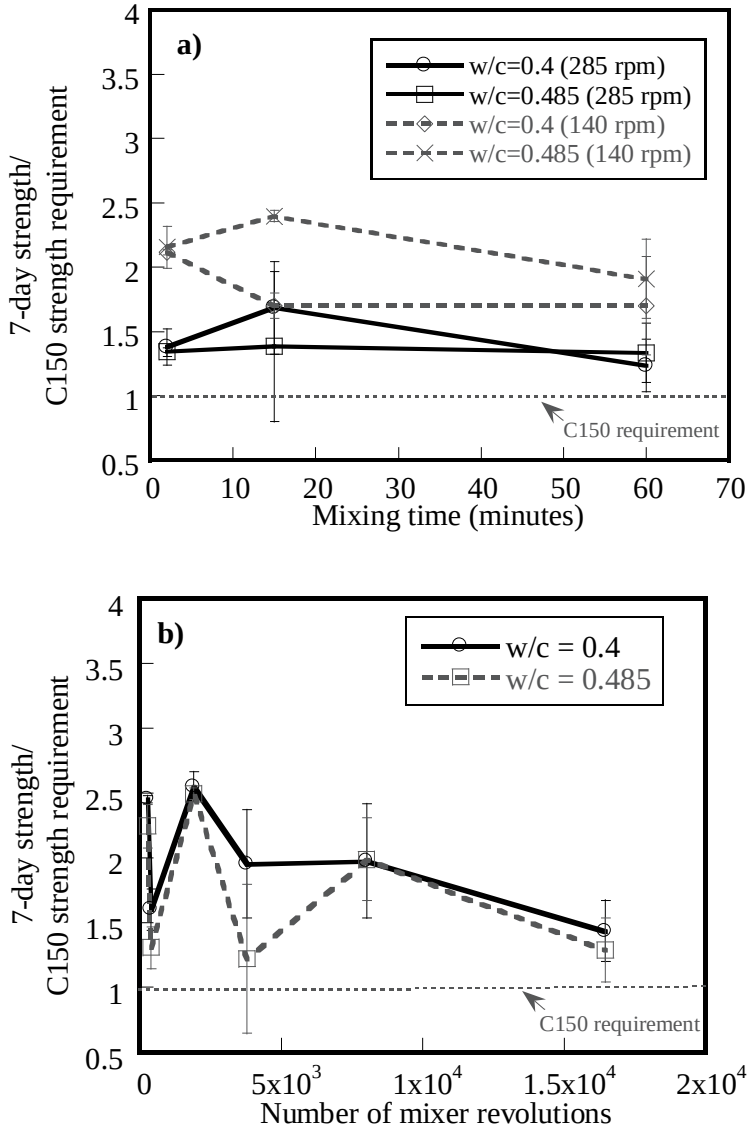

Fig. 6-7–Effect of a) mixing time and b) number of mixer revolutions on 7-day compressive strength/C150 strength requirement of PC mortars.

Fig. 6-7a shows the 7-day compressive strength ratio for mixtures with w/c values of 0.4 and 0.485 mixed at different mixing speeds and times. Results indicate that the compressive strengths of all mixtures meet the C150 7-day compressive strength requirements. The 7-day compressive strengths of the mortars mixed at lower speeds (140 rpm) are higher than the mortars mixed at higher speeds (285 rpm). **Fig. 6-7b** shows the 7-day compressive strength ratios of mixtures with w/c values of 0.4 and 0.485 as a function of number of mixer revolutions. Results indicate that the 7-day compressive strengths of all mixtures meet the C150 requirements. There is no significant difference in means of the compressive strength ratios between the mixtures with w/c value of 0.4 and the mixtures with w/c value of 0.485 (two-sample t-test with p-values > 0.05 for all systems).

The influence of the mixing time on the 28-day compressive strength ratio for mixtures with w/c values of 0.4 and 0.485 mixed at 140 and 285 rpm is shown in **Fig. 6-8a**. Results indicate that longer mixing times result in reduced compressive strength ratio values. All 28-day compressive strengths meet the C150 requirements except the 0.485 mixtures at 285 rpm for 60 minutes. The effect of the mixer revolutions counts on the 28-day compressive strength ratio for mixtures with w/c values of 0.4 and 0.485 is shown in **Fig. 6-8b**. Results indicate that the mortars mixed at 17,028 counts exhibited lower 28-day compressive strengths than the required strength. Although most mixtures meet the C150 requirements, mixtures mixed with higher w/c values and high revolutions did not meet the 28-day strength requirements.

Results indicate that the mortars mixed for longer times or higher mixer revolution counts can meet the compressive strength requirements at 1 and 7 days. Very high mixer revolutions resulted in 28-day compressive strengths being lower than the specified compressive strengths.

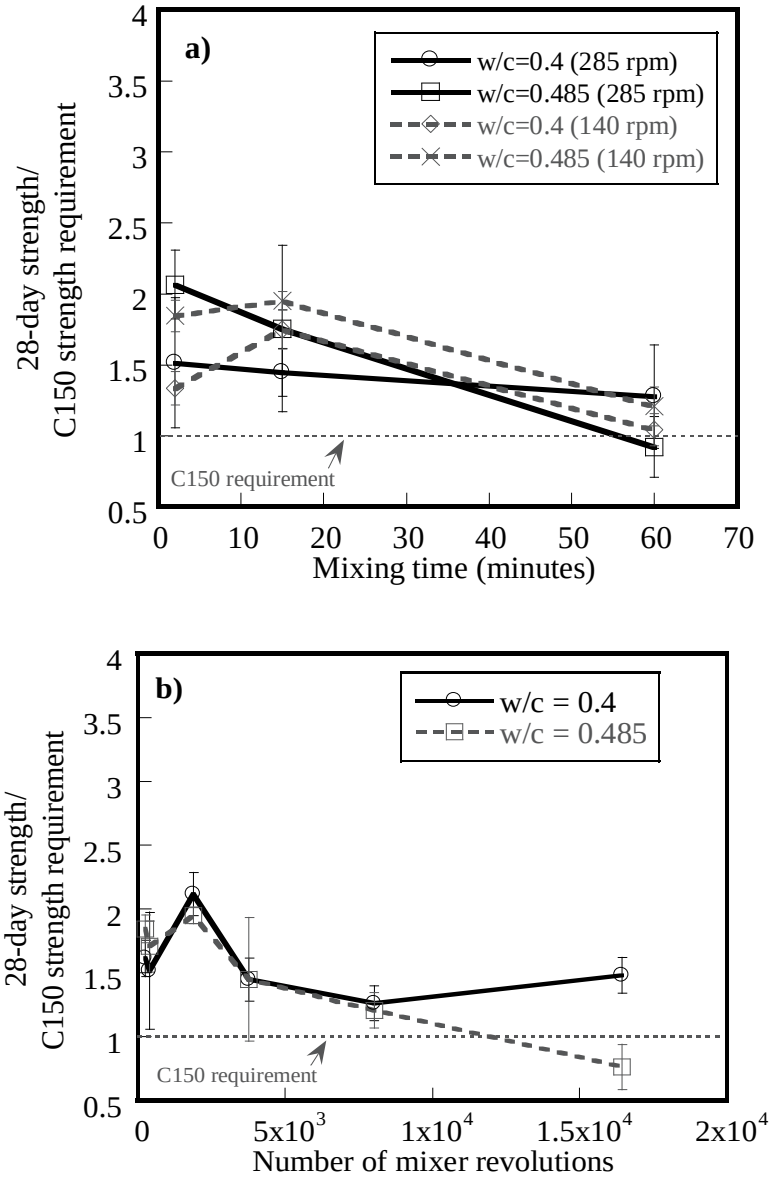

Fig. 6-8–Effect of a) mixing time and b) number of mixer revolutions on 28-day compressive strength/C150 strength requirement of PC mortars.

Fig. 6-9 shows the correlation between the normalized 28-day compressive strength and the 28-day hardened porosity of mixtures with w/c values of 0.4 and 0.485 for different mixer revolution counts. The 28-day compressive strengths are normalized with the average 28-day compressive strength for each w/c value. The logarithmic curve

fit was reported by Neveille (1996) and the exponential and linear curve fits were reported by Brandt (1995). Results indicate that compressive strength is correlated with porosity and porosity increases with increasing mixer revolution counts. This increased porosity can lead to lower compressive strength if the mixture is mixed at a higher number of mixer revolutions. Results also indicate that the increased porosity is due to decreased flow (**Fig. 6-5**).

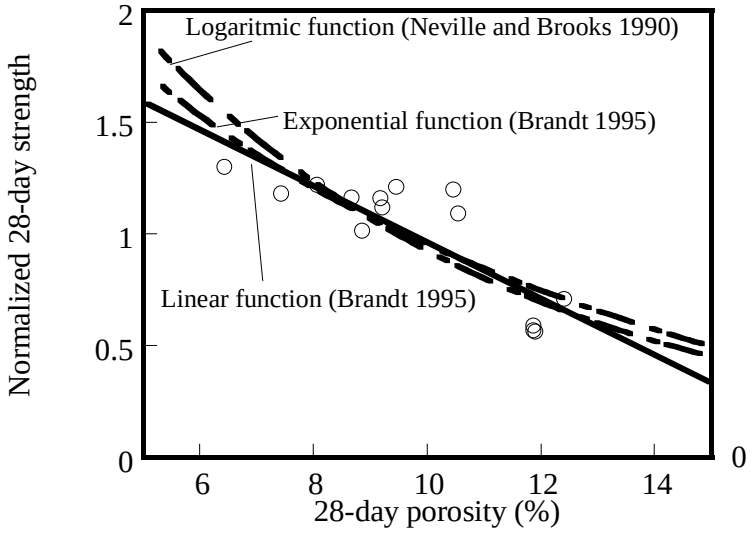

Fig. 6-9–Relationship and fitted-curves between normalized 28-day compressive strength and 28-day porosity of hardened PC mortars with the w/c values of 0.4 and 0.485 and mixed at different number of mixer revolutions.

6.4.3 *Apparent Chloride Diffusivity Coefficient*

The effect of the mixing time on the D_a of the mixtures mixed at 140 and 285 rpm for w/c values of 0.4 and 0.485 is shown in **Fig. 6-10a**. Results indicate that the D_a of mixtures with w/c values of 0.4 and 0.485 mixed at 140 rpm is not affected by mixing time (ANOVA test with p-value = 0.204 and 0.220, respectively). In addition, results also indicate that increased mixing time does not significantly influence the D_a of mixtures

with w/c values of 0.4 and 0.485 mixed at 285 rpm (ANOVA test with p-value = 0.599 and 0.203, respectively).

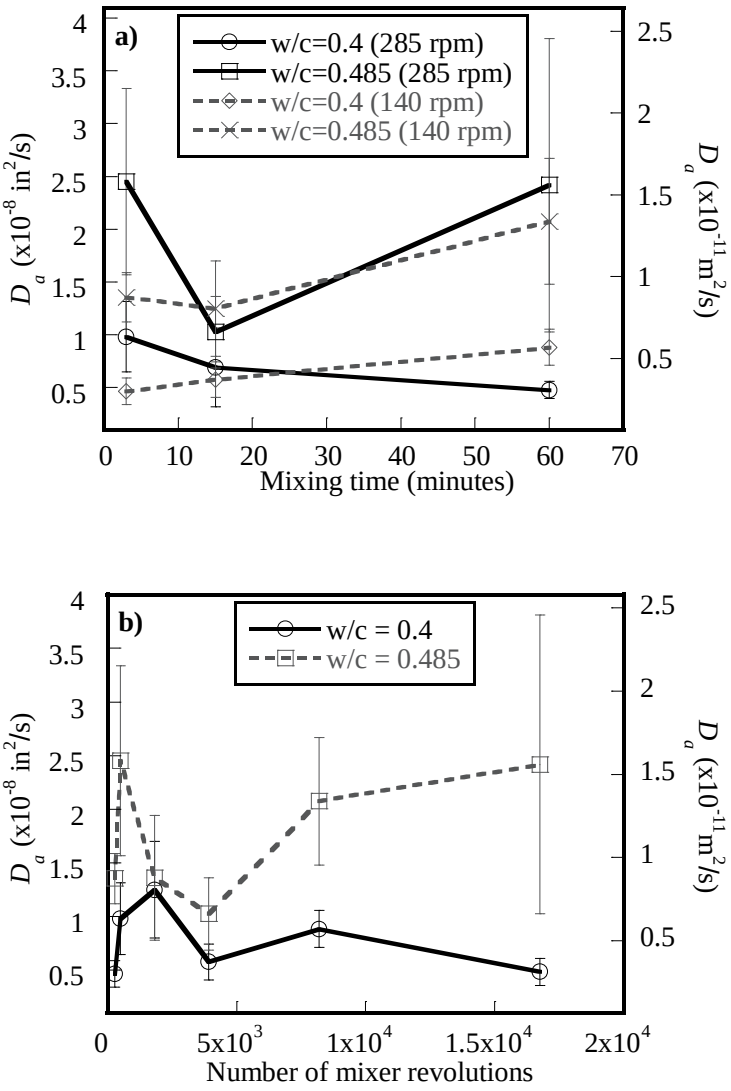

Fig. 6-10–Effect of a) mixing time and b) number of mixer revolutions on D_a of PC mortars for different w/c values.

The effect of the number of mixer revolutions on the D_a of the mixtures with w/c values of 0.4 and 0.485 is shown in **Fig. 6-10b.** Results indicate that increased number of mixer revolutions exhibited no significant difference in means of the D_a of mixtures with w/c values of 0.4 and 0.485 (ANOVA test with p-value = 0.084 and 0.203, respectively). Test results indicate that the D_a of the hardened mortars is not influenced by mixing time and number of mixer revolutions.

6.4.4 *Microstructure Assessment*

Fractured surfaces of specimens mixed for different times were observed using a SEM. **Figs. 6-11a**, **6-11b**, and 6-**11c** show representative SEM images of the microstructures of mortars with a w/c value of 0.485 and mixed for 3, 60, and 90 minutes, respectively. The microstructure of the specimens mixed for 3 minutes exhibited smoother and more gel-like surfaces than the specimens mixed for longer durations. The surfaces of specimens mixed for 60 minutes (**Fig. 6-11b**) exhibited irregular surfaces, and the microstructure of specimens mixed for 90 minutes (**Fig. 6-11c)** also exhibited irregular surfaces. As already noted, Diamond (2005) and Takahashi (2011) reported that larger mixing times can lead to changes in the microstructure. The extended mixing times resulted in higher porosity values. In preparing the SEM specimens, the fracture surfaces exhibited more irregular surfaces, which may be a result of the increased porosity. No clear differences in chemistry of hydrated products were observed and more research is needed to determine why the fractured surfaces changed.

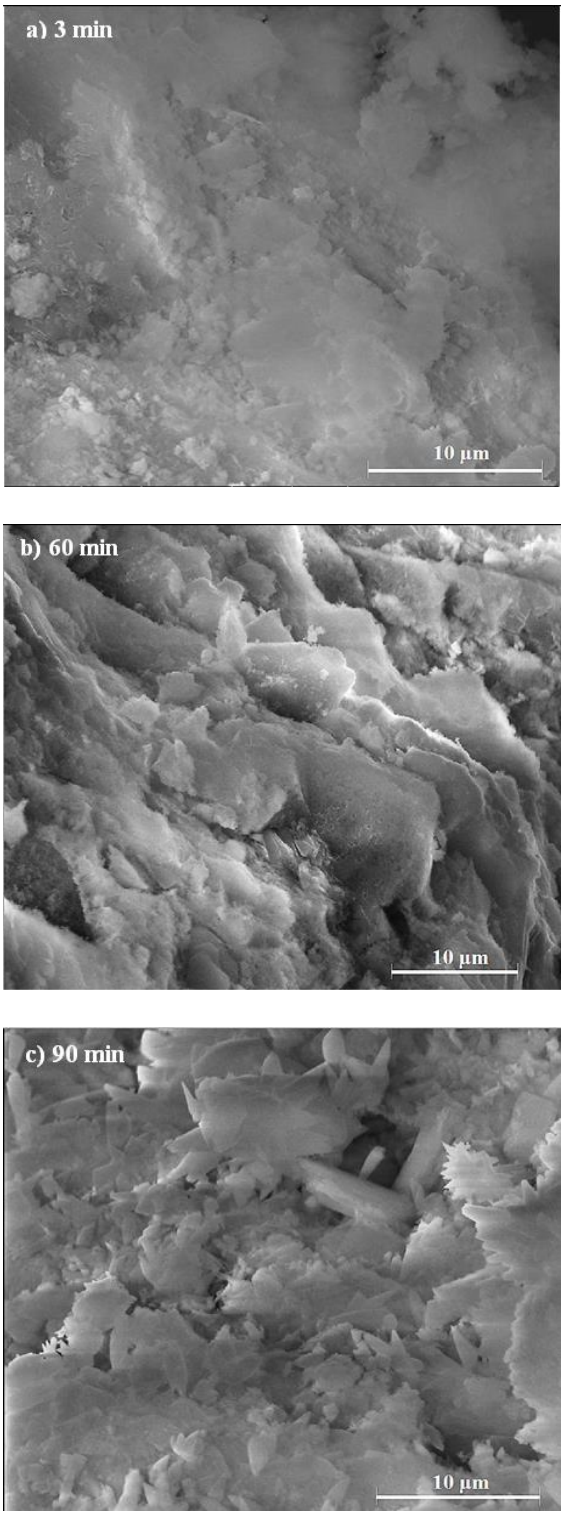

Fig. 6-11–Microstructure of PC mortars (w/c = 0.485) after cured for 30 days and mixed for a) 3 minutes, b) 60 minutes, and c) 90 minutes.

6.5 CONCLUSIONS

The effects of mixing time and mixer revolution counts of PC mortar systems on the hardened characteristics were investigated in this study. Based on the experimental results, the following conclusions can be made:

- Increased mixing time and increased mixer revolution counts results in rapid increases the 28-day porosity at early times and lower revolution counts. Beyond approximately 3000 mixer revolutions and 15 minutes of mixing, the porosity stabilizes to about 14%.
- All mixtures mixed at different mixing times and mixer revolution counts exceed the required predicted compressive strength except mixtures mixed at 17,028 revolutions. Mixtures mixed at 17,028 revolutions exhibited about 95% of the required compressive strength.
- The statistical analyses show that there is no significant influence of the mixing variables on the D_a.
- Increased mixing time results in modified microstructure of hydrated products. Microstructure of the mixtures mixed for shorter periods (e.g., 3 minutes) exhibited smooth surfaces; while, mixtures mixed for longer periods (e.g., 60 minutes and greater) exhibited irregular surfaces. The reasons for this are unknown at this time.

This research investigated the influence of mixing variables on hardened mortar characteristics. Studies are currently underway evaluating mixing variables on concrete

properties. Results from this study and the studies on concrete counts can be used to determine if time and mixer revolution requirements are still valid.

6.6 ACKNOWLEDGEMENTS

This study was conducted at the school of Civil and Construction Engineering, Oregon State University. The researchers acknowledge the support of Lafarge Cement, for provided the cement for this research.

6.7 REFERENCES

Al-Gahtani, H. J., Abbasi, A. G. F., and Al-Amoudi, O. S. B., *Concrete Mixture Design for Hot Weather: Experimental and Statistical Analyses*, in *Magazine of Conc. Res.*, 1998, Thomas Telford Services, London.

Al-Negheimish, A. I. and Alhozaimy, A. M. (2008), "Impact of Extremely Hot Weather and Mixing Method on Changes in Properties of Ready Mixed Concrete During Delivery," *ACI Mat. J.*, V. 105, No. 5, pp. 438-444.

Andersen, P. J. and Hodson, S. K., Concrete Having High Workability through Control of Fine-to-Coarse Particulates Ratio, A. Teasdale, Editor, 2009, iCrete, U.S., 28 pp.

Baskoca, A., Ozkul, M. H., and Artirma, S. (1998), "Effect of Chemical Admixtures on Workability and Strength Properties of Prolonged Agitated Concrete," *Cem. Con. Res.*, V. 28, No. 5, pp. 737-747.

Bloem, D. L. and Gaynor, R. D. (1971), "Factors Affecting the Homogeneity of Ready-Mixed Concrete," *J. ACI*, V. 68, No. 7, pp. 521-525.

Brandt, A. M. (1995), Cement Based Composites: Materials, Mechanical Properties and Performance, UK, E & FN Spon.

Chen, C. T. and Struble, L. J. (2009), "Influence of Mixing Sequnce on Cement-Admixture Interaction," *ACI Mat. J.*, V. 106, No. 6, pp. 503-508.

Cook, G. C. (1943), "Effect of Time of Haul on Strength and Consistence of Ready-Mixed Concrete " *J. ACI*, V. 14, No. 5, pp. 413-428.

Dewar, J. D. and Anderson, R. (1992), *Manual of Ready Mixed Concrete*, 2nd ed., Glasgow, UK, Blackie Academic and Professional, 72 pp.

Diamond, S. (2005), "The Patch Microstructure in Concrete: Effect of Mixing Time," *Cem. Con. Res.*, V. 35, No. 5, pp. 1014-1016.

Erdogdu, S. (2005), "Effect of Retempering with Superplasticizer Admixtures on Slump Loss and Compressive Strength of Concrete Subjected to Prolonged Mixing," *Cem. Con. Res.*, V. 35, No. 5, pp. 907-912.

Erdogdu, S., Arslanturk, C., and Kurbetci, S. (2011), "Influence of Fly Ash and Silica Fume on the Consistency Retention and Compressive Strength of Concrete Subjected to Prolonged Agitating," *Constr. Build. Mater.*, V. 25, No. 3, pp. 1277-1281.

Han, V., Ros, S., and Shima, H. (2013), "Effects of Sand Content, Superplasticizer Dosage, and Mixing Time on Compressive Strength of Mortar," *ACI Mat. J.*, V. 110, No. 1, pp. 23-31.

Kirca, O., Turanli, L., and Erdogan, T. Y. (2002), "Effect of Retempering on Consistency and Compressive Strength of Concrete Subjected to Prolonged Mixing," *Cem. Con. Res.*, V. 32, No. 3, pp. 441-445.

Lollini, F., Redaelli, E., and Bertolini, L. (2013), "Effects of Portland Cement Replacement with Limestone on the Properties of Hardened Concrete," *Cem. Con. Comp.*

Mahboub, K. C. and Cutshaw, Q. A. (2001), "Effects of Fresh Concrete Temperature and Mixing Time on Compressive Strength of Concrete," *ACI Mat. J.*, V. 98, No. 1, pp. 59-62.

Nehdi, M. and Al-Martini, S. (2009), "Coupled Effects of High Temperature, Prolonged Mixing Time, and Chemical Admixtures on Rheology of Fresh Concrete," *ACI Mat. J.*, V. 106, No. 3, pp. 231-240.

Neville, A. M. (1996), *Properties of Concrete*, 4th ed., New York, John Wiley & Sons.

Ozkul, M. H., Baskoca, A., and Artirma, S. (1997), "Influence of Prolonged Agitation on Water Movement Related Properties of Water Reducer and Retarder Admixtured Concretes," *Cem. Con. Res.*, V. 27, No. 5, pp. 721-732.

Payá, J., Monzó, J., Borrachero, M. V., Peris, E., and González-López, E. (1997), "Mechanical Treatments of Fly Ashes. Part III: Studies on Strength Development of Ground Fly Ashes (GFA) — Cement Mortars," *Cem. Con. Res.*, V. 27, No. 9, pp. 1365-1377.

Ravina, D. (1975), "Retempering of Prolong-Mixed Concrete with Admixtures in Hot Weather," *J. ACI*, V. 72, No. 6, pp. 291-295.

Ravina, D. (1996), "Effect of Prolonged Agitating on Compressive Strength of Concrete with and without Fly Ash and/or Chemical Admixtures," *ACI Mat. J.*, V. 93, No., pp. 451-456.

Takahashi, K., Bier, T. A., and Westphal, T. (2011), "Effects of Mixing Energy on Technological Properties and Hydration Kinetics of Grouting Mortars," *Cem. Con. Res.*, V. 41, No. 11, pp. 1167-1176.

Trejo, D. and Prasittisopin, L., Effects of Mixing Variables on Early-Age Characteristics of PC Systems, 2014. (Under review)

7 EFFECTS OF MIXING VARIABLES ON CHARACTERISTICS OF BLENDED CEMENT SYSTEMS CONTAINING RICE HUSK ASH

ABSTRACT

The performance and economy of our infrastructure is dependent on specifications used to construct it. Good specifications should be responsive to a current construction technologies. Many existing specifications for ready-mixed concrete contain limits on mixing time and drum revolution counts. A comparison paper assessed the influence of mixer revolution counts and time on the characteristics of portland cement (PC) pastes and mortars. This paper will assess the influence of time and revolution counts on the characteristics of PC systems containing rice husk ash (RHA).

Specifically, this study assesses the effects of mixing time and revolution count on the ion concentration, flowability, setting time, chemical shrinkage, porosity, compressive strength, and chloride diffusivity of pastes and mortars containing RHA. Systems assessed include as-received RHA (AR-RHA), transformed RHA (t-RHA), and AR-RHA with retarder (AR-RHA+R). Results indicate that although the mixing variables influence the characteristics, RHA type has a greater effect on these characteristics.

Keywords: Rice Husk Ash; Mixing Time; Mixer Revolution Count; Chemical Transformation; Retarder

Submitted to
American Concrete Institute Materials Journal

7.1 INTRODUCTION

Rice husk ash (RHA) is an agricultural waste product and is obtained from burning rice husks for generation of electricity. Its composition is reported to contain high amorphous silica (Trejo and Prasittisopin 2014a). This amorphous silica can react with portlandite ($Ca(OH)_2$) to form pozzolanic (C-S-H) products. The C-S-H products can lead to improved concrete performance characteristics. RHA has the potential for being used as a supplementary cementing material (SCM). Cementitious systems containing RHA have been reported to exhibit good early-age characteristics (Bui *et al.* 2005). Replacement of portland cement (PC) with RHA is reported to lead to improved mechanical properties (Vayghan *et al.* 2011, Muthadhi and Kothandaraman 2013), improved resistance to chloride penetration and sulphate attack (Sakr 2006, Venkatanarayanan and Rangaraju 2013), good freeze-thaw performance (Azevedo *et al.* 2001, Maeda *et al.* 2001, Nehdi *et al.* 2003, Gastaldini *et al.* 2007), good resistance to alkali-aggregate reaction (AAR) expansion (Shuichi et al. 1992), and improved resistance to deicing salt scaling (Mehta and Folliard 1995). The use of RHA in concrete can lead to improved overall system performance. Although reported to be a beneficial SCM, the use of RHA has not been as widespread, such as fly ash. However, improvements in processing and transformation of the cellular, honeycomb-like structure are making RHA a more economically viable material, especially in the wake of decreasing coal production and reduced availability of fly ash. To further enhance the use of RHA, more research is needed on how mixing, transporting, and placing systems containing RHA influence the fresh and hardened characteristics. This paper addresses these issues.

Specifications are critical in ensuring that our infrastructure is constructed to save minimum standard. These specifications can also significantly influence the cost to construct our infrastructure. Standard specifications that place limits on materials, suppliers, and/or contractors may result in increased construction and life cycle costs, especially if these specifications do not result in improved economy, constructability, or concrete performance. Hooton (2008) reported that historically prescriptive specifications should be switched to performance-based specifications so as not to limit the

development of alternative materials and construction practices (e.g., concrete systems with SCMs and chemical additives). These specifications include the standard specifications and guidelines for ready-mixed concrete.

The American Society for Testing and Materials (ASTM) defines ready-mixed concrete as concrete manufactured and delivered to a purchaser in a fresh state. Specifications for ready-mixed concrete from the American Association of State Highway and Transportation Officials (AASHTO), the American Concrete Institute (ACI), ASTM, and many State Highway Agencies (SHAs) place limits for mixing and agitating truck mixed concrete. These specifications place limits on mixing time, total number of drum revolution counts, and/or concrete temperature. ASTM placed the first limit on the concrete discharge time at 90 minutes in 1935 and this limit is still in place. In the U.S., 48 SHAs limit the maximum discharge time of concrete system (from 45 to 90 minutes); 30 SHAs limit the maximum truck drum revolution counts (from 250 to 300 counts); and 45 SHAs limit the maximum placement temperature (from 28 to 38˚C [82 to 100˚F]).

Many SHAs limit these mixing variables because increased mixing times, drum revolution counts, and concrete temperatures can result in reduced workability of fresh concrete. In addition, high concrete temperatures can lead to later deterioration. Trejo and Prasittisopin (2014b) reported that increasing mixing times and laboratory mixer revolution counts can alter not only flowability of mortars but also influence setting time (ST) and chemical shrinkage (CS) of PC pastes (without SCMs). Reduced workability makes it more difficult to place and consolidate fresh concrete. Al-Gahtani *et al.* (1998) and Lynsdale and Khan (2000) reported that improper placement and consolidation processes can result in reduction of compressive strengths (f_c) and durability issues.

Specification limits have been in place for most ready-mixed concrete systems (conventional systems and systems containing SCMs) for approximately 80 years. The Portland Cement Association (2000), reported that more than 50% of ready-mixed concrete contains SCMs. The utilization of the SCMs in ready-mixed concrete should be

even higher because using SCMs makes concrete more sustainable and economical and by using the materials, there are long-term ecological benefits. Concrete systems having SCMs are ubiquitous. Some studies have been performed to investigate the effects of mixing time and mixer revolution counts on the characteristics of cementitious material systems containing fly ash (Ravina 1996, Prasittisopin and Trejo 2013) and silica fume (Erdogdu et al. 2011). The study by Prasittisopin and Trejo (2013) reported that the reduction in flowability and f_c of PC systems resulting from increased mixing times and mixer revolution counts could be reduced by replacing PC with fly ash. The researchers also reported that specification limits of mixing time and mixer revolution counts for ready-mixed concrete may need to be modified when fly ash is present in the systems.

RHA can lead to the improvement of overall performance of cementitious systems. However, limited research has been performed on how mixing variables (i.e., mixing times and mixer revolution counts) influence the performance characteristics of the cementitious systems containing RHA. As important, limited research has been performed to determine if limits in specifications are applicable to concrete systems containing RHA.

This paper presents results from a laboratory research program assessing the influence of mixing times and mixer revolution counts on the fresh and hardened characteristics of paste and mortar systems containing RHA. The systems contained as-received RHA (AR-RHA), chemically transformed RHA (t-RHA), and AR-RHA with a retarder (AR-RHA+R) systems. Fresh characteristics evaluated include the time-variant concentrations of hydroxyl, calcium, and aluminate ions in solution, flowability, ST, and CS and the hardened characteristics included porosity, f_c, and apparent chloride diffusivity coefficient (D_a).

7.2 RESEARCH SIGNIFICANCE

Although the use of SCMs in ready-mixed concrete is ubiquitous, the applicability of specifications and guidelines that limit mixing times and drum revolution counts for these

systems is unknown. The cement and concrete industries continually work to become greener industries. Yet specifications that limit the implementation or use of materials that make the industries greener, especially when there is no correlation between the limits and the performance of the concrete systems, are counterproductive and add no value. This paper reports on the effects of mixing time and mixer revolution counts, two parameters limited in many specifications, of systems containing different types of RHA. This information can be used to determine the applicability of current limits in mixing specifications.

7.3 EXPERIMENTAL INVESTIGATION

7.3.1 *Materials*

Type I/II PC met ASTM C150 requirements was used for all mixtures in this study. AR-RHA was procured from a power plant company in Lake Charles, LA. The chemical composition of PC and AR-RHA is shown in **Table 7-1**. The average particle size of AR-RHA is 192 µm (0.0075 in). Standard graded sand meeting ASTM C778 was used for the flowability, porosity, and D_a studies. Fine aggregate, used for the f_c specimens, was procured from a local source in Corvallis, OR and met ASTM requirements C33. The fineness modulus of the fine aggregate was 3.1 determined following ASTM C136. The specific gravity of the fine aggregate was 2.47 and the absorption was 3.08%. The specific gravity and absorption values were determined following ASTM C128. Type II de-ionized (DI) water [1 MΩ·cm at 25˚C (0.394 MΩ·in at 77 ˚F)] was used for all mixtures and experiments. The liquid retarder is classified as a retarding and water-reducing admixture and met Type D requirements of ASTM C494/C494M. The composition consists of sodium gluconate and sucrose and the admixture has a pH of 5.9. The solution used to transform the RHA was made with sodium hydroxide (NaOH). Details on the chemical transformation process are reported in Trejo and Prasittisopin (2014a). Using the chemical transformation process is reported to result in a reduction of RHA particle size and elimination of the cellular, honeycomb-like morphology of the AR-RHA particles. When using t-RHA in cement systems, the authors reported that the

mixtures exhibited accelerated hydration, faster ST, improved flow, higher CS, higher early-age f_c, and reduced 28-day porosity (Prasittisopin and Trejo 2014b, c).

Table 7-1. Chemical composition of PC and AR-RHA

Composition	PC (%)	RHA (%)*
SiO_2	20.3	89.65 - 96.90
Al_2O_3	4.80	0.006 - 0.039
Fe_2O_3	3.50	0.006 - 0.052
MgO	0.70	0.13 - 0.53
SO_3	2.80	0.018 - 0.24
CaO	63.9	0.48 - 0.81
C	-	2.09 - 7.59
Ti_2O_3	-	0.003 - 0.020
P_2O_5	-	0.74 -1.23
Mn_3O_4	-	0.00 - 0.20
Loss on Ignition	2.60	-
Insoluble Residue	0.11	-
Limestone	3.20	-
$CaCO_3$ in limestone	97.8	-
Na_{eq}	0.54	-

*data from producer

7.3.2 *Preparation Method*

The mixing procedure followed ASTM C305. The mixtures were prepared with 10% RHA replacement levels. A control mixture (100% PC) was mixed and tested for comparison. The retarder was mixed with the DI water prior to mixing with the PC (3.25 ml/kg [0.05 fl oz/lb). The paste specimens were prepared with a water-binder ratio (w/b) of 0.4. The mortar specimens were prepared with the w/b of 0.485 and cement-fine aggregate ratio of 1:2.75. The C305 standard requires that mixing of pastes and mortars include two consecutive stages: low speed mixing (140 rpm) followed by intermediate speed mixing (285 rpm). This evaluation included adjusting the mixing time and mixing speed of the second stage only. **Table 7-2** shows the mixing procedures for the cement pastes and mortars. Three different mixing times (2, 15, and 60 minutes) and two different mixing speeds (140 and 285 rpm) were evaluated. This resulted in 210, 355,

2030, 4060, 8330, and 16,885 revolution counts for paste mixing and 350, 568, 2170, 4273, 8330, and 17,098 revolution counts for mortar mixing. All test results are based on triplicate tests.

Table 7-2. Mixing condition for cement pastes and mortars

Mix. No.	Paste				Mix. No.	Mortar			
	First stage		Second stage			First stage		Second stage	
	Time (minutes)	Speed (rpm)	Time (minutes)	Speed (rpm)		Time (minutes)	Speed (rpm)	Time (minutes)	Speed (rpm)
P1	0.5	140	1	140	M1	1	140	1.5	140
P2	0.5	140	1	285	M2	1	140	1.5	285
P3	0.5	140	14	140	M3	1	140	14.5	140
P4	0.5	140	14	285	M4	1	140	14.5	285
P5	0.5	140	59	140	M5	1	140	59.5	140
P6	0.5	140	59	285	M6	1	140	59.5	285

7.3.3 *Characterization Methods*

The hydroxyl ion concentration and related pH in solution is believed to influence the fresh characteristics of hydrating cement systems. This study evaluated the time-variant hydroxyl ion concentration in solution at early ages using a pH electrode. The w/b of the solutions was 4.0. Mixing for all systems was performed using a magnetic stirrer rotating at 400 and 800 rpm throughout the mixing period. The time elapsed after introducing the unhydrated portland cement (UPC) to the solution is referred to here as the "hydration time." Solutions used for evaluating hydroxyl ion concentrations were analyzed at 5, 10, 15, 30, 45, 60, 90, 120, 150, 180, 210, and 240 minutes (mixed at 400 and 800 rpm).

In addition to evaluating the hydroxyl ion concentration, the aluminate and calcium ion concentrations were determined using atomic absorption spectroscopy (AAS). Mixing for this study was similar to the mixing process for hydroxyl ion concentration study and concentrations were determined at the same hydration times. Additional tests were performed at 300, 360, and 420 minutes for the calcium and aluminate ion study. Methods for solution preparation are reported in Trejo and Prasittisopin (2014a).

The flowability of mortars was determined following ASTM C1437. The ST of pastes was assessed following ASTM C191. The CS of pastes was assessed following ASTM C1608. Details on the CS test are reported in Fu *et. al.* (2012). The 28-day porosity of mortars was determined following a modified procedure of ASTM C642. Methods for modified porosity test was reported in Prasittisopin and Trejo (2014a). The 1-, 7-, and 28-day f_c values were determined following ASTM C109. The D_a was evaluated following ASTM C1556 and C1152.

7.3.4 *Statistical Data Analysis*

Statistical analyses of two-sample t-test and analysis of variances (ANOVA) analyses were performed to compare the sample means with two groups and more than two groups, respectively. Before the analyses, the Shapiro-Wilk test was used to analyze the normal distribution of data and the Levene's test was used to analyze the equal-variance of the data. The statistical hypotheses were defined in Eq. (7-1) and (7-2):

$$\text{Null hypothesis } (H_0): \mu_1 = \mu_2 = ... = \mu_a \tag{7-1}$$

$$\text{Alternative hypothesis } (H_a): \mu_1 \neq \mu_j \text{ for some } i \neq j \tag{7-2}$$

The 95% confidence intervals were used for all analyses. If the H_0 is rejected (p-value ≤ 0.05), it is concluded that there is statistically significant difference at the 5% level between the means of group populations. Alternatively, if the H_0 is not rejected (p-value > 0.05), it is concluded that there is no statistically significant difference at the 5% level between the means of group populations.

7.4 **RESULTS AND DISCUSSION**

7.4.1 *Ion Concentration*

The effect of mixing time on the hydroxyl ion concentration of the RHA systems mixed at 400 rpm is shown in **Fig. 7-1a**. Results indicate that with increasing mixing times, the

hydroxyl ion concentration in solution for all systems increases rapidly at early ages and then stabilizes (i.e., logarithmic function). The hydroxyl ion concentration of the t-RHA system is higher than the control, AR-RHA, and AR-RHA+R systems. This is likely a result of the NaOH used in the transformation process. The AR-RHA system has lower hydroxyl ion concentrations than the control system because the AR-RHA particles are initially "inert" and the system contains less cement. The AR-RHA+R system also exhibits lower hydroxyl ion concentrations than the AR-RHA system. This would be expected as the retarder prevents the dissolution of ions from the UPC.

The slopes of the fitted curves shown in **Fig. 7-1a** represent the dissolution rates of the hydroxyl ions in solution. Larger slopes are associated with higher dissolution rates of hydroxyl ions. The slopes of the control, AR-RHA, t-RHA, and AR-RHA+R systems mixed at 400 rpm are 17.0, 16.0, 4.0, and 3.6 mmol/l/min, respectively. The slope of the control system is similar to the AR-RHA system, indicating that the dissolution rates of hydroxyl ions are similar. Because the AR-RHA initially acts as the inert filler, the dissolution rates would be expected to be similar (although the overall concentrations would be lower because of lower cement contents). Results also indicate that the dissolution rate of hydroxyl ions of the t-RHA system is approximately 75% lower than the control systems. The slower dissolution rate of the t-RHA system may be caused by the higher initial concentrations of hydroxyl ions from the NaOH contained in the t-RHA. This higher hydroxyl ion concentration consequently makes the solution closer to the supersaturated level before the addition of UPC to the solution. This leads to fewer hydroxyl ions being dissolved into solution. The dissolution rate of the hydroxyl ions of the AR-RHA+R system is 79% lower than the control system. The presence of the retarding admixture is believed to prevent the hydroxyl ions from dissolving in solution.

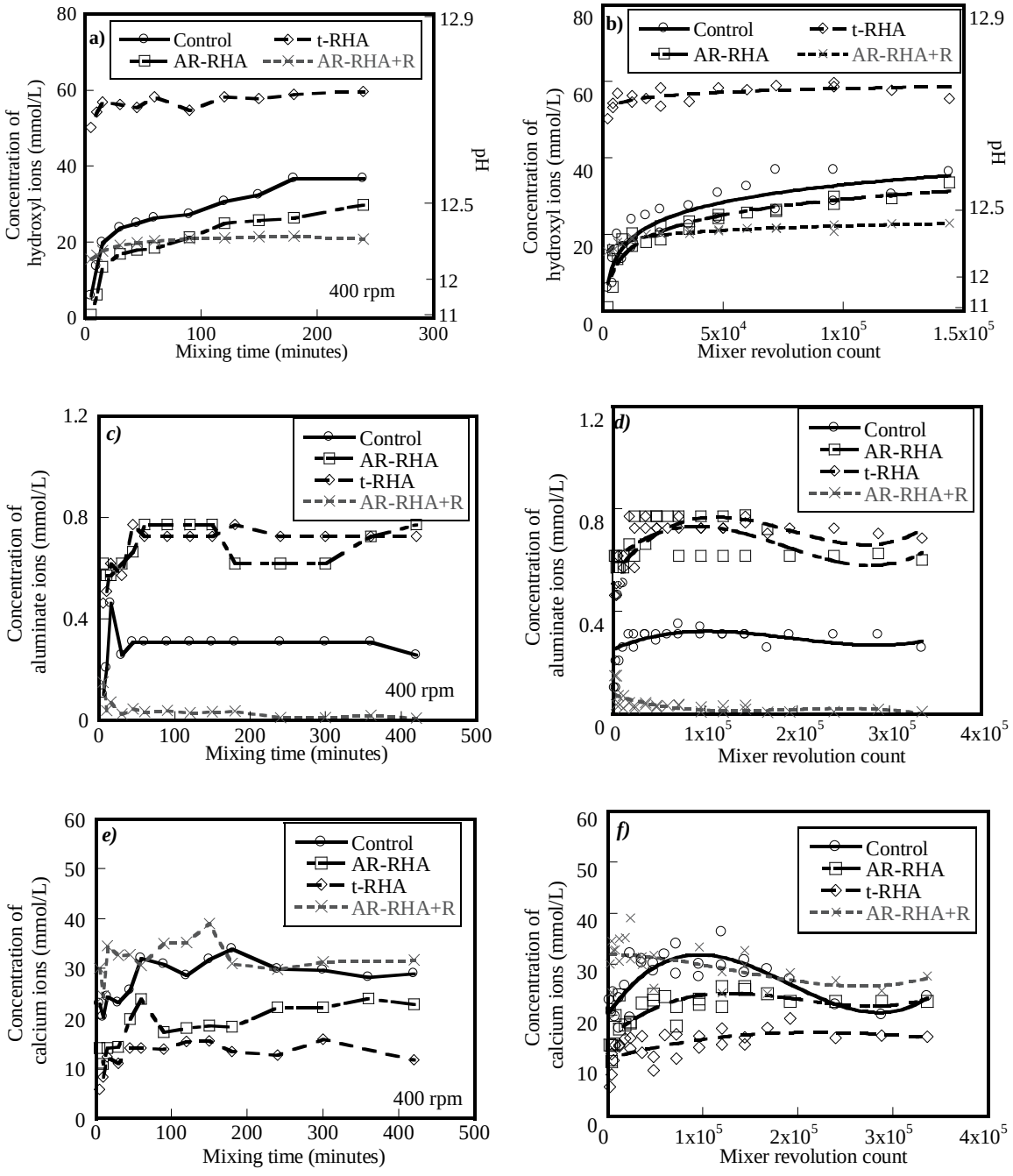

Fig. 7-1–Effect of *a)* mixing time and *b)* mixer revolution count on concentration of hydroxyl ions; *c)* mixing time and *d)* mixer revolution count on concentration of aluminate ions; *e)* mixing time and *f)* mixer revolution count on concentration of calcium ions of control, 10% AR-RHA, 10% t-RHA, and 10% AR-RHA+R systems.

Fig. 7-1b shows the effect of mixer revolution counts on the hydroxyl ion concentration of the control, AR-RHA, t-RHA, and AR-RHA+R systems. Results indicate that increased mixer revolution counts result in increased hydroxyl ion concentration in solutions for all systems. The figure shows that the concentration of hydroxyl ions increases rapidly when mixed at lower counts and then stabilizes at higher counts. Similar with the results in **Fig. 7-1a**, the hydroxyl ion concentration of the t-RHA system is higher than the hydroxyl ion concentration of the control, AR-RHA, and AR-RHA+R systems, respectively. Results indicate that the effect of mixer revolution counts on hydroxyl ion concentration of RHA systems is similar to the effect of mixing time on the hydroxyl ion concentration at RHA systems.

Fig. 7-1c shows the influence of mixing time on the aluminate ion concentration of the control, AR-RHA, t-RHA, and AR-RHA+R systems mixed at 400 rpm. Results indicate that when mixing time increases, the aluminate ion concentration rapidly increases at early ages, decreases, and then stabilizes. The aluminate ion concentration of the control system is lower than the AR-RHA and t-RHA systems, while higher than the AR-RHA+R system. Increased aluminate ion concentrations for the AR-RHA and t-RHA systems is likely a result of additional silicate ions from the RHA. Hong and Glasser (2002) reported that increased silicate ion concentrations from the replacement of SCMs results in increased concentration of aluminate ions at early ages. In contrast, the average concentration of aluminate ions of the AR-RHA+R system is 87% lower than the control system. Cheung et al. (2011) reported that when the retarder is present in the system, the dissolution rate of aluminate ions decreases because the retarder forms a layer on the aluminate surfaces of the UPC grains.

The aluminate ion concentrations for the control, AR-RHA, t-RHA, and AR-RHA+R systems as a function of mixer revolution count is shown in **Fig. 7-1d**. Results indicate that the aluminate ion concentration increases, decreases, and then stabilizes with increasing revolution counts. Similar with the results of the time study in **Fig. 7-1c**, the aluminate ion concentration of the control system is lower than the AR-RHA and t-RHA systems, but higher than the AR-RHA+R system.

Figs. 7-1e and **7-1f** show the plot of the calcium ion concentrations as a function of mixing time and mixer revolution count for the control, AR-RHA, t-RHA, and AR-RHA+R systems. Results shown in **Fig. 7-1e** indicate that the calcium ions of all systems increase at early ages and then stabilize at later ages. The calcium ion concentrations of the control and AR-RHA+R systems are higher than the AR-RHA and t-RHA systems. Cheung et al. (2011) reported that the systems containing retarders can liberate more calcium ions from the UPC particles. This is due to the chelation of calcium ions when retarders are present, leading to a formation of new compounds. The influence of the mixer revolution counts on the calcium ion concentration (**Fig. 7-1f**) indicates that the mixing revolutions counts has similar effects as the mixing time.

The study assessing ion concentrations of systems containing different RHA particles indicate that adding AR-RHA results in increased concentrations of aluminate and decreased concentration of calcium ions. Adding t-RHA increases the hydroxyl ions in solution. Lastly adding a retarder results in lower concentrations of aluminate ions in solution. From these results, it could be expected that the t-RHA systems would exhibit earlier set (because of higher hydroxyl and aluminate ions) and the systems containing the retarder would exhibit longer set (because of lower hydroxyl and aluminate ions). The influence of RHA addition on flow, ST, CS, porosity, f_c, and D_a is shown next.

7.4.2 *Flowability*

The effect of mixing time on flowability of the AR-RHA, t-RHA, and AR-RHA+R systems mixed at 285 rpm is shown in **Fig. 7-2a**. Results indicate that increased mixing time results in a nearly constant decrease in flow for all systems. Dewar and Anderson (1992) reported that decreased flow could occur as a result of increased water evaporation rates and increased hydration reaction rates. Results also indicate that the flow of the AR-RHA system is lower than the control, t-RHA, and AR-RHA+R systems. The AR-RHA system has lower flow values due to the high water absorption characteristics of the AR-RHA particles, leading to less water being available for flow.

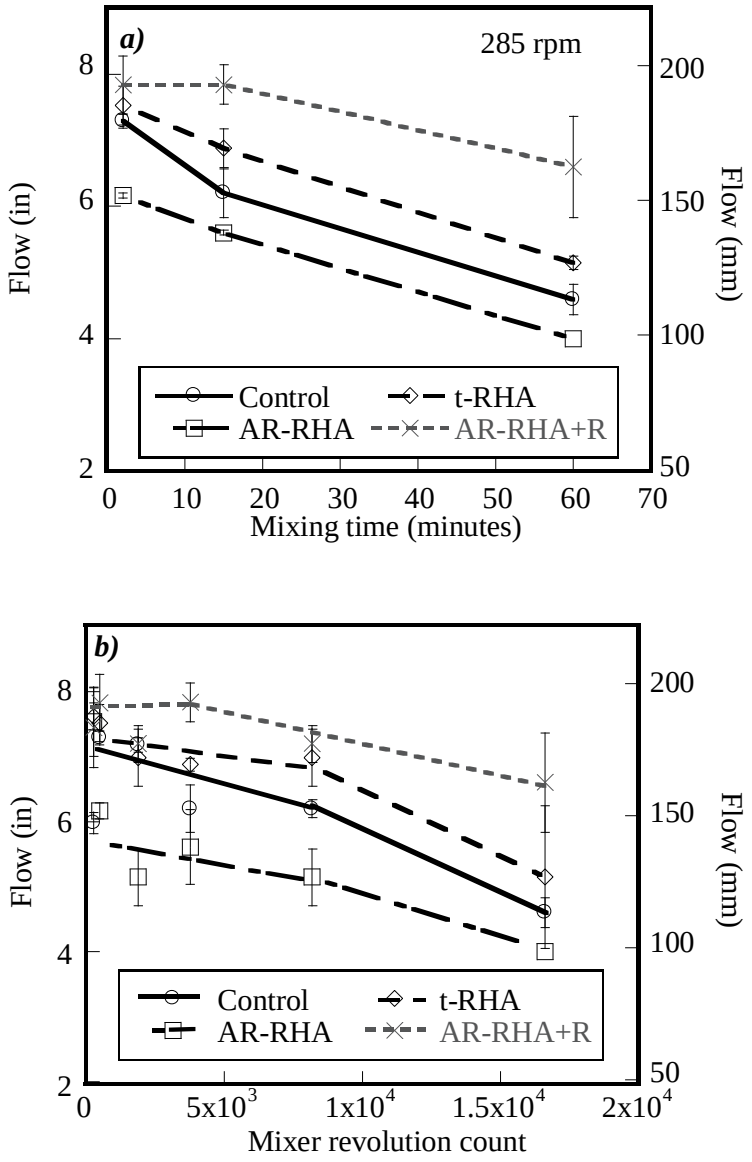

Fig. 7-2–Effect of *a)* mixing time and *b)* mixer revolution count on flow of control, 10% AR-RHA, 10% t-RHA, and 10% AR-RHA+R systems.

The negative slopes of the fitted curves in **Fig. 7-2a** for the control, AR-RHA, t-RHA, and AR-RHA+R systems are -0.043, -0.043, -0.040, and -0.022 in/min (-1.09, -1.08, -1.01, and -0.57 mm/min), respectively. This indicates that replacing cement with AR-RHA and t-RHA has limited effect on the flow reduction rate when compared with

the control system. However, the presence of a retarder in the AR-RHA system can decrease the flow reduction rate.

Fig. 7-2b shows the flow of the control, AR-RHA, t-RHA, and AR-RHA+R systems as a function of mixer revolution count. Results indicate that the flow of all systems is reduced with increasing mixer revolution counts. Similar to **Fig. 7-2a**, the reduction in flow rate of the AR-RHA+R system is less than the reduction in flow rates for the t-RHA, control, and AR-RHA systems.

7.4.3 *Setting Time*

Figs. 7-3a and 7-**3b** show the effect of mixing time and mixer revolution counts on the initial ST of the control, AR-RHA, t-RHA, and AR-RHA+R systems mixed at 285 rpm. Results indicate that the mixing time has less effect on the initial ST when compared to the effect of the RHA type. The ST of the AR-RHA system is higher than the control system. This is likely due to the lower cement contents in the AR-RHA system. The reduction in setting time of the t-RHA system is likely due to the presence of NaOH from the transformation process. The AR-RHA+R exhibited a significant increase of ST. This is because the presence of retarders limits the liberation of ions (hydroxyl and aluminate) from the UPC.

Based on the ST results, RHA type and the presence of a retarder influences the ST of the RHA systems. The mixing time and mixer revolution counts have less effect on ST. The ST can be extended by adding a retarder or AR-RHA.

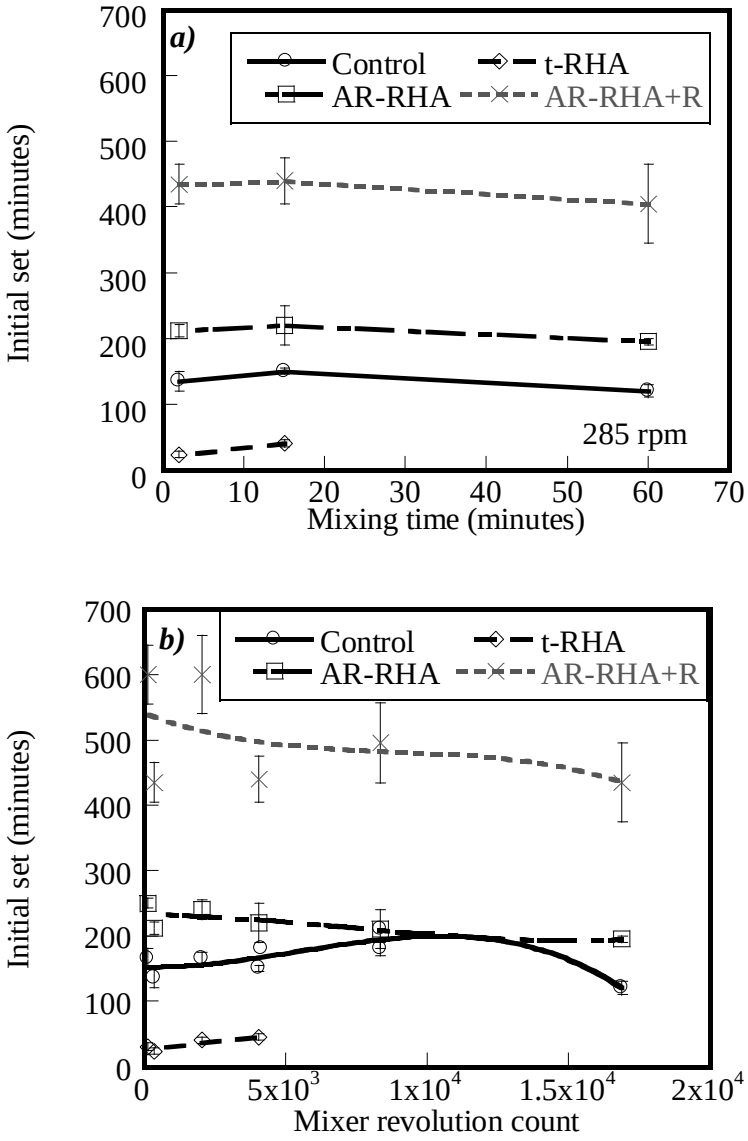

Fig. 7-3–Effect of *a)* mixing time and *b)* mixer revolution count on initial ST of control, 10% AR-RHA, 10% t-RHA, and 10% AR-RHA+R systems.

7.4.4 *Chemical Shrinkage*

The relationships of mixing time and mixer revolution counts on CS values for the control, AR-RHA, t-RHA, and AR-RHA+R systems are shown in **Figs. 7-4a**, **7-4b**, **7-4c**, and **7-4d**, respectively.

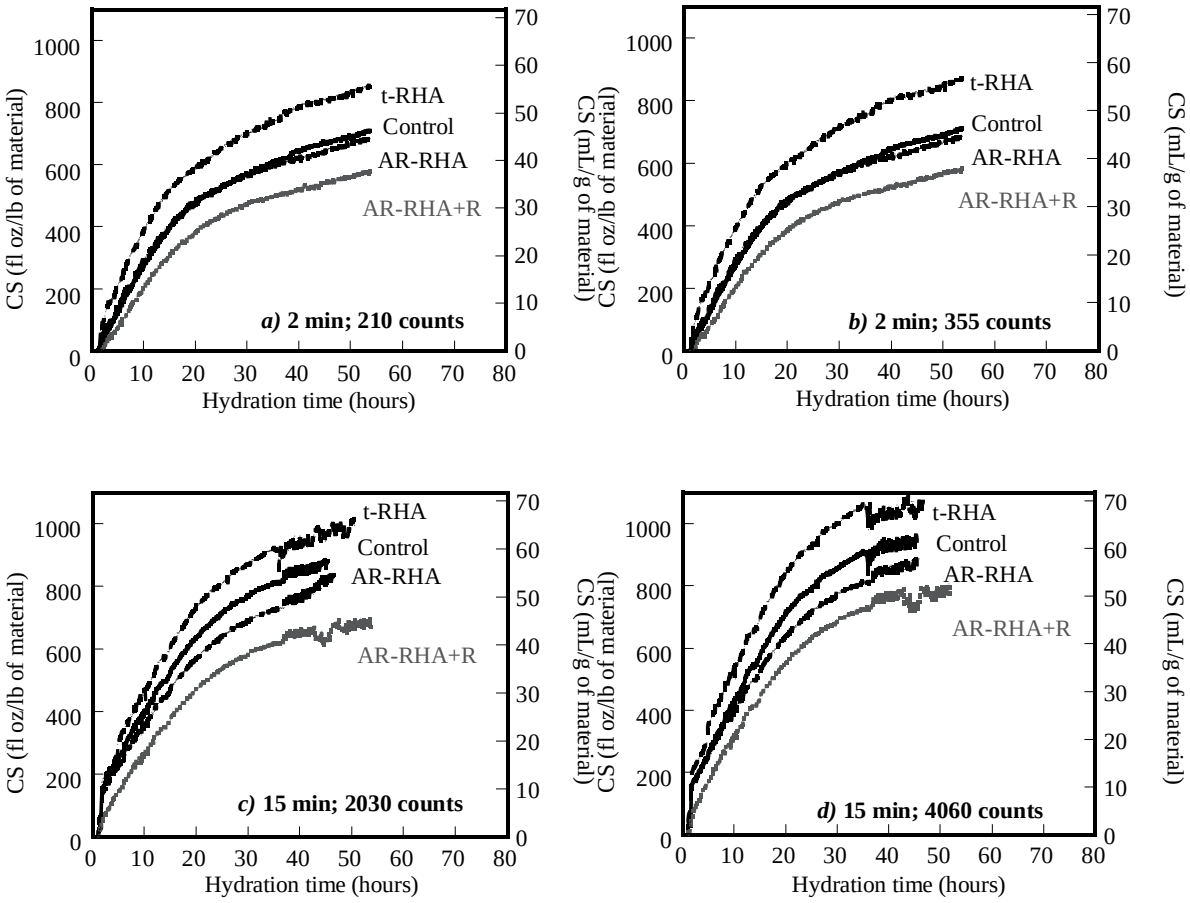

Fig. 7-4–Effect of mixing processes on CS of control, 10% AR-RHA, 10% t-RHA, and 10% AR-RHA+R systems mixed at *a)* 2 minutes and 210 counts, *b)* 2 minutes and 355 counts, *c)* 15 minutes and 2030 counts, and *d)* 15 minutes and 4060 counts.

The figures show the RHA systems mixed for different mixing times and mixer revolution counts and indicate that the CS values of the t-RHA system are higher than the control, AR-RHA, and AR-RHA+R systems. The systems that were mixed for 2 minutes and 210 revolutions, shown in **Fig. 7-4a**, exhibited similar CS values than the systems mixed for 2 minutes and 355 revolutions (shown in **Fig. 7-4b**). The systems mixed for 15 minutes at 2030 revolutions, shown in **Fig. 7-4c** also exhibited lower CS values than the systems mixed for 15 minutes at 4060 revolutions (as shown in **Fig. 7-4d**). In addition,

the CS values of the systems mixed for 15 minutes were higher than the CS for the systems mixed for 2 minutes. This indicates that extended mixing could lead to higher CS. Ravina and Soroka (1996) reported that mixing time or mixer revolution counts are associated with "grinding effects." Longer mixing times and higher mixer revolution counts can break the PC particles, resulting in smaller particles. These smaller PC particles are reported to lead to higher CS values (Bentz *et al.* 2008). This is due to the larger contact area of the smaller PC particles and water.

The CS after 40 hours as a function of mixer revolution counts is shown in **Fig. 7-5**. Results indicate that the CS values increase with increasing mixer revolutions and that the a 25% increase occurs when the mixer revolution counts increase from 210 to 4060 counts. This is believed to occur due to faster hydration from the smaller PC particles, leading to increased contact area between PC particles and water.

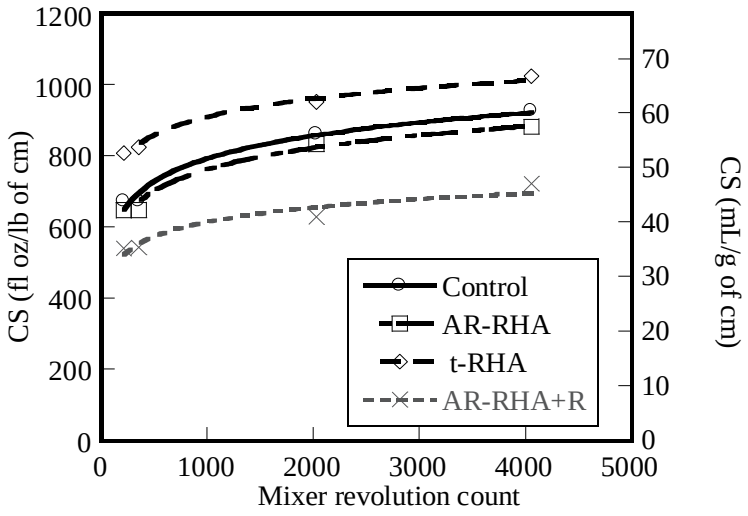

Fig. 7-5–Effect of mixer revolution count on CS at 40 hours of control, 10% AR-RHA, 10% t-RHA, and 10% AR-RHA+R systems.

7.4.5 *Hardened Porosity*

The effect of mixing time on the 28-day porosity of the control, AR-RHA, t-RHA, and AR-RHA+R systems mixed at 285 rpm is shown in **Fig. 7-6a**. Results indicate that as mixing time increases, the porosity of hardened mortars for all systems increases. As already discussed, increased mixing time results in reduced flow of the fresh mixtures. The fresh mixtures with lower flowability values require more consolidation energy input to achieve similar porosity values. Because specimens were fabricated with one energy input, it would be expected that the porosity increases with decreasing flow. All mixtures mixed for 60 minutes had reduced flow values (shown in **Fig. 7-2a**) and resulted in increased porosity in the specimens. Results indicate that the porosity of the AR-RHA+R system is not significant different from the AR-RHA system (two-sample t-test with p-value = 0.82, 0.077, 0.169 for systems mixed for 3, 15, and 60 minutes, respectively). In addition, the porosity of the t-RHA systems increases by 167% when mixing time increases from 15 to 60 minutes. As presented earlier, the initial ST of the t-RHA systems was approximately 30 minutes. After 30 minutes of mixing, the t-RHA mixtures began to set; therefore, it was difficult to consolidate this mixture. This consequently led to a significant increase in porosity.

Fig. 7-6b shows the effect of mixer revolution counts on 28-day porosity for the control, AR-RHA, t-RHA, and AR-RHA+R systems. Results indicate that increased revolution counts result in increased porosity. The porosity of the AR-RHA+R system is similar to the porosity of the AR-RHA, but higher than the control and t-RHA systems.

Previous studies (Bui *et al.* 2005, Rukzon *et al.* 2009) investigated the effects of RHA particle size on the porosity of cement systems. The authors reported that RHA particle size is correlated with the porosity in the mixtures. A reduction in RHA particle size can result in reduced porosity of the mixtures. This is because the smaller RHA particles in the mixtures enhance constituent particle packing. The results shown in **Figs. 7-6a** and **7-6b** show that the porosities of the t-RHA systems (smaller RHA particles) are lower than the porosity of the AR-RHA (having larger RHA particles) only at shorter

mixing times and lower mixer revolution counts. Increased times and counts lead to significant increases in porosity due to reduction in the flow and the increase in energy needed to cast the specimens.

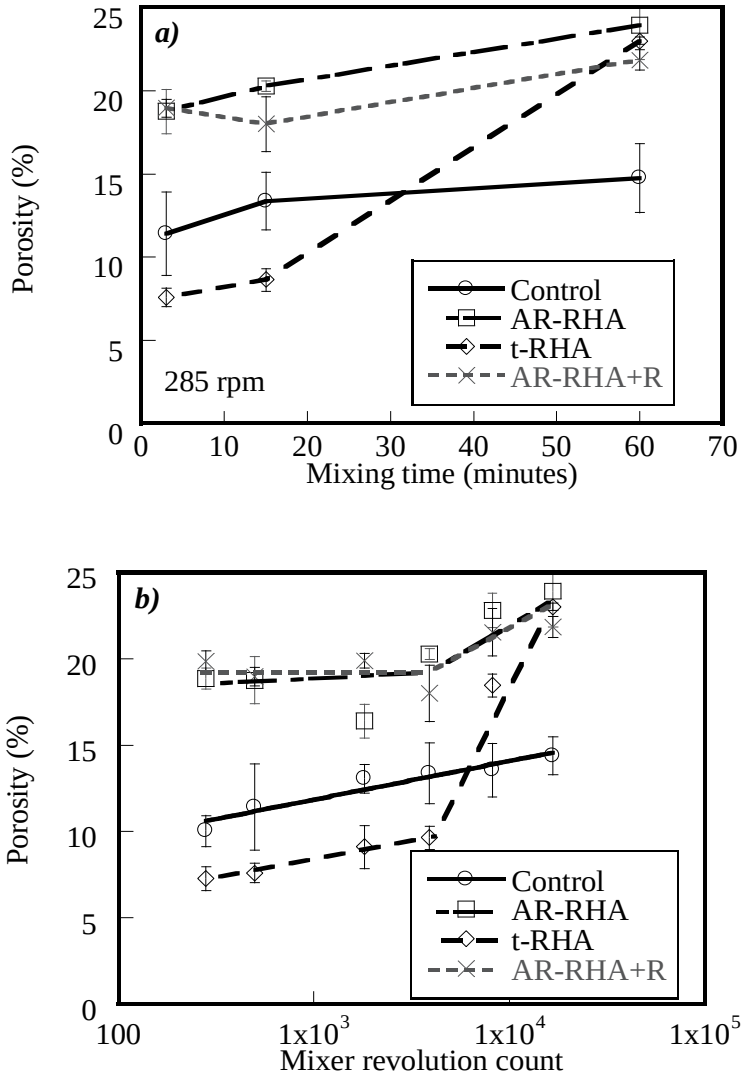

Fig. 7-6–Effect of *a)* mixing time and *b)* mixer revolution count on 28-day porosity of control, 10% AR-RHA, 10% t-RHA, and 10% AR-RHA+R blended cementitious systems.

7.4.6 *Compressive Strength*

Fig. 7-7a shows the effect of mixing time on 1-day f_c of the control, AR-RHA, t-RHA, and AR-RHA+R systems mixed at 285 rpm. Results indicate that the 1-day f_c of the control, AR-RHA, t-RHA, and AR-RHA+R systems is not significantly influenced by increasing mixing time. The 1-day f_c of the control system is higher than the AR-RHA and AR-RHA+R systems, but not significantly higher than the t-RHA system. **Fig. 7-7b** shows the influence of mixer revolution counts on the 1-day f_c for the control, AR-RHA, t-RHA, and AR-RHA+R systems. Results indicate that the 1-day f_c increases with increasing mixer revolution counts for all systems. The 1-day f_c of the control system is higher than the AR-RHA and AR-RHA+R systems, but not higher than the t-RHA system.

The effect of mixing time on the 7-day f_c of the control, AR-RHA, t-RHA, and AR-RHA+R systems mixed at 285 rpm is shown in **Fig. 7-7c**. Results indicate that the 7-day f_c of the control, AR-RHA, t-RHA, and AR-RHA+R systems is not influenced by mixing time. This is similar to the results of the effects of mixer revolution counts on the 7-day f_c shown in **Fig. 7-7d**.

A plot of the 28-day f_c for the control, AR-RHA, t-RHA, and AR-RHA+R systems mixed at 285 rpm as a function of mixing time is shown in **Fig. 7-7e**. Results indicate that there is no significant effect of mixing time on the 28-day f_c for all systems (ANOVA test with p-values > 0.05). The plot of the 28-day f_c of the control, AR-RHA, t-RHA, and AR-RHA+R systems as a function of mixer revolution counts is shown in **Fig. 7-7f**. Results indicate that the 28-day f_c of the control system decreases with increasing mixer revolution counts; however, the 28-day f_c of the AR-RHA, t-RHA, and AR-RHA+R systems does not show significant decreases with increasing mixer revolution counts.

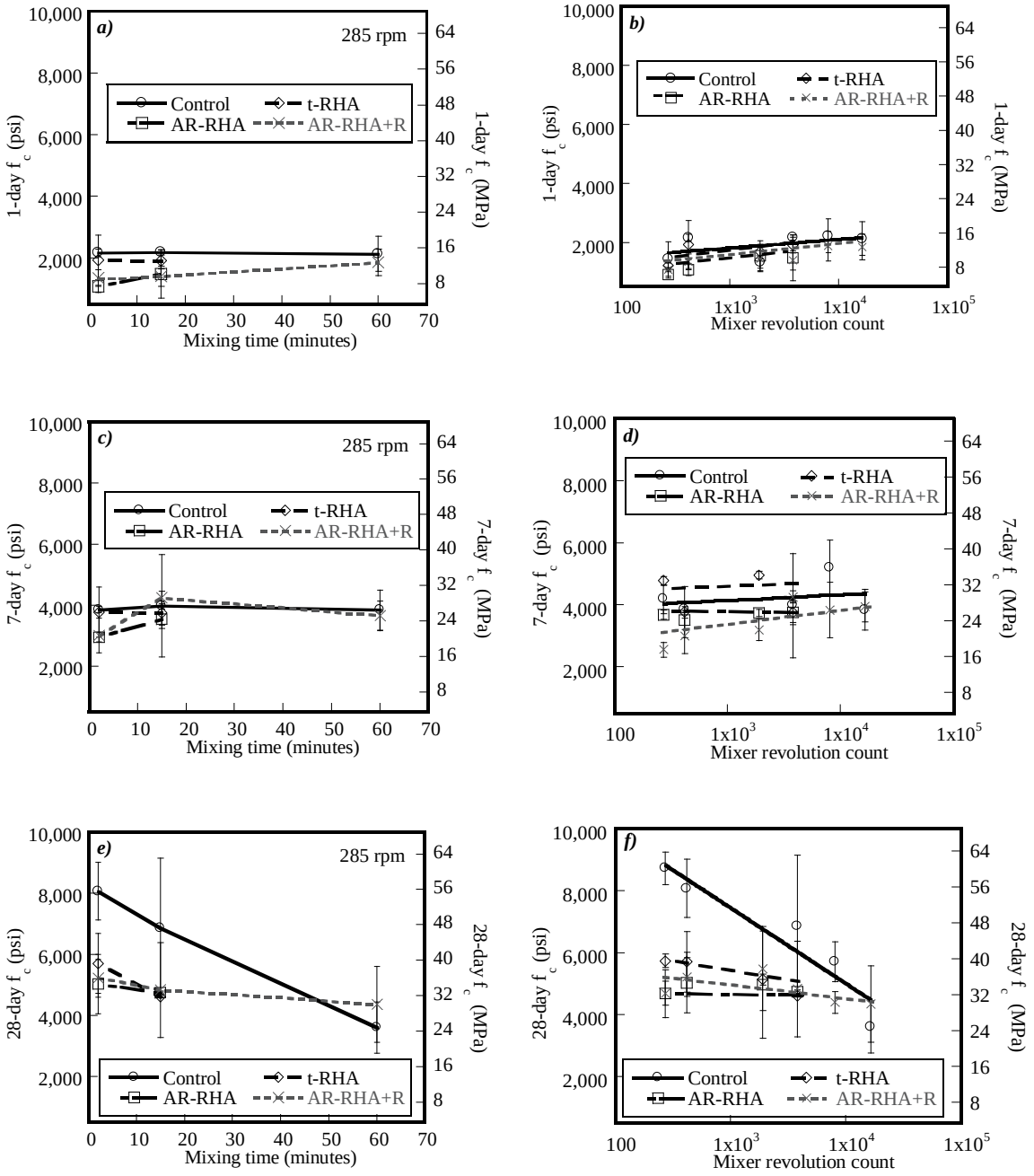

Fig. 7-7–Effect of *a)* mixing time and *b)* mixer revolution count on 1-day f_c; *c)* mixing time and *d)* mixer revolution count on 7-day f_c; *e)* mixing time and *f)* mixer revolution count on 28-day f_c of control, 10% AR-RHA, 10% t-RHA, and 10% AR-RHA+R blended cementitious systems.

A summary of the effect of mixer revolution counts on the f_c of the control, AR-RHA, t-RHA, and AR-RHA+R systems at different ages is shown in **Table 7-3**. Results indicate that increased mixer revolution counts have no significant influence on f_c for the RHA systems, but do result in a reduction in the mean 28-day f_c for the control system.

Table. 7-3 Summary of the effect of mixer revolution count on the f_c of mixtures at different ages (↑ = increase; ↓ = decrease; and - = similar).

fc	Systems			
	Control	AR-RHA	t-RHA	AR-RHA+ret
1-day	-	-	-	-
7-day	-	-	-	-
28-day	↓	-	-	-

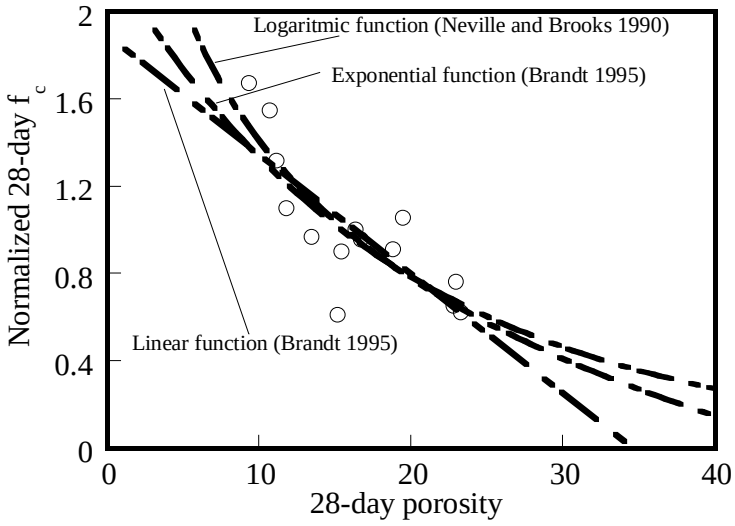

Fig. 7-8–Relationship and fitted-curves between normalized 28-day f_c and 28-day porosity of hardened PC mortars containing different types of RHA and mixed at different mixer revolution counts.

Fig. 7-8 shows the correlation between the normalized 28-day compressive strength and the 28-day hardened porosity of the RHA systems for different mixer revolution counts. The 28-day f_c values are normalized with the mean 28-day f_c for all mixtures. The logarithmic fitted curve shown is reported by Neveille (1996) and the

exponential and linear fitted curves are reported by Brandt (1995). Results indicate that f_c is reduced with increasing porosity and this increased porosity is likely due to reduced flow caused by a larger mixer revolution counts.

7.4.7 *Apparent Chloride Diffusivity Analysis*

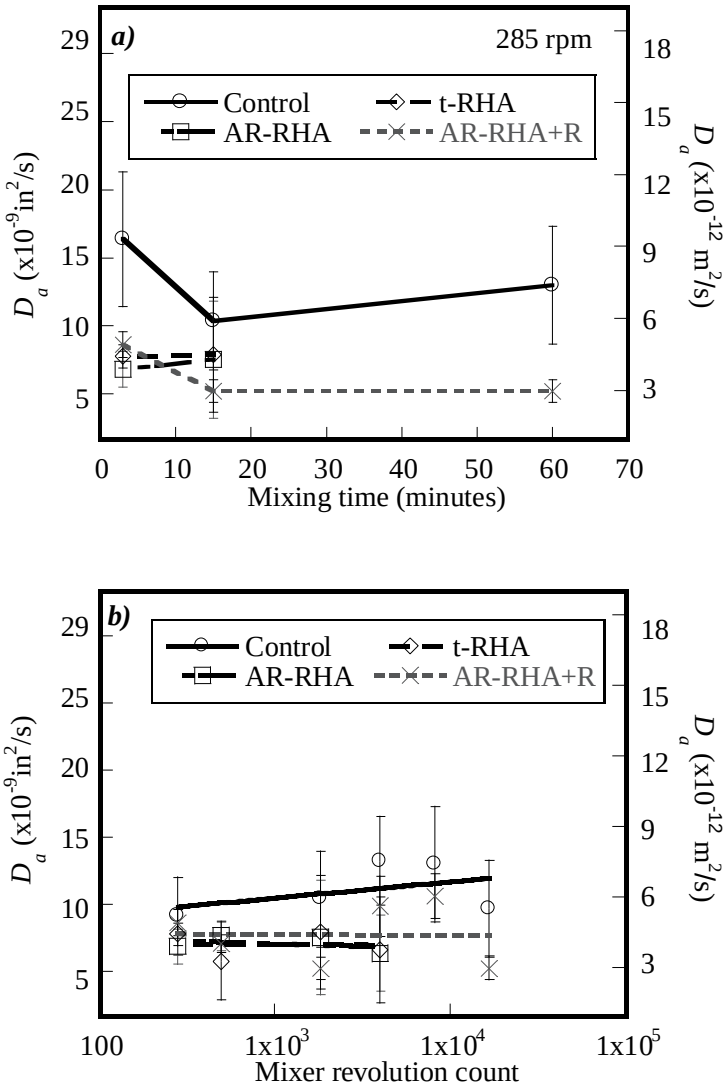

Fig. 7-9–Effect of a) mixing time and b) mixer revolution count on D_a of control, 10% AR-RHA, 10% t-RHA, and 10% AR-RHA+R blended cementitious systems.

Figs. 7-9a and **7-9b** show the effects of mixing time and mixer revolution counts on the D_a of the control, AR-RHA, t-RHA, and AR-RHA+R systems, respectively. Results indicate that neither mixing time nor mixer revolution counts has a significant effect on the D_a for all systems. The control system exhibits higher D_a than the t-RHA, AR-RHA, and AR-RHA+R systems. The presence of RHA in the cement systems can react with $Ca(OH)_2$ to produce C-S-H products, which make the hydrated portland cement denser and reduce transport rates. In addition, the RHA can either "block" or "absorb" the chloride ions (Prasittisopin and Trejo 2014b), resulting in lower D_a values.

7.5 CONCLUSIONS

The effects of mixing time and mixer revolution counts on the fresh and hardened characteristics of cementitious systems incorporating different types of RHA were assessed. Based on the experimental results, the following conclusions can be made:

- Ion concentration in solution is dependent on the chemistry of the RHA systems.
- The reduction in flow with increasing mixing time and mixer revolution counts results in the increase of the porosity of all systems.
- Increased mixing times and mixer revolution counts result in higher CS values.
- For the conditions of this research, an ANOVA analysis indicates that the 1-, 7-, and 28-day f_c for the RHA systems are not influenced by mixing time and mixer revolution counts. However, the 28-day f_c of the control mortar is reduced with increasing mixer revolution counts.

- ANOVA analysis indicates that the D_a is not affected by mixing time and mixer revolution counts; however, the replacement of RHA results in a significant reduction of the D_a.
- When mixing times and mixer revolution counts increase, the rate in the reduction of flow is approximately 1.1 mm/minute (0.04 in/minute). Adding retarder into AR-RHA systems significantly slows the flow reduction rates and also results in a significant increase in ST.

The type of RHA has a greater influence on the fresh and hardened characteristics than the effects from mixing time and mixer revolution counts. Future research should examine the effects of the mixing time and mixer revolution counts on the characteristics of conventional concrete and concrete systems containing different RHA types and different RHA particle sizes.

7.6 ACKNOWLEDGEMENTS

The authors express gratitude the support of Agrilectric Companies for provided the rice husk ash and Lafarge Cement for providing cement for this research.

7.7 REFERENCES

Al-Gahtani, H. J., Abbasi, A. G. F., and Al-Amoudi, O. S. B., *Concrete Mixture Design for Hot Weather: Experimental and Statistical Analyses*, in *Magazine of Conc. Res.*, 1998, Thomas Telford Services, London.

Azevedo, A. A., Martins, M. L. C., and Molin, D. C. D., A Study of the Penetration of Chloride Ions in Rice-Husk Ash Concrete, in Third CANMET/ACI Intern. Symp. on Sustainable Development of Cement and Concrete, V.M. Malhotra, Editor, 2001, ACI, San Francisco, CA, 379-396.

Bentz, D., Sant, G., and Weiss, J. (2008), "Early-Age Properties of Cement-Based Materials. I: Influence of Cement Fineness," *J. Mater. Civil Eng.*, V. 20, No. 7, pp. 502-508.

Brandt, A. M. (1995), Cement Based Composites: Materials, Mechanical Properties and Performance, UK, E & FN Spon.

Bui, D. D., Hu, J., and Stroeven, P. (2005), "Particle Size Effect on the Strength of Rice Husk Ash Blended Gap-Graded Portland Cement Concrete," *Cem. & Con. Comp.*, V. 27, No. 3, pp. 357-366.

Cheung, J., Jeknavorian, A., Roberts, L., and Silva, D. (2011), "Impact of Admixtures on the Hydration Kinetics of Portland Cement," *Cem. Con. Res.*, V. 41, No. 12, pp. 1289-1309.

Dewar, J. D. and Anderson, R. (1992), *Manual of Ready Mixed Concrete*, 2nd ed., Glasgow, UK, Blackie Academic and Professional, 72 pp.

Erdogdu, S., Arslanturk, C., and Kurbetci, S. (2011), "Influence of Fly Ash and Silica Fume on the Consistency Retention and Compressive Strength of Concrete Subjected to Prolonged Agitating," *Constr. Build. Mater.*, V. 25, No. 3, pp. 1277-1281.

Fu, T., Deboodt, T., and Ideker, J. (2012), "Simple Procedure for Determining Long-Term Chemical Shrinkage for Cementitious Systems Using Improved Standard Chemical Shrinkage Test," *J. Mater. Civil Eng.*, V. 24, No. 8, pp. 989-995.

Gastaldini, A. L. G., Isaia, G. C., Gomes, N. S., and Sperb, J. E. K. (2007), "Chloride Penetration and Carbonation in Concrete with Rice Husk Ash and Chemical Activators," *Cem. Con. Comp.*, V. 29, No., pp. 176-180.

Hong, S.-Y. and Glasser, F. P. (2002), "Alkali Sorption by C-S-H and C-A-S-H Gels: Part II. Role of Alumina," *Cem. Con. Res.*, V. 32, No. 7, pp. 1101-1111.

Hooton, R. D. (2008), "Bridging the Gap between Research and Standards," *Cem. Con. Res.*, V. 38, No. 2, pp. 247-258.

Lynsdale, C. J. and Khan, M. I. (2000), "Chloride and Oxygen Permeability of Concrete Incorporating Fly Ash and Silica Fume in Ternary Systems," *ACI SP*, V. 192, pp. 739-753.

Maeda, N., Wada, I., Kawakami, M., Ueda, T., and Pushpalal, G. K. D. (2001), "Chloride Diffusivity of Concrete Incorporating Rice Husk Ash," *ACI SP*, V. 200, pp. 291-308.

Mehta, P. K. and Folliard, K. J. (1995), "Rice Husk Ash--a Unique Supplementary Cementing Material: Durability Aspects," *ACI SP*, V. 154, pp. 531-542.

Muthadhi, A. and Kothandaraman, S. (2013), "Experimental Investigations of Performance Characteristics of Rice Husk Ash–Blended Concrete," *J. Mater. Civil Eng.*, V. 25, No. 8, pp. 1115-1118.

Nehdi, M., Duqette, J., and El Damatty, A. (2003), "Performance of Rice Husk Ash Produced Using a New Technology as a Mineral Admixture in Concrete," *Cem. Con. Res.*, V. 33, No. 8, pp. 1203-1210.

Neville, A. M. (1996), *Properties of Concrete*, 4th ed., New York, John Wiley & Sons.

Portland Cement Association, Survey of Mineral Admixtures and Blended Cements in Ready Mixed Concrete, 2000, 16 pp.

Prasittisopin, L. and Trejo, D. (2013), "Effects of Mixing and Transportation on Characteristics of Cementitious Systems Containing Fly Ash," in *World of Coal Ash Conference*, Lexington, KY.

Prasittisopin, L. and Trejo, D., Effects of Mixing Variables on Hardened Characteristics of PC Mortars, 2014a. (Under review)

Prasittisopin, L. and Trejo, D., Fresh and Hardened Characteristics of Blended Cementitious Systems Incorporating Chemically Transformed Rice Husk Ash, 2014b. (Under review)

Prasittisopin, L. and Trejo, D., Hydration and Phase Formation of Blended Cementitious Systems Incorporating Chemically Transformed Rice Husk Ash, 2014.

Ravina, D. (1996), "Effect of Prolonged Agitating on Compressive Strength of Concrete with and without Fly Ash and/or Chemical Admixtures," *ACI Mat. J.*, V. 93, pp. 451-456.

Rukzon, S., Chindaprasirt, P., and Mahachai, R. (2009), "Effect of Grinding on Chemical and Physical Properties of Rice Husk Ash," *Inter. J. Minerals, Metall. and Mater.*, V. 16, No. 2, pp. 242-247.

Sakr, K. (2006), "Effects of Silica Fume and Rice Husk Ash on the Properties of Heavy Weight Concrete," *J. Mater. Civil Eng.*, V. 18, No. 3, pp. 367-376.

Shuichi, S., Shoya, M., and Tokuda, H. (1992), "Evaluation of Pozzolanic Activity of Rice Husk Ash," *ACI SP*, V. 132, pp. 495-512.

Trejo, D. and Prasittisopin, L., *Chemical Transformation of Rice Husk Ash Morphology*, 2014a. (Under review)

Trejo, D. and Prasittisopin, L., Effects of Mixing Variables on Early-Age Characteristics of PC Systems, 2014b. (Under review)

Vayghan, A., Khaloo, A., Nasiri, S., and Rajabipour, F. (2011), "Studies on the Effect of Retention Time of Rice Husk Combustion on the Ash's Chemo-Physical Properties and Performance in Cement Mixtures," *J. Mater. Civil Eng.*, V. 24, No. 6, pp. 691-697.

Venkatanarayanan, H. and Rangaraju, P. (2013), "Evaluation of Sulfate Resistance of Portland Cement Mortars Containing Low-Carbon Rice Husk Ash," *J. Mater. Civil Eng.*

8 SUMMARY AND RECOMMENDATIONS

This section provides a summary of the research performed to assess the chemical transformation process of rice husk ash. The summary is followed by recommendation for future research.

8.1 SUMMARY OF RESEARCH

- A 2M NaOH solution mixed with AR-RHA for 3 hours was found to be the most efficient process assessed to reduce RHA particle size and to eliminate the cellular, honeycomb-like morphology of AR-RHA (i.e., to produce t-RHA).
- The addition of PVA is an effective dispersant for the t-RHA slurry. The PVA does not have any significant effect on the fresh and hardened characteristics of the mixtures.
- Using t-RHA in cementitious systems was found to lead to shorter setting times, higher chemical shrinkage values, and higher 1- and 7-day compressive strengths. These changes are likely a result of faster hydration. The faster hydration occurs because gypsum rapidly precipitates from the solution.
- The workability challenges associated with the cellular, honeycomb-like morphology of RHA can be minimized by using the chemical transformation process. Specimens containing t-RHA exhibited good performance characteristics (e.g., mechanical and durability characteristics).
- The hardened porosities of PC mortars increase with increasing mixing time and mixer revolution counts. This was a result of the reduction in flow of the mixtures and resulted in decreased compressive strength.
- Mortars mixed for longer times or higher mixer revolution counts met the minimum C150 requirements for the 1- and 7-day compressive strengths. However, if the mixtures were mixed for very long durations and very high

mixer revolutions, the 28-day compressive strengths were lower than the specified strength requirements.

- The influence of RHA addition (both AR-RHA and t-RHA) had more influence on hardened characteristics than mixing variables did.

8.2 RECOMMENDATIONS FOR FUTURE RESEARCH

As with all research, limitations exist. This research evaluated a chemical transformation process used to alter the size and morphology of RHA particles. The findings of this research are specific to the materials and methods used in this research program. However, findings from this research may be used to further the science in developing more sustainable infrastructure materials. The following recommendations for future research can further advance the science. Note that this list is the author's recommendations on future needs and may not be comprehensive. Recommendations for the future research based on the findings from this dissertation include:

- The t-RHA system has high alkali contents due to the mixing with 2M NaOH. If the alkali content can be reduced, potential long-term issues with using the t-RHA slurry may be avoided. The development and assessment of a filtration system for the t-RHA slurry could be beneficial.
- The cost analysis for the chemical transformation process is needed.
- Because the t-RHA is in slurry form, logistics of using t-RHA slurry in a concrete plant are needed.
- The current research was conducted in the laboratory on pastes and mortars. Further assessments are needed for concrete containing t-RHA. In addition, studies on the influence of *truck-mixer* revolution counts on concrete properties are needed.
- The development of a pilot-scale equipment and process for the chemical transformation process of RHA may be beneficial.

9 BIBLIOGRAPHY

Ahmed, A., R. Clowes, E. Willneff, H. Ritchie, P. Myers, and H. Zhang (2009). "Synthesis of uniform porous silica microspheres with hydrophilic polymer as stabilizing agent." *Indust. & Eng. Chem. Res.* **49**(2): 602-608.

Al-Gahtani, H. J., A. G. F. Abbasi, and O. S. B. Al-Amoudi (1998). Concrete mixture design for hot weather: Experimental and statistical analyses. *Magazine of Conc. Res.* London, Thomas Telford Services.

Al-Negheimish, A. I., and A. M. Alhozaimy (2008). "Impact of extremely hot weather and mixing method on changes in properties of ready mixed concrete during delivery." *ACI Mat. J.* **105**(5): 438-444.

Andersen, P. J., and S. K. Hodson (2009). Concrete having high workability through control of fine-to-coarse particulates ratio. A. Teasdale. U.S., iCrete. **US 2009/0158965 A1:** 28 pp.

Azevedo, A. A., M. L. C. Martins, and D. C. D. Molin (2001). A study of the penetration of chloride ions in rice-husk ash concrete. *Third CANMET/ACI Intern. Symp. on Sustainable Development of Cement and Concrete*. V. M. Malhotra. San Francisco, CA, ACI**:** 379-396.

Ball, J. W., and D. K. Nordstrom (1991). User's manual for WATEQ4F, with revised thermodynamic data base and test cases for calculating speciation of major, trace, and redox elements in natural waters. U.S. Department of Interior. Menlo Park, CA, U.S. Geological Survey**:** 55 pp.

Bapat, J. D. (2012). Rice husk ash. *Mineral admixtures in cement and concrete*. Boca Raton, FL, CRC Press**:** 75-96.

Baskoca, A., M. H. Ozkul, and S. Artirma (1998). "Effect of chemical admixtures on workability and strength properties of prolonged agitated concrete." *Cem. Con. Res.* **28**(5): 737-747.

Begarin, F., S. Garrault, A. Nonat, and L. Nicoleau (2011). "Hydration of alite containing aluminum." *Adv. Applied Ceram.* **110**(3): 127-130.

Bentz, D., G. Sant, and J. Weiss (2008). "Early-age properties of cement-based materials. I: Influence of cement fineness." *J. Mater. Civil Eng.* **20**(7): 502-508.

Bentz, D. P., and O. M. Jensen (2004). "Mitigation strategies for autogenous shrinkage cracking." *Cem. Con. Res.* **26**(6): 677-685.

Bhagiyalakshmi, M., L. J. Yun, R. Anuradha, and H. T. Jang (2010). "Utilization of rice husk ash as silica source for the synthesis of mesoporous silicas and their application to CO_2 adsorption through TREN/TEPA grafting." *J. Hazard. Mater.* **175**(1-3): 928-938.

Bloem, D. L., and R. D. Gaynor (1971). "Factors affecting the homogeneity of ready-mixed concrete." *J. ACI* **68**(7): 521-525.

Brandt, A. M. (1995). Cement based composites: Materials, mechanical properties and performance. UK, E & FN Spon.

Bui, D. D. (2001). Rice husk ash as a mineral admixture for high performance concrete. Delft, Delft University of Technology. **PhD:** 122 pp.

Bui, D. D., J. Hu, and P. Stroeven (2005). "Particle size effect on the strength of rice husk ash blended gap-graded portland cement concrete." *Cem. & Con. Comp.* **27**(3): 357-366.

Bullard, J. W., H. M. Jennings, R. A. Livingston, A. Nonat, G. W. Scherer, K. L. Scrivener, and J. J. Thomas (2011). "Mechanisms of cement hydration." *Cem. Con. Res.* **41**(12): 1208-1223.

Chandrasekhar, S., P. N. Pramada, P. Raghavan, K. G. Satyanarayana, and T. N. Gupta (2002). "Microsilica from rice husk as a possible substitute for condensed silica fume for high performance concrete." *J. Mater. Sci. Letters* **21**(16): 1245-1247.

Chandrasekhar, S., K. G. Satyanarayana, N. Pramada, and P. Raghavan (2003). "Review processing, properties and applications of reactive silica from rice husk—an overview." *J. Mater. Sci.* **38**(15): 3159-3168.

Charonnat, Y., and H. Beitzel (1997). "Report: Efficiency of concrete mixers towards qualification of mixers." *Mater. Struct.* **30**(1): 28-32.

Chen, C. T., and L. J. Struble (2009). "Influence of mixing sequnce on cement-admixture interaction." *ACI Mat. J.* **106**(6): 503-508.

Cheung, J., A. Jeknavorian, L. Roberts, and D. Silva (2011). "Impact of admixtures on the hydration kinetics of portland cement." *Cem. Con. Res.* **41**(12): 1289-1309.

Cizer, Ö., K. Van Balen, J. Elsen, and D. Van Gemert (2006). *Carbonation and hydration of calcium hydroxide and calcium silicate binders with rice husk ash*. 2nd Intern. RILEM Symp. "Advances in Concrete Through Science and Engineering", Quebec.

Cook, G. C. (1943). "Effect of time of haul on strength and consistence of ready-mixed concrete " *J. ACI* **14**(5): 413-428.

Cordeiro, G., R. Toledo Filho, and E. Moraes Rego Fairbairn (2009). "Use of ultrafine rice husk ash with high-carbon content as pozzolan in high performance concrete." *Mater. Struct.* **42**(7): 983-992.

Cordeiro, G. C., R. D. Toledo Filho, L. M. Tavares, E. d. M. R. Fairbairn, and S. Hempel (2011). "Influence of particle size and specific surface area on the pozzolanic activity of residual rice husk ash." *Cem. Con. Comp.* **33**(5): 529-534.

Da Costa, H. M., L. L. Y. Visconte, R. C. R. Nunes, and C. R. G. Furtado (2000). "The effect of coupling agent and chemical treatment on rice husk ash-filled natural rubber composites." *J. Appl. Polymer Sci.* **76**(7): 1019-1027.

Damidot, D., and F. P. Glasser (1993). "Thermodynamic investigation of the CaO-Al_2O_3-$CaSO_4$-H_2O system at 25°C and the influence of Na_2O." *Cem. Con. Res.* **23**(1): 221-238.

Datta, A., and R. K. Rajamani (2002). "A direct approach of modeling batch grinding in ball mills using population balance principles and impact energy distribution." *Inter. J. Mineral Processing* **64**(4): 181-200.

Della, V. P., I. Kuhn, and D. Hotza (2002). "Rice husk ash as an alternate source for active silica production." *Mater. Letter* **57**(4): 818-821.

Dewar, J. D., and R. Anderson (1992). *Manual of ready mixed concrete*. Glasgow, UK, Blackie Academic and Professional.

Diamond, S. (2005). "The patch microstructure in concrete: Effect of mixing time." *Cem. Con. Res.* **35**(5): 1014-1016.

Diamond, S., and S. Ong (1994). "Effects of added alkali hydroxides in mix water on long-term SO_4^{2-} concentrations in pore solution." *Cem. Con. Comp.* **16**(3): 219-226.

Double, D. D. (1983). "New developments in understanding the chemistry of cement hydration." *Phil. Trans. R. Soc. Lond.* **A 310**: 53-66.

Erdogdu, S. (2005). "Effect of retempering with superplasticizer admixtures on slump loss and compressive strength of concrete subjected to prolonged mixing." *Cem. Con. Res.* **35**(5): 907-912.

Erdogdu, S., C. Arslanturk, and S. Kurbetci (2011). "Influence of fly ash and silica fume on the consistency retention and compressive strength of concrete subjected to prolonged agitating." *Constr. Build. Mater.* **25**(3): 1277-1281.

Fajun, W., M. W. Grutzeck, and D. M. Roy (1985). "The retarding effects of fly ash upon the hydration of cement pastes: The first 24 hours." *Cem. Con. Res.* **15**(1): 174-184.

Feng, Q., H. Yamamichi, M. Shoya, and S. Sugita (2004). "Study on the pozzolanic properties of rice husk ash by hydrochloric acid pretreatment." *Cem. Con. Res.* **34**(3): 521-526.

Ferraris, C. F. (2001). "Concrete mixing methods and concrete mixers: State of the art." *J. Res. Nat. Stand. Technol.* **106**(2): 391-399.

Food and Agriculture Organization of the United Nations (2009). FAO statistical databases.

Fraay, A. L. A. (1990). Fly ash a pozzolan in concrete. *Civil Engineering and Geosciences*. Delft, Netherlands, Delft University of Technology**:** 165 pp.

Frigione, G., and S. Marra (1976). "Relationship between particle size distribution and compressive strength in portland cement." *Cem. Con. Res.* **6**(1): 113-128.

Fu, T., T. Deboodt, and J. Ideker (2012). "Simple procedure for determining long-term chemical shrinkage for cementitious systems using improved standard chemical shrinkage test." *J. Mater. Civil Eng.* **24**(8): 989-995.

Gastaldini, A. L. G., G. C. Isaia, N. S. Gomes, and J. E. K. Sperb (2007). "Chloride penetration and carbonation in concrete with rice husk ash and chemical activators." *Cem. Con. Comp.* **29**: 176-180.

Gholizadeh Vayghan, A., A. R. Khaloo, and F. Rajabipour (2013). "The effects of a hydrochloric acid pre-treatment on the physicochemical properties and pozzolanic performance of rice husk ash." *Cem. Con. Comp.* **39**(0): 131-140.

Giaccio, G., G. R. de Sensale, and R. Zerbino (2007). "Failure mechanism of normal and high-strength concrete with rice-husk ash." *Cem. Con. Comp.* **29**(7): 566-574.

Givi, N. A., S. A. Rashid, F. N. A. Aziz, and M. A. M. Salleh (2010). "Experimental investigation of the size effects of SiO_2 nano-particles on the mechanical properties of binary blended concrete." *Comp. Part B: Eng.* **41**(8): 673–677.

Gouda, G. R. (1986). Microstructure and properties of high-alkali clinker. *8th Intern. Congress on the Chemistry of Cement*. Rio de Janeiro, Brazil, Alba Grafica e Editora Ltda. **2:** 234-239.

Habeeb, G. A., and H. B. Mahmud (2010). "Study on properties of rice husk ash and its use as cement replacement material." *Mater Res* **13**(2): 185-190.

Halim, S. C. (2008). Application of reactive and partly soluble nanomaterials. *Department of Chemistry and Applied Biosciences*. Zurich, ETH **Doctor of Science**.

Han, V., S. Ros, and H. Shima (2013). "Effects of sand content, superplasticizer dosage, and mixing time on compressive strength of mortar." *ACI Mat. J.* **110**(1): 23-31.

Hanafi, S., S. A. Abo-El-Enein, D. M. Ibrahim, and S. A. El-Hemaly (1980). "Surface properties of silicas produced by thermal treatment of rice-husk ash." *Thermochimica Acta* **37**(2): 137-143.

He, J., Y. Jie, J. Zhang, Y. Yu, and G. Zhang (2013). "Synthesis and characterization of red mud and rice husk ash-based geopolymer composites." *Cem. Con. Comp.* **37**: 108-118.

Hong, S.-Y., and F. P. Glasser (2002). "Alkali sorption by C-S-H and C-A-S-H gels: Part II. Role of alumina." *Cem. Con. Res.* **32**(7): 1101-1111.

Hooton, R. D. (2008). "Bridging the gap between research and standards." *Cem. Con. Res.* **38**(2): 247-258.

Hutchins, M. J., and J. W. Sutherland (2008). "An exploration of measures of social sustainability and their application to supply chain decisions." *Journal of Cleaner Production* **16**(15): 1688-1698.

Isaia, G. C., A. L. G. Gastaldini, and R. Moraes (2003). "Physical and pozzolanic action of mineral additions on the mechanical strength of high-performance concrete." *Cem. Con. Comp.* **25**(1): 69-76.

Jawed, I., and J. Skalny (1978). "Alkalies in cement: A review: II. Effects of alkalies on hydration and performance of portland cement." *Cem. Con. Res.* **8**(1): 37-51.

Jensen, O. M., and P. F. Hansen (2001). "Autogenous deformation and RH-change in perspective." *Cem. Con. Res.* **31**(12): 1859-1865.

Juenger, M. C. G., and H. M. Jennings (2001). "Effects of high alkalinity on cement pastes." *ACI Mat. J.* **98**(3): 251-255.

Kalapathy, U., A. Proctor, and J. Shultz (2000). "Silica xerogels from rice hull ash: Structure, density and mechanical strength as affected by gelation pH and silica concentration." *J. Chem. Tech. & Biotech.* **75**(6): 464-468.

Kalapathy, U., A. Proctor, and J. Shultz (2000). "A simple method for production of pure silica from rice hull ash." *Bioresor. Tech.* **73**(3): 257-262.

Kalapathy, U., A. Proctor, and J. Shultz (2002). "An improved method for production of silica from rice hull ash." *Bioresor. Tech.* **85**(3): 285-289.

Kamath, S. R., and A. Proctor (1998). "Silica gel from rice hull ash: Preparation and characterization." *Cereal Chem.* **75**(4): 484-487.

Kibriya, T. (2006). *Performance of blended cement in high strength self compacting concrete*. 17th Analysis and Computation Specialty Conf. at Structures, St. Louis, MI, ASCE.

Kielland, J. (1937). "Individual activity coefficients of ions in aqueous solutions." *J. ACS* **59**(9): 1675-1678.

Kirca, O., L. Turanli, and T. Y. Erdogan (2002). "Effect of retempering on consistency and compressive strength of concrete subjected to prolonged mixing." *Cem. Con. Res.* **32**(3): 441-445.

Lagier, F., and K. E. Kurtis (2007). "Influence of portland cement composition on early age reactions with metakaolin." *Cem. Con. Res.* **37**(10): 1411-1417.

Liou, T. H., F. W. Chang, and J. J. Lo (1997). "Pyrolysis kinetics of acid-leached rice husk." *Indust. & Eng. Chem. Res.* **36**(3): 568-573.

Lollini, F., E. Redaelli, and L. Bertolini (2013). "Effects of portland cement replacement with limestone on the properties of hardened concrete." *Cem. Con. Comp.* (In press)

Lothenbach, B., K. Scrivener, and R. D. Hooton (2011). "Supplementary cementitious materials." *Cem. Con. Res.* **41**(3): 217-229.

Lothenbach, B., and F. Winnefeld (2006). "Thermodynamic modelling of the hydration of portland cement." *Cem. Con. Res.* **36**(2): 209-226.

Lowke, D., and P. Schiessl (2007). Effect of mixing energy on fresh properties of scc, Technical University of Munich, Centre of Building Materials**:** 6 pp.

Lu, D., and S. Wei (1992). "Effect of grinding aids on producing ultrafine particles." *Adv. Powder Tech.* **3**(1): 47-53.

Lura, P., J. Couch, O. M. Jensen, and J. Weiss (2009). "Early-age acoustic emission measurements in hydrating cement paste: Evidence for cavitation during solidification due to self-desiccation." *Cem. Con. Res.* **39**(10): 861-867.

Lynsdale, C. J., and M. I. Khan (2000). "Chloride and oxygen permeability of concrete incorporating fly ash and silica fume in ternary systems." *ACI SP* **192**: 739-753.

Maeda, N., I. Wada, M. Kawakami, T. Ueda, and G. K. D. Pushpalal (2001). "Chloride diffusivity of concrete incorporating rice husk ash." *ACI SP* **200**: 291-308.

Mahboub, K. C., and Q. A. Cutshaw (2001). "Effects of fresh concrete temperature and mixing time on compressive strength of concrete." *ACI Mat. J.* **98**(1): 59-62.

Maskara, A., and D. M. Smith (1997). "Agglomeration during the drying of fine silica powders, part ii: The role of particle solubility." *J. Am. Ceram. Soc.* **80**(7): 1715-1722.

Massazza, F. (2008). Pozzolana and pozzolanic cements. *Lea's chemistry of cement and concrete*. P. C. Hewlett. Oxford, UK, Butterworth-Heinemann**:** 471-635.

Mehta, P. K. (1983). "Pozzolanic and cementitious by-products as mineral admixtures for concrete - a critical review." *ACI SP*. **79**: 1-46.

Mehta, P. K. (1994). *Rice husk ash - a unique supplementary cementing material*. Proc. Intern. Advances in Concrete Tech., CANMET.

Mehta, P. K. (2004). *High-performance, high-volume fly ash concrete for sustainable development*. Intern. Workshop Sustain. Develop. Concr. Tech., Beijing, China, Iowa State University.

Mehta, P. K., and K. J. Folliard (1995). "Rice husk ash--a unique supplementary cementing material: Durability aspects." *ACI SP* **154**: 531-542.

Mehta, P. K., and P. J. M. Monteiro (2006). *Concrete: Structure, properties, and materials*. New York, McGraw-Hill.

Meyer, C. (2009). "The greening of the concrete industry." *Cem. Con. Comp.* **31**(8): 601-605.

Mindess, S., J. F. Young, and D. Darwin (2002). *Concrete*. NJ, Prentice Hall.

Misra, K. C. (2012). Introduction to geochemistry: Principles and appliations. Hoboken, NJ, John Wiley & Sons.

Muthadhi, A., and S. Kothandaraman (2013). "Experimental investigations of performance characteristics of rice husk ash–blended concrete." *J. Mater. Civil Eng.* **25**(8): 1115-1118.

Nair, D. G., A. Fraaij, A. A. K. Klaassen, and A. P. M. Kentgens (2008). "A structural investigation relating to the pozzolanic activity of rice husk ashes." *Cem. Con. Res.* **38**(6): 861-869.

Naiya, T. K., A. K. Bhattacharya, and S. K. Das (2009). "Adsorptive removal of Cd(II) ions from aqueous solutions by rice husk ash." *Env. Prog. Sustain. Energy* **28**(4): 535-546.

Naiya, T. K., A. K. Bhattacharya, S. Mandal, and S. K. Das (2009). "The sorption of lead (II) ions on rice husk ash." *J. Hazard. Mater.* **163**(2-3): 1254-1264.

Nakane, K., T. Yamashita, K. Iwakura, and F. Suzuki (1999). "Properties and structure of poly(vinyl alcohol)/silica composites." *J. Appl. Polymer* **74**(1): 133-138.

Nehdi, M., and S. Al-Martini (2009). "Coupled effects of high temperature, prolonged mixing time, and chemical admixtures on rheology of fresh concrete." *ACI Mat. J.* **106**(3): 231-240.

Nehdi, M., J. Duqette, and A. El Damatty (2003). "Performance of rice husk ash produced using a new technology as a mineral admixture in concrete." *Cem. Con. Res.* **33**(8): 1203-1210.

Neville, A. M. (1996). *Properties of concrete*. New York, John Wiley & Sons.

Nordstrom, D. K., and J. L. Munoz (2006). *Geochemical thermodynamics*. Palo Alto, CA, The Blackburn Press.

Odler, I. (2008). Hydration, setting and hardening of portland cement. *Lea's chemistry of cement and concrete*. P. C. Hewlett. Burlinton, MA, Butterworth-Heinemann**:** 241-297.

Osbaeck, B. (1984). On the influence of alkalis on strength development of blended cements. British Ceramic Proc.

Ozkul, M. H., A. Baskoca, and S. Artirma (1997). "Influence of prolonged agitation on water movement related properties of water reducer and retarder admixtured concretes." *Cem. Con. Res.* **27**(5): 721-732.

Parkhurst, D. L., and C. A. J. Appelo (1999). User's guide to PHREEQC (version 2)— a computer program for speciation, batch-reaction, one-dimensional transport, and inverse geochemical calculations. U. S. D. o. t. Interior. Denver, CO.

Payá, J., J. Monzó, M. V. Borrachero, A. Mellado, and L. M. Ordoñez (2001). "Determination of amorphous silica in rice husk ash by a rapid analytical method." *Cem. Con. Res.* **31**(2): 227-231.

Payá, J., J. Monzó, M. V. Borrachero, E. Peris, and E. González-López (1997). "Mechanical treatments of fly ashes. Part III: Studies on strength development of ground fly ashes (GFA) — cement mortars." *Cem. Con. Res.* **27**(9): 1365-1377.

PCA. (2010). "Green in practice 102 - concrete, cement, and CO_2." Retrieved 12/23, 2010.

Perkins, R. B., and C. D. Palmer (1999). "Solubility of ettringite ($Ca_6[Al(OH)_6]^2(SO_4)^3 \cdot 26H_2O$) at 5–75°C." *Geochimica et Cosmochimica Acta* **63**(13–14): 1969-1980.

Portland Cement Association (2000). Survey of mineral admixtures and blended cements in ready mixed concrete**:** 16 pp.

Prasittisopin, L., and D. Trejo (2013). Effects of mixing and transportation on characteristics of cementitious systems containing fly ash. World of Coal Ash Conference, Lexington, KY.

Prasittisopin, L., and D. Trejo (2014). Effects of mixing variables on hardened characteristics of PC mortars. (Under review)

Prasittisopin, L., and D. Trejo (2014). Fresh and hardened characteristics of blended cementitious systems incorporating chemically transformed rice husk ash. (Under review)

Prasittisopin, L., and D. Trejo (2014). Hydration and phase formation of blended cementitious systems incorporating chemically transformed rice husk ash. (Under review)

Pratson, L. F., D. Haerer, and D. Patiño-Echeverri (2013). "Fuel prices, emission standards, and generation costs for coal vs natural gas power plants." *Environ. Sci. Technol.* **47**(9): 4926-4933.

Qing, Y., Z. Zenan, K. Deyu, and C. Rongshen (2007). "Influence of nano-SiO_2 addition on properties of hardened cement paste as compared with silica fume." *Constr. Build. Mater.* **21**(3): 539-545.

Quennoz, A., and K. L. Scrivener (2012). "Hydration of C_3A–gypsum systems." *Cem. Con. Res.* **42**(7): 1032-1041.

Rangaraju, P., and K. C. Harish (2010). Optimization of use of rice husk ash for use as SCM in cementitious mortars. *Concrete Sustainability Conference*. Tempe, AZ, National Ready Mixed Concrete Association.

Ravina, D. (1975). "Retempering of prolong-mixed concrete with admixtures in hot weather." *J. ACI* **72**(6): 291-295.

Ravina, D. (1996). "Effect of prolonged agitating on compressive strength of concrete with and without fly ash and/or chemical admixtures." *ACI Mat. J.* **93**: 451-456.

Reinschmidt, K., and D. Trejo (2006). "Economic value of building faster." *J. Construc. Eng. Management* **132**(7): 759-766.

Rejeb, S. K. (1996). "Improving compressive strength of concrete by a two-step mixing method." *Cem. Con. Res.* **26**(4): 585-592.

Rodrigues, F. A. (2003). "Low-temperature synthesis of cements from rice hull ash." *Cem. Con. Res.* **33**(10): 1525-1529.

Rodríguez de Sensale, G. (2010). "Effect of rice-husk ash on durability of cementitious materials." *Cem. Con. Comp.* **32**(9): 718-725.

Rothstein, D., J. J. Thomas, B. J. Christensen, and H. M. Jennings (2002). "Solubility behavior of Ca-, S-, Al-, and Si-bearing solid phases in portland cement pore solutions as a function of hydration time." *Cem. Con. Res.* **32**(10): 1663-1671.

Roumain, J. C. (2004). Holcim. (Cited by Hooton (2008))

Roy, D. M., and G. M. Idorn (1993). Concrete microstructure. Washington DC, Strategic Highway Research Program.

Rukzon, S., P. Chindaprasirt, and R. Mahachai (2009). "Effect of grinding on chemical and physical properties of rice husk ash." *Inter. J. Minerals, Metall. and Mater.* **16**(2): 242-247.

Rupnow, T. D., V. R. Schaefer, K. Wang, and B. L. Hermanson (2007). Improving portland cement concrete mix consistency and production rate through two-stage mixing. Ames, IA, Iowa State University**:** 96 pp.

Sakr, K. (2006). "Effects of silica fume and rice husk ash on the properties of heavy weight concrete." *J. Mater. Civil Eng.* **18**(3): 367-376.

Salas, A., S. Delvasto, R. M. de Gutierrez, and D. Lange (2009). "Comparison of two processes for treating rice husk ash for use in high performance concrete." *Cem. Con. Res.* **39**(9): 773-778.

Samson, E., G. Lemaire, J. Marchand, and J. J. Beaudoin (1999). "Modeling chemical activity effects in strong ionic solutions." *Comp. Mater. Sci.* **15**: 285-294.

Sasaki, S. (1993). Method for preventing agglomeration of colloidal silica and silicon wafter polishing composition using the same. *U.S. Patent*. Yokkaichi, Monsanto Japan, Ltd. **526930:** 5 pp.

Sata, V., J. Tangpagasit, C. Jaturapitakkul, and P. Chindaprasirt (2012). "Effect of w/b ratios on pozzolanic reaction of biomass ashes in portland cement matrix." *Cem. Con. Comp.* **34**(1): 94-100.

Saucier, F., M. Pigeon, and P. Plante (1990). "Air-void stability, part III: Field tests of superplasticized concretes." *ACI Mat. J.* **87**(1): 3-11.

Schutz, R. J. (1981). Admixtures and method for accelerating the setting of portland cement compositions. U.S., Sika Chemical Corp. **4264367**.

Shearer, C. R., N. Yeboah, K. E. Kurtis, and S. E. Burns (2011). The early-age behavior of biomass fired and co-fired fly ash in concrete. *WOCA conf*. Denver, CO.

Shuichi, S., M. Shoya, and H. Tokuda (1992). "Evaluation of pozzolanic activity of rice husk ash." *ACI SP* **132**: 495-512.

Snow, R. H., E. Allen, B. J. Ennis, and J. D. Litster (2008). Size reduction and size enlargement. *Perry's chemical engineers' handbook*. R. H. Perry and D. W. Green. New York, McGraw-Hill.

Souza Rodrigues, C., K. Ghavami, and P. Stroeven (2010). "Rice husk ash as a supplementary raw material for the production of cellulose–cement composites with improved performance." *Waste and Biomass Valorization* **1**(2): 241-249.

Stroeven, P., D. D. Bui, and E. Sabuni (1999). "Ash of vegetable waste used for economic production of low to high strength hydraulic binders." *Fuel* **78**(2): 153-159.

Sugita, S., M. Shoya, and H. Tokuda (1992). "Evaluation of pozzolanic activity of rice husk ash." *ACI SP* **132**: 495-512.

Sujivorakul, C., C. Jaturapitakkul, and A. Taotip (2011). "Utilization of fly ash, rice husk ash, and palm oil fuel ash in glass fiber–reinforced concrete." *J. Mater. Civil Eng.* **23**(9): 1281-1288.

Suprenant, B. A., and W. R. Malisch (2000). The cost of waiting. *Concrete Construction*. Washington DC, Hanley Wood.

Takada, K. (2004). Influence of admixtures and mixing efficiency on the properties of self compacting concrete: The birth of self compacting concrete in the netherlands. *Civil Engineering and Geosciences*. Delfts, Netherlands, Delft University of Technology. **PhD:** 256 pp.

Takahashi, K., T. A. Bier, and T. Westphal (2011). "Effects of mixing energy on technological properties and hydration kinetics of grouting mortars." *Cem. Con. Res.* **41**(11): 1167-1176.

Taylor, H. F. W. (1997). *Cement chemistry*, Thomas Telford Publishing.

Thomas, J. J., H. M. Jennings, and A. J. Allen (1999). "The surface area of hardened cement paste as measured by various techniques." *Concr. Sci. Eng.* **1**(1): 45-64.

Tishmack, J. K., J. Olek, S. Diamond, and S. Sahu (2001). "Characterization of pore solutions expressed from high-calcium fly-ash–water pastes." *Fuel* **80**(6): 815-819.

Trejo, D., and L. Prasittisopin (2014). Chemical transformation of rice husk ash morphology. (Under review)

Trejo, D., and L. Prasittisopin (2014). Effects of mixing variables on early-age characteristics of PC systems. (Under review)

van Tuan, N. (2011). Rice husk ash as a mineral admixture for ultra high performance concrete. Delft, Netherlands, Delft University of Technology. **PhD:** 183 pp.

van Tuan, N., G. Ye, K. van Breugel, and O. Copuroglu (2011). "Hydration and microstructure of ultra high performance concrete incorporating rice husk ash." *Cem. Con. Res.* **41**(11): 1104-1111.

Vayghan, A., A. Khaloo, S. Nasiri, and F. Rajabipour (2011). "Studies on the effect of retention time of rice husk combustion on the ash's chemo-physical properties and performance in cement mixtures." *J. Mater. Civil Eng.* **24**(6): 691-697.

Venkatanarayanan, H., and P. Rangaraju (2013). "Evaluation of sulfate resistance of portland cement mortars containing low-carbon rice husk ash." *J. Mater. Civil Eng.*

Wang, L., R. K. Seals, and A. Roy (2001). "Investigation of utilization of amorphous silica residues as supplementary cementing materials." *Adv. Cem. Res.* **13**(2): 85-89.

Yu, Q., K. Sawayama, S. Sugita, M. Shoya, and Y. Isojima (1999). "The reaction between rice husk ash and $Ca(OH)_2$ solution and the nature of its product." *Cem. Con. Res.* **29**(1): 37-43.

Zhang, M. H., R. Lastra, and V. M. Malhotra (1996). "Rice-husk ash paste and concrete: Some aspects of hydration and the microstructure of the interfacial zone between the aggregate and paste." *Cem. Con. Res.* **26**(6): 963-977.

Zhang, M. H., and V. M. Malhotra (1996). "High-performance concrete incorporating rice husk ash as a supplementary cementing material." *ACI Mater. J.* **93**(6): 629-636.

VITA

Name:	Lapyote Prasittisopin
Address:	School of Civil and Construction Engineering, Oregon State University, Corvallis, OR, 97331
Email Address:	prasittl@engr.orst.edu
Education:	Ph.D., Civil Engineering, Oregon State University, 2013
	M.S., Materials Science, Oregon State University, 2009
	B.Eng., Chemical Engineering, Chulalongkorn University, 2006